University of Alberta

DEVELOPMENT OF A NEW GENERATION OF HYBRID ORTHOSES FOR PARAPLEGIC LOCOMOTION

by

Adam Thrasher ©

A thesis submitted to the Faculty of Graduate Studies and Research in partial fulfillment of the requirements for the degree of Doctor of Philosophy

in

Medical Science – Biomedical Engineering

Edmonton, Alberta

Spring 2002

National Library of Canada
Acquisitions and Bibliographic Services
395 Wellington Street
Ottawa ON K1A 0N4
Canada

Bibliothèque nationale du Canada
Acquisitions et services bibliographiques
395, rue Wellington
Ottawa ON K1A 0N4
Canada

Your file Votre référence

Our file Notre référence

The author has granted a non-exclusive licence allowing the National Library of Canada to reproduce, loan, distribute or sell copies of this thesis in microform, paper or electronic formats.

L'auteur a accordé une licence non exclusive permettant à la Bibliothèque nationale du Canada de reproduire, prêter, distribuer ou vendre des copies de cette thèse sous la forme de microfiche/film, de reproduction sur papier ou sur format électronique.

The author retains ownership of the copyright in this thesis. Neither the thesis nor substantial extracts from it may be printed or otherwise reproduced without the author's permission.

L'auteur conserve la propriété du droit d'auteur qui protège cette thèse. Ni la thèse ni des extraits substantiels de celle-ci ne doivent être imprimés ou autrement reproduits sans son autorisation.

0-612-68630-2

Canada

University of Alberta

Library Release Form

Name of Author: Timothy Adam Thrasher

Title of Thesis: Development of a new generation of hybrid orthoses for paraplegic locomotion

Degree: Doctor of Philosophy

Year this Degree Granted: 2002

Permission is hereby granted to the University of Alberta Library to reproduce single copies of this thesis and to lend or sell such copies for private, scholarly or scientific research purposes only.

The author reserves all other publication and other rights in association with the copyright in the thesis, and except as herein before provided, neither the thesis nor any substantial portion thereof may be printed or otherwise reproduced in any material form whatever without the author's prior written permission.

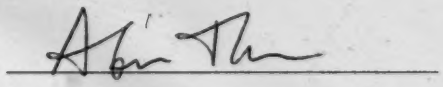

Adam Thrasher
Box 52207
Garneau Postal Outlet
Edmonton, Alberta
T6G 2T5

Submitted to the Faculty of Graduate Studies on January 31, 2002

University of Alberta

Faculty of Graduate Studies and Research

The undersigned certify that they have read, and recommended to the Faculty of Graduate Studies and Research for acceptance, a thesis entitled *Development of a new generation of hybrid orthoses for paraplegic locomotion* submitted by Adam Thrasher in partial fulfillment of the requirements for the degree of Doctor of Philosophy in Medical Science – Biomedical Engineering.

Dr. Brian J. Andrews (supervisor)

Dr. William K. Durfee

Dr. M. Gary Faulkner

Dr. Kenneth Fyfe

Dr. Zoltan J. Koles

Dr. Arthur Prochazka

Dr. Hasan Uludag

Dr. Ronald F. Zernicke

Date: Dec. 17, 2001

To Mom

Abstract

Five novel biomechanics studies were aimed at improving the medially linked knee-ankle-foot orthosis, a hybrid orthosis for paraplegic gait. An objective technique for quantifying trunk stability was developed, and experiments revealed that individuals with spinal cord injuries could resist only the smallest perturbations without using their arms. Open loop FES applied to the erector spinae via skin electrodes caused significant improvement in stability for one subject, but no improvement for another. Further study is required.

Computer modeling established that unassisted sit-to-stand is theoretically possible even with the reduced knee extensor strength associated with FES. The hip extensors must be stimulated with isometric moments of up to 200 Nm, and the trunk must be flexed at a rate of at least 75 deg/s. Trunk momentum prior to lift-off does not significantly reduce the required hip and knee moments.

Computer modeling also revealed that passive gait is theoretically possible if certain precise kinematic conditions are met at toe-off. Segment angles and angular velocities must be within less than 5% of desired values or else swing phase will fail. Passive gait is more energy efficient when the knees are locked in full extension than when the knees are allowed to flex during swing phase. The drawback is that stiff-legged gait is slower and foot clearance is more difficult to achieve. A strategy of oscillating the upper body laterally can produce foot clearance for stiff-legged gait. Only able-bodied subjects were able to successfully produce this effect in the laboratory. A certain amount of lumbosacral stiffness or active control of the lateral trunk flexors is required.

An adaptive neuro-fuzzy controller was designed for closed loop control of swing phase using reinforcement learning. Given no information about the plant, it was able to find to a successful control strategy in usually about 150 trials (failed swing phase). After training, it had the ability to continually adapt to large changes in the system parameters, which caused other controllers to fail. When initialized with expert knowledge, the controller was able to converge to a successful strategy in typically less than 30 trials.

Acknowledgments

I am extremely grateful to everyone who helped and supported and tolerated me during my work leading up to this thesis. Thank you especially, Dr. Brian Andrews, for introducing me to the field of FES and for guiding me through my research with the utmost patience. It was an honor to work under your supervision.

Thank you, Melanie Olin and Finn Mortensen from the Glenrose Rehabilitation Hospital and Dr. Garry Wheeler and Joeri Verellen from the Steadward Centre, for contributing your time and expertise to my clinical experiments. I also thank the dozens of people who selflessly volunteered to be subjects. I very much appreciate your assistance.

Thank you, Dr. Bill Lipsett from the Department of Mechanical Engineering, for your advice and intriguing conversations that got me hooked on biomechanics when I started this program. Sincere thanks also go to my colleagues Rahman Davoodi, Richard Williamson, Feng Wang and all the other staff and students in the Department of Biomedical Engineering, for your generosity, enthusiasm and humor.

Special thanks go to my wonderful family and friends for reassuring me every step of the way. So often I turned to you for support. I also thank the Natural Science and Engineering Research Council of Canada (NSERC) and the Alberta Heritage Foundation for Medical Research (AHFMR) for providing financial support.

TABLE OF CONTENTS

1 Introduction 1
- 1.1 Thesis overview 1
- 1.2 Spinal cord injury 3
- 1.3 Functional electrical stimulation 8
- 1.4 Trunk stability: theoretical and clinical background 16
- 1.5 Sit-to-stand 30
- 1.6 Paraplegic gait 36
- 1.7 Anthropometric data 49
- 1.8 Restatement of objectives 51
- 1.9 References 52

2 FES assisted trunk stability 83
- 2.1 Abstract 83
- 2.2 Introduction 83
- 2.3 Methods 85
- 2.4 Results 91
- 2.5 Discussion 97
- 2.6 References 101

3 The potential role of trunk momentum in FES assisted sit-to-stand 115
- 3.1 Abstract 115
- 3.2 Introduction 115
- 3.3 Methods 119
- 3.4 Results 121
- 3.5 Discussion 123
- 3.6 References 125

4 Passive gait in the medially linked knee-ankle-foot orthosis 136
- 4.1 Abstract 136
- 4.2 Introduction 136
- 4.3 Methods 140
- 4.4 Results 146
- 4.5 Discussion 149
- 4.6 References 154

5 Dynamic lateral articulation of the rigid trunk produces foot clearance in MLKAFO gait 171
5.1 Abstract 171
5.2 Introduction 171
5.3 Methods 174
5.4 Results 178
5.5 Discussion 181
5.6 Bibliography 184
6 Adaptive neuro-fuzzy control of paraplegic gait: reinforcement learning versus supervised learning 197
6.1 Abstract 197
6.2 Introduction 197
6.3 Methods 199
6.4 Results 203
6.5 Discussion 204
6.6 References 206
7 General discussion and conclusions 216
7.1 Discussion 216
7.2 Conclusions 219
7.3 Future work 220
Appendices 222
A Equations for sit-to-stand model 222
B Equations for ballistic walking models 227
C Equations for frontal plane rocking models 233
D Equations for 2-segment swing phase model 237

LIST OF FIGURES

Figure 1-1: ASIA neurological classification form. 69
Figure 1-2: Distribution of spinal cord injuries (epidemiology) 70
Figure 1-3: Distribution of spinal cord injuries by neurologic level of lesion 71
Figure 1-4: Schematic representation of electrical stimulation 72
Figure 1-5: Cross section through the abdomen 73
Figure 1-6: Da Vinci's notebook 74
Figure 1-7: Simple inverted pendulum models of the trunk 75
Figure 1-8: Phase description of the sit-to-stand maneuver 76
Figure 1-9: General biomechanical modeling scheme 77
Figure 1-10: Normal reciprocal gait cycle 78
Figure 1-11: Mechanical orthoses 79
Figure 1-12: Some typical gait models 80
Figure 1-13: Forward dynamics biomechanical modeling scheme 81
Figure 1-14: Spring-dashpot diagram of Hill-type muscle model 82
Figure 1-15: Block diagram of Hill-type muscle model 82
Figure 2-1: Prototype tilt-seat apparatus 103
Figure 2-2: SCI subject #13 shown on tilt-seat apparatus 104
Figure 2-3: Raw data and filtered signals (4-camera Vicon system) 105
Figure 2-4: Raw data and filtered signals (7-camera Vicon system) 106
Figure 2-5: Raw data and filtered signals (portable sensor system) 107
Figure 2-6: Typical data from an able-bodied trunk stability trial 108
Figure 2-7: Typical data from able-bodied trunk stability trials 109
Figure 2-8: Distribution of transient response time 110
Figure 2-9: Boxplots of the able-bodied data 111
Figure 2-10: Typical data from subject #11 trunk stability trials 112
Figure 2-11: Typical data from subject #13 trunk stability trials 113
Figure 2-12: Typical data from subject #14 trunk stability trials 114
Figure 3-1: "Momentum transfer" argument 129
Figure 3-2: 3-segment sagittal plane model of STS in the MLKAFO brace 130

Figure 3-3: Three STS strategies analyzed in this study 131
Figure 3-4: Flat foot static trials - failure regions 132
Figure 3-5: Stick figure illustration of rock-back failure 132
Figure 3-6: Successful STS using the flat foot dynamic strategy 133
Figure 3-7: Success and failure regions for flat foot dynamic trials 134
Figure 3-8: Trials starting from the Kralj position 135
Figure 3-9: Stick figure illustration of a fall-forward failure 135
Figure 4-1: The ballistic walking model 157
Figure 4-2: Illustration of modeling methodology 158
Figure 4-3: Model with stretched elastic cables spanning the hip and knee 159
Figure 4-4: Comparison of model simulation to actual gait data 160
Figure 4-5: Heights and weights of randomly generated subjects 161
Figure 4-6: A typical successful simulation 162
Figure 4-7: Four 2-dimensional "slices" through the input space 163
Figure 4-8: Optimal energy cost versus step length for free-knee gait 164
Figure 4-9: Normalized energy cost 165
Figure 4-10: A successful simulation of stiff-legged gait 166
Figure 4-11: Stiff-legged gait. Four 2-dimensional "slices" 167
Figure 4-12: Optimal energy cost versus step length for stiff-legged gait 168
Figure 4-13: Normalized optimal energy cost 169
Figure 4-14: Swing phase with ideal motor at hip joint 170
Figure 5-1: Three methods of generating foot clearance in MLKAFO 187
Figure 5-2: The medially linked knee-ankle-foot orthosis 188
Figure 5-3: Two-segment models of a person rocking laterally in MLKAFO ... 189
Figure 5-4: Experimental data (subject A, trial 2) smoothed 190
Figure 5-5: Subject A rocking in MLKAFO while holding handrails 191
Figure 5-6: Subject A rocking in MLKAFO without hands 192
Figure 5-7: Mean trunk flexion angle versus rocking frequency 193
Figure 5-8: Subject B walking in MLKAFO 194
Figure 5-9: Mean trunk flexion angle versus rocking frequency 195
Figure 5-10: Frequency vs. stiffness relationship according to linear model 196

Figure 6-1: Two-segment sagittal plane model of swing leg 208
Figure 6-2: Schematic diagram of the Adaptive Fuzzy Network 209
Figure 6-3: Reinforcement learning control scheme 210
Figure 6-4: The SL controller learned to mimic the open loop controller 211
Figure 6-5: Control surfaces for the adapted RL controller 212
Figure 6-6: The RL controller converged to this unique scheme 213
Figure 6-7: Phase plane of swing phase trajectory of RL controller 214
Figure 6-8: The RL controller re-adapted 215

LIST OF TABLES

Table 1-1; Relative effect of individual muscle groups on stability 18
Table 1-2; Numerical solutions of linear pendulum 44
Table 2-1; Able-bodied subjects 88
Table 2-2; Spinal cord injured subjects 88
Table 2-3; Average duration of transient response (able-bodied subjects) 93
Table 2-4; Summary of subject #11 results 95
Table 2-5; Maximum perturbation angles - subject #13 96
Table 2-6; Maximum perturbation angles - subject #14 96
Table 3-1; Optimal hip and knee moments for dynamic strategy 123
Table 4-1; Energy cost of gait from literature 148
Table 5-1; Summary of rocking trials for paraplegic subject A 179

Abbreviations

AFN	Adaptive fuzzy network
AFNa	Adaptive fuzzy network (action net)
COP	Center of pressure
EMG	Electromyography (sometimes electromyogram)
ES	Erector spinae
FC	Foot clearance
FES	Functional electrical stimulation
HA	Hip angle
KA	Knee angle
MLKAFO	Medially linked knee-ankle-foot orthosis
SCI	Spinal cord injury
STS	Sit-to-stand

1 Introduction

1.1 Thesis overview

For decades, rehabilitation devices featuring functional electrical stimulation have been giving paraplegics the ability to stand and walk. However, the technology is limited in that gait is slow, muscles fatigue rapidly, and the arms must bear enormous loads. The technology is unavailable to many paraplegics whose level of injury is too high. The central aim of my research is to present new methodologies based on biomechanical theory and clinical experimentation that will address these limitations. My ultimate goal is to produce a new generation of hybrid orthoses that will be useful and applicable to a significant proportion of the spinal cord injured population.

Contained in this document are five detailed research studies. Each study addresses a different issue concerning spinal cord injuries and hybrid orthoses. The first is trunk stability (chapter 2), which we opted to improve by artificially stimulating the lumbar trunk muscles. The method was shown to work for one out of two subjects. The next issue is the role of the trunk during sit-to-stand transfers (chapter 3). Using a mathematical model, we demonstrated that a strategy involving trunk momentum and hip extension could reduce the required knee moment. Chapter 4 looks at passive gait, an energy efficient process where there is no muscle activity during the swing phase. With a mathematical model, we established that it is theoretically possible, however very precise control of the muscles during stance phase is necessary. Chapter 5 concerns a form of gait where the knees are locked in full extension, and oscillating the trunk from side to side lifts the feet. This rocking motion was demonstrated by a paraplegic, two able-bodied subjects and a mathematical model. Chapter 6 presents an advanced machine learning method for closed loop control of the swing phase of gait, by which a controller can learn to produce satisfactory results completely on its own or with some prior knowledge from a human expert. The cumulative result of this research is a broad foundation of knowledge upon which a new generation of hybrid orthoses can be developed.

My original training is in mechanical engineering. I have a deep appreciation for classical dynamics and the mathematical elegance that arises through subjects like vibration theory. Towards the end of my undergraduate program, I also became interested in medical science and was introduced to biomechanics, which I took to instantly. I chose to investigate the above hypotheses, because they present fascinating mechanical challenges that can ultimately benefit people living with disabilities.

My primary research goals were:

1. To investigate the effect of spinal cord injury on the trunk and the concomitant effect on locomotion.
2. To understand the biomechanical role of the trunk when sitting, standing and walking with hybrid orthoses.
3. To establish biomechanical theories of various modes of paraplegic locomotion that can serve as a basis for improving the design of hybrid orthoses.
4. To propose better strategies for paraplegic sit-to-stand and gait.

The following hypotheses form the basis of the studies:

H1. *Higher levels of spinal cord injury result in lower trunk stability.*
This seems an obvious assertion, but it has never been objectively established because there is no widely accepted measurement protocol for trunk stability in the context of spinal cord injury.

H2. *Open loop functional electrical stimulation of the erector spinae muscles will improve trunk stability after SCI.*
Very few hybrid orthoses address trunk instability by stimulating the paralyzed trunk muscles. Reports of these devices are positive, but no specific stability analysis has been done.

H3. *Thrusting the rigid trunk forward before lift-off during sit-to-stand in conjunction with hip extension moment will reduce required knee moment.*

The biomechanical role of the trunk in sit-to-stand is still a subject of debate. This hypothesis is one possible explanation, which has been made before but remains unproven.

H4. *Passive swing phase is feasible and beneficial during gait in the medially linked knee-ankle-foot orthosis.*

Paraplegic gait might be made more efficient is by harnessing the passive dynamics of the legs. Passive gait has been observed in normal gait and demonstrated in anthropometrically scaled robots, but never in paraplegia.

H5. *Passive gait in the medially linked knee-ankle-foot orthosis can be improved by a powered hip actuator or an elastic element across the knee.*

Powered hip orthoses have been considered, but never successfully implemented. The elastic element spanning the knee is an entirely new idea. The feasibility of these techniques needs to be analyzed.

H6. *Stiff-legged gait in the medially linked knee-ankle-foot orthosis can be improved by functional electric stimulation of the trunk.*

Electrical stimulation has been used to stabilize the trunk before (e.g. 6-channel Parastep system) but never to create useful trunk movements. There is a theory that the trunk acts like a "spinal engine" to drive gait; this may be applicable to paraplegic gait.

H7. *A particular closed loop electrical stimulator for paraplegic gait can be improved with reinforcement learning.*

Because paraplegic gait presents such a complex non-linear control task, it is extremely difficult to design a controller rule base. Machine learning can automate the process.

1.2 Spinal cord injury

Among the most catastrophic and disabling injuries that can occur to the human body are those that damage the spinal cord. The spinal cord is the major conduit through which the brain communicates with the rest of the body. Via sophisticated networks of nerve cells, it receives, integrates and propagates thousands of simultaneous signals between the brain, sensory organs and muscles.

Due to the tremendous importance of these functions, the results of SCI are many and profound.

Depending on the severity and location of the injury, one may experience complete or partial loss of sensation and motor function in one's legs, trunk or arms. For many, this means a wheelchair-centered lifestyle. Atrophy occurs because of muscle disuse. Osteoporosis occurs due to the lack of weight-bearing. Chronic reflex spasms and muscle contractures can occur – sometimes painfully. In addition, an individual living with a SCI is prone to experience changes in body heat regulation, impaired bowel and bladder function, sexual function and fertility. Where there is loss of sensation, continual precautions must be taken to prevent pressure sores. One may also experience increased susceptibility to cardiovascular disease due to reduced levels of physical activity and renal problems due to poor bladder control and urinary function. In short, SCI results in radical changes to one's lifestyle.

The research studies described in this document concern technologies that can give people with SCI greater function, enabling them to stand and walk. These technologies already exist, but they are in need of refinement so that they can do more for more people.

1.2.1 Classification

Not all spinal cord injuries are alike. They affect different body parts, and with different severity. SCI classifications, made according to these factors, assist in prognoses and allow for suitable regimens to be prescribed. They also indicate which users will benefit from which rehabilitation devices. One of the main objectives of this thesis is to examine the specific effect of muscle paralysis on trunk stability.

The American Spinal Injury Association (ASIA) endorses one of the more popular standards of SCI classification in use today (Maynard et al., 1997). Part of the neurological classification form published by ASIA is shown in Figure 1-1.

The four basic neurologic categories for SCI are complete tetraplegia, incomplete tetraplegia, complete paraplegia and incomplete paraplegia. *Tetraplegia*, also known as quadriplegia, refers to loss of motor and/or sensory

function in all four limbs resulting from an injury to one of the eight cervical segments of the spinal cord. *Paraplegia* refers to loss of function in the lower extremities, but no loss of arm function. Paraplegics have lesions in the thoracic, lumbar or sacral regions of the spinal cord.

SCI is said to be *complete* when the spinal cord is completely transected thus severing all ascending and descending tracts. When this is the case, all sensations and voluntary movements are lost below the injury. However, when the spinal cord is not completely transected, some voluntary movement may still be possible and the injury is said to be *incomplete*. ASIA strictly defines complete injuries as those resulting in no anal sensation or voluntary anal contraction.

The neurologic level of injury is an indicator of what parts of the body will be impaired. It refers to the highest segment of the spinal cord that is damaged. The spinal cord is divided into 30 segments corresponding to the vertebrae. There are 8 cervical, 12 thoracic, 5 lumbar and 5 sacral segments. Attached to each segment is a pair of nerves, or roots, that enter/exit the spinal column via gaps called intervertebral foramina. The cervical segments are named according to the vertebra directly *below* the gap through which their roots pass, while all other segments are named according to the vertebra directly *above*. For example, the segment with roots emerging between the fourth and fifth cervical vertebrae is called C5, and the segment with roots passing through the fourth and fifth thoracic vertebrae is called T4. By convention, the segment between the C7 and T1 vertebrae is named C8.

Each root receives sensory information from skin areas called dermatomes, as illustrated in Figure 1-1. Each root also *innervates* (furnishes with nerves) a group of muscles called a myotome. When SCI occurs, it potentially impairs all the muscles and sensory organs that are innervated by the roots at and below the site of the injury. For example, a C7 injury jeopardizes the hand, the arm, all of the trunk and leg muscles, as well as bowel, bladder and sexual function. By determining which dermatomes and myotomes are impaired, the level of SCI can be classified.

Damaged peripheral nerve cells die through a process called *Wallerian degeneration*. Upon injury, the cell becomes slightly swollen and then breaks up into fragments three to five days later. In almost all cases, Wallerian degeneration occurs to the spinal roots at the level of SCI. The result is *denervation* at the myotome, meaning the muscle fibers are no longer furnished with nerves.

1.2.2 Epidemiology

It is estimated that the annual incidence of SCI in North America is 40 cases per million population (NSCISC, 1999). This does not include those who die at the scene of the accident. The number of people alive today with injured spinal cords is estimated to be between 721 and 906 per million population.

According to the National Spinal Cord Injury Statistical Center (NSCISC) (1999), the most common cause of SCI are motor vehicle accidents followed by acts of violence and falls. The distribution shown in Figure 1-2(a) is based on totals from the NSCISC database, compiling data from 1973 to 1999.

Tragically, the majority of SCI happen to young, active adults. Fifty-six percent of SCI occur to people between the ages of 16 and 30. The average age at injury is 31.7 years. Men comprise 81.8% of the SCI population.

The ratio of SCI resulting in tetraplegia to paraplegia is almost 1:1, with a slight majority to paraplegia. While paraplegic injuries are more likely to be complete, tetraplegic injuries are more likely to be incomplete. The distribution by neurologic category is shown in Figure 1-2(b).

The most common site of injury is in the mid-cervical region, C4 toC6. This can partially be explained by anatomy. The thoracic spine is more rigid and surrounded by body mass, making it more resilient to large shearing and bending forces. A detailed breakdown by neurologic level is shown in Figure 1-3.

1.2.3 Rehabilitation

SCI is incurable. The damaged neurons in the spinal cord do not regenerate naturally, and in almost all cases, the impairment caused by SCI is permanent. The damage resulting from SCI is so profound that rehabilitation was once thought impossible. Fortunately, this is no longer the case. Following is a very brief summary of how SCI was dealt with historically.

One of the earliest descriptions of SCI on record comes from ancient Egypt. Contained in the Edwin Smith papyrus, dated 1700 BC, it reads: "One having a dislocation in a vertebra of his neck while he is unconscious of his two legs and his two arms, and his urine dribbles. An ailment not to be treated (Breasted, 1930)." That hopeless prognosis was maintained for a very long time.

Experimental studies of SCI began near the end of the nineteenth century (Collins, 1995). By World War I, progress had been made towards understanding the mechanisms of SCI, and some treatment regimens were in development. However, medical science and facilities were scarcely sufficient to deal with the many spinal casualties caused by the war. The life expectancy after SCI was in the order of weeks, and most of those who did survive never returned to productive life (Collins, 1995, Guttmann, 1976).

The prognosis remained the same until World War II when Sir Ludwig Guttmann, a German exile living in Britain, was appointed to operate a special center for war casualties at Stoke Mandeville Hospital. It was there that SCI ceased to be a hopeless affliction. Guttmann's comprehensive treatment and care regimens were so successful that a majority of his patients were able to return to happy and productive lives (Guttmann, 1976).

Today, research into SCI treatment and care persists at all levels. Surgeons, physiatrists, neurologists, pharmacists, nurses, physiotherapists and rehabilitation engineers have built upon many of Guttmann's techniques and introduced new ones. Not only has the life expectancy of people with SCI been extended to almost that of the general population, technologies such as orthotics and functional electrical stimulation allow for greater independence, and expand the range of opportunities for people with SCI.

One of the most important aspects of an independent lifestyle is mobility. Currently, most people with SCI rely upon wheelchairs. The obvious limitations to wheelchair users are environmental obstacles, such as stairs and uneven terrain. But there are also physiological problems associated with wheelchair use, such as shoulder pain from overuse of the arms (Goldstein et al., 1997, Lal, 1998) and the risk of pressure sores. Many of these problems have been addressed by

technologies such as electric motors, seating materials, all-terrain wheels, and hydraulic pistons that extend the seat and occupant into a standing position.

The ability to stand and walk after SCI has functional, therapeutic and psychological benefit. Guttmann extolled the importance of standing and walking:

> *"The great therapeutic value of daily standing and walking exercises, and the need for the paraplegic to continue these permanently at home, after leaving hospital, should always be stressed." (Guttmann, 1976)*

Standing and walking after SCI was first possible with standing frames and mechanical braces.

Once thought impossible, partial spinal cord regeneration is now being demonstrated in adult mammals (Fawcett, 1998, Lu and Waite, 1998). One can only speculate as to whether and when spinal cord regeneration may be possible in humans. Regeneration is unlikely to be complete. Often techniques demonstrated in non-human species fail to work clinically – the nature of the induced SCI in the animal model has little in common with actual SCI. Until a cure is found, advances in rehabilitation technology are necessary to improve the lives of people living with SCI.

1.3 Functional electrical stimulation

The assistive devices analyzed in this thesis feature a technology that artificially stimulates paralyzed muscles. Involuntary contractions are induced by an electrical stimulus. My research explores new methods of applying electrical stimulation to paralyzed muscles in order to promote stability and restore ambulation.

Functional electrical stimulation (FES) is defined generally as the application of an electrical current to the nervous system to produce or restore some function. FES is differentiated from therapeutic electrical stimulation in that FES promotes functions that have an immediate purpose, e.g. locomotion or voiding of the bladder. However, therapeutic benefits often follow from use of FES. Following SCI, a regular regimen of electrical stimulation can increase

muscle size, strength and endurance and also reverse some of the osteoporosis in bones that are stressed by the targeted muscles (Stein, 1999). While FES refers to a general class of technologies, including sensory prostheses such as cochlear implants for the hearing impaired, the term *functional neuromuscular stimulation* (FNS) is sometimes used when specifically referring to stimulation of the neuromuscular system. FES systems, sometimes called *neural prostheses*, are devices that produce and control electrical stimulation.

1.3.1 Brief history of electrical stimulation

The research in this thesis concerns techniques for applying FES to people with SCI. FES technology has come a long way over the years. At first it was a little understood phenomenon. Now it is widely utilized in many areas of rehabilitation medicine. This section describes how the technology was discovered and developed over time.

Before the electrical nature of the nervous system was understood, people experienced the curious effects of external electrical currents on the body and, in some cases, derived medical applications. In 46 AD, Scribonius Largus described methods of pain relief and healing using torpedo fish (the torpedo fish generates an electric potential of 25 to30 Volts):

> *"For any type of gout a live black torpedo should, when the pain begins, be placed under the feet. The patient must stand on a moist shore washed by the sea and he should stay like this until his whole foot and leg up to the knee is numb. This takes away present pain and prevents pain from coming on if it has not already arisen. In this way Anteros, a freedman of Tiberius, was cured." (Schechter, 1971)*

For centuries, torpedo fish were prescribed for all sorts of ailments including headaches, hemorrhoids and even mental illness.

The next developments in electrical stimulation did not happen until the invention of the electrostatic generator by Otto von Geuricke in 1672. Immediately, the relationship between electricity and biology became a topic of

great interest. Weak electrostatic discharges from the generator were found to excite limbs and animal preparations. Stronger discharges, and hence stronger biological responses, were made possible when the first capacitor was invented 1745. Physicians began treating a wide range of diseases by applying electrical discharges to their patients. Some even reported success. Benjamin Franklin pioneered these techniques, and today stimulation by electrostatic shocks, alone or in series, is called *Franklinism*.

In 1791, Luigi Galvani published his discovery that dissected frog legs could be stimulated by touching a bimetallic rod to nerve and muscle (McNeal, 1977). Although it was Alessandro Volta who explained that the bimetallic rod was a source of electricity, not the nerves or muscles themselves, Galvani is credited with the method of electrical stimulation by making and breaking direct electrical current: *Galvanism*.

Michael Faraday built the first electric generator in 1831. His device introduced the possibility of applying a series of electrical pulses to nerves at high frequency. Such a technique, called *Faradism*, is the basis for all modern electrical stimulation. G. B. Duchenne used Faradism extensively in the latter part of the nineteenth century to treat various neurological disorders. Among his accomplishments was the development of localizing electrical currents using electrodes and a set of maps of the body indicating locations, called *motor points*, where electrical stimulation can be applied to excite individual muscles. His maps are still used today.

Electrical stimulation took off again in the mid-twentieth century following developments in microelectronics. The first FES device is generally credited to Liberson who designed and patented a stimulator for preventing drop-foot in hemiplegics (Liberson et al., 1961). Around the same time, Kantrowitz excited the SCI rehabilitation community by demonstrating a sit-to-stand transfer by a T7 complete paraplegic using FES (Kantrowitz, 1960). Over the following decades, FES sit-to-stand was refined by Kralj and colleagues in Ljubljana, Slovenia (Kralj and Grobelnik, 1973, Bajd and Kralj, 1982), and it continues to be

a subject of interest in SCI research (Dolan, 1997, Davoodi and Andrews, 1998, Miyamoto et al., 1999, Durfee, 1999).

Around the same time as FES sit-to-stand, studies into FES assisted gait began. A much more complex form of locomotion than sit-to-stand, gait poses very difficult problems in terms of stimulation and control. Several groups around the world have contributed to the far from complete FES gait corpus – notably, in Ljulbljana (Strojnik et al., 1979) and Cleveland (Chizeck et al., 1988). In 1994, the first FES gait device – the Parastep system – received approval by the United States Federal Drug Association (FDA), and it now has approximately 500 users worldwide (Kordylewski and Graupe, 2001).

Representing the growing interest in FES research, the International FES Society (IFESS) was founded in 1995. Annual conferences put on by IFESS attract hundreds of researchers from all over the world. Other organizations, for example the Engineering in Medicine and Biology Society (EMBS) branch of IEEE and the Rehabilitation Engineering Society of North America (RESNA), offer FES symposia at their annual conferences.

1.3.2 Principles of FES

Muscle contractions are stimulated naturally by motor signals transmitted via motoneurons. The signals carry coded commands from the central nervous system. The "code" is made up of individual pulses about one millisecond in duration and 100 millivolts in amplitude. Called *action potentials*, these impulses propagate along motoneurons at a rate of 70-120 m/s (Benton et al., 1981). The strength of the resulting muscle contraction is a function of the frequency of the action potentials. A maximal contraction occurs at approximately 60 Hz. (Unfortunately, this is the standard frequency of AC power lines in North America.)

FNS is the process of inducing action potentials in a group of nerve cells and then exploiting the resulting muscle action. Denervated muscle fibers are not accessible through FNS, because they have no motoneurons to stimulate.

Figure 1-4 shows how an external electrical field produces current that penetrates a nerve cell. In doing so, the current causes depolarization of the cell

membrane where it exits the nerve fiber, thus inducing an action potential. Modern applications of FES apply controlled electrical stimuli via electrodes placed on the skin, inserted transcutaneously or surgically implanted. The stimulus is a controlled series of electrical pulses.

There are three ways to regulate the strength of an FES induced muscle contraction. *Amplitude modulation* is when the current amplitude is increased causing a greater number of nerves to be affected, thus a greater number of motor units are recruited. The more motor units activated, the stronger the resulting muscle contraction. *Pulse width modulation* also varies recruitment number by varying the duration, or "width," of each pulse. A wider pulse results in a greater number of motor units recruited. Pulse width modulation is preferred over amplitude modulation, because it involves less risk of electrode corrosion and tissue damage. The third method is frequency modulation, which varies the rate of induced action potentials. Some researchers advocate using pulse width modulation and frequency modulation in combination for the best control performance (Chizeck et al. 1991), but most use pulse width modulation alone, because it is easy to implement electronically.

Typically, when using surface electrodes, pulse widths and amplitudes vary up to 300 μs and 120 mA respectively. Stimulation frequency is usually kept around 20 to 25 Hz. Higher frequencies will produce stronger contractions, but muscles tend to fatigue more rapidly. Unfortunately, muscles fatigue more rapidly than normal at any stimulation frequency. This is one of the major limitations of FES. Another limitation is that stimulated muscle contractile strength is reduced compared to normal muscle. For example, the knee extensors generate 10-50 Nm of moment undergoing FES (Kralj et al., 1983) while normal healthy knee extensors can easily produce up to 150 Nm (Schultz et al., 1992).

Some FES applications target sensory nerves instead of motoneurons. The purpose of this is to trigger a reflex arc that will produce a pattern of muscle contractions. For example, stimulation of the common peroneal nerve can elicit the flexor withdrawal reflex (the reflex experienced immediately after stepping on something sharp). This technique has been employed widely to initiate swing

phase in reciprocal gait (Kralj et al., 1983, Andrews and Kirkwood, 1989, Kralj and Bajd, 1989, Graupe and Kohn, 1994, Malezic and Hesse, 1995). The response of the reflex to electrical stimulation weakens after prolonged FES use, a phenomenon known as *habituation*.

1.3.3 Modern neural prostheses

A goal of my research is to suggest new ways of employing FES, including methods of stimulus control and coordination. How these methods would be practically employed will require special equipment, such as electronic sensors and microprocessors. Following is a brief summary of FES devices that are currently in use and development.

Neural prostheses (sometimes *neuroprostheses*) are devices that control and deliver FES. FES systems for paraplegic locomotion can involve anywhere from four to 18 channels of stimulation. Stimulation can be provided *transcutaneously* via surface electrodes (e.g. Kralj and Bajd 1989, Graupe and Kohn, 1998), *percutaneously* using needle electrodes inserted through the skin (e.g. Moynahan et al. 1996), or by fully implanted electrodes (e.g. Marsolais et al. 1994, Davis et al. 1999, Davis et al., 2001). Surface electrodes are inexpensive and not invasive, but they require higher voltages to overcome the impedance of the skin; many deep muscles are inaccessible to surface stimulation. Percutaneous electrodes tend to fail and are therefore difficult to use on a long-term basis. Implanted systems involve a long, multistage surgical procedure, which only a small number of patients worldwide have undergone.

Modern systems are small and portable. The FDA approved Parastep system (Graupe and Kohn, 1998), for example, is powered and controlled by a Walkman-sized unit that can be comfortably attached to a belt or waistband.

A wide variety of FES control systems exist, ranging in sophistication from simple switch-initiated open loop controllers to self-adapting intelligent closed loop controllers. Closed loop controllers require some kind of sensory feedback, either artificial or natural. Artificial sensors include goniometers, accelerometers, and rate gyroscopes (Davis et al., 1999, Williamson and Andrews, 2001). Although the main purpose of sensors is to provide continuous

state feedback to closed loop controllers, they are also used for intention detection (i.e. when does the user wish to initiate or terminate a stimulation sequence?). Kordylewski and Graupe (2001) have implemented a controller that uses EMG recordings of voluntary upper body contractions to determine the user's intention.

1.3.4 Hybrid orthoses

Most of my research concerns a specific device that combines FES with mechanical bracing – a hybrid orthosis. My objective is to suggest ways in which this particular device can be improved.

An orthosis is a device designed to give mechanical support to weak or ineffective joints or muscles, i.e. a brace. "Hybrid orthoses" is the name given to a class of devices that combine mechanical braces with FES. This approach, originally proposed by Tomovic et al. (1972), seems to get the best of both worlds. By stiffening certain joints, the braces compensate for denervated muscles, delay the onset of FES induced muscle fatigue and simplify motion control by reducing the number of degrees of freedom. At the same time, FNS provides a means to actuate the otherwise passive brace. The mechanical orthoses also provide convenient surfaces for mounting stimulator leads, electronics, sensors and batteries.

Some hybrid orthoses include externally powered actuators (Popovic et al., 1989, Edwards and Rithalia, 1996). Thus far, *active braces* have not had much success in the area of paraplegic locomotion due to their weight and bulkiness. However, as battery and actuator technology advance, the potential of active braces increases.

See sections 1.6.2 to 1.6.4 for a detailed review of hybrid orthoses.

1.3.5 Control strategies

One way in which I foresee significant improvements to FES devices is to employ more sophisticated control strategies. Currently, general control theory is very advanced, but only the simplest closed loop control schemes have been put into practice in the context of FES.

There are many different ways to control FES signals. The simplest method is open loop. That is, when the controller is activated, a prescribed

sequence of stimulation signals is sent through the electrodes; there is no feedback. If something goes wrong, for example, the swing leg fails to achieve toe-off, the controller will be unaware and will continue providing stimulation as though nothing happened. Most FES controllers today operate without feedback.

Closed loop control has the ability to alter stimulation according to continuous sensor feedback. In the previous example, a toe switch might detect that the swing leg foot is in contact with the ground longer than it should be, and the controller could respond with stronger stimulation of the hip and/or knee flexors.

One of the simplest forms of closed loop control is the old proportional-integral-derivative (PID) scheme. PID controllers are linear and hence limited when applied to non-linear systems. Muscular dynamics and biomechanics tend to be very non-linear and time-variant, so PID controllers are generally insufficient for anything but the simplest postural stability tasks. Still, PID control is often used in FES systems (e.g. Durfee and Hausdorff, 1990, Chizeck, 1992). The PID architecture has also been successfully combined with other, non-linear control schemes (Abbas and Chizeck, 1991).

Fuzzy logic is a popular control approach that can potentially address the neuromuscular system's non-linearity and time-variance. Fuzzy systems are rule based; feedback signals are interpreted by a series of if-then rules and synthesized according to weighted membership functions. Due to its use of semantic variables, human operators can easily construe the rule base of a fuzzy control system. No other control scheme is quite as lucid. Fuzzy logic controllers can be designed to have learning capabilities. Adaptive fuzzy logic controllers for FES assisted sit-to-stand have been devised, however only in theory (Davoodi and Andrews, 1998, Bahrami et al. ,1999).

Neural networks are another popular type of non-linear control scheme. They are said to be *connectionist,* because they are made up of a group of interconnected nodes. Together, the nodes behave as a single processing unit. The popularity of connectionist control schemes is, in part, because they are simple in form, and amenable to gradient learning methods. Sepulveda et al. (1998) built an

adaptive neural network controller, and collected somewhat encouraging evidence that it could be used to control FES assisted gait.

Adaptive closed loop controllers, be they fuzzy based, connectionist or otherwise, have the ability to learn. Machine learning methods can be separated into two general classes. The first is *supervised learning* (SL). This requires some prior expert knowledge regarding what output is needed. An SL controller will alter its parameters until it produces something close to the desired output every time. For example, the hip and knee angles of normal gait could be used as the supervisor data for an adaptive FES gait controller. The other machine learning class is *reinforcement learning* (RL). Controllers in this class are merely given objectives to achieve. Each time the controller attempts to achieve the objectives, a simple reinforcement signal is returned indicating success or failure. The controller then upgrades its parameters, sometimes randomly, and tries again until success occurs routinely. The advantage of RL is that it does not require prior knowledge about the plant. Sometimes, RL will discover novel control strategies, because it does not converge to specified output. RL, however, generally takes much longer to converge than SL.

Neuro-fuzzy control is a promising new concept that combines fuzzy logic and neural networks. Neuro-fuzzy controllers bear the connectionist structure of neural networks, allowing SL and RL methods to be applied, while using a fuzzy rule base. The fuzzy rules accommodate human-type thinking and make it easy to incorporate expert knowledge directly. To date, adaptive neuro-fuzzy controllers for FES have only been theorized.

Of course, many different FES control schemes have been devised and implemented over the years, encompassing an enormous range of ideas. The above review is by no means exhaustive.

1.4 Trunk stability: theoretical and clinical background (H1 & H2)

Hypothesis H2 states that FES of the trunk muscles can improve trunk stability for people with SCI. Such a technique would hopefully enable subjects with high thoracic lesions to use braces that have no mechanical components

above the waist. Currently, there are very few hybrid orthoses that stimulate the trunk muscles.

Many researchers have sought to quantify the trunk stability. The need for such a measure has been identified as a means to statistically compare treatments for severe motor disabilities. Others have noted that a trunk stability index could be useful as a prognostic indicator and a measure of rehabilitation for clinical practice (McGill and Cholewicki, 2001). The choice of variables and method of measurement, however, vary radically from study to study. Following is a discussion on the concept of trunk stability and a summary of the different quantifying methods that have been used in published literature.

1.4.1 Anatomy and physiology of the paralyzed trunk

The basis for hypothesis H2 is anatomical. The muscles spanning the lumbar spine are arranged like guy ropes to promote stability in all directions through co-contraction. When not stimulated, they lack the stiffness to support the upper body mass. Following is a brief summary of the lumbar musculature.

The trunk is a vital structural component of the human body. In addition to housing many of the vital organs, it consists of a sturdy skeletal structure and a complex arrangement of muscles to support it. The muscles that stabilize and articulate the vertebral column are many. They have multiple origins and insertions, which overlap considerably. Nerves branching from multiple spinal roots innervate these muscles. A spinal cord lesion results in denervation of myotomes at the level of injury and paralysis of myotomes below the level of injury. FES is not applicable to the denervated myotomes, but it can be applied to the innervated, paralyzed myotomes.

For example, the iliocostalis lumborum (one of the erector spinae muscles) connects the inferior six ribs to the iliac crests of the pelvis, and runs posterior and lateral to the spine. Nerves from each lumbar root innervate its fibers. A lesion at L3 would paralyze some of the fibers, leaving the iliocostalis lumborum partially paralyzed. Furthermore, nerve degeneration is likely to occur at the lesion level, leaving the muscle fibers corresponding to L3 denervated. FES could still be delivered to the paralyzed fibers innervated from L4 and L5, but not the

denervated fibers of L3. The unaffected fibers of L1 and L2 would remain under voluntary control. The practical issues of combining FES with voluntary contraction of a partially paralyzed muscle are not well known.

It is practical to group the trunk muscles according to the general direction of the muscle bundles and their approximate length. Table 1-1 below identifies the major muscle groups that apply potentially stabilizing moments on the thoracic and lumbar spine (Tortora and Grabowski, 1996). Figure 1-5 is a transverse plane cross section through the lumbar region of the trunk where most of these muscles groups can be seen.

Table 1-1; Relative effect of individual muscle groups on stability

Muscle group	Lateral stability	Anterior-posterior stability
Erector spinae	medium	large
Rectus abdominis	small	large
External oblique	large	none
Internal oblique	large	none
Quadratus lumborum	small	medium
Psoas	small	none
Latissimus dorsi	small to medium	small
Transversospinalis	very small	very small
Segmental	very small	very small

The largest group is the erector spinae (ES), located posterior to the spine, which act to extend the vertebral column. The ES span five to fifteen vertebrae each, and have the greatest moment arms posterior to the spine of any other paraspinal muscles. In terms of stability, the ES are best at resisting perturbations that push the trunk in the anterior direction. The rectus abdominis muscles (RA) act anterior to the spine, connecting the pubic crest of the pelvis to the cartilage of the rib cage. Antagonist to the ES, the RA can provide resistance to perturbations in the posterior direction.

The external and internal oblique abdominal muscles connect the rib cage to the pelvis to the connective tissue of the abdomen. The oblique abdominals laterally flex the lumbar spine with a large moment arm. In terms of stability, they are effective at resisting perturbations that occur in the medial-lateral direction (i.e. in the frontal plane). The quadratus lumborum (QL) connects the lumbar

spine to the pelvis, and it also provides medial-lateral stability, however with less of a moment arm than the obliques. The psoas are massive muscles that connect the lumbar spine to the lesser trochanter of the femur. They also provide stability in the frontal plane, however with a very small moment arm.

Latissimus dorsi (LD) is a large, unique muscle that connects the upper arm to the spine. The origin includes every vertebra from T6 to the sacrum, plus the iliac crests of the pelvis. Thus, it produces forces that tend to laterally flex the whole spine. LD is innervated from C6 to C8. In tetraplegia, LD is often one of the only trunk muscle not paralyzed. It is very common for tetraplegics to have extremely well developed latissimus dorsi, which they rely on heavily for stability.

The transversospinalis and segmental muscles connect adjacent vertebrae (except in the mid-thoracic region where transversospinalis can span up to five vertebrae). They are relatively small, their moment arms are short, and their contribution to spinal stability is minimal.

The trunk muscles that are most accessible to surface FES are the ones closest to the surface of the skin. These are the ES, RA, LD and external obliques. Surface electrodes may affect the internal obliques, although minimally. The QL and psoas are too deep to be stimulated by surface electrodes. However, Percutaneous electrodes can access the nerves that innervate them via the dorsal rami.

The transverse abdominis is shown in Figure 1-5, but it is not included in the table, because it acts horizontally to compress the abdomen. This might possibly promote trunk stability by increasing intra-abdominal pressure, a mechanism that has yet to be proven (Cholewicki et al., 1999).

A spinal injury often results in permanent vertebral damage, which may further reduce the stability of the trunk. Bony fusion could fix a group of vertebra into a position that might be detrimental to stability (e.g. scoliosis). On the other hand, spinal fixation devices are often implanted to repair damaged vertebrae, thus increasing spinal rigidity and stability.

1.4.2 Stability definitions

In order to address hypotheses H1 and H2, it is first necessary to define "trunk stability" in such a way that it can be objectively measured. This section discusses the concept of stability, and reviews how it has been used (and misused) in the scientific and clinical literature.

As a concept, stability has evolved through the course of history, but it has never converged upon one universally accepted interpretation. Its meaning has always been adjusted to fit the requirements of specific problems, and there is still, within many disciplines, widespread disagreement on how the term ought to be applied. Leipholz acknowledged that there is no absolute definition of stability, and put forward a general statement outlining the concepts that are common to all well accepted definitions of stability:

> *"An unperturbed state, whose stability is being studied, is specified. A perturbation is then applied to the unperturbed state, so that it is transformed into a perturbed state. Certain characteristics are emphasized, which we shall call norms, which characterize the states at any desired time. The change in the norms during the transition from the unperturbed state to the perturbed state under the influence of the perturbation is determined. Based on this behavior, a conclusion may be reached regarding the stability of the unperturbed state or its instability."*
> *(Leipholz, 1970)*

The differences between specific definitions of stability are therefore based on (1) what kind of perturbation is applied, (2) what state characteristics are observed, and (3) how the change in state characteristics is interpreted. Note that since it must be assessed by its response to perturbation, stability of an object or system cannot be determined solely by its equilibrium position. Let trunk stability then be defined generally as the ability of the unsupported human trunk to remain erect without the use of arms when subjected to perturbation.

"Spine stability," or sometimes "vertebral stability," typically refers to the spine as a mechanical structure. The application of formal stability theory to the spine has been a popular topic in the biomechanics literature recently, particularly in reference to the lumbar spine. This area of research seeks to understand the individual mechanisms that stabilize the vertebral column such as spinal ligaments, paraspinal muscles and intra-abdominal pressure. Although generally aimed at quantifying global trunk stability in vivo, most studies of spine stability use theoretical models or cadaver dissections instead of living human subjects. Some noteworthy studies are included in this review.

Balance is defined as "stability produced by even distribution of weight on each side of the vertical axis" (Merriam-Webster, 1989). In the context of trunk mechanics, balance is equivalent to stability with the added implication of vertical symmetry. The term "balance," although largely avoided in the biomechanics literature, is popular within Phys Ther reports and clinical procedure. Many physiotherapists use the term "sitting balance," or sometimes "independent sitting balance," to refer to one's ability to maintain an upright posture without external support. It is a binary attribute; either one has it or one does not. Sometimes, this includes the ability to sit up from a prone position unassisted. Others assess sitting balance based on the vertical alignment of the spine at static equilibrium. The problem with these definitions is that they do not directly consider one's ability to cope with perturbations, which is central to the concept of stability.

"Postural stability" usually refers to the stability of an individual who is standing upright, however some researchers use it to refer to seated individuals. When it does refer to upright standing, it involves whole body stability, not just the trunk.

Other terms that come up frequently in both the physical therapy and biomechanics literature are "postural control," "balance control" and "trunk control." These generally refer to one's ability to perform non-equilibrium tasks, for example leaning and reaching, but the exact definition varies greatly from study to study. Although trunk control deals with many of the same neuromuscular mechanisms as trunk stability, the two terms must not be

confused. Control deals with the performance of willful acts that result in transitions to new states; Stability is one's ability to retain a desired equilibrium state in spite of perturbations.

1.4.3 Formal stability theory

Further to the discussion in the previous section, "stability" is often used in a very formal, mathematical sense. Briefly, this section discusses formal stability theory and how it is generally applied to various classes of mathematical problems.

Stability theory is a branch of mathematical physics that deals with special types of mechanical problems, both static and kinetic. The history of stability theory begins in ancient Greece. Aristotle and Archimedes expressed two different ways to assess stability by observing the response of a system to a perturbation (Magnus, 1959). Aristotle's method, generally, was to observe the resulting course of motion. Archimedes was only interested in the purely geometric situation after perturbation. Both methods have been used extensively in all fields of mechanics since. A third general method involving energy eventually came about, contributing largely to the theory of elastic bodies.

In order to determine stability of a system, one or more stability criteria are often defined. A system is said to be stable if the criteria are satisfied, and unstable otherwise. A single parameter is usually varied until a value is found where the system makes a transition from stable to unstable. In 1744, Euler determined a stability criterion for static elastic columns in terms of the maximum compressive force they could support before buckling. This critical load was found to be a simple function of the height and stiffness characteristics of the column. Critical load is a common indicator of structural stability.

Adolf Hurwitz, near the end of the nineteenth century, determined another popular stability criterion. The Hurwitz stability criterion applies to all systems that can be described by linear differential equations. Around the same time, Aleksandr Lyapunov introduced groundbreaking new definitions and theorems that form the basis of modern stability theory. Lyapunov's definition of stability can be applied to any system, linear or nonlinear, time-variant or time-invariant,

expressed as a set of ordinary differential equations. Following Aristotle's original idea, Lyapunov stability considers the course of motion following perturbations of the initial conditions. Typically, one determines the set of initial conditions for which Lyapunov's stability criteria are met, and that set is interpreted to reflect overall stability.

1.4.4 Spine stability

There has been a great deal of research into the specific mechanics of the normal spine, and its surrounding tissues and muscles. This section reviews that work and discusses how the theories of spine stability relate to understanding trunk instability after SCI.

For decades, trunk and spine models have been used to represent the human torso in such a way that formal stability theory could be applied. Lucas and Bresler (1961) made inroads to this idea by modeling the ligamentous spine (vertebrae and ligaments only – no muscles or intra-abdominal pressure) as a continuous elastic Euler column. They accurately determined the critical buckling load to be 20.5 N. Belytschko et al. (1973) reported similar results using a discrete elastic column model. Crisco and Panjabi (1992) followed their lead and produced a discrete model of the ligamentous lumbar spine. They determined the critical buckling load to be approximately 90 N by treating the equations of motion as a generalized eigenvalue problem. Of course, this result is not comparable to those of Lucas and Belytschko, because it dealt with only the lumbar spine while the others dealt with the entire thoracolumbar column.

The very low buckling loads reported illustrate a well-known fact: the neuromuscular system must fulfill a contributing role to stabilizing the spine. This was first noted by Leonardo da Vinci who observed that the muscles of the cervical spine supported the neck like the guy ropes of a ship's mast (Figure 1-6) (Keele, 1983). Anders Bergmark examined the stabilizing role of muscles about the lumbar spine (Bergmark, 1989). With various 2- and 3-dimensional inverted pendulum models, he studied spine stability in terms of energy. He defined his models as stable if the total potential energy, which incorporated both the ligamentous and muscular stiffness, was a minimum at the equilibrium position.

He reported critical muscular stiffness as an indicator of overall spinal stability. Crisco and Panjabi (1991) later used critical stiffness to evaluate different muscular architectures of the lumbar spine. Unsatisfied with their findings, Gardner-Morse et al. (1995) developed a highly detailed, anatomically precise, 3-dimensional model of the lumbar spine and subjected it to a minimal potential energy stability analysis. From the values of critical stiffness determined, they importantly concluded that, "under normal circumstances at maximal efforts, muscle stiffness can stabilize the lumbar spine without the need for active control."

In addition to the ligaments and paraspinal muscles, several researchers have proposed intra-abdominal pressure as a third mechanism that contributes to stability of the lumbar spine (Tesh et al., 1987, McGill and Norman, 1987, Cresswell et al., 1994). The abdominal cavity is a chamber filled with semisolid fluid. Under the influence of trunk muscles, it exerts pressure on the pelvis and diaphragm thereby providing additional stability to the spine. This hypothesis has yet to be proven. A modeling study by Cholewicki et al. (1999) showed no increase in critical load when IAP was applied.

The spine stability studies of Lucas, Bergmark, Crisco, Gardner-Morse, etc. mentioned thus far have all been static. Instead of actually perturbing their models, they applied a theory of elastic bodies and determined some critical variable, usually load or muscle stiffness. Cholewicki and McGill (1996) introduced a theory of stability that could be applied to the dynamic trunk in vivo. They recorded the motion, force and EMG of able-bodied subjects performing a series of basic trunk movements, for example a two-handed lift. The recorded data was used to determine the muscle and inertial forces in an 18-degree of freedom lumbar spine model. Then, a minimum potential energy method was used to calculate a relative stability index at every point in time. Their major finding was that the stability of the lumber spine increases during demanding muscle tasks and diminishes during periods of low muscle activity. This supports the theory that muscle force is the primary mechanism in spinal stability. Gardner-Morse and

Stokes (2001) recently clarified the relationship between trunk muscle coactivation and trunk stiffness.

1.4.5 In vivo evaluation of trunk and postural stability

In order to test hypotheses H1 and H2, a method of objectively measuring trunk stability in living subjects is needed. Such methods have been developed before in a number of different contexts, however no widely accepted standard has been established (at least not in the context of SCI). Following is a review of those methodologies.

The earliest and crudest methods of quantifying trunk stability in living persons involve qualitative assessment scales. Patients are asked to perform various tasks, such as sitting up from a prone position, sitting quietly, raising the arms, etc., and scores are accumulated according to a point-value system based on an observer's judgment. Many scales exist, for example the Barthel Index (Mahoney and Barthel, 1965), Fugl-Meyer Assessment (Fugl-Meyer, 1974), Trunk Control Test (Franchignoni et al., 1997), Trunk Stability Test (Vezina et al., 2000) and Motor Assessment Scale (Carr et al., 1985). As well, there are many ad hoc scales that are used for one or two studies and then discarded. Although many of the scales are useful in assessing general level of impairment and have demonstrated inter-rater repeatability, none of them look specifically at the response of the subject to perturbations. Hence, they are not true measures of stability.

To reiterate, the three basic elements of a stability assessment are: (1) equilibrium state, (2) perturbation, and (3) response measurement. Some methods alter the equilibrium state, for example vertical shoulder force, until the slightest perturbation results in failure (e.g. buckling) as defined by some characteristic response variable. Other methods involve altering the perturbation until failure occurs. Tests to failure are generally not applied in vivo due to the risk of injury. Other methods apply controlled perturbations or random perturbations, which do not result in failure, and conclusions are based on measured response. A summary of the different experimental designs reported in the literature follows.

1.4.5.1 Equilibrium states

In postural stability studies, the subject is typically asked to assume a relaxed standing position, with no external support except for the feet on the ground (Cresswell et al., 1994, Lavender and Marras, 1995, Crane and Demer, 1998, Pai et al., 1998). In some unusual cases, subjects are placed in special frames that reduce the degrees of freedom (Mihelj et al., 2000, Chiang and Potvin, 2001, Matjacic et al., 2001). In almost all experimental designs, subjects are instructed to fold their arms. However, when unassisted quiet standing is not possible, for example in complete paraplegia, a pair of handrails or a walking frame is permitted (Moynahan and Chizeck, 1993, Fujita et al., 1995).

Ideally, trunk stability measurements should be designed in such a way that no part of the body other than the trunk can effectively respond to the perturbation. Of course, this can be difficult to achieve. Some researchers simply sit subjects on a seat with hips and knees flexed in neutral positions (Hardcastle et al., 1987, Kamper et al., 1996, Yang et al., 1996, Pavec et al., 1999). This approach is not perfect, because the legs can push against the ground or footrests causing the pelvis to tilt. Forssberg and Hirschfeld (1994) had their subjects sit on a platform with legs fully extended, and hips flexed approximately 90 degrees. Again, in such an experiment, the legs can partake in the response to the perturbation.

Some apparatuses fix the subjects in a frame that restricts hip and/or pelvic movement (Cholewicki et al., 1997, Thomas et al., 1998). When a subject is in a position where his hips are extended, i.e. standing, stretched tendons and ligaments of the hip joint can create moments that induce anterior rotation of the pelvis. This problem is exacerbated in subjects with contractures of the hip. Care must be taken to immobilize the pelvis as much as possible. Lateral force should be applied to iliac crests via a belt or a carefully positioned brace to prevent anterior rotation of the pelvis.

Cholewicki et al. (1997) varied the equilibrium state. The subjects began each trial in a position with the trunk either flexed or extended. Also, a mass of 32 kg was placed on the subjects' shoulders for half of the trials. Another study by

Radebold et al. (2001) had the subjects sitting on a platform with a hemispherical underside that was free to wobble upon a flat surface.

1.4.5.2 Perturbations

Figure 1-7 illustrates a simple inverted pendulum model of the trunk and upper body of a seated or standing individual. Two basic perturbations can be applied to this model: (1) external force, and (2) moving base of support. In the latter case, the base may undergo rotation or translation or both. Both types of perturbation have been published. Most often implemented are step perturbations that come on at some point in time and remain on thereafter. Occasionally, ramps or brief impulses are used instead when a step perturbation is too difficult to implement.

Perturbations to the base of support are usually applied via specially designed apparatuses, for example a movable platform. These can be motorized or operator driven (Bernard et al., 1994, Forssberg and Hirschfeld, 1994, Yang et al., 1996, Crane and Demer, 1998). Less conventional experimental designs have involved a wheelchair rolling down a twisted ramp (Pavec et al., 1999), and a wheelchair mounted in a van that is driving in circles (Kamper et al., 1996).

External force perturbations have been applied no less creatively. Dropped weights are commonly used to produce controlled, repeatable forces. Typically, the dropped weight is attached to a stiff cable that is passed through a system of pulleys and attached to a thoracic harness worn by the subject (Cresswell et al., 1994, Fujita et al., 1995, Thomas et al., 1998, Chiang and Potvin, 2001). In one experiment, instead of using a cable and harness a weight was dropped into a bucket held by the subject (Lavender and Marras, 1995). In other experiments, the force was generated by an electric motor (Pai et al., 1998, Gardner-Morse and Stokes, 2001) or servo-controlled hydraulic actuators (Matjacic et al., 2001). Sometimes, an external force perturbation is simply a push from an operator (Hardcastle et al., 1987, Moynahan and Chizeck, 1993, Rietdyk et al., 1999). Typically, experiments of this nature are designed such that the subject cannot anticipate the exact time of perturbation.

1.4.5.3 Response variables

Some kinematic data are almost always collected for stability measurements. Kinematic data can be acquired using video cameras with anatomical markers, goniometers (angle sensors), rate gyroscopes (angular velocity sensors), accelerometers or any combination of these devices. In addition to what data to collect, stability analysts must also decide how to reduce their data. From the kinematics recorded before and after the onset of the perturbation, a characteristic *response variable* is calculated. Many researchers look solely at the maximum angles achieved during the response, thus ignoring temporal factors such as settling time (Hardcastle et al., 1987, Cresswell et al., 1994, Lavender and Marras, 1995, Krajcarski et al., 1999). There are many other ways that kinematic data can be reduced. Moynahan and Chizeck (1993) as well as Forssberg and Hirschfeld (1994) measured latency by noting the timing of events such as peak angular displacement. Fujita et al. (1995) recorded the inclination of the trunk (treating the trunk and upper body as an inverted pendulum supported only at the lumbosacral joint even though the subject was standing with arm support). The response variable was defined as the average angle recorded 5 to 10 seconds after the onset of the perturbation minus the average angle recorded in the 5 seconds immediately prior to the perturbation.

Some studies look at the center of pressure (COP) instead of (or in addition to) kinematic data. This requires a force platform or similar apparatus. As with kinematic data, there is no standard for data reduction of COP data. One study used root mean-squared (RMS) COP velocity as the response variable (Crane and Demer, 1998), while another defined a "Dispersion Index" based on RMS displacements (Yang et al., 1996). Popovic et al. (2000) used COP data to define a stability criterion for FES standing systems based on "stability zones" of able-bodied subjects.

Electromyography (EMG) is yet another type of data that is commonly collected in stability experiments, usually in addition to some other kind of data. EMG signals are typically collected via surface electrodes or transcutaneous needle electrodes, which are sampled at 800Hz or greater, then rectified, filtered

and normalized. Peak values are often used as response variables (Thomas et al., 1998, Chiang and Potvin, 2001), as well as the timing of peaks (Cresswell et al., 1994). In one case, the area under the rectified EMG signals was used (Forssberg and Hirschfeld, 1994). In another, the EMG data were converted into muscle moments using some scaling theory (Lavender and Marras, 1995).

1.4.6 FES assisted trunk stability

One of my objectives is to prove that trunk stability can be improved by stimulating the erector spinae muscles. There are some hybrid orthoses in existence that target the ES, but the actual effect of ES stimulation on stability has never been objectively established. Following is a review of those orthoses, plus one recorded attempt to quantitatively measure the effect.

SCI impairs trunk stability due to paralysis of the paraspinal muscles. Theoretically, some of the lost muscle activity can be recovered using FES. To date, there have been a very limited number of applications involving FES of the trunk muscles. The efficacy of these applications has yet to be objectively studied.

Graupe and Kohn's (1994) Parastep system includes stimulation of the paraspinal muscles during gait. Surface electrodes are located 7 to 10 cm above the iliac crests on the subject's back, 4 to 7 cm apart. The designers claim that when this, in addition to gluteal stimulation, is used, "patients with lesions at T7 and higher will usually benefit … in terms of improved stability during standing."

Marsolais et al. (1994) included the ES in their implanted 16-channel FES system. Unfortunately, they reported nothing about the specific effect of the ES stimulation. Similarly, Moynahan et al. (1996) stimulated the ES in some subjects, merely citing "spine extension" as the stimulated response.

At a small conference in Japan, Fujita et al. (1995) reported a pilot study where they applied closed loop FES to the lumbar erector spinae and rectus abdominalis muscles of a standing SCI patient. They conducted a true stability analysis with a force perturbation (dropped weight) applied to the thorax of a standing patient. Maximum inclination of the thorax relative to the vertical was the response variable. The researchers concluded that FES of the ES had a positive effect on stability only in the sagittal plane. One limitation of their study

was that the subject's trunk was not isolated. The pelvis was not fixed, and the hip joints were observed to flex during the response to perturbation, especially when FES was used. Also, the subject was permitted to hold onto handrails during the perturbation. This study involved only one subject.

1.5 Sit-to-stand (H3)

Another objective of my research is to examine the biomechanical role of the trunk during sit-to-stand transfers. In normal sit-to-stand, the trunk is often seen to flex and extend rapidly. How exactly does this contribute to the entire process, and can it be useful for paraplegic sit-to-stand? Following is an encapsulated review of the sit-to-stand literature that relates to these questions.

Standing has been prescribed as an effective therapeutic exercise for paraplegics (Guttman, 1976, Kralj and Bajd, 1989, Andrews and Wheeler, 1995). In addition to the therapeutic benefits, standing offers SCI individuals greater independence to work at high counters, reach objects, transfer from one seat to another and to interact face to face. It is also a prerequisite to walking. The transfer from a sitting position to a standing position is difficult for paraplegics, because the muscle forces available through FES are much weaker than normal. Other complicating factors include contractures, spasticity and shoulder pain (Kralj and Bajd, 1989, Kagaya et al., 1998).

Moving from a sitting position to a standing position has been described as one of the most physically demanding tasks of daily life in terms of joint moments (Riley et al., 1991). This maneuver has many names. In casual conversation, one might say "standing." This term is somewhat ambiguous as it may refer to rising from a seat, or simply maintaining a standing posture. In the biomechanics and Phys Ther literature, terms such as "standing up," "rising from a chair," "standing from sitting" and "transfer from sit to stand" are used. Currently, the most popular term seems to be "sit-to-stand," (abbreviated STS). As it is the most concise, "STS" will be used exclusively throughout this thesis.

Another term that requires clarification is "unassisted STS." In most reports, this refers to STS without external forces on the arms – i.e. no handrails, crutches or armrests are used – and the subject does not push against the seat with

his arms. Sometimes, particularly in the geriatric literature, "unassisted" refers to STS without another person helping. In this thesis, "unassisted" will be used only in reference to STS that is performed with no external forces except for the feet on the ground and the buttocks and thighs on the seat.

In addition to the strength requirements, which are greater than gait and on par with stair climbing (Berger et al., 1988, Jevsevar et al., 1993), STS involves intricate balance control. An individual while seated has a large base of support (the buttocks and the feet). In the standing position, the base of support is much smaller (feet only). A typical unassisted STS maneuver is illustrated in Figure 1-8. One basic objective of STS is to maneuver the body center of mass from above the large area of support to above the small one. Another objective is to erect the body such that the hip and knee joints are near full extension.

1.5.1 Phase description

Hypothesis H3, which concerns STS, states that creating trunk momentum prior to losing contact with the seat (in combination with hip extension moment) can reduce the extension moment required at the knees. In understanding the biomechanics of any maneuver, it is often useful to break the movements down into *phases*. Well-chosen phases will isolate specific actions, thus allowing for detailed examination. Phases are divided by instantaneous *events* that can be determined from objective measurements. *Lift-off* is a standard event in STS marked by the loss of contact of the buttocks and thighs with the seat. Events must be chosen in such a way that any performance of the maneuver, normal or pathological, will produce all of the events in order.

Motivated by the success of phase divisions in gait analysis, Kralj et al. (1990) devised phase divisions for unassisted STS based on standardized recordings of 20 able-bodied subjects. They defined events that could be objectively determined after an entire STS maneuver was performed and recorded. Required data were ground reaction force, knee angle and seat contact throughout the entire maneuver. Four distinct phases were defined:

- Initiation (0 to 27% of maneuver) – Upper body momentum is generated by rotating the trunk toward flexion; end of phase marked by rapid

increase of vertical ground reaction force (rate of change greater than 10% of peak-to-peak value).

- Seat unloading (27 to 34%) – Whole body center of mass accelerates upward; end of phase marked by *lift-off*.
- Ascending (34 to 73%) – Center of gravity continues to ascend, upward acceleration changes to deceleration mid phase; end of phase marked by extension of knee within 2% of quiet standing.
- Stabilization (73 to 100%) – Tuning of balance until a stable posture is achieved; end of phase marked by vertical ground force settling within 1% of quiet standing.

Although several other phase descriptions have been offered (e.g. Schenkman et al., 1990), this thesis uses the one detailed above, which is best suited for analysis of FES assisted STS. Nuzik et al. (1986) and Rodosky et al. (1989) both divided STS into two phases – flexion and extension – however they differed on which event defines the division of those phases. Pai and Rogers (1990) defined four phases, simply numbered I through IV, with events based on vertical and horizontal momentum maxima and lift-off. Yet another phase description was offered by Millington et al. (1992), a three-phase system marked by events based on knee and trunk angles.

In all phase descriptions, STS starts with the first discernable movement. This is typically characterized by flexion of the trunk. Three of the five studies recognized lift-off (sometimes by a different name, such as "seat off"). The phases identified in the Kralj and Schenkman systems are similar. They both identify momentum generating activity before lift-off and upward acceleration after lift-off. Schenkman's wording goes further than Kralj's to suggest that the momentum generated prior to lift-off is useful in the latter phases, a theory that remains unproven.

1.5.2 Patterns and strategies

Hypothesis H3 suggests a strategy for paraplegic STS that is not commonly used by paraplegics. The justification for it comes from the STS literature, which is summarized here.

STS has three basic objectives: (1) unload the seat, (2) move the whole body center of mass over the new base of support (the feet), and (3) extend the knees, hips and trunk such that quiet standing can be maintained with minimal muscle effort. There are many different ways to achieve these objectives. For one, it can be done with or without the use of arms. Studies of able-bodied STS typically reveal that the objectives listed above are achieved in numerical order via a smooth pattern of muscle contractions, resulting in standard trajectories of the joints and center of mass (e.g. Kelley et al., 1976, Nuzik et al., 1986, Kralj et al., 1990, Millington et al., 1992). There are many patterns and trajectories that will achieve the objectives. Able-bodied subjects adapt their strategy to different conditions, e.g. chair height, or the need to rise quickly. However, some basic processes remain the same. Goulart and Valls-Solé (1999) hypothesized that the activation patterns of certain muscles remain more or less unchanged when different STS strategies are employed. They found that the lumbar paraspinals, quadriceps and hamstrings were activated in a pattern that was invariable and time locked to the instant of lift-off.

In disabled populations, normal strategies are often precluded by physical impairments; therefore, some alternate strategy must be adopted to compensate. For example, it has been reported that people with bilateral knee osteoarthritis start STS from a position of greater knee extension and ankle plantar flexion, use a smaller range of motion at the knee, use more hip extension moment, and perform STS slower than able-bodied people (Pai et al., 1994). This alternate strategy is likely the result of adaptive motor behavior designed to overcome the reduced strength of the knee extensors. Individuals who suffer from back pain (Hsieh and Pringle, 1994) and sensory/motor impairments (Alexander et al., 1991) have also been observed to use alternate STS strategies.

Initial body position is one factor that is commonly altered in disabled STS strategies. Several studies have investigated how STS is affected by variations in chair height (Ellis et al., 1984, Burdett et al., 1985, Wheeler et al., 1985, Hughes et al., 1996) and foot placement (Fleckenstein et al., 1988, Vander Linden et al., 1994, Shepherd and Koh, 1996, Khemlani et al., 1999). Other

factors that have been investigated are use of arms (Seedhom and Terayama, 1976, Ellis et al., 1984), speed of execution (Pai and Rogers, 1991) and normal versus maximum trunk flexion (Doorenbosch et al., 1994). "Ejector chairs" are commercially available for persons who have difficulty performing STS. In one particular design, a spring-loaded cushion pushes the subject's buttocks upward and forward several inches from the seat's original position (Munro et al., 1998).

1.5.3 FES assisted sit-to-stand

The reason why a better strategy for paraplegic STS is needed is because current methods are limited. This section briefly describes these limitations and some solutions that have been offered.

In paraplegia, motor impairment is so severe that radical STS strategies are required. Some subjects can perform the maneuver using just the strength of their arms (Riener and Fuhr, 1998, Bahrami et al., 2000). Others can do it with FES of the quadriceps muscles. Kralj and Bajd (1989) prescribe a strategy in which the paraplegic subject moves his buttocks to the edge of the seat and assumes a static posture with the ankles, knees and trunk almost fully flexed. This way, the center of mass is directly above the feet, and the subject can rise by pushing straight up. Even when FES is used, large vertical forces are carried in the arms, up to 30-45% of the total body weight (Dolan, 1997, Riener and Fuhr, 1998, Kuzelicki et al., 1999, Davoodi et al., 2001). This is very undesirable because the shoulder girdle is ill adapted for weight bearing, and many paraplegics already suffer from shoulder dysfunction (Goldstein et al., 1997, Lal, 1998).

Maximum knee extension moments from FES are estimated to be between 10 and 50 Nm per leg (Kralj and Bajd, 1989, Kagaya et al., 1995). Peak knee extension moments during able-bodied unassisted STS range from 80-220 Nm (both legs combined) (Kelley et al., 1976, Bajd et al., 1982, Burdett et al., 1985, Fleckenstein et al., 1988, Berger et al., 1989, Kralj and Bajd, 1989, Pai and Rogers, 1991, Schultz et al., 1992, Hutchinson et al., 1994, Shepherd and Gentile, 1994, Hughes et al., 1996, Kamnik et al., 1999). This suggests that a small number of paraplegics may have the FES knee extensor strength for unassisted

STS. Davoodi and Andrews (1997) supported this idea with a computer simulation study in which a 5-segment model with reduced knee extensor strength performed STS using a trunk momentum strategy. The model failed when trunk momentum was not developed prior to lift-off. This is compelling evidence in favor of the momentum transfer theory.

Stimulation of the hip extensors in addition to the knee extensors has been shown to reduce the vertical loads placed on the arms during FES STS (Wibowo et al., 1998). Also, closed loop control has had success in reducing the upper limb demands (Riener and Fuhr, 1998).

1.5.4 Sit-to-stand models

In this thesis, hypothesis H3 is addressed using a computer model. Biomechanical models of the human body are used to examine the dynamic relationship between kinematics (displacement, velocity and acceleration) and kinetics (forces, moments and inertia) during movement. Models are commonly employed to derive joint moments and muscle forces from recorded motion and force plate data. This approach is called *inverse dynamics*. Following the development of precise motion capture systems, inverse dynamics has seen widespread use in STS analysis (Kelley et al., 1976, Bajd et al., 1982, Burdett et al., 1985, Fleckenstein et al., 1988, Berger et al., 1989, Pai and Rogers, 1991, Schultz et al., 1992, Shepherd and Gentile, 1994, Hutchinson et al., 1994, Kagaya et al., 1995, Hughes et al., 1996, Munro et al., 1998, Kamnik et al., 1999, Riener et al., 1999)

The other approach is *forward dynamics*, or *direct dynamics*, in which muscle forces or joint moments are specified and the resulting kinematics are computed. Forward dynamics models are often used in the development of FES STS controllers and STS strategies for FES users (Khang and Zajac, 1989, Mulder et al., 1992, Donaldson and Yu, 1996, Veltink et al., 1997, Davoodi and Andrews, 1998, Kagaya et al., 1998, Riener and Fuhr, 1998, Bahrami et al., 1999, Davoodi and Andrews, 1999). Figure 1-9 illustrates a general scheme by which biomechanical models are employed. See section 1.6.5 below for an extended review of forward dynamics techniques.

The majority of biomechanical STS models are 2-dimensional representing symmetrical motion in the sagittal plane. Lundin et al. (1995) addressed the issue of bilateral symmetry, and concluded that the assumption of symmetry was invalid in terms of ground reaction force and joint moments. However, most studies continue to assume bilateral symmetry.

1.6 Paraplegic gait (H4 through H7)

Improving paraplegic gait is the ultimate objective of this thesis. A portion of the paraplegic population can perform sit-to-stand with the aid of FES and/or mechanical braces. Some can also walk. So far, paraplegic gait is crude. At best, it is approximately one tenth as fast as normal gait (Brissot et al., 2000) and requires heavy use of handrails, walking frames, or crutches. Paraplegic gait puts a very large physical and cognitive load on the individual. Due to muscle fatigue, it can rarely be performed for more than 10 minutes at a time.

Guttman described three basic forms of paraplegic gait (Guttman, 1976):

1. Four-point gait. Using handrails, a walking frame or a pair of crutches, the subject bears his weight in his arms and one leg while swinging the other leg forward by tilting the pelvis. After the foot lands, the corresponding hand or crutch (or the entire frame) is advanced. Then the other leg is swung through.
2. Swing-to gait. Using handrails, a walking frame or a pair of crutches, the subject lifts his entire weight with his arms and drags or hops his feet forward a short distance. The feet always remain behind the hands or crutches.
3. Swing-through gait. Using handrails or a pair of crutches, the subject lifts his entire weight with his arms and swings his legs forward such that the feet return to the ground in front of the hands or crutches. This mode of gait is less stable than the others, due to the two-point base of support during swing. Abdominal and hip spasms can cause falls.

All of the above techniques involve passive legs. Required is some means of keeping the knees fully extended such that the legs can bear weight, i.e. mechanical braces or FES. Advances in FES and orthotics technology have improved four-point gait considerably, making it more energy efficient and cosmetic (closer to normal biped gait).

1.6.1 Normal gait

For insight into better strategies for paraplegic gait, we first look to normal gait. The gait of able-bodied people is fast, efficient and graceful compared to paraplegic gait. *Normal gait* is a highly controlled, coordinated, repetitive series of limb movements whose function is to advance the body safely from place to place with a minimum expenditure of energy (Gage et al., 1995). Although most paraplegic gait systems do not aspire to fully restore it, normal gait serves as a prevailing ideal from which biomechanical insight can be gained.

The literature on normal gait is extensive. What follows is a brief outline of basic definitions and principles.

Figure 1-10 depicts a phase representation of normal reciprocal gait. In relation to a specific leg, the gait cycle is divided into two phases (approximate durations with respect to the entire gait cycle are given in parentheses): swing (40%) and stance (60%). In relation to both legs, the cycle consists of four phases: left swing (40%), double support (10%), right swing (40%) and double support again (10%). The cycle begins with the left toe leaving the ground, and the events that mark phase transitions are respectively: left heel-strike, right toe-off, right heel strike.

Perry (1992) pointed out four priorities of normal gait: (1) stability of the stance leg throughout stance phase, (2) clearance of the foot during swing phase, (3) appropriate positioning and extension of the swing leg at the end of swing phase, and (4) adequate step length. Gage et al. (1995) added energy conservation to this list. Normal walking has an average speed of about 1.5 m/s. The typical energy expended is 10.5 kJ per minute (compare to that of quiet standing: 6.3 kJ) (Gage et al., 1995). Deviations from normal gait increase the energy cost, e.g. fast walking (60% increase).

1.6.2 Gait orthoses

Before we can suggest improvements to paraplegic gait, we must review methods that have been tried before. The first attempts to restore gait after paraplegia involved mechanical braces. Figure 1-11 illustrates some popular designs that have seen clinical and home use. The classical long leg braces (LLB),

depicted in Figure 1-11(a), are also known as knee-ankle-foot orthoses (KAFO), because they restrict the motion of the knee and ankle joints. For decades, these heavy, cumbersome devices were the only possibility for people with paraplegia to stand and walk. Because the legs are locked in full extension with no actuation in LLB, gait is slow and awkward. The user must rely heavily on crutches and upper body strength to unload and swing his legs in a four-point gait pattern.

Later, a new class of braces called *reciprocating gait orthoses* was created by linking a pair of KAFOs to a trunk brace via joints located lateral to the hips. Reciprocating gait orthoses, sometimes called hip-knee-ankle-foot orthoses (HKAFOs), make possible faster and more efficient four-point gait. One of the most well-known and widely used members of this class is the Louisiana State University Reciprocating Gait Orthosis (LSU-RGO), shown in Figure 1-11(c) (Douglas et al., 1983). The LSU-RGO included a dual cable linkage between the hip joints, such that when one hip flexes, the other hip extends, thus reducing the brace to a single degree of freedom. After shifting his weight off one leg, the user can create hip flexion to advance it by exaggerating lordosis, pushing back on the trunk segment of the brace. One study concluded that experienced RGO users do not load the cables to create significant hip flexion moments (Dall et al., 1999), while another concluded that removal of the cable linkage was undesirable (Ijzerman et al., 1997).

Most reciprocating gait orthoses are extremely difficult to don and doff, partially due to the cumbersome trunk components. The medially linked knee-ankle-foot orthosis (MLKAFO), shown in Figure 1-11(b), is an alternative that does away with trunk components altogether by linking the KAFOs by a single uniaxial joint located in the crotch. The lack of above-waist components makes it far less bulky and easier to don and doff than reciprocating gait orthoses (Kirtley, 1992), however trunk instability typically makes it impractical for individuals with spinal cord lesions above the low thoracic region. The MLKAFO facilitates easier sit-to-stand transfers than reciprocating gait orthoses, however gait is slower and often requires assistance from a third party (Harvey et al. 1997).

None of these gait orthoses are considered alternatives to the wheelchair. As auxiliary devices, they can augment a wheelchair user's mobility in places where the wheelchair is insufficient, for example around high shelves and countertops. Or, they can act as exercise devices. Most follow-up studies have found that, given any kind of gait orthosis, a majority of paraplegics use them only for exercise purposes, or abandon them altogether (Franceschini et al., 1997). Still, there is a small population of people who use them on a daily basis for functional locomotion both in and out of the home.

1.6.3 FES assisted gait

Hypotheses H4, H6 and H7 concern FES assisted gait. For many paraplegics (mainly thoracic-level without major spasticity or contractures), gait without braces can be achieved using FES. The earliest systems merely kept the knees in full extension by continuously stimulating the quadriceps. This enabled patients to perform swing-to, swing-through or four-point gait as though they were wearing LLBs.

Kralj and Bajd (1989) improved paraplegic gait with a four channel transcutaneous FES system that stimulated the knee extensors and flexor withdrawal reflex of each leg to produce reciprocal gait. Stimulated via the common peroneal nerve, the flexor withdrawal reflex causes simultaneous hip flexion, knee flexion and ankle dorsiflexion in the affected leg, thus providing foot clearance for swing phase. During this time, stance phase is maintained in the contralateral leg by quadriceps stimulation. Open loop algorithms tuned to practical walking frequencies controlled the stimulation. In later versions, thumb switches were mounted on the handgrips of the walking frame allowing the user control over step frequency.

The main drawbacks of Kralj and Bajd's system are (Karcnik et al., 1996): (1) low walking speed, approximately 0.15 m/s, which is about 10% of normal walking, (2) high energy cost, about 14 J/kg.m compared to 3.3 J/kg.m for normal walking, (3) Insufficient propulsive forces in the direction of walking, about 40 N for paraplegia, which is one fifth of healthy subjects, and (4) postural stability is maintained by large arm forces. Also, there is significant habituation of the flexor

withdrawal reflex after prolonged electrical stimulation (Malezic and Hesse, 1995).

Still, Kralj and Bajd's system remains one of the most popular neural prostheses today due to its simplicity and ease of implementation. Operating in four-channel mode, Graupe and Kohn's (1994) Parastep system is very similar to the Kralj & Bajd method. The Parastep has a six-channel option that stimulates the gluteal and erector spinae muscles as well. This is believed to improve trunk stability during gait. Still other systems include stimulation of the ankle dorsiflexors to augment ground clearance during swing phase (Greene and Granat, 2000).

These systems are generally easy to don and doff compared to mechanical orthoses, because they simply involve sticking 8 to 12 electrodes on the skin. Percutaneous systems are more convenient, once installed, because they can be in place for months at a time (Moynahan et al., 1996). Fully implanted systems are the most convenient, as they remain installed for years (Davis et al., 1999). However, an arduous surgical procedure is required to install them (Davis et al., 2001).

In general, the energy cost of FES four-point gait is high and on par with LLB swing-to gait (Marsolais et al., 1988). It has been shown to improve walking speeds for incomplete SCI (Ladouceur and Barbeau, 2000), and theories are evolving to further improve speed (Babic et al., 2001).

The therapeutic benefits of FES gait are far greater than walking with LLBs alone (Gallien et al., 1995), and users generally prefer FES (Bonaroti et al., 1999).

1.6.4 Hybrid orthoses

Hypotheses H4, H5 and H6 concern a device that uses both FES and braces. Systems that combine FES with mechanical braces are called *hybrid orthoses*. They address the problems of fatigue associated with FES and the lack of actuation associated with passive mechanical braces. Many types of hybrid orthoses exist, from largely braced systems with one or two muscle groups activated by FES to largely FES systems with minimal bracing.

Ankle-foot orthoses (AFO) are simple braces that restrict ankle articulation. They are light, easy to don and doff, and small enough to be worn under pant legs and inside the shoes. AFOs prevent plantar flexion during swing phase, and promote extension of the stance leg during the latter part of stance phase when the ground reaction force vector passes anterior to the knee joint (Andrews et al., 1988).

The first hybrid orthosis to receive FDA approval is the Parastep system, which consists of a pair of AFOs and 4 or 6 channels of FES (Graupe and Kohn, 1994). The Parastep system has enabled many people with thoracic-level spinal cord injuries to stand and walk for short distances (Klose et al., 1997). Brissot et al. (2000) reported that the Parastep system is limited as a functional device because of its modest performance and high physiological cost. However, they could not deny its usefulness as an exercise device.

Kagaya et al. (1996) developed a hybrid orthosis with a mechanical knee lock that would maintain extension in the stance leg instead of relying on electrical stimulation of the knee extensors. Thus, muscle fatigue was reduced.

RGO gait has been improved by stimulation of the hip extensors during stance phase (Stallard, 1998, Ferguson et al., 1999). Solomonow et al. (1997) and Merati et al. (2000) unlocked the knees of the RGO and used FES of the quadriceps and hamstrings to control the knee. This approach was found to improve locomotion compared to gait in the RGO without FES, but the energy expenditure was no different.

1.6.5 Gait models

Hypotheses H4, H5 and H6 are addressed in this thesis using computer models of gait. When designing a controller for FES gait, many test trials are necessary to determine feasibility and to tune parameters. The most direct way to test an FES controller is on a paralyzed subject, in a clinical setting. However, clinical trials require a great deal of time and effort to arrange. Support personnel must be scheduled, as well as the test subject. The lab must be prepared with adequate safety measures, fully functional equipment, backup hardware and contingency plans. Before any experiment takes place, ethical approval must be

obtained. Furthermore, only a limited number of trials can be performed in a single lab session.

A great deal of time and money can be saved by first testing new control strategies on computer simulated models. Clinical testing is still a necessary step in controller development, but much of the preliminary testing can be performed on biomechanical models, or *virtual patients*, that do not require safety precautions or ethical clearance.

As discussed in section 1.5.4 above, biomechanical models describe the relationship between kinematics and kinetics. Models of gait have been useful for both inverse dynamics (trajectory matching) and forward dynamics (simulations). As with any model, a gait model must strike a balance between complexity and accuracy. A very complex model may provide extremely precise output that may or may not be accurate. The more complex a model, the more parameters are required to describe it. A model can only be as accurate as the estimation of its parameters. Also, complex models make great demands on computers. Models that were once considered too complex for simulation have been made practical by improvements in computer memory and processor speed. There are still practical limitations, however. In some applications, real-time simulations are required – that is, simulations that calculate time steps as quickly as the steps occur in real life. Even with today's computer power, only fairly simple models can function in real-time.

1.6.5.1 Model computation

Equations of motion for any n degree of freedom mechanical system described by a vector of angular displacements, $\phi = \{\phi_1, \phi_2, \ldots, \phi_n\}$, can be expressed in the following form:

$$I\ddot{\phi} = G\dot{\phi}^2 + g + M \qquad (1\text{-}1)$$

where I is the *inertia matrix* representing the inertial properties of the system, $\ddot{\phi} = \{\ddot{\phi}_1, \ddot{\phi}_2, \ldots, \ddot{\phi}_n\}$, G is the *gyroscopic matrix* representing the Coriolis components, $\dot{\phi}^2 = \{\dot{\phi}_1^2, \dot{\phi}_2^2, \ldots, \dot{\phi}_n^2\}$, g is the *gravitational vector* representing the effects created by gravity, and M is the *internal moment vector* representing all of

the internal joint moments. I, G and g all typically vary nonlinearly with respect to ϕ. M is typically dependent on time and ϕ. The result is a very nonlinear system of second order differential equations.

Citing the difficulty of deriving equations of motion by hand, Pandy and Berme (1988) recommended a method for automatically deriving equations based on Newtonian mechanics. Today, several software packages are commercially available that provide quick and easy ways to simulate models of almost limitless complexity. Working Model 3D (1997) and SD/FAST are two examples. Both use Kane's method to derive equations of motion (Kane and Levinson, 1985). The software derives equations of motion and solves them as a system of ordinary differential equations using numerical integration techniques.

There are several methods for numerical solution of ordinary differential equations. The simplest is Euler's method, which is easy to implement and useful for quick estimates. Its accuracy is limited, however, because truncation errors occur at every time step. Reducing the step size will reduce the truncation error, however doing so inversely increases the number of operations needed, and the round-off errors of floating point numbers can accumulate significantly.

Runge-Kutta methods are convenient and widely used. They are designed to reduce truncation error, and they range in order from 2 to 5 (Euler's method is considered a first-order Runge-Kutta method). As order increases, truncation error decreases, but the number of computations necessary at each step increases. In choosing an appropriate order, one must consider the trade-offs between accuracy and computation time. Runge-Kutta methods can be made more efficient by implementing a variable step-size that responds to an estimate of the truncation error. The effect is intelligent integration that speeds through regions where the changes are small and slows down where the changes are great. Other numerical integration techniques, such as the Adams formulas, require initial conditions at multiple time steps, which are generally not available in forward dynamics applications but can be estimated using Runge-Kutta as the first step.

MATLAB offers a suite of advanced numerical integrators. Among them are three general modules: a low order Runge-Kutta algorithm (ODE23), a high

order Runge-Kutta algorithm (ODE45), and an Adams-Bashforth-Moulton algorithm (ODE113). These algorithms vary order based on error estimation to minimize computation time without compromising accuracy. They can use fixed or variable step sizes. For the sake of comparison, the various methods were used to compute the motion of a simple, linearly damped pendulum. The equation of motion is given as

$$\ddot{\phi} + 2\gamma\dot{\phi} + \beta^2 \sin\phi = 0 \qquad (1\text{-}2)$$

where ϕ is the angle of the pendulum. γ and β are variables representing the damping and natural frequency. $\gamma = 0.5$ rad/s and $\beta = 6$ rad/s were chosen to roughly represent a human leg. Initial conditions were arbitrarily chosen to be $\phi(0) = 0.2$ rad and $\dot{\phi}(0) = 0$ rad/s.

Equation 1-2 can be solved easily when it is assumed that the angle is always small enough that $\sin\phi \cong \phi$. When this is the case, the solution becomes

$$\phi(t) = 0.2 * e^{-\gamma t} \cos\sqrt{\beta^2 - \gamma^2}\, t \qquad (1\text{-}3)$$

For large angles, Equation 1-2 remains non-linear, and there are analytical solutions, however they are more complex than is necessary for the purpose of validation. Therefore, the non-linear case was omitted from the present analysis.

The linear pendulum was solved over a range of five seconds using various solution methods. The results are summarized in Table 1-2. Error was calculated by summing the squares of the difference between the numerical approximation and the analytical solution at 50 evenly spaced points in time.

Table 1-2; Numerical solutions of linear pendulum

Method	Step size (ms)	Total error	# of floating point operations
Euler	10	0.1972	7500
Euler	1.0	0.0145	75000
Euler	0.1	0.0138	750000
ODE23	10	0.0139	61951
ODE23	variable	0.0139	19391
ODE45	10	0.0136	98721
ODE45	variable	0.0137	23574
ODE113	10	0.0138	116869
ODE113	variable	0.0141	23892

The methods shown in Table 1-2 estimated the pendulum's motion with excellent accuracy, except for Euler's method with 10 ms time step. The methods differed in the number of floating point operations; methods using variable step sizes were significantly faster. In this thesis, ODE45 with variable step size was used to solve all forward dynamics problems, because it quickly produces highly accurate solutions to equations of motion of human scale.

1.6.5.2 Forward dynamics

The forward dynamics approach to modeling tends to be very sensitive. Schutte and Risher (1994) expressed the following admonishment, "small changes in the inputs can lead to initially small but exponentially growing changes in the kinematics, and very large changes in the objective function. (The difference between inputs that produce a coordinated motion resembling walking and inputs that produce a wildly uncoordinated movement can be very small)."

Walking models reported in the literature range in complexity from one (Bajd et al., 1993) to over 20 degrees of freedom (Schutte and Risher, 1994). Although gait motion is 3-dimensional, some models only concern themselves with motion in the sagittal plane. One of the most complicating aspects of gait is that it involves open chain dynamics during swing phase, and closed chain dynamics during double support phase. Therefore, models that examine the whole gait cycle must be able to switch from one form to the other, and account for the collision during heel-strike. Some researchers avoid these complications by looking solely at swing phase, which they consider the critical phase due to its static instability.

Mochon and McMahon (1980) developed one of the earliest swing phase models for what they coined *ballistic walking*. The term refers to reciprocal gait in which the muscles of the swing leg are completely inactive. Today, the term most commonly used is *passive dynamic gait*, or simply *passive gait* (more on this in section 1.6.8). Shown in Figure 1-12(a) is the original ballistic walking model, a three-segment compound pendulum. The stance leg was assumed to be rigid while the swing leg was jointed at the knee. The upper body mass was lumped at the hip. All joints were modeled as simple frictionless pin joints, except the knee,

which would suddenly lock when it reached full extension. Mochon and McMahon derived the equations of motion using Lagrangian mechanics. The Lagrange method is a tidy alternative to the more rigorous Newton-Euler approach. However, since it involves differentiation, the Lagrange method is only best suited to models with easily differentiable elements.

Onyshko and Winter (1980) also derived a mathematical model of human gait using Lagrangian mechanics. Their model, shown in 1-12(b), was 2-dimensional with seven segments. It covered both the swing and double support phases of the gait cycle. Initial conditions at the start of swing phase were taken from recorded gait trials. Then an open loop pattern of joint moments that produced a successful gait cycle was found through trial-and-error.

Addressing a lack of biomechanical understanding of paraplegic gait in an RGO, Tashman et al. (1995) developed a 3-dimensional 4-segment model with a total of eight degrees of freedom, shown in Figure 1-12(d). Unlike the other models discussed thus far, Tashman's model included external forces on the shoulders via arms and crutches. Their simulations revealed that upper body forces during swing phase could be reduced substantially by producing a ballistic swing.

Yamaguchi and Zajac (1990) modeled the walking human as seven segments in 3-dimensions with eight degrees-of-freedom, shown in Figure 1-12(c), deriving equations of motion using Kane's method. Their study sought optimal open loop FES control schemes by minimizing a weighted cost function. They found, amongst other things, that an ankle-foot orthosis was "especially useful, as it helped to stabilize the stance leg and simplified the task of controlling the ankle during swing."

1.6.6 Muscle models

Some of the biomechanical models used in this thesis include muscles. *Muscle model* is the term generally used to refer to a model of the neuromuscular system that translates a stimulation signal into a generated muscle force. Often in FES controller design, it is more meaningful to input nerve activation or FES stimulation signals instead of muscle forces/joint moments (Bobet, 1998). Figure

1-13 illustrates a modeling scheme that includes both muscle contraction dynamics and the rigid body mechanics of the walking person.

In the context of dynamic simulations and FES controllers, there are two main types of muscle models: Hill-based and systems based. The first type is named after A. V. Hill (1938) who devised a model of isolated muscle that consisted of basic mechanical elements connected in series and parallel (Winters, 1990). In Hill-based models, there is always one active element, called the *contractile element*, and the remaining elements are passive springs or dashpots. The contractile element is characterized by two fundamental relationships: force-length and force-velocity. Each of these is modulated by activation input. Without the contractile element, a Hill-type model is a passive viscoelastic system. Many musculoskeletal motion studies have employed Hill-type muscle models (e.g., Audu and Davy, 1985, Yamaguchi and Zajac, 1990, Piazza and Delp, 1996, Munih and Kralj, 1997). More recent studies offer simplified Hill-type models that describe forces produced by muscles undergoing FES based on stimulus frequency (Dorgan and O'Malley, 1998, Watanabe et al., 1999, Eom et al., 2000). Such models are ideal for simulations of neural prostheses. Some Hill-based muscle models even address the issue of fatigue and recovery during FES (Giat et al., 1996).

In systems based muscle models, an isolated muscle, or a group of muscles spanning a joint, is treated like a black box. The properties of the black box are determined by formal identification techniques of systems engineering. (Incidentally, this approach is commonly used to identify the force-length-velocity relationship of the contractile element in Hill-based models.) Muscles are complex, nonlinear, multiple-input systems, which pose a very challenging identification problem (Durfee, 1992). One way to simplify the problem is to assume linearity. Ferrarin et al. (1995) devised a fairly accurate single pole transfer function model for FES-activated knee extensors. The linear assumption, however, is usually considered an oversimplification. Non-linear formulations are the subject of some research related to neural prosthesis design (Crago et al.,

1990, Flaherty et al., 1995), but Hill-based models remain the more popular representation.

In this thesis, all muscles were modeled using a common Hill-type system. It is illustrated in Figure 1-14. This is a popular model that appears in many FES studies (e.g. Watanabe et al., 1999). The series element (SE) consists of a linear spring, and the parallel element (PE) consists of a linear spring and linear dashpot in parallel. The force output of the contractile element (CE) is a non-linear function of its length and velocity as well as the frequency and intensity of the stimulus provided. It is described by the following equation:

$$F_{CE} = \bar{F}k(l_{CE})g(\dot{l}_{CE})a(s) \qquad (1\text{-}2)$$

where $\bar{F}$ is the maximum isometric force developed by electrical stimulation, $k(l_{CE})$ is the force-length relationship of the CE, $g(\dot{l}_{CE})$ is the force-velocity relationship of the CE, and $a(s)$ is the activation/recruitment level determined by stimulus s. The computational scheme is illustrated in Figure 1-15.

The force-length and force-velocity relationships were derived via the method described by Epstein and Herzog (1998). Eccentric contractions were modeled according to Krylow and Sandercock (1997). The activation dynamics were based on a normalization function with first-order delay. Parameters for the specific models were chosen from various sources of data, which are indicated in the relevant chapters.

1.6.7 Biped robots

The issues of passive gait and motor control during gait, come up frequently in the biomechanics literature and also in the robotics literature. Biped gait has long been a subject of interest in robotics research. Legged robots are widely regarded as best suited for various types of terrain. Robots with four or more legs achieve gait easily due to the inherent stability of a 3-(or more)-point base of support, but they may not be ideal in some human working environments. Biped robots, sometimes termed *dynamic walking machines* because they do not maintain static equilibrium throughout their motion, tend to travel faster and may be able to better negotiate some environments.

Today, biped robots are being developed in over 30 major research centers in 8 different countries, with Japan and the United States leading. Anthropometric robots – that is, robots scaled to human body mass and dimension – are all the rage. In terms of control and mechanics, designers of anthropometric robots face many of the same problems as bioengineers in the field of gait restoration (lower limb prosthetics and orthotics). There is a great deal of overlap in the two fields. Robotics researchers draw upon the biomechanics literature, while biomechanics researchers draw upon the robotics literature.

McGeer (1990) was one of the first to unite the two fields. Using both computer simulations and physical models, he demonstrated that some anthropomorphic mechanisms can exhibit stable, human-like walking down shallow slopes with no actuation – purely passive gait. McGeer achieved passive gait with both stiff legged robots (sometimes called *compass robots* because they resemble a drawing compass) and robots with flexible knee joints. Of course, the compass robots had difficulty achieving foot clearance.

Garcia et al. (1998) studied McGeer's compass robot in more detail, describing it as "the simplest walking model." They found perpetual gait cycles for walking down various gentle slopes. Goswami et al. (1998) also studied the compass robot walking passively down a slope, focusing on chaotic behavior and energy loss due to ground impact. They found that, "additional dissipative elements in the robot joint result in a significant improvement in the stability and the versatility of the gait, and provide a rich repertoire for simple control laws." In a similar vein, Reisinger and Moskowitz (1999) addressed the energy loss due to ground collision for stiff-legged gait on level surfaces. However, they used a 3-segment model with a trunk segment instead of the simple compass robot. The energy could be recovered, they reported, by a brief, impulsive hip moment of sufficient magnitude.

1.6.8 Passive gait

Passive gait is the subject of hypotheses H4 and H5. Mochon and McMahon (1980), McGeer (1990), Garcia et al. (1998) and Goswami et al. (1998) all demonstrated that passive gait is possible in anthropometric biped robots.

These findings suggest that the geometric and inertial properties of the human body are ideally suited for biped gait, since passive dynamics are inherent. Furthermore, Eng et al. (1997) provided evidence that the nervous system utilizes passive dynamics to control the swing leg, as one way to minimize energy costs. In an excellent review of biped robots, Sardain et al. (1998) state, "it is widely known that the existence of natural gaits is closely linked to the intrinsic dynamic characteristics of the mechanical structure of the biped robot." Sardain's group analyzed both the lateral stability and sagittal plane progression of several biped robots.

Lateral stability is a major issue during passive biped gait. During the single support phase, the body is unstable in the frontal plane much like an inverted pendulum. Kuo (1999) studied lateral instability of the compass robot, and proposed five possible methods of stabilizing the lateral "roll" motion. The one method Kuo studied in depth was variable step width accomplished by hip abduction/adduction. Active control of the step width was sufficient to stabilize the lateral motion. Later, Bauby and Kuo (2000) confirmed that able-bodied humans achieve lateral stability during normal gait through active control, but they did not identify a specific mechanism.

1.6.9 "Spinal engine"

Hypothesis H6 concerns the "spinal engine." Among Kuo's proposed solutions to the lateral stability problem of compass robots was a torso that sits atop the hip joints and rocks laterally like a metronome, thus transferring upper body momentum to the legs via the spine. In his book *The Spinal Engine*, Gracovetsky (1988) promoted the theory that the oscillating trunk drives the pelvis during gait. Prior to Gracovetsky, it was widely believed that trunk oscillation during gait was merely a reaction to ground impact and lower body activity.

Nichols and Witt (1974) were possibly the first to model the rocking motion of a stiff-legged walking model with a laterally oscillating torso. They found a muscle pattern that resulted in steady gait with a step frequency similar to natural gait, but a walking speed of only about 20% of natural gait. No

conclusions about the stability of the system could be made, since the sensitivity to perturbation was not examined. Interestingly, Nichols and Witt started their model from rest, which is an unconventional approach today.

Li et al. (1993) built a roughly anthropometric robot with a heavy trunk segment. They studied stabilizing effect of the rocking trunk during biped gait by using a "Zero Moment Point" (ZMP) stability criterion. The ZMP is a point projected on the ground representing the centroid of all the dynamic forces of the model. When the ground reaction force coincided with the ZMP, the robot was considered to be stable. They programmed an adaptive back-propagation trunk controller to keep the ZMP within the robot's ground support polygon using trunk motion.

1.7 Anthropometric data

Multi-segment mechanical models of the human body comprise a large portion of this thesis. Therefore, a few words regarding the body segment parameters are required. How much does a thigh weigh? Where is its center of mass? What is its moment of inertia? These types of questions are not easily answered, yet every model requires specific answers.

It is easy to directly measure the length of a body segment. However, it is impossible to directly measure its mass or moment of inertia, or to locate its center of mass while it is still attached to the rest of the body. Dempster (1955) solved this problem by dissecting a small population of cadavers. He devised scaling factors by which lengths and masses and the location of center of mass for individual segments could be determined given the subject's total height and weight. Dempster's scaling factors are accurate within 4% 19 times out of 20. Chandler et al. (1975) conducted cadaver studies similar to Dempster, and developed even more accurate scaling methods based on length and circumference measurements of the individual segments in addition to body mass. The cadaver studies are old, but fairly accurate. More advanced techniques of body segment parameter identification include radiation scanning and geometric modeling.

In theoretical modeling studies, body parameters for a typical individual are usually used. But what is a "typical" body type? Anthropometric

measurements (e.g. height and weight) of large samples of people have been collected in many studies. One of the most comprehensive data sets that is publicly available comes from NASA (1978). Several hundred members of the U.S. Air Force and their families were measured. The height and weight distributions of men and women can be approximated from this data, as well as the variance of individual segment dimensions. Private anthropometric data can be purchased from agencies whose clients are automotive companies and furniture designers with an interest in ergonomics, but they are expensive.

Anthropometric data on the SCI population is not as complete. It has been established that paraplegics with complete injuries weigh significantly less than able-bodied individuals and have a higher center of gravity (Duval-Beaupere and Robain, 1991). This is due to atrophy of the lower extremities and abdominal obesity due to sedentary lifestyles.

1.8 Restatement of objectives

The primary goals of my research are:

1. To investigate the effect of SCI on the trunk and the concomitant effect on locomotion.
2. To understand the biomechanical role of the trunk when sitting, standing and walking with hybrid orthoses.
3. To establish biomechanical theories of various modes of paraplegic locomotion that can serve as a theoretical basis in improving the design of hybrid orthoses.
4. To propose better strategies for paraplegic locomotion.

1.8.1 Justification

There exist many devices, mechanical and electrical, that are designed to assist paraplegic STS and gait. However, they are imperfect and not very popular among users. For these devices to become useful rehabilitation aids, improvements must be made to overcome the problems of excessive arm loads, rapid muscle fatigue, slow gait, etc.

I propose that solutions will be found by first establishing a better theoretical basis for paraplegic STS and gait. One area that needs to be thoroughly considered is the trunk. The effect of the paralyzed trunk on locomotion may

seem obvious, but is not completely understood. My first two objectives are to investigate this. Some researchers (e.g. Graupe and Kohn, 1994) have already reported that stimulation of the erector spinae improves gait somewhat.

Current methods of paraplegic STS are very hard on the shoulders. The strategy of throwing the trunk forward has not been adequately scrutinized. Using mechanical theory, I proposed some new ideas.

It is unclear whether or not the passive dynamics of the legs can be exploited during paraplegic gait. I hypothesize that it can, and it may result in significant energy savings. It has not been established if stiff-legged gait is better or worse than free-knee gait. I feel that this needs to be analyzed to contribute to the theoretical basis of hybrid orthoses.

Ultimately, I hope my contributions lead to a hybrid orthosis that is practical for regular use by people with SCI. I hope that it has both functional and therapeutic benefits.

1.9 References

Abbas J, Chizeck H. Feedback control of coronal plane hip angle in paraplegic subjects using functional neuromuscular stimulation, *IEEE Trans Biomed Eng*, 38(7):687-698, 1991.

Alexander NB, Schultz Ab, Warwick DN. Rising from a chair: effects of age and functional ability on performance biomechanics, *J Gerontol*, 46(3):M91-98, 1991.

Andrews BJ, Baxendale RH, Barnett R, Phillips GF, Yamazaki T, Paul JP, Freeman PA. Hybrid FES orthosis incorporating closed loop control and sensory feedback, *J Biomed Eng*, 10:189-195, 1988.

Andrews BJ, Kirkwood CA, Mowforth P, Baxendale RH. Control of hybrid FNS orthoses for paraplegic locomotion, *Proc Osaka Int Works FNS*, 19-21 Nov, Osaka, Japan, pp. 143-158, 1989.

Andrews BJ, Wheeler GD. Functional and therapeutic benefits of electrical stimulation after spinal cord injury, *Curr Opin Neurol*, 8:461-466, 1995.

Audu ML, Davy DT. The influence of muscle model complexity in musculoskeletal motion modeling, *J Biomech Eng*, 107:147-157, 1985.

Babic J, Karcnik T, Bajd T. Stability analysis of 4-point walking, *Gait & Posture*, 14(1):56-60, 2001.

Bahrami F, Erfani M, Jabedar P. Integrating the voluntary movements of paraplegic patients intact limbs in FES-controllers: part I, virtual patient, *Proc 4th Ann Conf Int FES Society*, Sendai, Japan, pp. 271-274, 1999.

Bahrami F, Riener R, Jabedar-Maralani P, Schmidt G. Biomechanical analysis of sit-to-stand transfer in healthy and paraplegic subjects, *Clin Biomech*, 15(2):123-133, 2000.

Bajd T, Kralj A, Turk R. Standing-up of a healthy subject and a paraplegic patient, *J Biomech*, 15(1):1-10, 1982.

Bajd T, Kralj A, Zefran M. Unstable states in four-point walking, *J Biomed Eng*, 15:159-162, 1993.

Bauby BE, Kuo AD. Active control of lateral balance in human walking, *J Biomech*, 33(11):1433-1440, 2000.

Belytschko T, Andriacchi T, Schultz A, Galante J. Analog studies of forces in the human spine: computational techniques, *J Biomech*, 6:361-372, 1973.

Benton LA, Baker LL, Bowman BR, Waters RL. *Functional electrical stimulation: a practical clinical guide*, Rancho Los Amigos, Downey, California, 1981.

Berger RA, Riley PO, Mann RW, Hodge WA. Total body dynamics in ascending stairs and rising from a chair following total knee arthroplasty, *Proc 34th Ann Meeting Orthop Res Society*, 13:542, 1988.

Berger RA, Schenkman ML, Riley PO, Hodge WA. Advantages of rising from a chair to quantitate human performance, *Proc 35th Ann Meeting Orthop Res Society*, 6-9 Feb, Las Vegas, Nevada, p.91, 1989.

Bergmark A. Stability of the lumbar spine: a study in mechanical engineering, *Acta Orthop Scand*, supplement 230, vol. 60, 1989.

Bernard P-L, Peruchon E, Micallef J-P, Hertog C, Rabischong P. Balance and stabilization capability of paraplegic wheelchair athletes, *J Rehabil Res Dev*, 31(4):287-296, 1994.

Bobet J. Can muscle models improve FES assisted walking after spinal cord injury, *J Electromygr Kinesiol*, 8:125-132, 1998.

Bonaroti D, Akers JM, Smith BT, Mulcahey MJ, Betz RR. Comparison of functional electrical stimulation to long leg braces for upright mobility for children with complete thoracic level spinal injuries, *Arch Phys Med Rehabil*, 80:1047-1053, 1999.

Breasted JH. *The Edwin Smith surgical papyrus*, University of Chicago press, Chicago, 1930.

Brissot R, Gallien P, Le Bot M-P, Beaubras A, Laisné D, Beillot J, Dassonville J. Clinical experience with functional electrical stimulation-assisted gait with Parastep in spinal cord-injured patients, *Spine*, 25(4):501-508, 2000.

Burdett RG, Habasevich R, Pisciotta J, Simon SR. Biomechanical comparison of rising from two types of chairs, *Phys Ther*, 65(8):1177-1183, 1985.

Carr JH, Shepherd RB, Nordholm L, Lynne D. Investigation of a new motor assessment scale for stroke patients, *Phys Ther*, 65(2):175-80, 1985.

Chandler RF, Clauser CE, McConville JP, Reynolds HM, Young JW. *Investigation of inertial properties of the human body, Final report, Apr. 1, 1972 – Dec. 1974*, AMRL-TR-74-137, Aerospace Medical Research Laboratories, Wright-Patterson Air Force Base, Dayton, Ohio, 1975.

Chiang J, Potvin JR. The in vivo dynamic response of the human spine to rapid lateral bend perturbation, *Spine*, 26(13):1457-1464, 2001.

Chizeck HJ, Kobetic R, Marsolais EB, Abbas JJ, Donner IH, Simon E. Control of functional neuromuscular stimulation systems for standing and locomotion in paraplegics, *Proc IEEE*, 76(9):1155-1165, 1988.

Chizeck HJ, Lan N, Palmieri LS, Crago PE. Feedback control of electrically stimulated muscle using simultaneous pulse width and stimulus period modulation, *IEEE Trans Biomed Eng*, 38(12):1124-1134, 1991.

Chizeck HJ. Apadtive and nonlinear control methods for neural prostheses. In: Stein R and Peckham H (eds) *Neural Prostheses: Replacing Motor Function After Disease or Disability*, pp. 298-328, Oxford University Press, 1992.

Cholewicki J, McGill SM. Mechanical stability of the in vivo lumbar spine: implications for injury and chronic low back pain, *Clin Biomech*, 11(1):1-15, 1996.

Cholewicki J, Panjabi MM, Khachatryan A. Stabilizing function of trunk flexor-extensor muscles around a neutral spine posture, *Spine*, 22(19):2207-2212, 1997.

Cholewicki J, Juluru K, McGill SM. Intra-abdominal pressure mechanism for stabilizing the lumbar spine, *J Biomech*, 32(1):13-17, 1999.

Crago PE, Lemay MA, Lui L. External control of limb movements involving environmental interactions. In: Winters JM and Woo SL (eds.) *Multiple Muscle Systems*, Springer-Verlag, New York, 1990.

Crane BT, Demer JL. Gaze stabilization during dynamic posturography in normal and vestibulopathic humans, *Exp Brain Res*, 122(2):235-246, 1998.

Cresswell AG, Oddsson L, Thorstensson A. The influence of sudden perturbationa on the trunk muscle activity and intra-abdominal pressure while standing, *Exp Brain Res*, 98:336-341, 1994.

Crisco JJ, Panjabi MM. The intersegmental and multisegmental muscles of the lumbar spine, *Spine*, 16(7):793-99, 1991.

Crisco JJ, Panjabi MM. Euler stability of the human ligamentous lumbar spine, part I: theory, *Clin Biomech*, 7:19-26, 1992.

Crosbie J, Herbert RD, Bridson JT. Intersegmental dynamics of standing from sitting, *Clin Biomech*, 12(4):227-235, 1997.

Dall PM, Müller B, Stallard I, Edwards J, Granat MH. The functional use of the reciprocal hip mechanism during gait for paraplegic patients walking in the Louisiana State University reciprocating gait orthosis, *Prosthet Orthot Int*, 23:152-162, 1999.

Davis R, Houdayer T, Andrews BJ, Barriskill A. Paraplegia: prolonged standing using closed-loop functional electrical stimulation and Andrews ankle-foot orthosis, *Artif Organs*, 23(5):418-420, 1999.

Davis JA, Triolo RJ, Uhlir JP, Bhadra N, Lissy DA, Nandurkar S, Marsolais EB. Surgical technique for installing an eight-channel neuroprosthesis for standing, *Clin Orthop & Rel Res*, 385:237-252, 2001.

Davoodi R, Andrews BJ. Standing up in paraplegia: a comparative study of fixed parameter controllers. *Proc 2nd Ann Conf Int FES Society*, Burnaby, Canada, pp. 93-94, 1997.

Davoodi R, Andrews BJ. Computer simulation of FES standing-up in paraplegia: a self-adaptive fuzzy controller with reinforcement learning, *IEEE Trans Rehabil Eng*, 6(2):1-11, 1998.

Davoodi R, Andrews BJ. Optimal control of FES assisted standing up in paraplegia using genetic algorithms, *Med Eng Phys*, 21:609-617, 1999.

Davoodi R, Kamnik R, Andrews BJ, Bajd T. Predicting the voluntary arm forces in FES-assisted standing up using neural networks, *Biological Cybernetics*, 85(2):133-143, 2001.

Dempster WT. Space requirements of the seated operator. *WADC Technical Report*, pp. 55-159, Wright-Patterson Air Force Base, 1955.

Dolan MJ. *Restoration and biomechanical evaluation of standing up and sitting down in paraplegics using functional electrical stimulation*. Dissertation, University of Glasgow, 1997.

Donaldson NN, Yu CH. FES standing: control by handle reactions of leg muscle stimulations (CHRELMS), *IEEE Trans Rehab Eng*, 4(4):280-284, 1996.

Doorenbosch CAM, Harlaar J, Roebroeck ME, Lankhorst GJ. Two strategies of transferring from sit-to-stand; the activation of monoarticular and biarticular muscles, *J Biomech*, 27(11):1299-1307, 1994.

Dorgan SJ, O'Malley MJ. A mathematical model for skeletal muscle activated by N-let pulse trains, *IEEE Trans Rehab Eng*, 6(3):286-299, 1998.

Douglas R, Larson PF, D'Ambrosia R, McCall RE. The LSU reciprocating gait orthoses, *Orthopedics*, 6:834-839, 1983.

Durfee WK, Hausdorff JM. Regulating knee joint position by combining electrical stimulation with a controllable friction brake, *Ann Biomed Eng*, 18:575-596, 1990.

Durfee WK. Muscle model identification in neural prosthesis systems. In: Stein R and Peckham H (eds) *Neural Prostheses: Replacing Motor Function After Disease or Disability*, Oxford University Press, 1992.

Durfee WK. Electrical stimulation for restoration of function, *Neurorehabilitation*, 12(1):53-62, 1999.

Duval-Beaupere G, Robain G. Upward displacement of the center of gravity in paraplegic patients, *Paraplegia*, 29:309-317, 1991.

Edwards J, Rithalia SVS. Powered hip orthosis. In: Pedotti A, Ferrarin M, Quintern J, Riener R (eds) *Neuroprosthetics: from Basic Research to Clinical Applications*, Springer-Verlag, Berlin, 1996.

Ellis MI, Seedhom BB, Wright V. Forces in the knee joint whilst rising from a seated position, *J Biomed Eng*, 6:113-120, 1984.

Eng JJ, Winter DA, Patla AE. Intralimb dynamics simplify reactive control strategies during locomotion, *J Biomech*, 30(6):581-588, 1997.

Eom G-M, Watanabe T, Futami R, Hoshimiya N, Handa Y. Computer-aided generation of stimulation data and model identification for functional electrical stimulation (FES) control of lower extremities, *Frontiers Med Biol Engng*, 10(3):213-231, 2000.

Epstein M, Herzog W. *Theoretical Models of Skeletal Muscle: Biological and Mathematical Considerations*, Wiley & Sons, pp. 23-57, 1998.

Fawcett, JW. Spinal cord repair: from experimental models to human application, *Spinal Cord*, 36(12):811-817, 1998.

Fergusen KA, Polando G, Kobetic R, Triolo RJ, Marsolais EB. Walking with a hybrid orthosis system, *Spinal Cord*, 37:800-804, 1999.

Ferrarin M, Iacuone P, Baglioni P, Mingrino A, Frigo C. Transfer function identification between muscle torque and stimulus in electrically activated knee muscles, *RESNA '95*, pp. 387-389, June 9-14, 1995.

Flaherty B, Robinson C, Agarwal G. Identification of nonlinear model of ankle joint dynamics during electrical stimulation of soleus, *Med & Biol Eng & Comput*, 33:430-439, 1995.

Fleckenstein SJ, Kirby RL, MacLeod DA. Effect of limited knee-flexion range on peak hip moments of force while transferring from sitting to standing, *J Biomech*, 21(11):915-918, 1988.

Franceschini M, Baratta S, Zampolini M, Loria D, Lotta S. Reciprocating gait ortheses: a multicenter study of their use by spinal cord injured patients, *Arch Phys Med Rehabil*, 78:582-586, 1997.

Franchignoni FP, Tesio L, Ricupero C, Martino MT. Trunk control test as an early predictor of stroke rehabilitation outcome, *Stroke*, 28:1382-1385, 1997.

Forssberg H, Hirschfeld H. Postural adjustments in sitting humans following external perturbations: muscle activity and kinematics, *Exp Brain Res*, 97:515-527, 1994.

Fugl-Meyer AR. Assessment of motor function in hemiplegic patients, In: Buerger & Tobis (eds) *Neurophysiologic aspects of rehabilitation medicine*, pp. 231-50, Springfield, Ill., Thomas, 1976.

Fujita K, Hoshimiya N, Handa Y, Ichie M. Feedback postural control of trunk in paraplegic standing via FES, *Proc 2nd Int FES Symposium*, 160-5, 1995.

Gage JR, Deluca PA, Renshaw TS. Gait analysis: principles and applications, *J Bone Joint Surg Am*, 77-A(10):1607-1623, 1995.

Gallien P, Brissot R, Eyssette M, Tell L, Barat M, Wiart L, Petit H. Restoration of gait by functional electrical stimulation for spinal cord injured patients, *Paraplegia*, 33:660-664, 1995.

Garcia M, Chatterjee A, Ruina A, Coleman M. The simplest walking model: stability, complexity, and scaling, *J Biomech Eng*, 120:281-288, 1998.

Gardner-Morse MG, Stokes IAF, Laible JP. Role of muscles in lumbar spine stability in maximum extension efforts, *J Orthop Res*, 13(5):802-808, 1995.

Gardner-Morse MG, Stokes IAF. Trunk stiffness increases with steady-state effort, *J Biomech*, 34(4):457-463, 2001.

Giat Y, Mazrahi J, Levy M. A model of fatigue and recovery in paraplegic's quadriceps muscle subjected to intermittent FES, *J Biomech Eng*, 118:357-366, 1996.

Gracovetsky S. *The Spinal Engine*, Springer-Verlag, Wien-New York, 1988.

Graupe D, Kohn KH, Basseas S, Maccarato E. Electromyographic control of functional electrical stimulation in selected patients, *Orthopedics*, 7:1134, 1984.

Graupe D, Kohn KH. *Functional electrical stimulation for ambulation by paraplegics*, Krieger Publishing Company, Malabar, Florida, 1994.

Graupe D, Kohn KH. Functional neuromuscular stimulator for short-distance ambulation by certain thoracic-level spinal-cord-injured paraplegics, *Surg Neurol*, 50:202-207, 1998.

Greene PJ, Granat MH. The effect of knee and ankle flexion on ground clearance in paraplegic gait, *Clin Biomech*, 15(7):536-540, 2000.

Goldstein B, Young J, Escobedo EM. Rotator cuff repairs in individuals with paraplegia, *Am J Phys Med Rehabil*, 76:316-322, 1997.

Goswami A, Thuilot B, Espiau B. A study of the passive gait of a compass-like biped robot: symmetry and chaos, *Int J Robot Res*, 17(12):1282-1301, 1998.

Goulart FR, Valls-Solé J. Patterned electromyographic activity in the sit-to-stand movement, *Clin Neurophysiol*, 110:1634-1640, 1999.

Guttmann, L. *Spinal Cord Injuries, Comprehensive Management and Research, 2nd Edition*. Blackwell Scientific Publications, Oxford, UK, 1976.

Hardcastle P, Bedbrook G, Curtis K. Long-term results of conservative and operative management in complete paraplegics with spinal cord injuries between T10 and L2 with respect to function, *Clin Orthop*, 224:88-96, 1987.

Harvey LA, Smith MB, Davis GM, Engel S. Functional outcomes attained by T9-T12 paraplegic patients with the walkabout and isocentric reciprocal gait orthoses, *Arch Phys Med Rehabil*, 78: 706-711, 1997.

Hill AV. The heat of shortening and the dynamic constants of muscle, *Proc Roy Soc*, B126:136-195, 1938. (cited by Winters, 1990)

Hsieh CJ, Pringle RK. Range of motion of the lumbar spine required for four activities of daily living, *J Manipulative Physiol Ther*, 17(6):353-358, 1994.

Hughes MA, Myers BS, Schenkman M. The role of strength in rising from a chair in the functionally impaired elderly, *J Biomech*, 1509-13, 1996.

Hutchinson EB, Riley PO, Krebs DE. A Dynamic analysis of the joint force and torques during rising from a chair, *IEEE Trans Rehab Eng*, 2:49-56, 1994.

Ijzerman MJ, Baardman G, Hermens HJ, Veltink PH, Boom HBK, Zilvold G. The influence of the reciprocal cable linkage in the advanced reciprocating gait orthosis on paraplegic gait performance, *Prosthet Orthot Int*, 21:52-61, 1997.

Jevsevar DS, Riley PO, Hodge WA, Krebs DE. Knee kinematics and kinetics during locomotor activities of daily living in subjects with knee arthroplasty and in healthy control subjects, *Phys Ther*, 73:229-239, 1993.

Kagaya H, Shimada Y, Ebata K, Sato M, Sato K, Yukawa T, Obinata G. Restoration and analysis of standing-up in complete paraplegia utilizing functional electrical stimulation, *Arch Phys Med Rehabil*, 76:876-881, 1995.

Kagaya H, Shimada Y, Sato K, Sato M, Iizuka K, Obinata G. An electrical knee lock system for functional electrical stimulation, *Arch Phys Med Rehabil*, 77:870-873, 1996.

Kagaya H, Sharma M, Kobetic R, Marsolais EB. Ankle, knee, and hip moments during standing with and without joint contractures, *Am J Phys Med Rehabil*, 77(1):49-54, 1998.

Kamnik R, Bajd T, Kralj A. Functional electrical stimulation and arm supported sit-to-stand transfer after paraplegia: a study of kinetic parameters, *Artificial Organs*, 23:413-417, 1999.

Kamper DG, Linden MA, Adams TC, Reger SI. Seated postural stability of wheelchair passengers in motor vehicles, *RESNA '96*, Salt Lake City, Utah, pp. 46-48, 1996.

Kane TR, Levinson DA. *Dynamics: Theory and Applications*, McGraw-Hill Publishing Company, 1985.

Kantrowitz A. In: *Electronic Physiological Aids: A Report of the Maimonides Hospital*, Brooklyn, New York, pp. 4-5, 1960.

Karenik T, Kralj A, Bajd T. Crutch assisted FES gait and upright stability assessment, In: Pedotti A, Ferrarin M, Quintern J, Riener R (eds) *Neuroprosthetics: from Basic Research to Clinical Applications*, Springer-Verlag, Berlin, 1996.

Keele KD. *Leonardo Da Vinci's Elements of the Science of Man*, Academic Press, New York, pp. 286-287, 1983.

Kelley DL, Dainis A, Wood GK. Mechanics and muscular dynamics of rising from a seated position, *Biomechanics VB*, Komi PV (ed.), Baltimore, Maryland, University Park Press, pp. 127-134, 1976.

Khang G, Zajac FE. Paraplegic standing controlled by functional neuromuscular stimulation, *IEEE Trans Biomed Eng*, 36(9):873-894, 1989.

Khemlani MM, Carr JH, Crosbie WJ. Muscle synergies and joint linkages in sit-to-stand under two initial foot positions, *Clin Biomech*, 14:236-246, 1999.

Kirtley C. Principles and practice of paraplegic locomotion: experience with the Walkabout Walking System,. *Aust Orthot Prosthet Magazine*, 7(2):4-7, 1992.

Klose KJ, Jacobs PL, Broton JG, Guest RS, Needham-Shropshire BM, Lebwohl N, Nash MS, Green BA. Evaluation of a training program for persons with SCI paraplegia using the Parastep 1 ambulation system: part 1, *Arch Phys Med Rehabil*, 78:789-793, 1997.

Kordylewski H, Graupe D. Control of neuromuscular stimulation for ambulation by complete paraplegics via artificial neural networks, *Neurol Res*, 23(5):472-481, 2001.

Krajcarski SR, Potvin JR, Chiang J. The in vivo dynamic response of the spine to perturbations causing rapid flexion: effects of pre-load and step input magnitude. *Clin Biomech*, 14(1):54-62, 1999.

Kralj A, Grobelnik S. Functional electrical stimulation – a new hope for paraplegic patients? *Bull Prosth Res*, 10-20:75-102, 1973.

Kralj A, Bajd T, Turk R, Krajnik J, Benko H. Gait restoration in paraplegic patients: a feasibility demonstration using multichannel surface electrode FES. *J Rehabil Res & Develop*, 20(1):3-20, 1983.

Kralj A, Bajd T. *Functional Electrical Stimulation: Standing and Walking after Spinal Cord Injury*. CRC Press Inc, Boca Raton, Florida, 1989.

Kralj A, Jaeger RJ, Munih M. Analysis of standing up and sitting down in humans: definitions and normative data presentation. *J Biomech*, 23(11):1123-1138, 1990.

Krylow AM, Sandercock TG. Dynamic force responses of muscle involving eccentric contraction, *J Biomech*, 30(1):27-33, 1997.

Kuzelicki J, Kamnik R, Bajd T, Andrews BJ. Dynamic modeling of paraplegic person's standing-up. *Proc the International Biomechatronics Workshop*, Enschede, The Netherlands, April 19-21, pp. 173-177, 1999.

Ladouceur M, Barbeau H. Functional electrical stimulation-assisted walking for persons with incomplete spinal injuries: longitudinal changes in maximal overground walking speed. *Scand J Rehab Med*, 32(1):28-36, 2000.

Lal S. Premature degenerative shoulder changes in spinal cord injury patients. *Spinal Cord*, 36:186-189, 1998.

Lavender SA, Marras WS. The effects of a temporal warning signal on the biomechanical preparations for sudden loading. *J Electromyogr Kinesiol*, 5(1):45-56, 1995.

Leipholz H. *Stability theory: an introduction to the stability of dynamic systems and rigid bodies*, New York: Academic Press, 1970.

Li Q, Takanishi A, Kato I. Learning control for a biped walking robot with a trunk. *Proc the 1993 IEEE/RSJ International Conference on Intelligent Robot Systems*, Yokohama, Japan, July 26-30, 1993.

Liberson WT, Holmquest HJ, Scot D, Dow M. Functional electrotherapy: stimulation of the peroneal nerve synchronized with the swing phase of the gait of hemiplegia patients. *Arch Phys Med Rehabil*, 42:101-105, 1961.

Lu J, Waite P. Spine update: advances in spinal cord regeneration. *Spine*, 24(9):926-930, 1998.

Lundin TM, Grabiner MD, Jahnigen DW. On the assumption of bilateral lower extremity joint moment symmetry during the sit-to-stand task. *J Biomech*, 28(1):109-112, 1995.

Lucas DB, Bresler B. *Stability of the Ligamentous Spine*. Report no. 40 from the Biomechanics Laboratory, University of California, San Francisco, Berkeley, 1961. (cited by Cholewicki and McGill, 1996)

Magdalena L, Monasterio F. Fuzzy controlled gait synthesis for a biped walking machine. In: R.J. Marks II (ed) *Fuzzy Logic Technology & Applications*, IEEE Press, pp. 117-122, 1994.

Magnus K. Development of the stability concept in mathematics, *Naturwissenschaften*, 46:590-595, 1959. (cited in Leipholz, 1970)

Matjacic Z, Voigt M, Popovic D, Sinkjaer T. Functional postural responses after perturbations in multiple directions in a standing man: a principle of decoupled control, *J Biomech*, 34(2):187-196, 2001.

Mahoney FI, Barthel DW. Functional evaluation: the Barthel Index, *Md State Med J*, 14:61-5, 1965.

Malezic M, Hesse S. Restoration of gait by functional electrical stimulation in paraplegic patients: a modified programme of treatment, *Paraplegia*, 33:126-131, 1995.

Marsolais EB, Scheiner A, Miller PC, Kobetic R, Jacobs-Daly J. Augmentation of transfers for a quadriplegic patient using an implanted FNS system, *Paraplegia*, 32:573-579, 1994.

Maynard FM, et al. International standards for neurological and functional classification of spinal cord injury, *Spinal Cord*, 35(5):266-274, 1997.

McGeer T. Passive dynamic walking, *Int J Robot Res*, 9(2):62-82, 1990.

McGill SM, Norman RW. Reassessment of the role of intra-abdominal pressure in spinal compression, *Ergonomics*, 30:1565-1588, 1987.

McGill SM, Cholewicki J. Biomechanical basis for stability: an explanation to enhance clinical utility, *J Orthop Sports Phys Ther*, 31(2):96-100, 2001.

McNeal DR. 2000 years of electrical stimulation. In: Hambrecht TF, Reswick JB (eds) *Functional Electrical Stimulation: Applications in Neural Prostheses*, Marcel Dekker, New York, 1977.

Merati G, Sarchi P, Ferrarin M, Pedotti A, Veicsteinas A. Paraplegic adaptation to assisted-walking: energy expenditure during wheelchair versus orthosis use, *Spinal Cord*, 38:37-44, 2000.

Merriam-Webster Inc. *Webster's Ninth New Collegiate Dictionary*, United States, 1989.

Mihelj M, Matjacic Z, Bajd T. Postural activity of constrained subject in response to disturbance in sagittal plane, *Gait and Posture*, 12:94-104, 2000.

Millington PJ, Myklebust BM, Shambes GM. Biomechanical analysis of the sit-to-stand motion in elderly person. *Arch Phys Med Rehabil*, 73:609-617, 1992.

Miyamoto S, Shimada Y, Sato K, Kagaya H, Matsunaga T, Obinata G. Hybrid functional electrical stimulation for energy-efficient restoration of standing-up motion, *Arch Phys Med Rehabil*, 80(1):40-47, 1999.

Mochon S, McMahon TA. Ballistic walking. *J Biomech*, 13:49-57, 1980.

Moynahan M, Chizeck HJ. Characterization of paraplegic disturbance response during FNS standing, *IEEE Trans Rehab Eng*, 1(1):43-48, 1993.

Moynahan M, Mullin C, Cohn J, Burns CA, Halden EE, Triolo RJ, Betz RR. Home use of a functional electrical stimulation system for standing and mobility in adoles cents with spinal cord injury. *Arch Phys Med Rehabil*, 77:1005-1013, 1996.

Mulder AJ, Veltink PH, Boom HBK. On/off control in FES-induced standing up: a model study and experiments. *Med & Biol Eng & Comput*, 30:205-212, 1992.

Munih M, Kralj A. Modelling muscle activity in standing with considerations for bone safety. *J Biomech*, 30(1):49-56, 1997.

Munro BJ, Steele JR, Bashford GM, Ryan M, Britten N. A kinematic and kinetic analysis of the sit-to-stand transfer using an ejector chair: implications for elderly rheumatoid arthritic patients. *J Biomech*, 31:263-271, 1998.

National Spinal Cord Injury Statistical Center. *1998 Annual Report*, University of Alabama at Birmingham, December 1998.

Nuzik S, Lamb R, VanSant A, Hirt S. Sit-to-stand movement pattern: a kinematic study, *Phys Ther*, 66(11):1708-1715, 1986.

Pai YC, Rogers MW. Control of body mass transfer as a function of speed of ascent in sit-to-stand, *Med Sci Sports Exerc*, 22(3):378-384, 1990.

Pai YC, Rogers MW. Speed variation and resultant joint torques during sit-to-stand, *Arch Phys Med Rehabil*, 72:881-885, 1991.

Pai YC, Chang HJ, Chang RW, Sinacore JM, Lewis JL. Alteration in multijoint dynamics in patients with bilateral knee osteoarthritis, *Arthritis Rheum*, 37(9):1297-1304, 1994.

Pai YC, Rogers MW, Patton J, Cain TD, Hanke TA. Static versus dynamic predictions of protective stepping following waist-pull perturbations in young and older adults, *J Biomech*, 31(12):1111-8, 1998.

Pandy MG, Berme N. A numerical method for simulating the dynamics of human walking, *J Biomech*, 21(12):1043-1051, 1988.

Pavec D, Dansereau J, Parent F, Aissaoui R, Aubin C-E. Stability measurement of the user in seating devices using a kinematic model, *RESNA '99*, June 25-29, pp. 278-280, 1999.

Perry J. *Gait Analysis: Normal and Pathological Function*, Thorofare, New Jersey, Slack, 1992.

Piazza SJ, Delp SL. The influence of muscles on knee flexion during the swing phase of gait, *J Biomech*, 29(6):723-733, 1996.

Popovic D, Tomovic R, Schwirtlich L. Hybrid active system – the motor neuroprosthesis, *IEEE Trans Biomed Eng*, 36(7):729-737, 1989.

Popovic MR, Pappas IPI, Nakazawa K, Keller T, Morari M, Dietz V. Stability criterion for controlling standing in able-bodied subjects, *J Biomech*, 33(11):1359-1368, 2000.

Radebold A, Cholewicki J, Polzhofer GK, Greene HS. Impaired postural control of the lumbar spine is associated with delayed muscle response times in patients with chronic idiopathic low back pain, *Spine*, 26(7):724-730, 2001.

Reisinger KD, Moskowitz GD. Bipedal locomotion: stopping and the standing/balance gait, *Int J Robot Res*, 18(3):333-343, 1999.

Riener R, Fuhr T. Patient-driven control of FES-supported standing up: a stimulation study, *IEEE Trans Rehab Eng*, 6:113-124, 1998.

Riener R, Boll M, Pavan E, Ferrarin M, Spadone R, Frigo C. Control experiments with a neuroprosthesis for standing-up and sitting-down, *Proc the International Biomechatronics Workshop*, Enschede, The Netherlands, pp. 168-172, 1999.

Rietdyk S, Patla AE, Winter DA, Ishac MG, Little CE. Balance recovery from medio-lateral perturbations of the upper body during standing, *J Biomech*, 32(11):1149-58, 1999.

Riley P, Schenkman ML, Mann RW, Hodge WA. Mechanics of a constrained chair rise, *J Biomech*, 24(1):77-85, 1991.

Rodosky MW, Andriacchi TP, Anderson GBJ. The influence of chair height on lower limb mechanics during rising, *J Orthop Res*, 7:266-271, 1989.

Sardain P, Rostami M, Bessonnet G. An anthropometric biped robot: dynamic concepts and technological design, *IEEE Transactions on Systems, Man, and Cybernetics – Part A: Systems and Humans*, 28(6):823-838, 1998.

Schechter DS. Origins of electrotherapy. *New York State Journal of Medicine*, 71:997-1008, 1971.

Schenkman M, Berger RA, Riley PO, Mann RW, Hodge WA. Whole-body movements during rising to standing from sitting, *Phys Ther*, 70(10):638-648, 1990.

Schultz AB, Alexander NB, Ashton-Miller JA. Biomechanical analyses of rising from a chair, *J Biomech*, 25(12):1383-1391, 1992.

Schutte L, Risher D. An inverse dynamics approach to dynamic optimization: application to a trajectory matching problem, *Proc 8th Biennial Conference, Canadian Society for Biomechanics*, Calgary, August 18-20, 1994.

Seedhom BB, Terayama K. Knee forces during the activity of getting out of a chair with and without the aid of arms, *J Biomed Eng*, 1:278-282, 1976.

Seelen HAM, Potten YJM, Drukker J, Reulen JPH, Pons C. Development of new muscle synergies in postural control in spinal cord injured subjects, *J Electromygr Kinesiol*, 8:23-34, 1998.

Seelen HAM, Potten YJM, Adams JJ, Drukker J, Spaans F, Huson A. Postural motor programming in paraplegic patients during rehabilitation, *Ergonomics*, 41(3):302-316, 1998.

Sepulveda F, Granat MH, Cliquet A. Gait restoration in a spinal cord injured subject via neuromuscular electrical stimulation controlled by an artificial neural network, *Int J Artif Organs*, 21(1):49-62, 1998.

Shepherd RB, Gentile AM. Sit-to-stand: functional relationship between upper body and lower limb segments, *Hum Movement Sci*, 13:817-840, 1994.

Shepherd RB, Koh HP. Some biomechanical consequences of varying foot placement in sit-to-stand in young women, *Scand J Rehab Med*, 28:79-88, 1996.

Solomonow M, Aguilar E, Reisin E, Baratta RV, Best R, Coetzee T, D'Ambrosia R. Reciprocating gait orthosis powered with electrical muscle stimulation (RGO II). Part I: performance evaluation of 70 paraplegic patients, *Orthopedics*, 20(4):315-324, 1997.

Stallard J. Mechanical orthoses and FES for patients with complete thoracic lesions, In: Pedotti A, Ferrarin M, Quintern J, Riener R (eds) *Neuroprosthetics: from Basic Research to Clinical Applications*, Springer-Verlag, Berlin, 1996.

Stein RB. Functional electrical stimulation after spinal cord injury. *J Neurotrauma*, 16(8):713-717, 1999.

Strojnik P, Kralj A, Ursic I. Programmed six-channel electrical stimulator for complex stimulation of leg muscles during walking, *IEEE Trans Biomed Eng*, BME-26:112-116, 1979.

Tashman S, Zajac FE, Perkash I. Modeling and simulation of paraplegic ambulation in a reciprocating gait orthosis, *J Biomech Eng*, 117:300-308, 1995.

Tesh KM, Dunn JS, Evans JH. The abdominal muscles and vertebral stability. *Spine*, 12(5):501-8, 1987.

Thomas JS, Lavender SA, Corcos DM, Andersson GB. Trunk kinematics and trunk muscle activity during a rapidly applied load, *J Electromyogr Kinesiol*, 8(4):215-25, 1998.

Tortora GJ, Grabowski SR. *Principles of anatomy and physiology*, 8th edition, HarperCollins, 1996.

Vander Linden DW, Brunt D, McColloch MU. Variant and invariant characteristics of the sit-to-stand task in healthy elderly adults, *Arch Phys Med Rehabil*, 75:653-660, 1994.

Veltink PH, Boiten O, Jacobs R, de Vries TJA, Baardman G. FES-supported standing up by independent control of three global variables – a modeling study, *Proc 2nd Ann Conf Int FES Society*, Burnaby, Canada, pp. 95-96, 1997.

Watanabe T, Futami R, Hoshimiya N, Handa Y. An approach to a muscle model with a stimulus frequency-force relationship for FES relationships, *IEEE Trans Rehab Eng*, 7(1):12-18, 1999.

Wheeler J, Woodward C, Ucovich RL, Perry J, Walker JM. Rising from a chair: influence of age and chair design, *Phys Ther*, 65:22-6, 1985.

Wibowo MA, Triolo RJ, Uhlir JP, Kobetic R. The effect of stimulated hip extensor moment on the loads imposed on the arms during standing with FES, *RESNA '98*, June 26-30, pp. 384-386, 1998.

Williamson R, Andrews BJ. Detecting absolute human knee angle and angular velocity using accelerometers and rate gyroscopes, *Med Biol Eng Comput*, 39(3):294-302, 2001.

Winters JM. Hill-based muscle models: a systems engineering perspective, In: Winters JM and Woo SL (eds) *Multiple Muscle Systems*, Springer-Verlag, New York, 1990.

Working Model, *Working Model 3D: user manual, version 2.0*, Knowledge Revolution, 1997.

Yamaguchi GT, Zajac FE. Restoring unassisted natural gait to paraplegics via functional neuromuscular simulation: a computer simulation study, *IEEE Trans Biomed Eng*, 37(9):886-902, 1990.

Yang TF, Chan RC, Wong TT, Bair WN, Kao CC, Chuang TY, Hsu TC. Quantitative measurement of improvement in sitting balance in children with spastic cerebral palsy after selective posterior rhizotomy, *Am J Phys Med Rehabil*, 75:348-352, 1996.

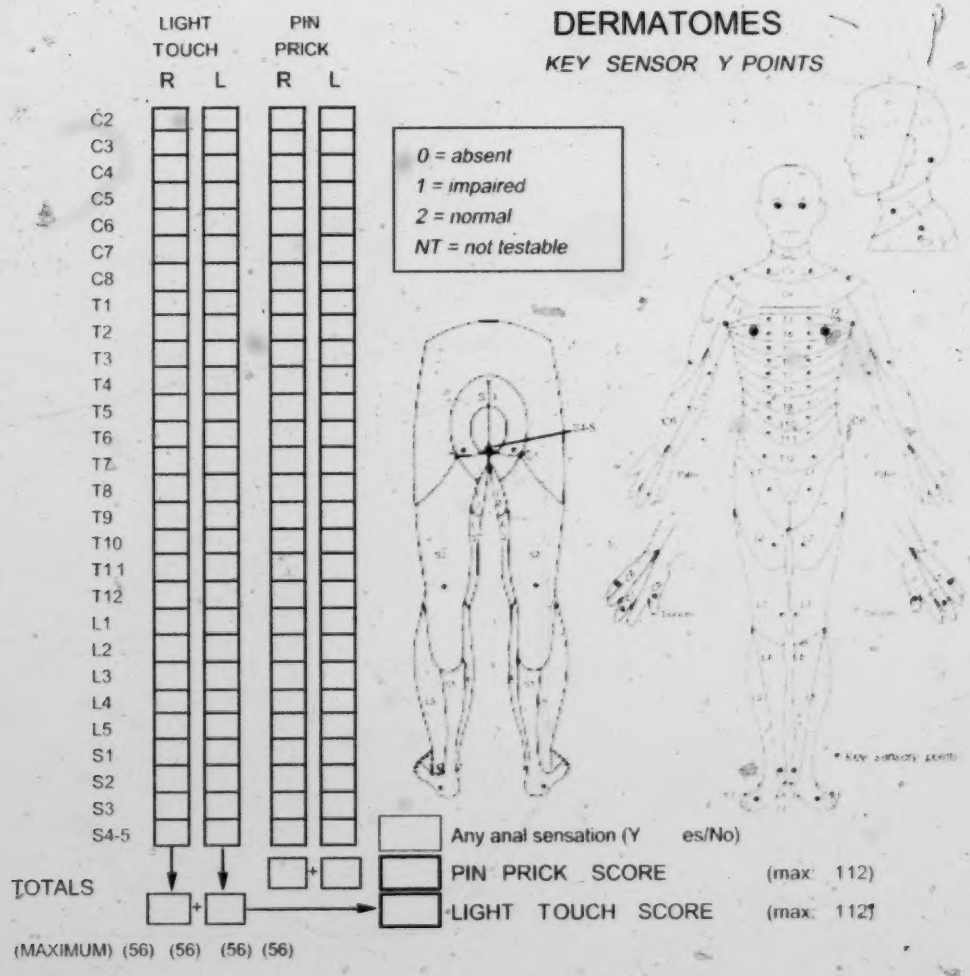

Figure 1-1: SCI classification by sensory region (dermatome), as proposed by the American Spinal Injury Association (ASIA).

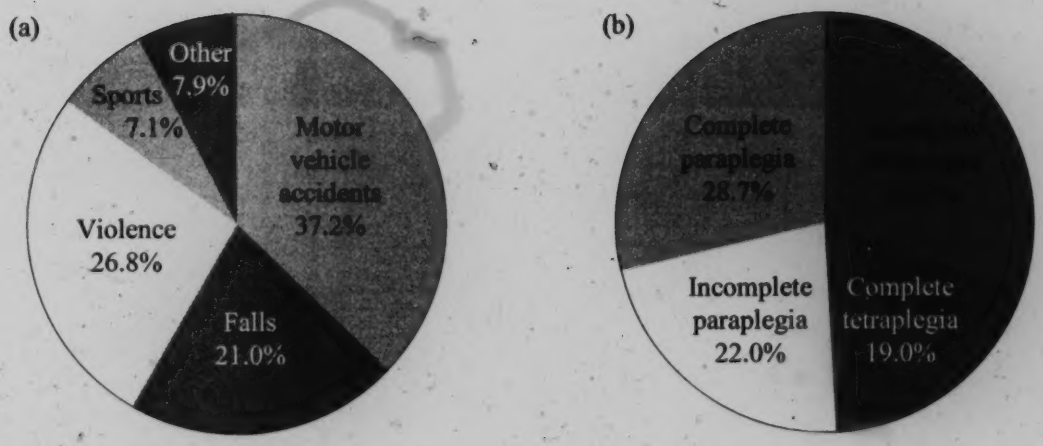

Figure 1-2: Distribution of spinal cord injuries by (a) epidemiology and (b) general injury classification.

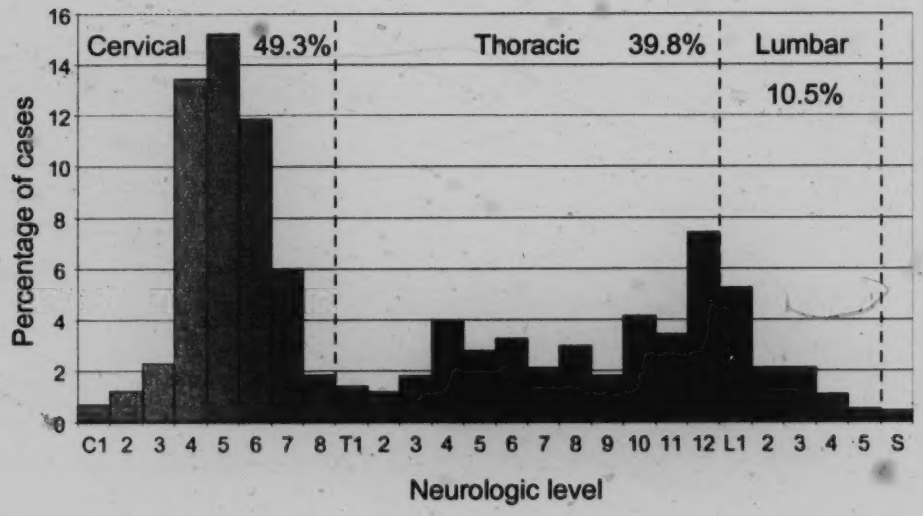

Figure 1-3: Distribution of spinal cord injuries by neurologic level of lesion.

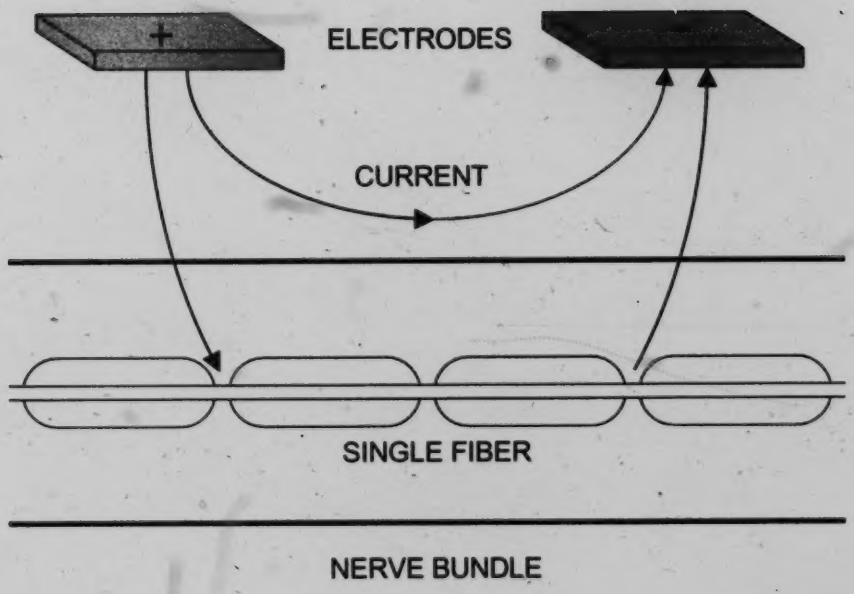

Figure 1-4: Schematic representation of electrical stimulation. Electrodes create a current through the motoneuron. Depolarization occurs near the positive (active) electrode, causing an action potential to propagate along the axon.

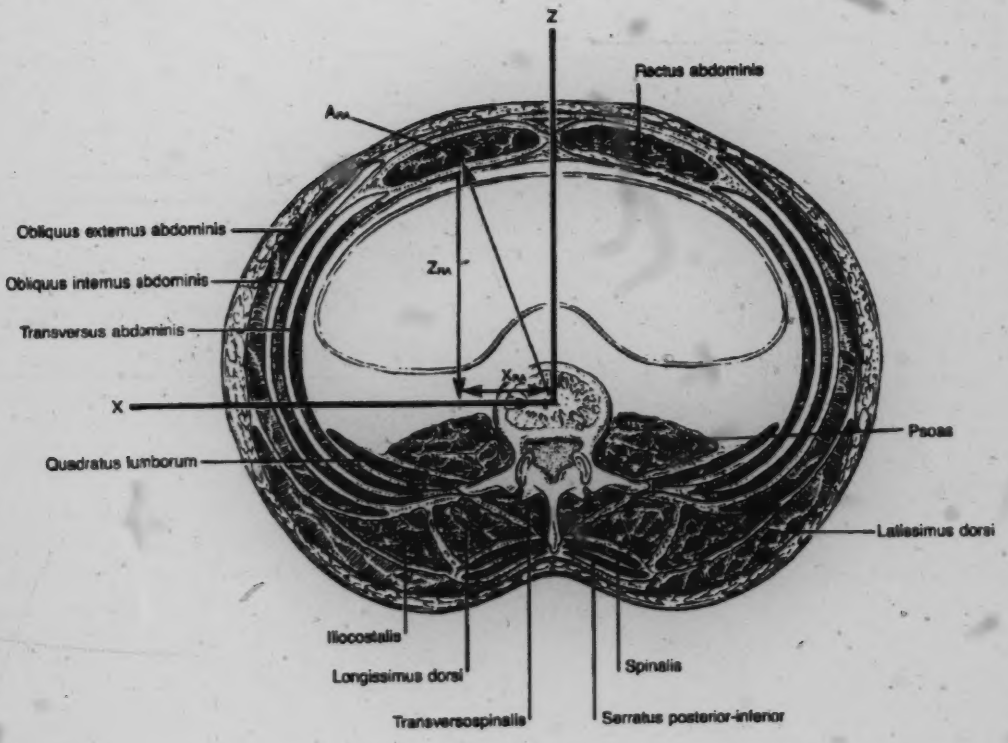

Figure 1-5: Cross section through the abdomen. Vertebra shown is L4.

Figure 1-6: A page from da Vinci's notebook describing how the neck muscles support the spine by means of tensile contractions, like the guy ropes supporting a ship's mast.

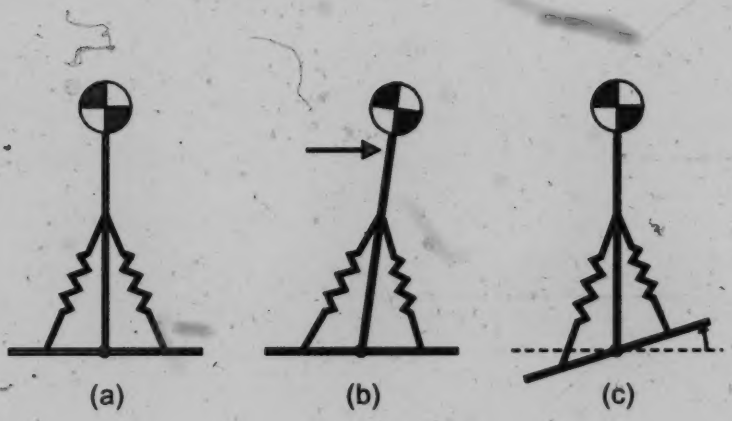

Figure 1-7: Simple inverted pendulum models of the trunk. The lumbosacral joint allows the trunk to pivot relative to the base of support (pelvis). (a) unperturbed equilibrium state, (b) horizontal force perturbation, (c) perturbation of base of support.

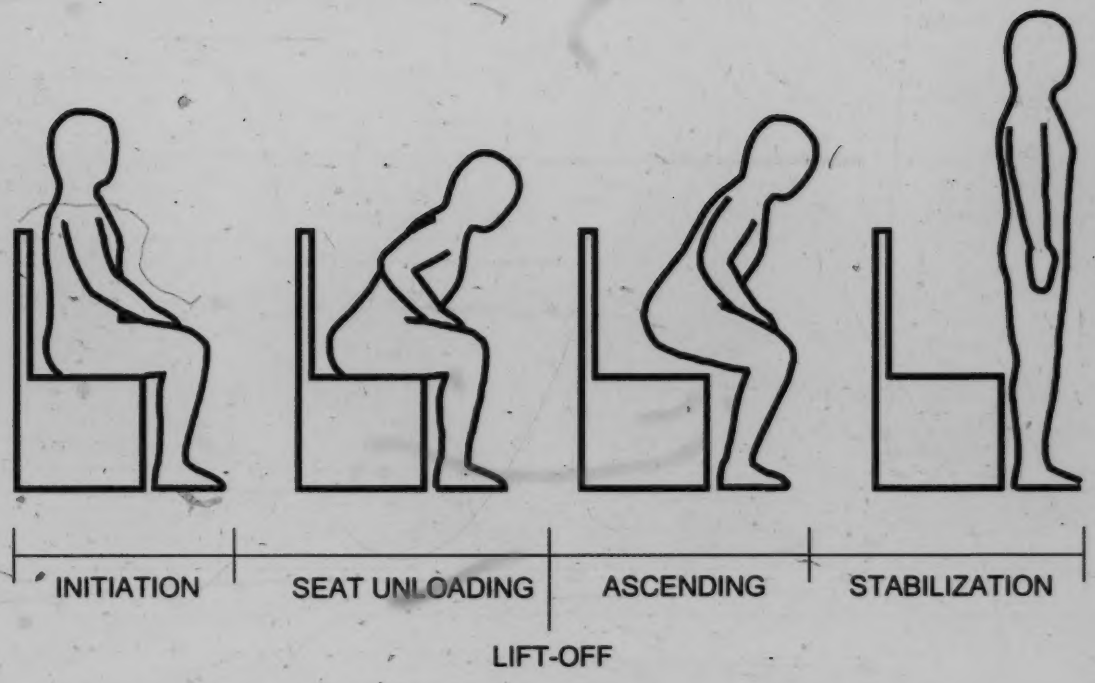

Figure 1-8: The sit-to-stand maneuver. Phase description of Kralj et al. (1990).

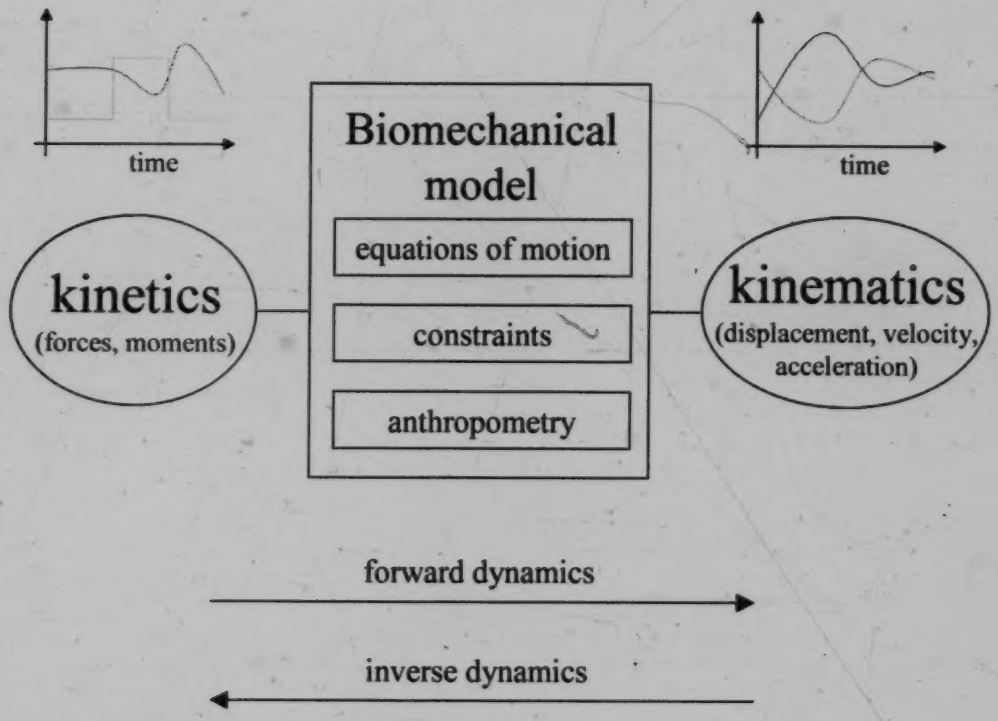

Figure 1-9: General biomechanical modeling scheme. Forward dynamics determines trajectories based on applied forces and moments. Inverse dynamics determines forces and moments based on recorded motion.

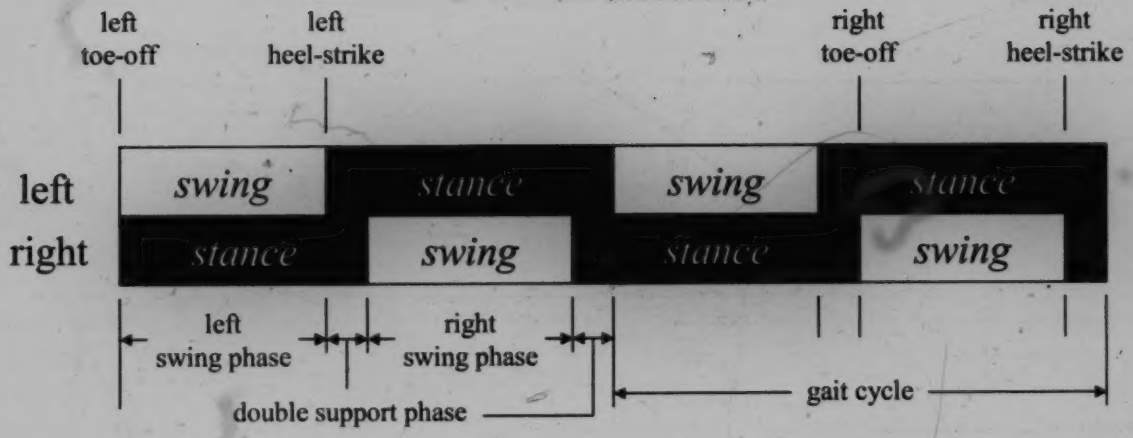

Figure 1-10: Normal reciprocal gait cycle (description from Perry, 1992).

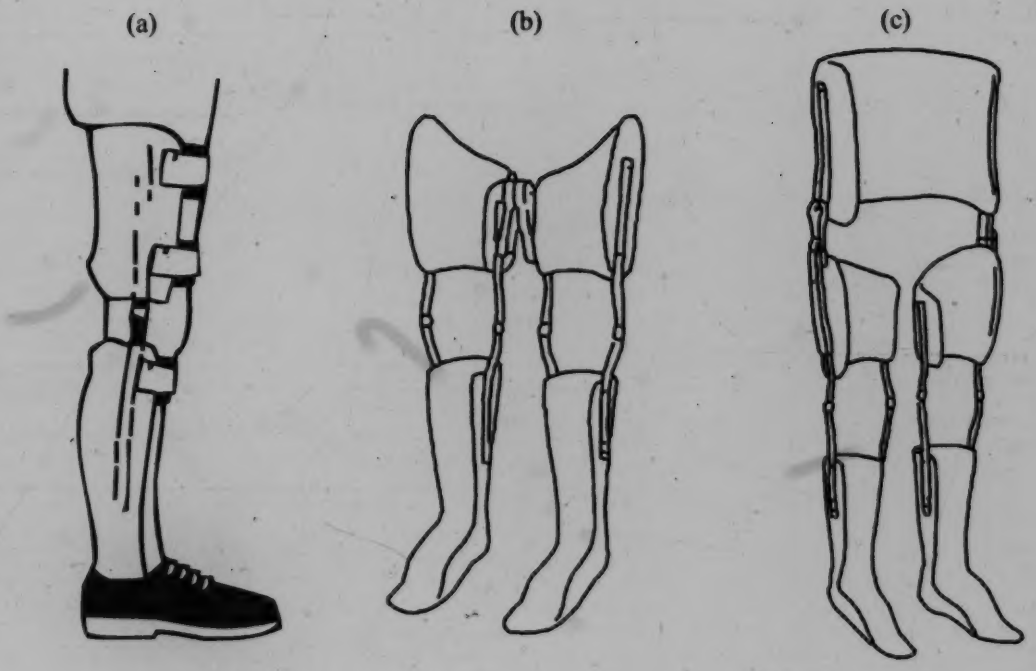

Figure 1-11: Mechanical orthoses. (a) Long leg braces; (b) medially linked knee-ankle-foot orthosis; (c) Louisiana State University Reciprocating Gait Orthosis.

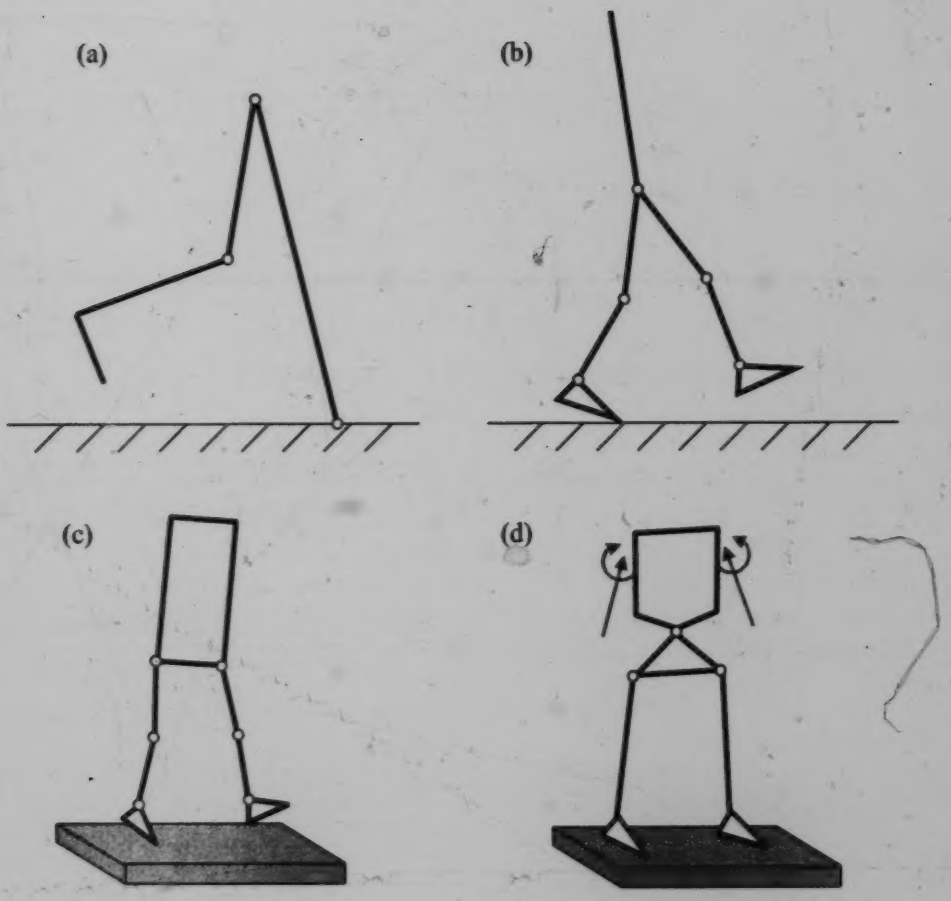

Figure 1-12: Some typical gait models. (a) Ballistic walking model (Mochon and McMahon, 1980); (b) seven-segment model of Onyshko and Winter (1980); (c) seven-segment model of Yamaguchi and Zajac (1990) ; (d) four-segment model of LSU-RGO (Tashman et al., 1995).

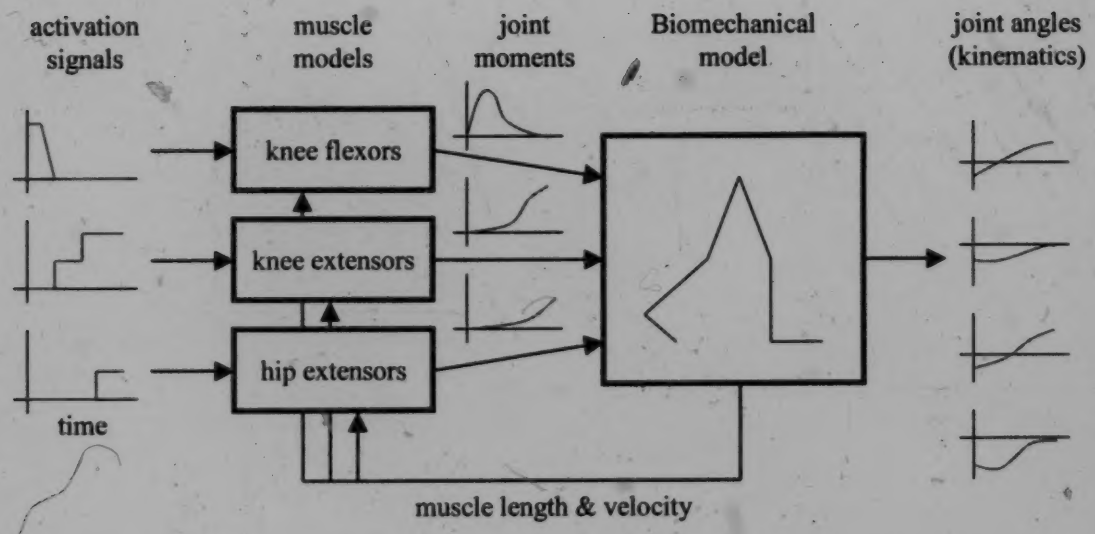

Figure 1-13: Biomechanical modeling scheme that uses forward dynamics with muscle activation signals as input.

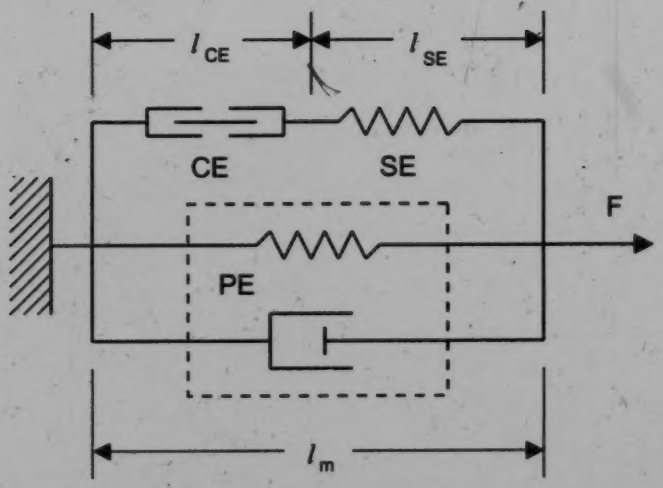

Figure 1-14: Hill-type muscle model consists of a contractile element (CE), a series elastic element (SE), and a parallel viscoelastic element (PE). Lengths of the elements are indicated. Total muscle length is denoted l_m. F indicates the muscle force. This is the same model used by Watanabe et al. (1999).

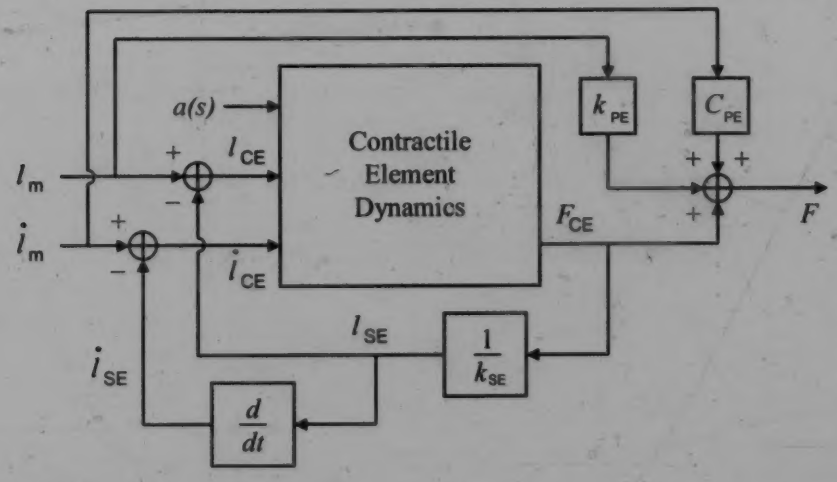

Figure 1-15: Block diagram of the method used to compute muscle forces given the whole muscle length, velocity and electrical stimulation level.

2 FES assisted trunk stability

2.1 Abstract

Trunk instability is a consequence of spinal cord injury that limits many important activities for people living with paraplegia. A method using functional electrical stimulation to stabilize the paralyzed trunk was investigated. As well, a novel approach to measuring trunk stability in vivo was devised. An apparatus was built that applied a controlled perturbation to the base of support of a seated subject. Trunk stability was objectively defined according to the subject's kinematic response. 2-channel surface stimulation was applied bilaterally to the erector spinae muscles at the levels of T12-L2 of three spinal cord injured subjects. Constant open loop stimulation was provided at a level such that a maximal contraction was observed. One subject, with a lesion at C6/7, exhibited a dysreflexic response to stimulation. Another subject (lesion level T5/6) showed improvement to lateral and anterior stability when the stimulation was on. The third subject (lesion level T3/4/5) showed no improvement to stability when stimulated. Ten able-bodied volunteers aided in the development of the experimental method and provided data for comparison to the paraplegic subjects. The results of this study suggest that trunk stimulation may be a means by which stability can be improved, however more muscle groups should probably be activated.

2.2 Introduction

This study is the first step towards a long-term objective to develop a paraplegic gait orthosis with no mechanical components above the waist. Trunk stability, or the ability of the torso to independently maintain an upright posture and resist perturbations, is diminished after SCI. The degree to which it is diminished is a factor of the neurological level of injury. This fact is easily observed and widely accepted. For example, in wheelchair sports where stability is crucial, classification based on the level of lesion provides a reasonably fair basis for competition (Shepherd, 1988). Loss of trunk stability makes difficult many everyday tasks, such as reaching, driving, wheeling over slopes and bumpy

terrain, and lateral transfers to and from seats. Also, instability often precludes the use of gait orthoses.

When seated, people with SCI generally address trunk instability by assuming postures that rely heavily on their arms or the backrests of their chairs. When performing certain tasks, such as reaching, one arm must be delegated to supporting the upper body. The necessity for trunk support at all times complicates most activities. Paraplegic gait demands an extraordinary degree of trunk stability. Users of even the most sophisticated FES gait systems and hybrid orthoses must rely heavily on handrails and crutches (Karcnik et al., 1996).

Special seating is one approach to improving trunk stability after SCI, but of course, it does not benefit out of seat movements such as lateral transfers, sit-to-stand or gait. Seats involving thoracic belts introduce additional risks of pressure sores, and are considered uncomfortable by most. The trend in wheelchairs today is towards lighter, smaller models that are easier to transfer in and out of. Corset-like trunk orthoses are another possibility (Shurr et al., 1990), but they are very cumbersome. They also present pressure sore risks, and are virtually never used by people with SCI. Some gait orthoses, such as the Louisiana State University Reciprocal Gait Orthosis (LSU-RGO), include a bulky trunk component that wraps around the subject's midsection. These require a great deal of time and effort to don and doff (Douglas et al., 1983), plus they present risks of pressure sores during long-term use.

2.2.1 Trunk FES

One approach to improving trunk stability after SCI, which has never been adequately assessed, is using FES. The paraspinal muscles are the major providers of stability to the spine (see section 1.4.4 for full discussion). Electromyography studies confirm that able-bodied subjects, when sitting quietly, coactivate the antagonistic trunk flexors and extensors (Cholewicki et al., 1997, Gardner-Morse and Stokes, 2001). As well, the paraspinal muscles contract and do work during normal gait (Gracovetsky, 1988).

Trunk FES remains almost completely unstudied. To date, there have been only a few FES systems that involve stimulation of trunk muscles (Graupe and

Kohn, 1994, Marsolais et al., 1994, Moynahan, 1996). The reports on these systems rarely discuss the results or benefits of trunk stimulation beyond one or two subjective observations. Information regarding motor points for trunk stimulation is even hard to find in current FES manuals. Only the old FES literature seems to include this information (e.g. Licht, 1967).

2.2.2 Hypotheses

H1. Higher levels of spinal cord injury result in lower trunk stability.

H2. Open loop functional electrical stimulation of the erector spinae muscles will improve trunk stability after SCI.

The following additional hypotheses were made in this study:

1. Some able-bodied subjects would exhibit different stability ratings than others. Also, that the measurement would differ depending on the direction of perturbation.

2.2.3 The need for quantification

In order to objectively assess the benefits of trunk stimulation, an objective measure of trunk stability is needed. There have been many attempts to quantify trunk stability for a variety of different pathologies (see section 1.4.5), but few deal specifically with SCI. Those that do, tend to be subjective, and do not necessarily fit a proper definition of stability (Hardcastle et al., 1987, Franchignoni et al., 1997, Vezina and Hubley-Kozey, 2000). In the context of spinal cord injury, trunk stability has yet to be objectively quantified. Thus, we devised a novel experiment that applies controlled perturbations to a seated subject while measuring the response of the trunk.

Beyond the present study, an objective measure of trunk stability would be useful as a clinical tool. For example, it could be incorporated into the battery of tests that classify spinal cord injuries. Also, a measure of trunk stability could be very useful in research of treatments that aim to restore trunk function.

2.3 Methods

An apparatus was designed that would constrain a seated subject below the trunk and then perturb his base of support. The kinematic response of the trunk was recorded. How to interpret the response was an important

consideration. We first devised a basic method of interpretation that was applicable to able-bodied subjects. This method was then applied to SCI subjects, but without success. Thus, a more meaningful method for SCI subjects was developed.

2.3.1 Definition of *trunk stability* (perturbation & measurement)

It was necessary to establish a rigid definition of the term "trunk stability" before beginning the experiments. In developing our definition, we reviewed a wide range of current literature on stability (see section 1.4). Generally stated, stability involves three elements: a system in equilibrium, a perturbation, and a measurable response that attempts to resist or recover from the perturbation. How definitions of stability differ is by the designation of those three elements, and how the final outcome is evaluated. Following are our designations.

The system of interest was the human trunk. Its equilibrium state was an upright sitting posture with no external support. The perturbation was an unexpected angular displacement of the seat, which remained constant once it was applied. The pelvis was immobilized relative to the seat. It was important that the perturbation was applied unexpectedly, as the response to an expected perturbation differs from the response to an unexpected perturbation (Lavender and Marras, 1995). We considered using force perturbations, but decided that angular displacements were easier to control and more representative of the perturbations experienced during locomotion in a wheelchair or gait orthosis. The response to the perturbation was a change in posture. This was quantified by measuring the displacement of the spine.

The response variable was defined differently for the able-bodied subjects and the SCI subjects. For the SCI subjects, the response variable was the maximum angle of perturbation that they could resist without failure. Failure was indicated when trunk angle exceeded 30 degrees. Generally, when the subject went beyond this range, one of the operators would catch him, or he would unfold his arms and catch himself. For the able-bodied subjects, all of who were able to resist the maximal perturbations that the apparatus could deliver, the response

variable was response time – the amount of time from the onset of perturbation to a steady-state offset displacement of the spine.

2.3.2 Apparatus – tilt seat

A unique apparatus was designed that could apply a controlled perturbation to the seated subject. The "tilt seat," as it came to be known, consists of a padded seat, a levered platform and a heavy wooden base. The assembled tilt seat is shown in Figure 2-1. The base was constructed from medium density fibreboard (MDF), and is therefore quite heavy – approximately 40kg. The lever arm is also made of MDF, but it is considerably lighter. It attaches to the base via a sturdy hinge, and it is able to tilt up to 20 degrees relative to the horizontal. A narrow tower connected firmly to the base acts as a guide. It contains graded markings for every degree of rotation. It also contains a latch at zero degrees that locks the platform in the horizontal position.

The seat was attached to the levered platform by a "Lazy Susan" joint. This allowed it to rotate in the horizontal plane. Two metal pegs could lock it into one of two positions. In the first position, the seat is oriented such that the front and back edges are perpendicular to the lever joint. In such a position, the subject can be tilted to the left or right. In the second position, the front and back edges of the seat are parallel to the hinge joint. So, a subject could be tipped forward or backwards. Because of this feature, we were able to apply perturbations to the subject in not just two, but four directions.

An operator standing behind the apparatus out of the subject's field of view controlled the seat angle by disengaging the latch, then manually pulling up or down on a handle attached to the lever arm. A heavy C-clamp was used as an adjustable stop, which limited the angle of tilt to a specified maximum.

Our apparatus is different from that of Forssberg and Hirschfeld (1994), but the concept is similar. They devised a platform that could both tilt and translate, perturbing the subject seated upon it. It is not clear whether their apparatus was motorized. Radebold et al. (2000) built a seat with a hemispherical underside that, when placed upon a horizontal force plate, could tilt freely in any

direction. The subjects simply attempted to remain upright; no external perturbations were applied.

2.3.3 Subjects

Ten able-bodied subjects were recruited to participate in the study. They are described in Table 2-1.

Table 2-1; Able-bodied subjects

Subject	Gender	Age (years)	Height (m)	Weight (kg)
1	M	28	1.83	81
2	M	28	1.88	87
3	F	26	1.73	50
4	F	27	1.63	64
5	M	22	1.68	62
6	M	25	1.75	73
7	M	49	1.79	68
8	M	24	1.71	75
9	M	26	1.70	70
10	M	47	1.83	86

Four spinal cord injured subjects volunteered for our study. They are described below in Table 2-2.

Table 2-2; Spinal cord injured subjects

Subject	Gender	Age (years)	Height (m)	Weight (kg)	Level of injury	Years post injury
11	M	67	1.68	86	T12	6
12	M	38	1.81	110	C6/C7	10
13	M	26	1.90	87	T5/6	5
14	M	27	1.80	90	T3/4/5	3

Each of the SCI subjects had experience with FES cycling and rowing exercises, which apply stimulation to the quadriceps and hamstrings, and in some cases, the common peroneal nerve (for the flexion-withdrawal reflex) or gluteal muscles. Since the subjects were not accustomed to trunk stimulation, each was tested prior to the experiment for autonomic dysreflexia. With the subject sitting on a regular bench, increasing stimulation was applied to the lumbar ES while heart rate and blood pressure were closely monitored.

Surface FES was applied using a small handheld stimulator (The Odstock Stimulator, England) and standard skin electrodes. The active electrodes were

placed on the back just below the rib cage. See Figure 2-2. The centers of the active electrodes were located approximately 5 cm to either side of the spinous process of L1. The passive electrodes were located just above the iliac crests.

FES was not applied to SCI subject #11 because his lesion was too low (T12). His lumbar muscles were mostly unaffected by his injury, and he had skin sensation at the location that we proposed to stimulate. Stimulation would have been uncomfortable and probably painful.

2.3.4 Instrumentation – Vicon and Pico

Two different measurement protocols were used. Under the original design, the kinematic data were collected using an optical marker system. Four motion analysis cameras (Vicon 140 manufactured by Oxford Metrics Ltd.) recorded the three-dimensional coordinates of six reflective markers taped to the skin over anatomical landmarks – the acromions and the spinous processes of vertebrae T4, T8, T12 and L4 – at a sampling rate of 60 Hz. By these markers, flexion of the spine was measured in both the anterior-posterior direction and the medial-lateral direction.

Four more markers mounted on the apparatus were used to record the seat angle. Data for the first seven able-bodied subjects were collected by this means. Unfortunately, these signals were noisy, and required filtering. An improved 7-camera Vicon system became available later in the study. It was used for able-bodied subjects #8 and #9. This system sampled at 50 Hz and reduced noise considerably.

Finally, a low-noise portable measurement system consisting entirely of electronic sensors was devised. This development was necessary in order to accommodate SCI subjects who were reluctant to travel to our laboratory at the Glenrose Rehabilitation Hospital. The portable system enabled us to move the experiment to the Robert Steadward Centre (formerly the Rick Hansen Centre) on the University of Alberta campus, where the subjects visited in the course of their regular exercise routines.

The portable sensor system consisted of a single axis potentiometer, a dual axis goniometer (XM180/B manufactured by Biometrics Ltd., formerly Penny &

Giles), a 10-bit analog-digital converter (ADC-11 manufactured by Pico Technology Ltd.), a custom-built transducer circuit, and a laptop computer. The single axis potentiometer was mounted on the apparatus in line with the fulcrum in order to measure the seat angle. The goniometer was designed specifically for in vivo spine measurement. The two terminals of the goniometer were taped to the subject's skin over the spinous processes of T4 and L2 (see Figure 2-2). The goniometer measured two relative angles between its terminals: one in the sagittal plane (anterior-posterior flexion) and one in the frontal plane (medial-lateral flexion). The system recorded three digital signals at a sampling rate of 50Hz.

Able-bodied subject #10 was measured with the portable sensor system, as well as able-bodied subject #3, who had previously been tested using the original 4-camera Vicon system. Subject #3 was tested under both measurement schemes to ensure commutability of the acquired data.

2.3.5 FES of the erector spinae

Since this was a pilot study, we sought to keep the complications few. We chose to use open-loop FES, avoiding the need for feedback control systems. According to Gardner-Morse et al. (1995), muscle stiffness can stabilize the lumbar spine without the need for active control. Furthermore, we chose to target only one muscle group: the lumbar erector spinae. Two independent active electrodes were positioned on the back with centers located approximately 3 cm below the most inferior ribs and 5 cm lateral to the spine, on either side. Thus, the ES innervated from T12-L2 were targeted.

The stimulus was generated by a portable FES unit using amplitude modulation (Odstock stimulator). For all trials, a frequency of 30 Hz and a pulse width of 180 μs were used. The amperage was adjustable from zero to 100 mA. Signal amplitude was increased until a full contraction was observed (usually approximately 60% of full power, or more if fatigue was setting in).

2.3.6 Trials – perturbed sitting

Perturbed sitting trials were conducted in the four cardinal directions: left, right, anterior, and posterior. Efforts were made to apply the perturbations unexpectedly. The operators communicated silently and minimally by nodding

their heads, and the apparatus was positioned such that the operators were out of the subject's field of vision at all times. The perturbation was roughly a step displacement applied at an arbitrary time (usually 5-30 seconds after the subject was informed that a trial has begun). The operator suddenly pushed the seat to a predetermined angle and held it there until the end of the trial. Trials lasted 15 to 20 seconds each, and were separated by rest periods of 1-3 minutes.

Each subject was instructed to "sit quietly with arms folded in front, and try to remain upright at all times." The SCI subjects were provided with handgrips in front of them so that they could catch themselves when necessary. In addition, an operator stood close to spot them in case they fell over. They were instructed that if they unfolded their arms or made contact with the operator, the trial would be unsuccessful.

With the able-bodied subjects, four trials were conducted with perturbations of 10 degrees in each direction while the subject was staring at a fixed point directly ahead. The duration of the transient response was used as an indication of stability.

With the SCI subjects, several trials were conducted in each direction with perturbations of increasing degrees. When failure occurred, the perturbation magnitude was reduced by a small amount, and the trial was repeated. Once an angle was found that resulted in success, and an increase of one degree resulted in failure, that value was taken as the maximum perturbation in that direction.

At the beginning of each FES trial, while the subject was sitting quietly in the unperturbed state, stimulation was slowly increased from zero until a full contraction was observed. 10-30 seconds later, the perturbation was applied. Stimulation was shut off at the end of every trial to minimize muscle fatigue and the risk of electrode burns.

2.4 Results

2.4.1 Noise and filtering

The 4-camera Vicon system produced fairly noisy data. The movements being measured were not fast. The amount of time required to perturb the seat from zero to maximum angle was typically about 0.50 to 0.75 s. Thus, the signals

were expected to consist primarily of frequencies less than 2.0 Hz. Analysis of the power spectral density suggested that a cut-off frequency of 3 Hz would preserve the essential information. A second-order Butterworth low-pass filter with a cut-off frequency of 3 Hz was used to remove noise. An example of unfiltered and filtered output signals is displayed in Figure 2-3.

The improved 7-camera Vicon system produced less noisy data. Again, a second-order Butterworth low-pass filter with a cut-off frequency of 3 Hz was used (see Figure 2-4). The measurement protocol was identical using both systems. The portable sensor system produced very low noise data. The same filter as above was used on the goniometer signal (see Figure 2-5).

2.4.2 Able-bodied data

All of the ten able-bodied subjects were able to cope with the perturbations without difficulty. The responses were varied. As expected, the change in seat angle resulted in an immediate change in trunk angle. Shortly after, the trunk would reach a more or less steady state. In most cases, there was some overshoot before the steady-state position was achieved. In some cases, the trunk angle oscillated above and below steady state, like an underdamped system. All attempts to fit a linear system to the data failed. The reason for this was that the "steady state" was not entirely steady. After the subject recovered from the perturbation, there were often random adjustments or a slow drift towards a more comfortable posture, which does not indicate instability. In fact, some minor movement prior to perturbation was often measured. This made it difficult to determine exactly when the transient response had ended. This problem was solved by ignoring slow movements of the trunk. A threshold of 1.00 deg/s was decided; the time when movements above this value ceased to appear was considered the end of the transient response.

Some typical data are shown in Figure 2-6. The perturbations were not perfect steps; it took 0.50 to 0.75 seconds to move the seat from zero to maximum angle. Aside from the duration of the perturbation, there was little variance in the seat angle signal between trials and between subjects. In the Figures, two vertical red lines mark the beginning and end of the "step" perturbation. The red dashed

line indicates the end of the transient response. Trunk stability was evaluated based on the time interval starting with the onset of perturbation and the end of all trunk motion in excess of 1.00 deg/s. In Figure 2-6, this value is 1.08 s.

Figure 2-7 contains eight more examples of typical data from the able-bodied trials. Note the lack of a true "steady state," and the varied shape of the different responses. All of the responses to lateral perturbations involved trunk flexion in the direction opposite to the perturbation. Often, a small change in anterior trunk angle occurred at the same time. Similarly, changes in lateral flexion occurred during anterior/posterior perturbations, indicating an asymmetrical response. Anterior perturbations produced the most peculiar results. Most subjects were somewhat startled when the seat tipped forward, as though it was ejecting them. On the other hand, posterior perturbations were qualitatively the easiest to cope with.

Before perturbation, the able-bodied subjects generally sat with little to no lateral trunk flexion and 5 to 15 degrees of anterior trunk flexion. During lateral perturbations, anterior trunk flexion sometimes changed a few degrees and usually returned to neutral after perturbation. Similarly, during anterior/posterior perturbations, lateral trunk flexion often occurred.

The complete results are summarized in Table 2-3 below. Each cell of the table represents four trials. The second to fifth columns report the average duration of transient response from the trials in each direction. The final column, labeled "combined," reports the mean value from all 16 trials performed by each subject followed by the standard deviation in parentheses. Subject #3 performed the test on two separate occasions under two different measurement protocols (4-camera Vicon and portable sensor system). Both trials are listed in the table as "3a" and "3b," with the later corresponding to the portable sensor system.

Table 2-3; Average duration of transient response (able-bodied subjects)

Subject	left	right	anterior	posterior	Combined
1	1.13 s	1.51 s	1.97 s	1.42 s	1.51 (0.37) s
2	0.99	0.88	1.30	1.06	1.06 (0.19)
3a	1.21	1.42	1.68	1.55	1.47 (0.22)
3b	1.10	0.98	1.41	1.20	1.17 (0.19)
4	0.93	1.22	1.20	0.74	1.02 (0.25)

5	1.48	1.31	1.92	1.71	1.61 (0.30)
6	1.19	1.27	1.60	1.15	1.30 (0.22)
7	1.27	1.33	2.07	1.38	1.51 (0.40)
8	1.32	0.97	1.34	1.37	1.25 (0.21)
9	1.01	0.91	1.57	1.66	1.29 (0.38)
10	1.03	1.20	1.59	1.12	1.24 (0.26)
mean std. dev.	1.15 (0.22)	1.18 (0.25)	1.60 (0.31)	1.31 (0.31)	1.31 (0.33)

The above data is compiled in a histogram in Figure 2-8 and a series of boxplots in Figure 2-9. In the latter, it appears that anterior perturbations resulted in greater mean response times than the other directions. This assertion was confirmed by a standard analysis of variance F-test (p-value < 0.0001). There was no significant difference between the responses to left and right perturbations.

There were very significant differences between subjects as well (p-value < 0.0001). Subject #3, who was measured on two separate occasions several months apart, performed significantly better during the latter session (p-value < 0.0001).

2.4.3 SCI data

The paralyzed subjects behaved very differently on the apparatus than the able-bodied group. In fact, all but subject #11 had difficulty maintaining an unperturbed equilibrium state. The others struggled to remain upright throughout their trials, and recorded many failures.

2.4.3.1 Subject #11 – complete lesion at T12

Subject #11 could resist lateral perturbations up to 10 degrees in magnitude in either direction. As well, he resisted anterior perturbations up to 4 degrees and posterior perturbations of 20 degrees, which was the maximum that the apparatus could deliver. Some typical trials of subject #11 are shown in Figure 2-10. Subject #11 was the only SCI subject that produced results comparable to the able-bodied sample. Table 2-4 summarizes these results. The values of response time given are for perturbations of 10 degrees, except in the case of anterior perturbations, which could only be done to 4 degrees.

Table 2-4; Summary of subject #11 results

Direction of perturbation	left	right	anterior	posterior	combined
Max. angle (deg)	10	11	4	+20	
Mean response time (s)	2.01	2.10	2.17	0.96	1.80 (0.55)

Subject #11 recorded response times in the lateral directions that were significantly higher than the able-bodied sample. (Due to the difference in variance between the two samples, a robust rank-sum statistical test was used, yielding a p-value = 0.0002). In the posterior direction, subject #11 recorded more rapid response times than the able-bodied sample ($p = 0.0202$). Because he was unable to resist perturbations of 10 degrees in the anterior direction, his stability in that direction could not be compared to the able-bodied sample.

Before perturbation, subject #11 generally sat with 20 to 30 degrees of anterior flexion. His initial lateral flexion ranged from 7 degrees to the right to 3 degrees to the left. In some trials where anterior perturbations were applied, for example that shown in Figure 2-10(c), he tended to flex strongly to the right, indicating a very asymmetric response.

It was observed that subject #11 assumed a very slumped posture in the apparatus, which may have augmented stability, particularly in the posterior direction. In the seat, his pelvis was not oriented vertically, i.e. the hip joints were less flexed than 90 degrees even though the thighs were parallel to the ground. Despite repeated attempts to adjust his posture, it was not possible to secure the pelvis vertically in the apparatus seat.

Subject #11 did not receive FES, because his spinal injury was at T12, exactly where we sought to stimulate. Thus, the target muscles were denervated.

2.4.3.2 Subject #12 – complete lesion at C6/C7

Subject #12 had quadriplegia. When FES was applied to the ES on one side of the body, the RA on that side was seen to contract in unison. During the preliminary FES testing, subject #12 exhibited signs of autonomic dysreflexia (sustained hypertension and lightheadedness). FES was stopped immediately. He

did not perform any stability trials, because without stimulation, he was unable to sit upright unassisted.

2.4.3.3 Subject #13 – complete lesion at T5/T6

Subject #13 had pronounced scoliosis of the spine, which resulted in permanent flexion to the left. As with subject #12, his RA was seen to contract when the ES was stimulated. When sitting unperturbed, subject #13's entire upper body tended to shake. As a result of his rapid movements, it was often impossible to apply the 1.00 deg/s threshold to determine when the transient response had ended.

Eight of subject #13's trials are shown in Figure 2-11. The scoliosis is evident by the constant lateral flexion of the spine to the left. His response to all lateral perturbations, both left and right, involved increased flexion to the left. Anterior/posterior perturbations resulted in either an increase or decrease in lateral flexion. The maximum perturbations that subject #13 could cope with are given in Table 2-5 below.

Table 2-5; Maximum perturbation angles – subject #13

Direction	FES off	FES on
left	4 deg	7 deg
right	6	8
anterior	3	10
posterior	12	12

When FES was applied, subject #13 showed only a slight decrease in anterior flexion. However the effect on anterior stability was significant.

2.4.3.4 Subject #14 – complete lesion at T3/T4/T5

Subject #14 was only able to resist very small perturbations. Table 2-6 below summarizes his results. Eight trials are shown in Figure 2-12. As with the previous subject, subject #14's upper body tended to move a lot when unperturbed, thus it was too difficult to determine the end of the transient response.

Table 2-6; Maximum perturbation angles – subject #14

Direction	FES off	FES on
Left	3 deg	4 deg
Right	2	2

Anterior	2	2
posterior	5	7

Subject #14 sat unperturbed with 20 to 35 degrees of anterior flexion and very little lateral flexion, if any. He responded to lateral perturbations with lateral flexion in the same direction.

When stimulation was applied to Subject #14, a large reduction in anterior flexion occurred. Since the pelvis was fixed at a steep posterior angle (approximately 30 degrees from the vertical), this resulted in the subject leaning far back beyond the sacral support of the apparatus. Subject #14 found this position precarious and uncomfortable.

2.5 Discussion

2.5.1 Major findings

Trunk instability is clearly a problem for people with SCI. Most cannot sit unassisted and resist perturbations without resorting to their arms. This makes it very difficult or impossible to perform many two-handed tasks. There are no FES systems in existence that address trunk stability, despite the obvious need for one.

Unfortunately, from the data gathered, conclusions could not be drawn regarding the efficacy of simple open-loop FES in improving trunk stability (H2). Subject #13 appeared to show an improvement in lateral stability and anterior stability when the ES were stimulated, while subject #14 exhibited no benefit. However, the groundwork was laid for subsequent studies.

FES of the ES muscle group did cause the trunk to extend giving the SCI subjects an unassisted posture they are not normally capable of. The sitting posture chosen by the SCI subjects without stimulation was very kyphotic, or "hunched." They all recorded anterior trunk flexion angles well above the range used by able-bodied subjects. Kyphosis is most likely a direct result of ES paralysis. It may also be an adaptation to wheelchair use. Whatever the case, it seemed effective in dealing with perturbations in the posterior direction. Wheelchair seats are generally designed with a posterior incline of 15 to 20 degrees – in some cases more – such that gravity pulls the user into the seat.

Only one SCI subject was able to perform the tests at a comparable level to the able-bodied subjects (subject #11). This was because his injury was very low (T12), thus he had voluntary control of most of his trunk muscles. Still, his results were significantly inferior to the able-bodied sample, particularly in the anterior direction. Interestingly, in the posterior direction, subject #11 recorded a superior performance to the able-bodied sample. This was likely due to the kyphotic posture and its inherent resistance to posterior perturbations.

The other SCI subjects had injuries in the upper thoracic region. As expected, they had far more difficulty coping with perturbations than the T12 subject and the able-bodied subjects. They struggled to sit unassisted without any perturbation. They could resist small perturbations, but the response was often erratic and prolonged. The sample of SCI subjects was insufficient to address the second hypothesis.

The third hypothesis was proven by the data gathered from the able-bodied subjects. The able-bodied subjects all responded to lateral perturbations with lateral spine flexion in the opposite direction. For example, if the seat tipped left, they would flex their trunk to the right, keeping their shoulders roughly parallel to the ground. The SCI subjects would also flex in the opposite direction by using exaggerated shoulder movements, often tilting their heads and bringing one shoulder right up to the jaw, thus stretching the latissimus dorsi to an extreme. They tended to overcompensate with two or three times as much trunk flexion as the perturbation angle, whereas the able-bodied subjects tended to flex roughly equal to the perturbation angle.

All three SCI subjects who performed trials on the apparatus exhibited a strong tendency to flex left or right in response to anterior and posterior perturbations. In other words, their response was asymmetric. Many of the able-bodied subjects responded this way as well, but to a much lesser degree.

The dysreflexic response to stimulation observed in subject #12 was likely triggered by pain receptors on the skin where the electrodes were placed, or possibly by muscle damage resulting from stimulation. None of the other subjects

exhibited any dysreflexia. It is uncertain what proportion of the SCI population will react similarly to trunk FES.

2.5.2 Usefulness of stability definition & measurement methodology

In order to assess FES systems that aim to bolster the paralyzed trunk, an objective measure of trunk stability is necessary. In the rehabilitation literature, there is disagreement regarding how trunks stability is defined and measured. We chose to define it in two different ways: (1) the maximum magnitude of perturbation that can be resisted, and (2) the amount of time it takes to respond to a standardized perturbation. The latter was only applicable to able-bodied subjects.

We developed a novel apparatus and measurement method based on these definitions. It is possible that the measurement method for SCI subjects could be used for injury classification. Our methods could conceivably be applied to other populations, for example, individuals with vestibulo-motor disorders. It could be a useful clinical tool for assessing treatments and rehabilitation programs for a wide range of neurological disorders that affect the trunk, not just SCI.

2.5.3 Further work

Foremost, more SCI data is needed in order to make reasonable conclusions about the efficacy of trunk FES. Unfortunately, we had a very difficult time recruiting SCI subjects for this study.

The trunk FES method needs to be extended. There are a lot of possibilities. In this study, FES was applied to a small region on the back targeting the ES innervated from L1 and L2. A multiple electrode system that targets ES from L5 all the way up to the level of injury may provide greater rigidity, and therefore more resistance to perturbations in the anterior and lateral direction. Furthermore, stimulation of the external obliques should be attempted, and its effect on lateral stability assessed. For a better understanding of what trunk muscles contribute to stability and how, an EMG study should be performed on able-bodied subjects. The apparatus from this study could be used.

The contraction of the RA when the ES was stimulated in subjects #12 and #13 warrants investigation. There is currently a lot of discussion in the

biomechanics literature concerning co-contraction of trunk muscles (e.g. Cholewicki et al., 2000). Knowledge of a reflex arc between ES and RA would be valuable to that discussion as well as to general physiology.

Further evaluation of the measurement method is required. Although we did not endeavor to assess the repeatability of the test protocol from session to session, our data concerning subject #3, who was measured on two separate occasions, suggested that the able-bodied test might not produce repeatable results. Why subject #3 performed so much better in the second session could be the result of many factors. For example, the first session may have taken place at a time when she was fatigued or under the weather.

We believe the kyphotic posture assumed by the SCI subjects is common among that population. Its affect on seated trunk stability merits close examination. Our experimental protocol did not account for different postures. In future experiments using the tilt-seat apparatus, posture should be standardized either by establishing a rigid procedure of entering the seat, or by adding some pelvic alignment features to the seat itself. For example, the sacral support could be mounted on a horizontal shaft such that once the subject is in the seat, it could be slid forward until the pelvis is aligned vertically.

The measurement apparatus used in this study was a far from perfect prototype. One major limitation is that it relied upon a human operator to apply the perturbation. Although great care was taken to apply similar perturbations to every trial, there was some variation. By replacing the human operator with a controlled actuator, for example a servomotor or a hydraulic cylinder, more consistent perturbations could be applied. Further analysis should be performed to determine the robustness of the measurement technique with respect to variations in perturbation.

Another way to improve the apparatus would be to install a load cell on the tilt arm. That way the moment at the hinge could be determined, and moments along the trunk could be estimated using inverse dynamics. Even better, the base could be redesigned to stand upon a force plate thus providing the ground reaction force and center of pressure location. Such data might be useful.

Although the Pico sensor system is very portable, the tilt-seat apparatus is not. The next version might include a quick release mechanism that allows the seat arm to be detached from the base so that the two can be packed together for easy transport. The base was made massive (approx. 40kg) to ensure that it would remain stationary during the experiment. Perhaps another method of securing it to the ground can be devised such that the base need not be so heavy and inconvenient to transport.

2.6 References

Cholewicki J, Panjabi MM, Khachatryan A. Stabilizing function of trunk flexor-extensor muscles around a neutral spine posture. *Spine*, 22(19):2207-2212, 1997.

Cholewicki J, Juluru K, McGill SM. Intra-abdominal pressure mechanism for stabilizing the lumbar spine. *Journal of Biomechanics*, 32(1):13-17, 1999.

Cholewicki J, Polzhofer GK, Radebold A. Postural control of trunk during unstable sitting. *Journal of Biomechanics*, 33(12):1733-1737, 2000.

Douglas R, Larson PF, D'Ambrosia R, McCall RE. The LSU reciprocating gait orthoses. *Orthopedics*, 6:834-839, 1983.

Forssberg H, Hirschfeld H. Postural adjustments in sitting humans following external perturbations: muscle activity and kinematics, *Experimental Brain Research*, 97:515-527, 1994.

Franchignoni FP, Tesio L, Ricupero C, Martino MT. Trunk control test as an early predictor of stroke rehabilitation outcome, *Stroke*, 28:1382-1385, 1997.

Fujita K, Hoshimiya N, Handa Y, Ichie M. Feedback postural control of trunk in paraplegic standing via FES. *Proceedings of the 2nd International FES Symposium*, 160-5, 1995.

Gardner-Morse MG, Stokes IAF. Trunk stiffness increases with steady-state effort, *Journal of Biomechanics*, 34(4):457-463, 2001.

Gracovetsky S. *The Spinal Engine*, Springer-Verlag, Wien-New York, 1988.

Hardcastle P, Bedbrook G, Curtis K. Long-term results of conservative and operative management in complete paraplegics with spinal cord injuries between T10 and L2 with respect to function. *Clinical Orthopaedics and Related Research*, 224:88-96, 1987.

Karcnik T, Kralj A, Bajd T. Crutch assisted FES gait and upright stability assessment. In: Pedotti A, Ferrarin M, Quintern J, Riener R (eds) *Neuroprosthetics: from Basic Research to Clinical Applications*, Springer-Verlag, Berlin, 1996.

Lavender SA, Marras WS. The effects of a temporal warning signal on the biomechanical preparations for sudden loading, *Journal of Electromyography and Kinesiology*, 5(1):45-56, 1995.

Licht S. *Therapeutic Electricity and Ultraviolet Radiation*. Waverly Press, Baltimore, 1967.

Lucas DB, Bresler B. *Stability of the Ligamentous Spine*. Report no. 40 from the Biomechanics Laboratory, University of California, San Francisco, Berkeley, 1961.

Shephard RJ. Sports medicine and the wheelchair athlete. *Sports Medicine*, 5(4):226-47, 1988.

Shurr DG, Goel VK, Weinstein JN. Spinal orthoses in lumbar spine disease. In: Goel VK, Weinstein JN (eds.) *Biomechanics of the Spine: Clinical and Surgical Perspective*, CRC Press, pp. 233-50, 1990.

Vezina MJ, Hubley-Kozey CL. Muscle activation in therapeutic exercises to improve trunk stability. *Archives of Physical Medicine and Rehabilitation*, 81(10):1370-1379, 2000.

Vicon 140 version 1.0, Movement analysis hardware & software, Oxford Metrics Ltd, Oxford, 1996.

(a) front view

(b) oblique view from behind and above

(c) seat and hinge from behind

Figure 2-1: Prototype tilt-seat apparatus shown from various points of view.

Figure 2-2: SCI subject #13 shown on tilt-seat apparatus between trials. The blue goniometer is attached to the skin over spinous processes of T4 and L2. The two visible white pads are the active electrodes. Passive electrodes are obscured behind sacral pad of apparatus.

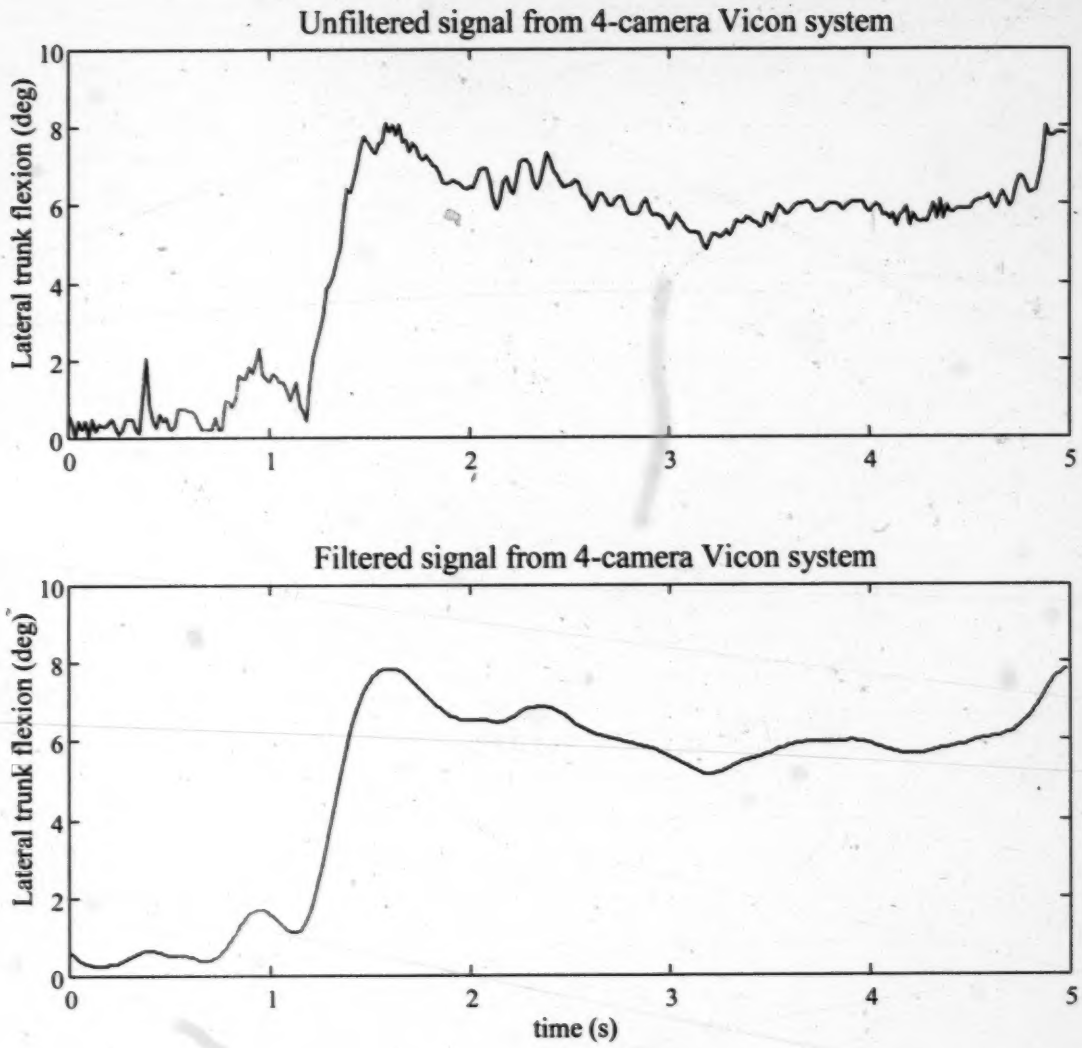
Unfiltered signal from 4-camera Vicon system
Lateral trunk flexion (deg)
Filtered signal from 4-camera Vicon system
Lateral trunk flexion (deg)
time (s)

Figure 2-3: Comparison between a raw data signal from the 4-camera Vicon system and the signal after being smoothed by a second-order Butterworth filter with a cutoff frequency of 3 Hz.

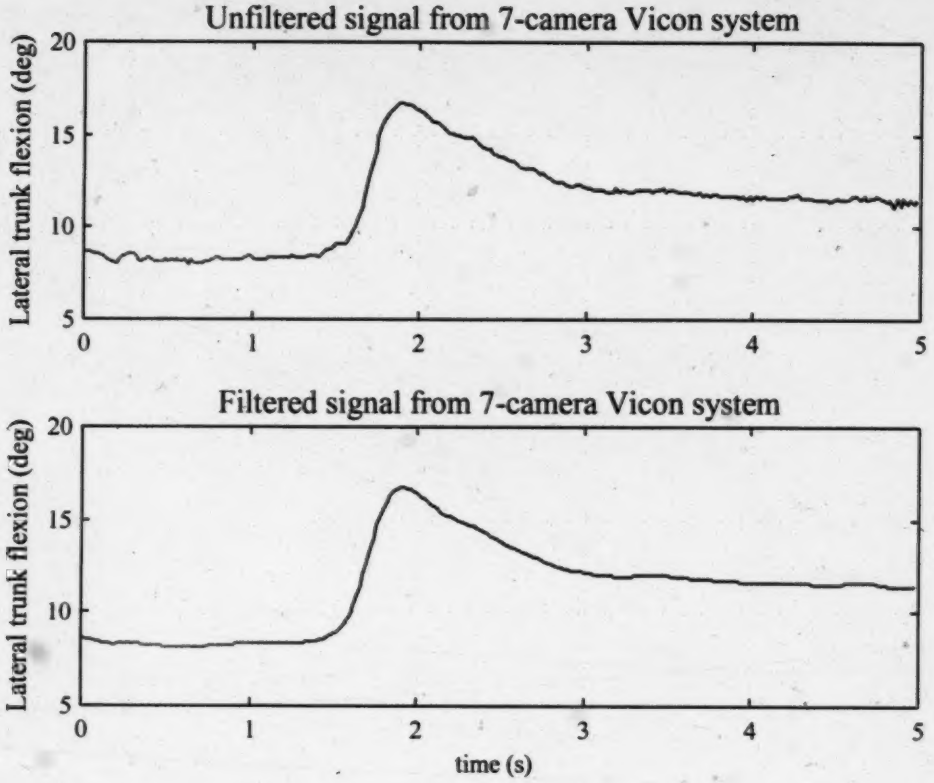

Figure 2-4: Comparison between a raw data signal from the 7-camera Vicon system and the signal after being smoothed by a second-order Butterworth filter with a cutoff frequency of 3 Hz.

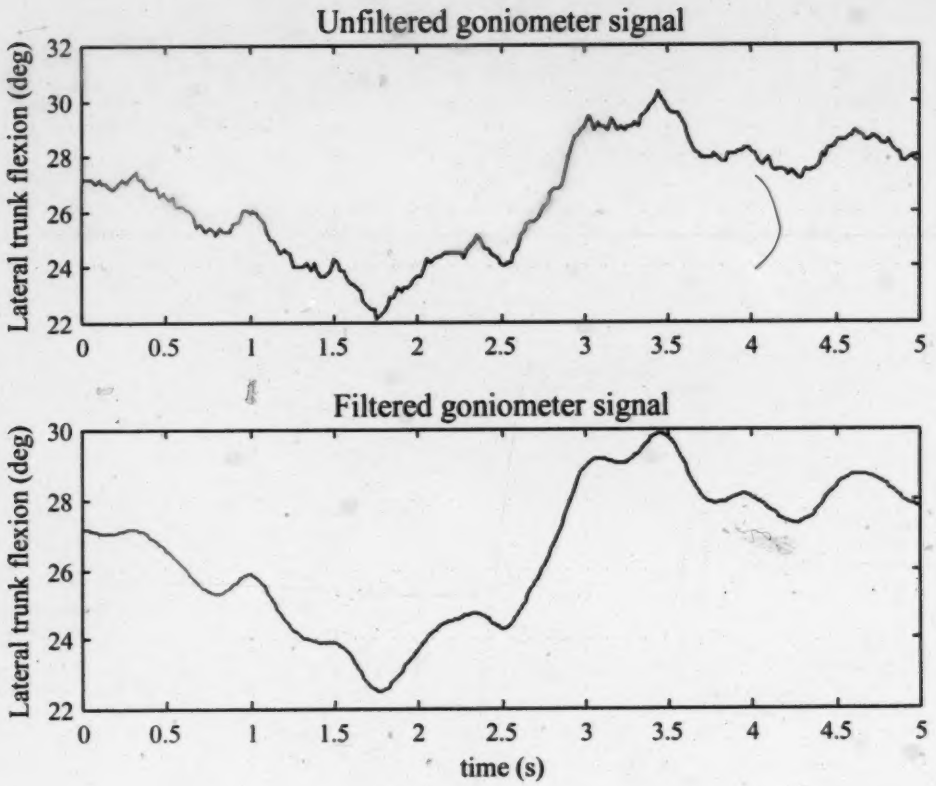

Figure 2-5: Comparison between a raw data signal from the portable sensor system and the signal after being smoothed by a second-order Butterworth filter with a cutoff frequency of 3 Hz.

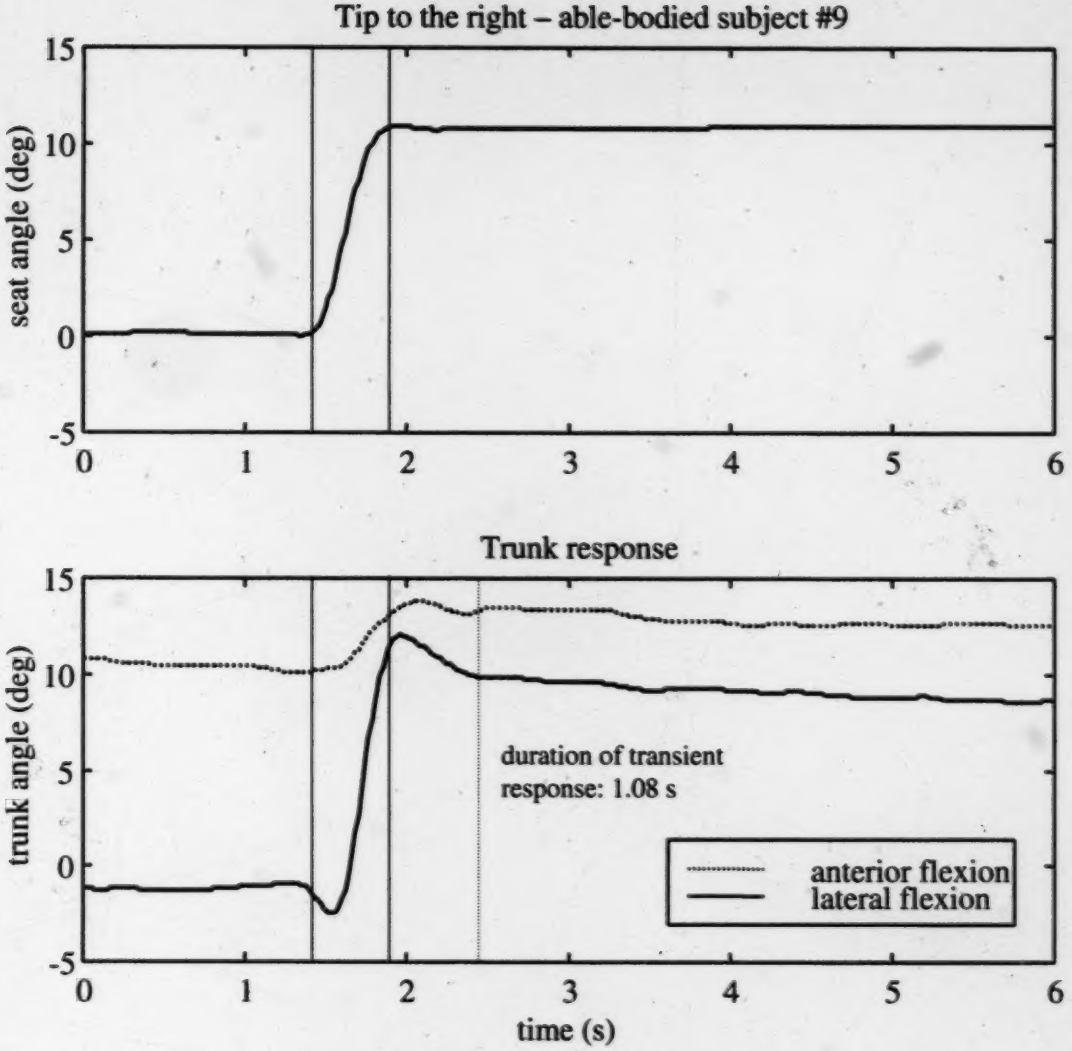

Figure 2-6: Typical data from an able-bodied trunk stability trial. The solid blue curve represents lateral flexion of the spine; (+)ve right, (-)ve left. The dashed green curve represents flexion in the anterior direction; (-)ve indicates posterior flexion. The solid vertical red lines indicate the onset of perturbation and the end of the perturbation. The dashed vertical red line indicates the end of the transient response, after which no movement greater than 1.00 deg/s was detected.

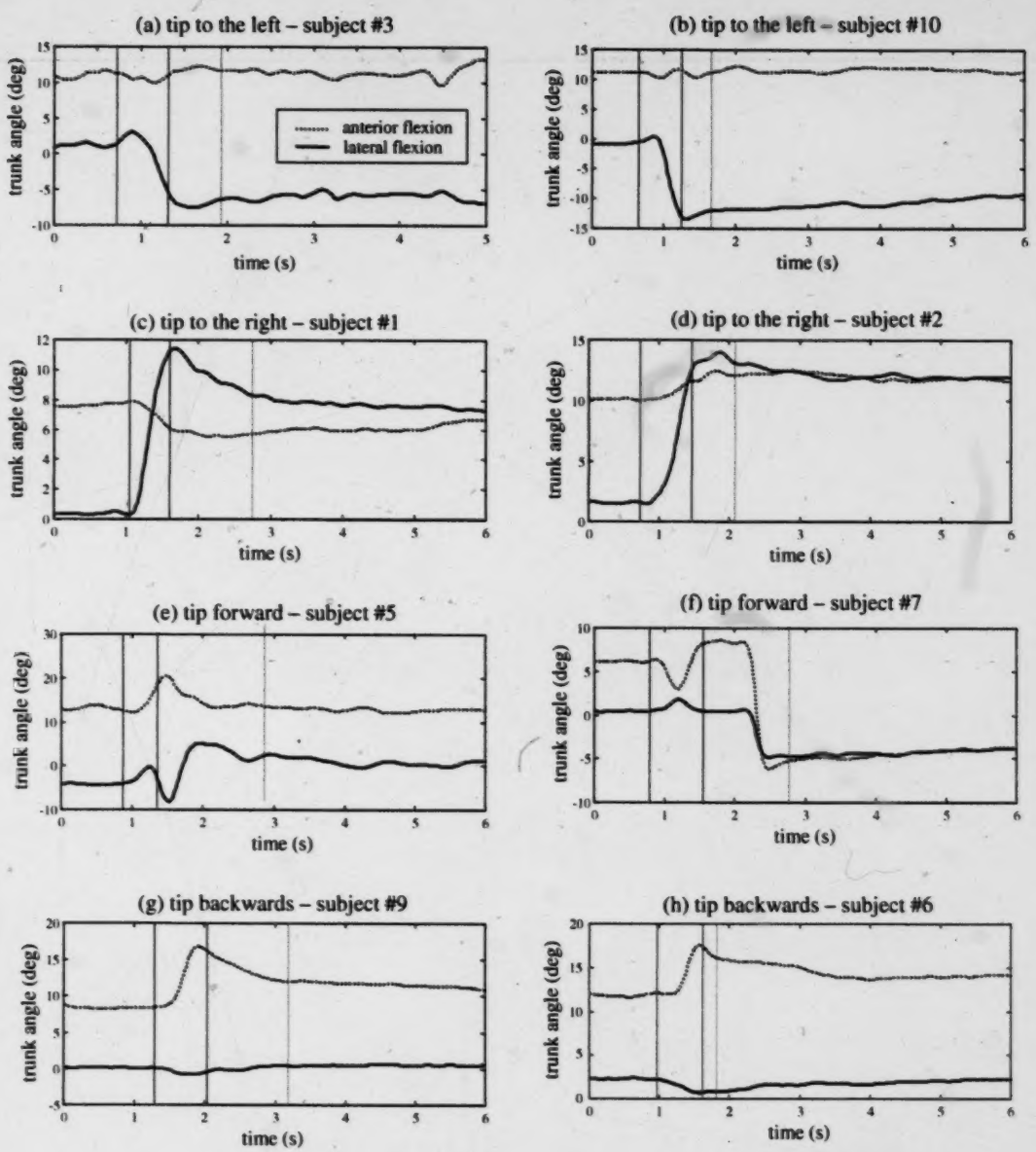

Figure 2-7: Typical data from able-bodied trunk stability trials. The solid blue curve represents lateral flexion of the spine; (+)ve left, (-)ve right. The dashed green curve represents flexion in the anterior direction; (-)ve indicates posterior flexion. The solid vertical red lines indicate the onset of perturbation and the end of the perturbation. The dashed vertical red line indicates the end of the transient response, after which no movement greater than 1.00 deg/s was detected.

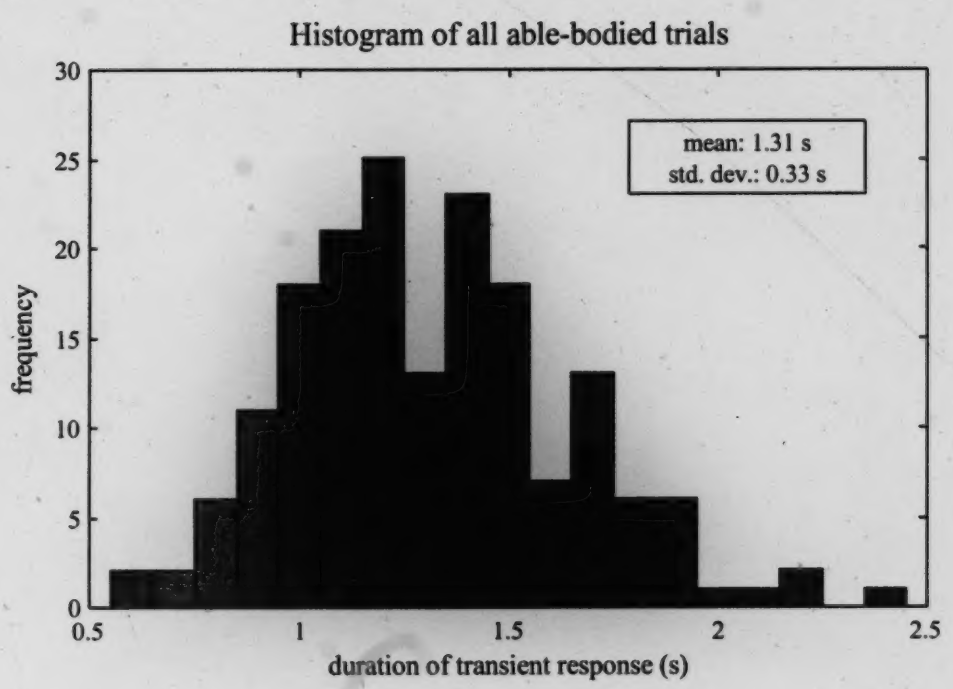

Figure 2-8: The distribution of transient response time was roughly normal for the entire able-bodied population.

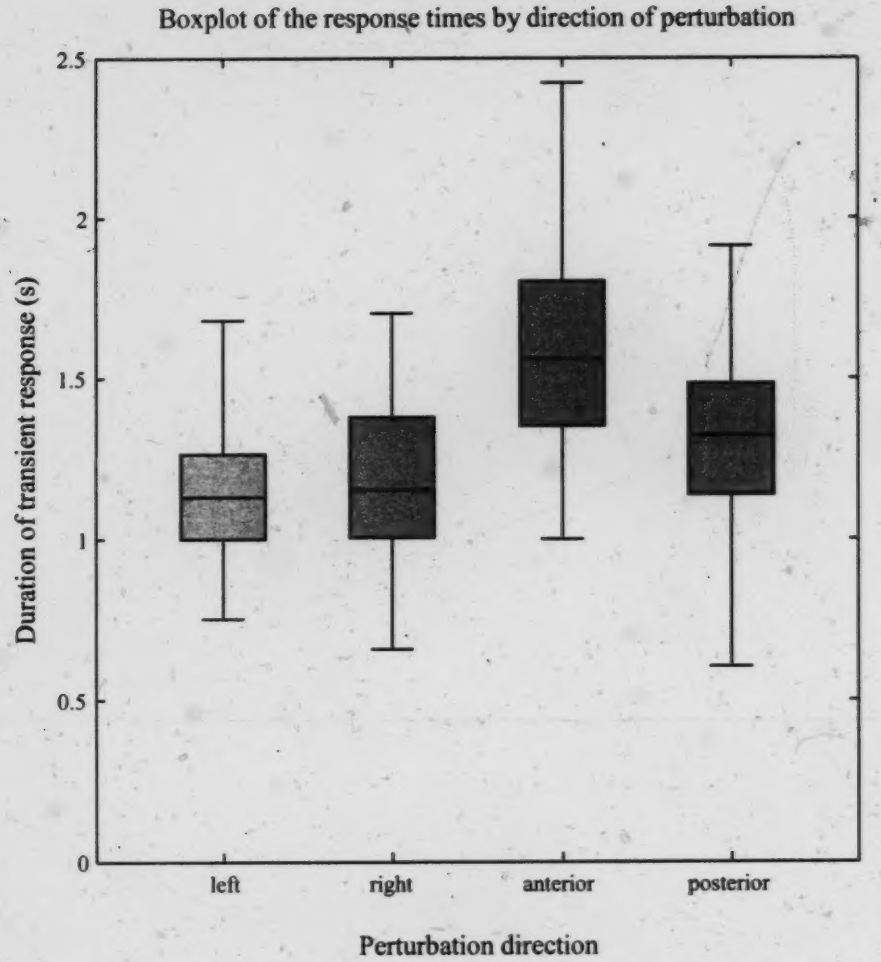

Figure 2-9: Boxplots of the able-bodied data illustrate the similarity and differences between response times for different types of perturbation (N = 40, boxes contain second and third quartiles, midline indicates median, whiskers span full range of data). Anterior perturbations elicited the slowest responses (p-value < 0.0001).

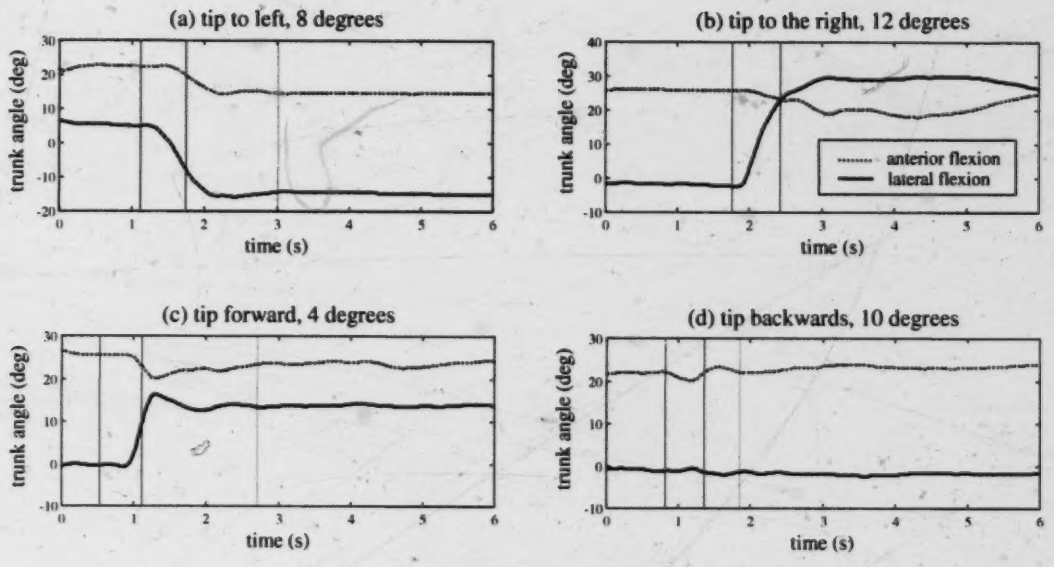
(a) tip to left, 8 degrees
(b) tip to the right, 12 degrees
(c) tip forward, 4 degrees
(d) tip backwards, 10 degrees
trunk angle (deg)
time (s)
anterior flexion
lateral flexion

Figure 2-10: Typical data from subject #11 trunk stability trials. All trials shown were successful, except for (b), in which an operator intervened at t = 3s. The solid blue curve represents lateral flexion of the spine; (+)ve left, (-)ve right. The dashed green curve represents flexion in the anterior direction; (-)ve indicates posterior flexion. The solid vertical red lines indicate the onset of perturbation and the end of the perturbation. The dashed vertical red line indicates the end of the transient response, after which no movement greater than 1.00 deg/s was detected.

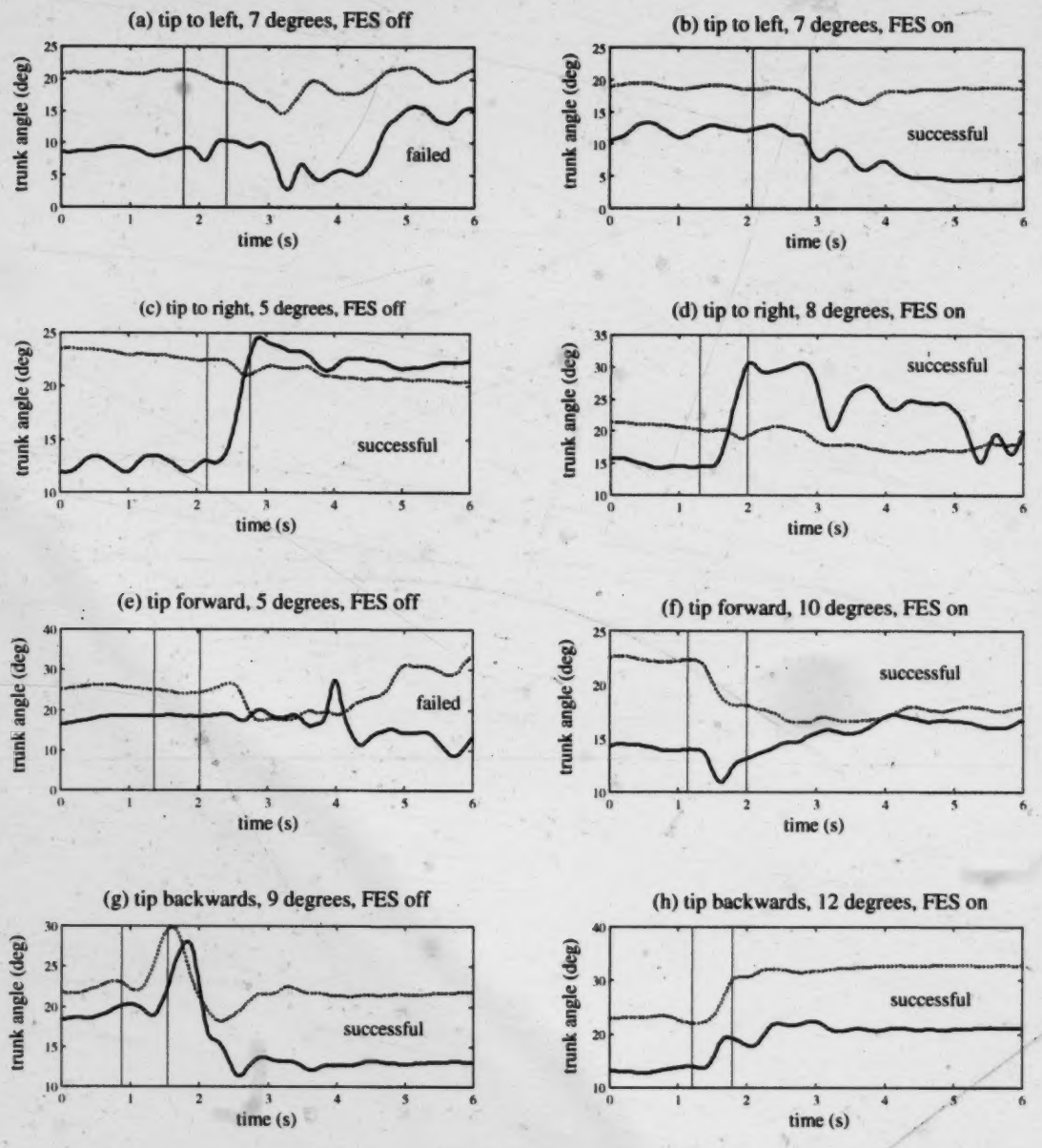
(a) tip to left, 7 degrees, FES off
failed
(b) tip to left, 7 degrees, FES on
successful
(c) tip to right, 5 degrees, FES off
successful
(d) tip to right, 8 degrees, FES on
successful
(e) tip forward, 5 degrees, FES off
failed
(f) tip forward, 10 degrees, FES on
successful
(g) tip backwards, 9 degrees, FES off
successful
(h) tip backwards, 12 degrees, FES on
successful
trunk angle (deg)
time (s)

Figure 2-11: Typical data from subject #13 trunk stability trials. The solid blue curve represents lateral flexion of the spine; (+)ve left, (-)ve right. The dashed green curve represents flexion in the anterior direction; (-)ve indicates posterior flexion. The solid vertical red lines indicate the onset of perturbation and the end of the perturbation.

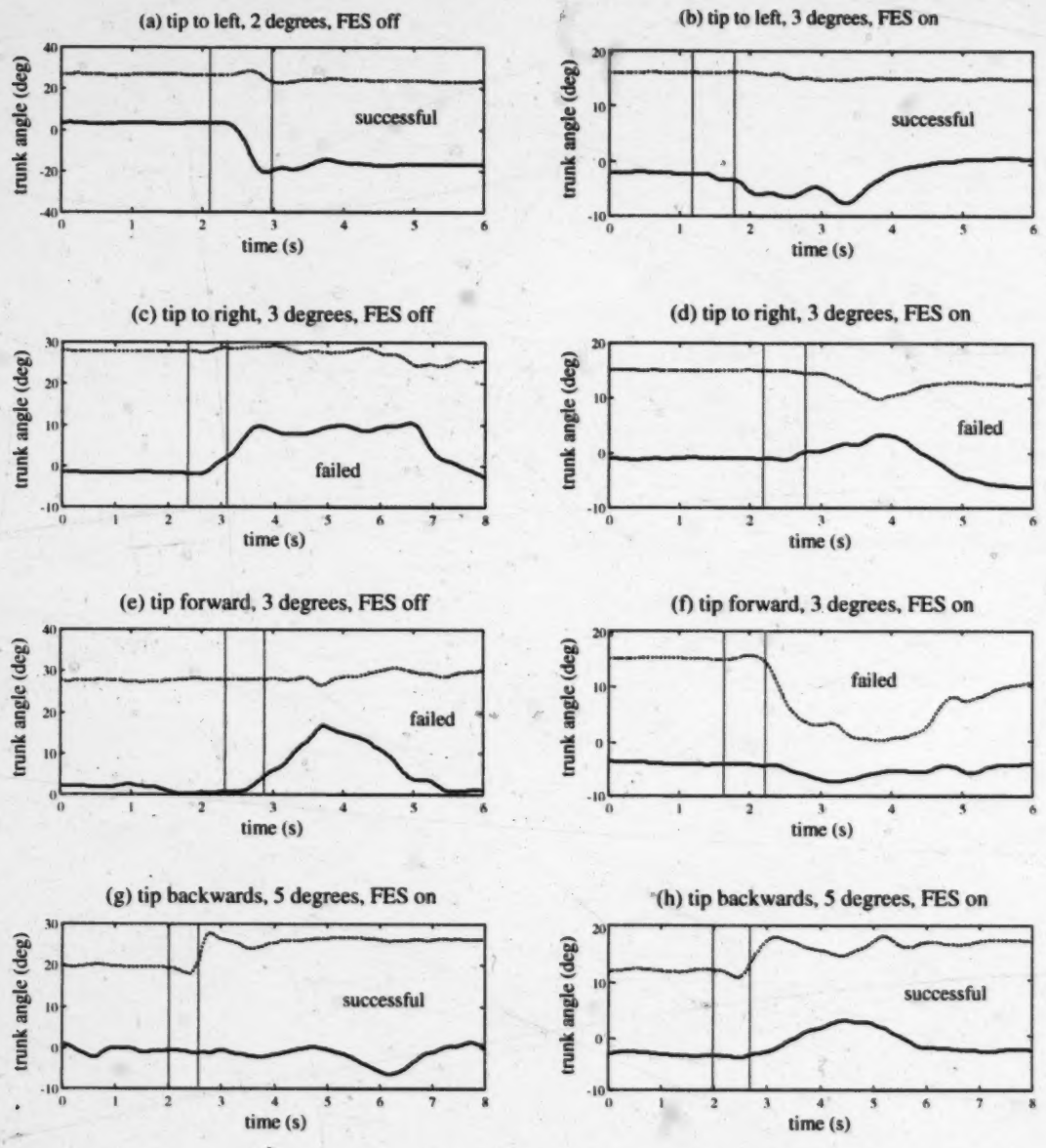
(a) tip to left, 2 degrees, FES off
successful
(b) tip to left, 3 degrees, FES on
successful
(c) tip to right, 3 degrees, FES off
failed
(d) tip to right, 3 degrees, FES on
failed
(e) tip forward, 3 degrees, FES off
failed
(f) tip forward, 3 degrees, FES on
failed
(g) tip backwards, 5 degrees, FES on
successful
(h) tip backwards, 5 degrees, FES on
successful
trunk angle (deg)
time (s)

Figure 2-12: Typical data from subject #14 trunk stability trials. The solid blue curve represents lateral flexion of the spine; (+)ve left, (-)ve right. The dashed green curve represents flexion in the anterior direction; (-)ve indicates posterior flexion. The solid vertical red lines indicate the onset of perturbation and the end of the perturbation.

3 The potential role of trunk momentum in FES assisted sit-to-stand

3.1 Abstract

The goal of this study was to find better strategies for paraplegic sit-to-stand. Current methods involve large, damaging loads on the shoulders that result from the overuse of the arms to overcome weak electrically stimulated leg muscles. A 3-segment planar model of the human body was devised, and it was used to simulate unassisted sit-to-stand using three different strategies. It was found that unassisted STS is theoretically possible for isometric knee moments as low as 50-70 Nm, if (1) the subjects sits with feet flat on the ground and knees flexed at right angles, (2) the hip extensors are stimulated with isometric moments of up to 200 Nm, and (3) the trunk is flexed at a rate of at least 75 deg/s at liftoff. The purpose of the trunk momentum was to carry the body's center of mass to a position above the new base of support – the feet. Trunk momentum reduced the risk of slipping and enabled larger than isometric hip extension moments by creating eccentric contractions. Trunk momentum did not significantly reduce the muscle strength requirements, as hypothesized. In fact, it increased the need for hip extension moment in order to prevent the trunk from falling too far forward. The hip extensors were found to be able to assist the knee extensors in creating lift-off. An increase of 5.6 Nm of hip extensor moment reduced the knee extensor demands by 1 Nm. The popular strategy of starting from a position where one's feet are directly under one's center of mass was found to require more muscle strength than was required by the flat foot strategies. This was largely because the knee extensors were stretched beyond their optimal length resulting in contractions that were weaker than the isometric strength of the muscles.

3.2 Introduction

Sit-to-stand (STS) is one of the most mechanically demanding maneuvers of daily life (Riley et al., 1991). In the last 20 years, it has been repeatedly demonstrated that some paraplegics can perform STS using functional electrical stimulation (FES) (e.g. Kralj and Bajd, 1989, Kagaya et al., 1995, Kordylewski and Graupe, 2001), however not all are candidates for this technology (Durfee,

1999). Since muscles undergoing FES lack the contractile strength of normal muscles, the subject must compensate with high arm forces resulting in shoulder loads up to 30-45% of the total body weight (Riener et al., 1998, Davoodi et al., 2001). This is problematic since many paraplegic individuals already suffer from shoulder pain and dysfunction (Goldstein et al., 1997, Sinnott et al., 2000), therefore alternative strategies for FES assisted STS must be found.

Studies on healthy, unassisted STS report maximum joint moments that range from 75-300 Nm at the hip, and 80-220 Nm at the knee (both legs combined) (e.g. Kralj and Bajd, 1989, Pai and Rogers, 1991, Kamnik et al., 1999, Lundin et al., 1999). Unfortunately, the maximum knee extension moment for a paraplegic undergoing FES is typically between 10 and 60 Nm per leg (Kralj and Bajd, 1989, Kagaya et al., 1995). Thus, few paraplegics are able to meet the apparent strength requirements for unassisted STS. It is not known exactly what moments are available from FES of hip extensors.

The primary objective of this study was to develop an improved STS strategy for users of the medially linked knee-ankle-foot orthosis (MLKAFO), a hybrid gait system. Before one can walk, one must stand. We desire a strategy that addresses the reduced muscle strength associated with FES, while significantly reducing vertical arm forces. In previous studies, closed loop FES control has successfully reduced arm forces compared to classical open loop control (Dolan, 1997, Riener and Fuhr, 1998). These methods, however, require special handgrips equipped with force and moment transducers to provide feedback signals. Such equipment is expensive and probably not accessible to a typical FES user outside of the laboratory. Our desired strategy is one that exploits the basic mechanics of the body, and which can be used in conjunction with a simple open loop FES scheme.

We also sought a strategy that would reduce the risk of slipping. In clinical practice, FES assisted STS sometimes results in one or both feet slipping forward, particularly in paraplegics with relatively strong quadriceps. To minimize slipping, Kralj and Bajd (1989) recommend that the paraplegic subject move to the edge of the seat and assume a static posture with the ankles, knees and trunk

almost fully flexed. This way, the center of mass is directly above the feet, and the subject can rise by pushing straight up. This strategy will be further analyzed in our study.

3.2.1 Biomechanics of STS

Several mechanical factors have been shown to affect the maximal hip and knee moments during unassisted STS. Among them: (1) increased chair height decreases the necessary knee extension moments (Rodosky et al., 1989); (2) anterior placement of the foot relative to the knee increases trunk flexion and hip moments (Shepherd and Koh, 1996); (3) when active trunk flexion is restricted, more muscle force is required (Shepherd and Gentile, 1994); (4) when STS is performed more rapidly, there is pronounced trunk flexion, and hip and knee moments increase (Kralj and Bajd, 1989, Pai and Rogers, 1990, Hutchinson et al., 1994). The last three findings illustrate that the trunk plays an important mechanical role in STS, one which is capable of reducing the muscle requirements at the hip and knee. If the trunk can alleviate the muscle demands on the legs somewhat, then certain trunk strategies may relieve the arms in FES assisted STS.

Some have postulated that the trunk momentum, built up during the flexion phase, may reduce the large demands on hip and knee extensors (Riley et al., 1991, Shepherd and Gentile, 1994). In a computer simulation study of FES assisted paraplegic standing, Davoodi and Andrews (1997) demonstrated that, at least theoretically, the arms could be unloaded completely using a strategy of trunk rotation, even with the reduced strength of stimulated knee extensors. Others have found evidence that the trunk momentum has little effect on the forces of STS (Hughes et al., 1996, Crosbie et al., 1997).

One relationship that remains largely unexplored is that of hip extension moment to knee extension moment. Can lower knee extension moments be used for STS if larger hip extension moments are produced? FES assisted STS often involves stimulation of the knee extensors only. Cooperative stimulation of the hip extensors is less common, but its effect on the moment required of the knee extensors has yet to be proven.

3.2.2 On "momentum transfer"

Schenkman et al. (1990) wrote, "momentum transfer occurred when the momentum of the upper body … was transferred to the total body and contributed to total-body upward and anterior movement." This is, in fact, quite a bold assertion. If it is true, then a strategy of accelerating the trunk prior to lift-off ought to augment the arms, hips and knees in raising the whole body mass.

During STS, the upper and lower bodies interact via the hip joints and the muscles, tendons, ligaments, and other tissues that span them. Can this interaction effectively turn upper body momentum into vertical lift, and if so, what conditions affect it? A simple mechanical argument for this theory is depicted in Figure 3-1. The upper body rotates forward and then suddenly impacts on the lower body through a taut cable wrapped around the joint (representing the hip extensors). A collision occurs, and some of the angular momentum of the upper body is transferred to the lower body. The result is overall upward movement of the center of mass. It is perhaps better to think of this action in terms of kinetic energy instead of momentum.

Some studies into the "kinetic energy transfer" theory – that is, the theory that upper body motion generated prior to lift-off mechanically contributes to raising the whole body – have taken place in the last decade. However, the results are not all in agreement. Riley et al. (1991) supported the theory somewhat with a study on able-bodied women. They found that immediately after lift-off, the center of pressure under the feet displaced from the whole body center of mass created a "gravity torque" of approximately 36 Nm opposing the angular momentum of the upper body. Based only on that, they concluded that the momentum generated prior to lift-off is important for the critical phase immediately following lift-off. Shepherd and Gentile (1994) agreed based on findings that when trunk momentum was absent at lift-off, a greater sum of extension moments at the hip, knee and ankle is required.

Conversely, Hutchinson et al. (1994) reported that dynamic loads (those resulting from momentum and inertia) during STS are dominated by static loads, and hence can be neglected. In other words, quasi-static analysis of STS is

reasonably accurate. This, however, did not hold true for joints at the neck and lower back. Nothing about the momentum transfer theory could be concluded from this study. Crosbie et al. (1997) came up with similar, but more definitive results, concluding that, "motion-dependent moments do not significantly reduce the muscle moments required to stand up."

3.2.3 Hypotheses

H3. Thrusting the rigid trunk forward before lift-off during sit-to-stand in conjunction with hip extension moment will reduce required knee moment.

The following additional hypotheses were made in this study:

1. Weakness of the knee extensors can be compensated by an increase in hip extensor stimulation.
2. An initial sitting position with the trunk flexed far forward and the point of contact between the foot and ground positioned directly below the whole body center of mass will reduce the risk of slipping.

3.3 Methods

3.3.1 STS model

A standard 3-segment sagittal plane model of a person performing sit-to-stand in the MLKAFO was devised. The model, shown in Figure 3-2, is similar to other models commonly used in biomechanical studies (e.g. Iqbal and Pai, 2000). The ankles are locked in the neutral position by the brace, such that the shank and foot can be treated as one rigid body that pivots about the heel or toe. The brace applied no constraint to the knee. The hip joint was situated where the actual hips are located, not the medial joint of the brace. The head and trunk were treated as a single rigid body connected to the hips. Passive joint dynamics were described by a non-linear spring in parallel with a linear dashpot (Davy and Audu, 1987). The equations of motion describing the model are provided in Appendix A. Body segment parameters were calculated for a typical male of 75 kg mass and 1.80 m height according to the scaling methods of Dempster (1955).

The mono-articular knee extensors (vasti) and hip extensors were simulated using the common Hill-type muscle model described in section 1.6.6.

Activation signals were provided to the muscles according to an open loop FES scheme (pulse-width modulated), described below. A first-order recruitment response determined the activation level, which in turn produced the appropriate muscle contraction. The maximum isometric force of each muscle was varied. For the knee extensors, it was varied between 0 and 150 Nm. The hip extensors were independently varied between 0 and 300 Nm.

The chair was treated as a rigid obstacle that would apply the necessary force on the hip joint to prevent it from accelerating downward when the buttocks were in contact with the chair. The chair also prevented horizontally sliding.

3.3.2 STS strategies using open loop FES

Three different STS strategies were simulated. All used open loop control of FES whereby each stimulus signal was off for some predefined delay period. Then the stimulus came on full power. The muscles remained stimulated until the Ascending phase of STS had been completed, as defined by Kralj et al. (1990), i.e. the acceleration vector of the whole body center of mass changed from upwards to downwards.

Such "full on" open loop strategies are undesirable in clinical practice because the knees tend to reach full extension at high speed, which can be damaging to the joints. In this study, however, we are solely interested in the maximal joint moments, which tend to occur immediately following lift-off (Riley et al., 1991, Kagaya et al., 1995). As such, these simulations cover only the first portions of the STS cycle. It is assumed that horizontal arm forces would be able to correct the posture in the latter Stabilization phase.

Typical coefficients of friction for shoe/floor interaction during various activities are in the range of 0.2 to 0.6 (Chaffin et al., 1992, Chiou et al., 1996). In this study, if the ratio of horizontal ground reaction force to vertical ground reaction force exceeded 0.4, slip was implied, and the trial was considered a failure.

The three strategies tested are illustrated in Figure 3-3 and described below.

3.3.2.1 Trials 1 – flat foot static

The feet were positioned flat on the ground, and the trunk was flexed forward 60 degrees from the vertical. The hip and knee extensors were activated simultaneously with zero delay. The subject either rose from his chair or not. Maximum isometric hip and knee moments were varied between trials.

3.3.2.2 Trials 2 – flat foot dynamic

The feet were again positioned flat on the ground. The trunk was positioned vertically such that the hip and knee joints were both in 90 degrees of flexion. The trunk was given some initial angular velocity and allowed to flex forward. After a handpicked time delay, the hip and knee extensors were fully stimulated and the resultant trajectory was generated.

Trials were executed for six different initial trunk angular velocities in the range of 25 to 150 deg/s. These values represent the high and low end of trunk velocities reported in the STS literature.

3.3.2.3 Trials 3 – Kralj position

The hip was moved to the very edge of the seat, and the trunk was flexed 60 degrees forward. The knees were flexed such that the point of contact between the toe and ground was 2.5 cm in front of the projection of the whole body center of mass on the floor. The hip and knee extensors were activated simultaneously with no delay.

3.4 Results

3.4.1 Validation of the model

It was confirmed that the equations of motion describing the model were conservative. Total mechanical energy remained constant when it was executed without damping elements.

3.4.2 Trials 1 – flat foot static

None of the flat foot static trials were successful. During most, the subject failed to achieve lift-off. The set of isometric hip and knee moments for which lift-off could not occur is illustrated as the darkest shaded region in Figure 3-4. The line dividing the "no lift-off" region from the other regions illustrated a negative relationship between hip and knee strength. The necessary isometric

knee extension moment could be reduced by 1.0 Nm by increasing the hip moment by 5.9 Nm.

There was a small set of joint moments that resulted in the foot slipping immediately after lift-off, indicated by the pink region in Figure 3-4. The remaining trials resulted no slip, however, the shank segment began to rotate backwards about the heel immediately following lift-off. Thus, the leg would strike the edge of the chair. Figure 3-5 illustrates a typical example of a rock-back failure. The reason for the rock-back failures is that as soon as the subject lifted off from the seat, his center of mass was located 13 cm behind his heels. Since the center of mass had no forward momentum, it could not travel to a position above the new base of support. At the instant of lift-off, the displacement of the whole body center of mass yielded a gravity torque of 96 Nm backwards.

3.4.3 Trials 2 – flat foot dynamic

Many of the dynamic trials were successful. A typical successful simulation is shown in Figure 3-6. The initial velocity of the trunk (75 deg/s) and joint moments (150 Nm and 100Nm, hip and knee respectively) prevented both rock-back and slipping. All trials in this part of the study involved eccentric contractions of the hip extensors prior to lift-off, which often yielded higher than isometric hip moments. This is seen in Figure 3-6. Also, it is indicated that the peak joint moments occur immediately following lift-off.

The majority of the dynamic trials, however, failed in one of four ways: 1) lift-off did not occur, 2) the feet slipped, 3) rock-back, or 4) the upper body center of mass fell forward and never began to rise. Figure 3-7 illustrates the failure and success regions for trials involving different initial trunk velocities. Successful trials did not occur for initial trunk velocities of 50 deg/s and less. The threshold line that divided the "no lift-off" region from the other regions was almost identical to the line found in the static trials. It had a negative slope of –5.8 to –5.5 for all initial trunk velocities. Increases in the trunk velocity tended to shift the lift-off threshold line to the left approximately one Nm per every 25 deg/s increase.

Many of the dynamic trials resulted in rock-back failures, but the occurrence was reduced with increasing initial trunk velocity. With increased trunk velocity, the upper body tended to flex too far forward and never recover. Large hip extension moments were required to resist this action.

The point on the graphs in Figure 3-7 where the lift-off threshold line meets the line that divided the "fall forward" and "success" regions represents optimal joint muscle strengths for STS. Table 3-1 summarizes these points for the four trunk velocities tested that yielded successful trials.

Table 3-1; Optimal hip and knee moments for dynamic strategy

Initial trunk velocity (deg/s)	Isometric knee moment (Nm)	Isometric hip moment (Nm)
75	70	140
100	67	148
125	59	158
150	51	185

3.4.4 Trials 3 – Kralj position

Higher isometric hip and knee moments were required to stand up from the Kralj position. Figure 3-8 shows the failure and success regions. There was no slipping and no roll-back failure. Fall-forward failures did occur when the hip extension moment was below approximately 120 Nm. Figure 3-9 illustrates such a failure. The threshold line between the "no lift-off" region and other regions was further to the right than it was for the flat foot strategies, indicating higher hip and knee moments. Here, it had a negative slope of –8.6. The optimal hip and knee moments were 123 Nm and 124 Nm, respectively.

3.5 Discussion

This study sought ways for paraplegics to overcome the very weak knee extension moments associated with FES while performing STS without relying on their arms. Three different strategies for unassisted STS were simulated. Simple open loop FES control schemes were defined with the purpose of reducing the strength requirements while avoiding failure modes such as slipping and falling backward or forward.

3.5.1 Major findings

According to the results, unassisted STS is theoretically possible for isometric knee moments as low as 50-70 Nm, if (1) the subject sits with feet flat on the ground and knees flexed at right angles, (2) the hip extensors are stimulated with isometric moments of up to 200 Nm, and (3) the trunk is flexed at a rate of at least 75 deg/s at liftoff.

It was found that the hip extensors can assist the knee extensors to create lift-off during unassisted STS, which validates the second hypothesis. From both static and dynamic initial conditions, there was a negative, linear correlation between isometric hip and knee moments required for lift-off. When starting from a sitting position with the foot flat on the ground, an increase of 5.6 Nm of hip extensor moment reduces the knee extensor demands by 1 Nm. The results suggest that the hip extensors should be stimulated in cooperation with the knee extensors during paraplegic STS, as this augments lift and will logically relieve the arms. This concurs with Pai et al. (1994), who reported that arthritis patients use increased hip extension moment as a means to overcome reduced knee extension moment.

When the foot was placed flat on the ground and the knees flexed at right angles, STS was only possible when trunk momentum was present. The trunk momentum carried the body's center of mass to a position over the feet. When trunk momentum was too small, the 96 Nm gravity torque caused the body to rock backward about the heels. In practice, this gravity torque would have to be counteracted by external forces, i.e. the arms would have to pull the body forward.

The results indicated that the minimum speed at which the trunk must flex to avoid rock-back failure is between 50 and 75 deg/s. The effect of trunk momentum on the hip and knee moment requirements for lift-off was negligible, thus invalidating the first hypothesis. This is in agreement with a number of other studies that suggest that STS is dominated by gravitational forces, not motion-dependent forces (Hutchinson et al., 1994, Hughes et al., 1996, Crosbie et al., 1997).

The drawback of large amounts of trunk momentum was that more hip extension moment was needed to prevent the subject from falling forward. The presence of trunk momentum at lift-off also reduced the risk of slipping. Also, slipping was prevented by starting in the Kralj position (third hypothesis confirmed). Another effect of the trunk momentum was that it enabled the hip extensors to create moments that were larger than the isometric moment in that the muscles were lengthening, and thus contractions were eccentric.

The present study found that the Kralj position required somewhat more muscle strength than was required by the flat foot strategies. This was largely because the knee extensors were stretched beyond their optimal length resulting in contractions that were weaker than the isometric strength of the muscles. There was no risk of slipping when beginning from the Kralj position.

3.5.2 Comments on methodology

As this was a computer simulation study, it addressed only the theoretical issues of STS biomechanics. The model used in this study was very similar to others that have been employed in FES assisted STS studies (e.g. Davoodi and Andrews, 1997, Riener and Fuhr, 1998). As in those studies, we treated the trunk as a rigid body. However, we know this to be untrue. That large moments can be carried through the paralyzed trunk is questionable. In some cases, SCI patients will have undergone spinal fixation. This is likely to positively affect the load carrying ability of the spine, but it remains to be studied in the context of STS.

3.5.3 Further work

As this was a theoretical study, a logical follow-up would be to collect clinical data on actual paraplegic subjects attempting to perform STS using the strategies that were described here.

Very little has been reported on the strength of electrically stimulated hip extensors. Although the results of the dynamic trials indicate that hip extensor moments of at least 140 Nm are needed for success, it is not known if contractions of such magnitude are possible through FES. In the STS literature, hip extension moments range from approximately 75 to 160 Nm for able-bodied individuals (Bajd et al., 1982, Berger et al., 1989), however some reports go as high as 300

Nm (Fleckenstein et al., 1988). Further study is necessary to determine if the values predicted by this study are feasible.

Some limitations of the model could be addressed in a future study. A multi-segmented model of the trunk should definitely be considered. Difficulty will lie in accurately modeling the spinal joints.

3.6 References

Bajd T, Kralj A, Turk R. Standing-up of a healthy subject and a paraplegic patient, *Journal of Biomechanics*, 15:1-10, 1982.

Berger RA, Riley PO, Mann RW, Hodge WA. Total body dynamics in ascending stairs and rising from a chair following total knee arthroplasty, *Proceedings 34th Annual Meeting of the Orthopaedic Research Society*, 13:542, 1988.

Berger RA, Schenkman ML, Riley PO, Hodge WA. Advantages of rising from a chair to quantitate human performance, *Proceedings 35th Annual Meeting of the Orthopaedic Research Society*, 6-9 Feb, Las Vegas, Nevada, p. 91, 1989.

Chaffin DB, Woldstad JC, Trujillo A. Floor/shoe slip resistance measurement, *American Industrial Hygiene Association Journal*, 53:283-289, 1992.

Chiou S-Y, Bhattacharya A, Succop PA. Effect of workers' shoe wear on objective and subjective assessment of slipperiness, *American Industrial Hygiene Association Journal*, 57:825-831, 1996.

Crosbie J, Herbert RD, Bridson JT. Intersegmental dynamics of standing from sitting, *Clinical Biomechanics*, 12:227-235, 1997.

Davoodi R, Andrews BJ. Standing up in paraplegia: a comparative study of fixed parameter controllers, *Proceedings 2nd Annual Conference of the International Functional Electrical Stimulation Society*, Burnaby, Canada, pp. 93-94, 1997.

Davoodi R, Kamnik R, Andrews BJ, Bajd T. Predicting the voluntary arm forces in FES-assisted standing up using neural networks, *Biological Cybernetics*, 85(2):133-143, 2001.

Davy DT, Audu ML. A Dynamic optimization technique for predicting muscle forces in the swing phase of gait, *Journal of Biomechanics*, 20(2):187-201, 1987.

Dempster WT. Space requirements for the seated operator, *WADC Technical Report 55-159*, 1955.

Dolan MJ. *Restoration and biomechanical evaluation of standing up and sitting down in paraplegics using functional electrical stimulation*, Ph.D. Thesis, University of Glasgow, Scotland, 1997.

Durfee WK. Electrical stimulation for restoration of function, *Neurorehabilitation*, 12(1):53-62, 1999.

Fleckenstein SJ, Kirby RL, Macleod DA. Effects of limited knee flexion range on peak hip moments of forces while transferring from sitting to standing, *Journal of Biomechanics*, 21:915-918, 1988.

Goldstein B, Young J, Escobedo EM. Rotator cuff repairs in individuals with paraplegia, *American Journal of Physical Medicine & Rehabilitation*, 76:316-322, 1997.

Kordylewski H, Graupe D. Control of neuromuscular stimulation for ambulation by complete paraplegics via artificial neural networks, *Neurological Research*, 23(5):472-481, 2001.

Hughes MA, Myers BS, Schenkman ML. The role of strength in rising from a chair in the functionally impaired elderly, *Journal of Biomechanics*, 29(12):1509-1513, 1996.

Hutchinson EB, Riley PO, Krebs DE. A Dynamic analysis of the joint force and torques during rising from a chair, *IEEE Transactions on Rehabilitation Engineering*, 2:49-56, 1994.

Iqbal K, Pai Y-C. Predicted region of stability for balance recovery: motion at the knee joint can improve termination of forward movement, *Journal of Biomechanics*, 33(12):1619-1627, 2001.

Kagaya H., Shimada Y, Ebata K, Sato M, Sato K, Yukawa T, Obinata G. Restoration and analysis of standing-up in complete paraplegia utilizing functional electrical stimulation, *Archives of Physical Medicine and Rehabilitation*, 76:876-881, 1995.

Kamnik R, Bajd T, Kralj A. Functional electrical stimulation and arm supported sit-to-stand transfer after paraplegia: a study of kinetic parameters, *Artificial Organs*, 23:413-417, 1999.

Kralj A, Bajd T. *Functional Electrical Stimulation: Standing and Walking after Spinal Cord Injury*, CRC Press Inc, Boca Raton, Florida, 1989.

Kralj A, Jaeger RJ, Munih M. Analysis of standing up and sitting down in humans: definitions and normative data presentation. *Journal of Biomechanics*, 23(11):1123-1138, 1990.

Lundin TM, Jahnigen DW, Grabiner MD. Maximum trunk flexion angle during the sit to stand is not determined by knee or trunk-hip extension strength in healthy older adults, *Journal of Applied Biomechanics*, 15:233-241, 1999.

Pai Y-C, Rogers MW. Control of body mass transfer as a function of speed of ascent in sit-to-stand, *Medicine and Science in Sports and Exercise*, 22:378-384, 1990.

Pai Y-C, Rogers MW. Speed variation and resultant torques during sit-to-stand, *Archives of Physical and Medical Rehabilitation*, 72:881-885, 1991.

Pai Y-C, Chang HJ, Chang RW, Sinacore JM, Lewis JL. Alteration in multijoint dynamics in patients with bilateral knee osteoarthritis, *Arthritis & Rheumatism*, 37:1297-1304, 1994.

Riener R, Fuhr T. Patient-driven control of FES-supported standing up: a stimulation study, *IEEE Transactions on Rehabilitation Engineering*, 6:113-124, 1998.

Riley PO, Schenkman ML, Mann RW, Hodge WA. Mechanics of a constrained chair-rise, *Journal of Biomechanics*, 24:77-85, 1991.

Rodosky MW, Andriacchi TP, Anderson GBJ. The influence of chair height on lower limb mechanics during rising, *Journal of Orthopedic Research*, 7:266-271, 1989.

Schenkman ML, Berger RA, Riley PO, Mann RW, Hodge WA. Whole-body movements during rising to standing from sitting, *Physical Therapy*, 70:638-648, 1990.

Shepherd RB, Gentile AM. Sit-to-stand: functional relationship between upper body and lower limb segments, *Human Movement Science*, 13:817-840, 1994.

Shepherd RB, Koh HP. Some biomechanical consequences of varying foot placement in sit-to-stand in young women, *Scandinavian Journal of Rehabilitation Medicine*, 28:79-88, 1996.

Sinnott KA, Milburn P, McNaughton H. Factors associated with thoracic spinal cord injury, lesion level and rotator cuff disorders, *Spinal Cord*, 38(12):748-753, 2000.

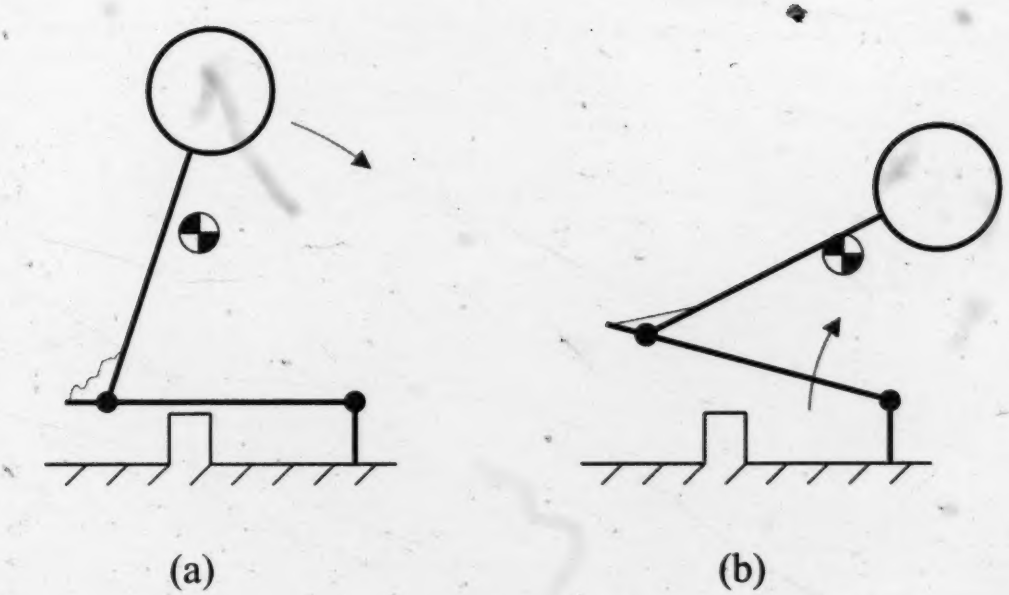

Figure 3-1: "Momentum transfer" argument. The moving trunk (a) creates lift-off (b) by pulling on taut hip extensors.

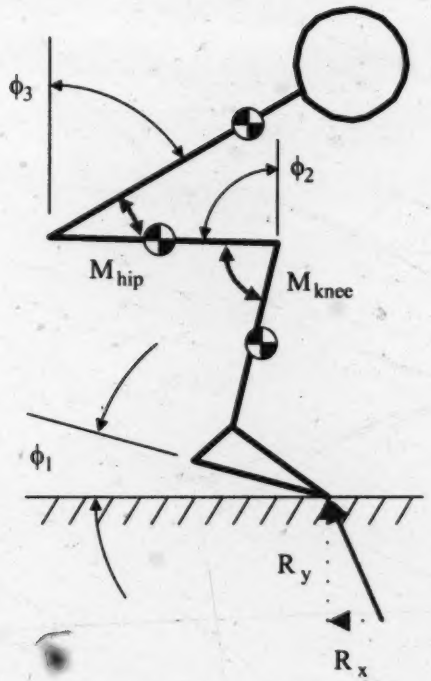

Figure 3-2: 3-segment sagittal plane model of STS in the MLKAFO brace.

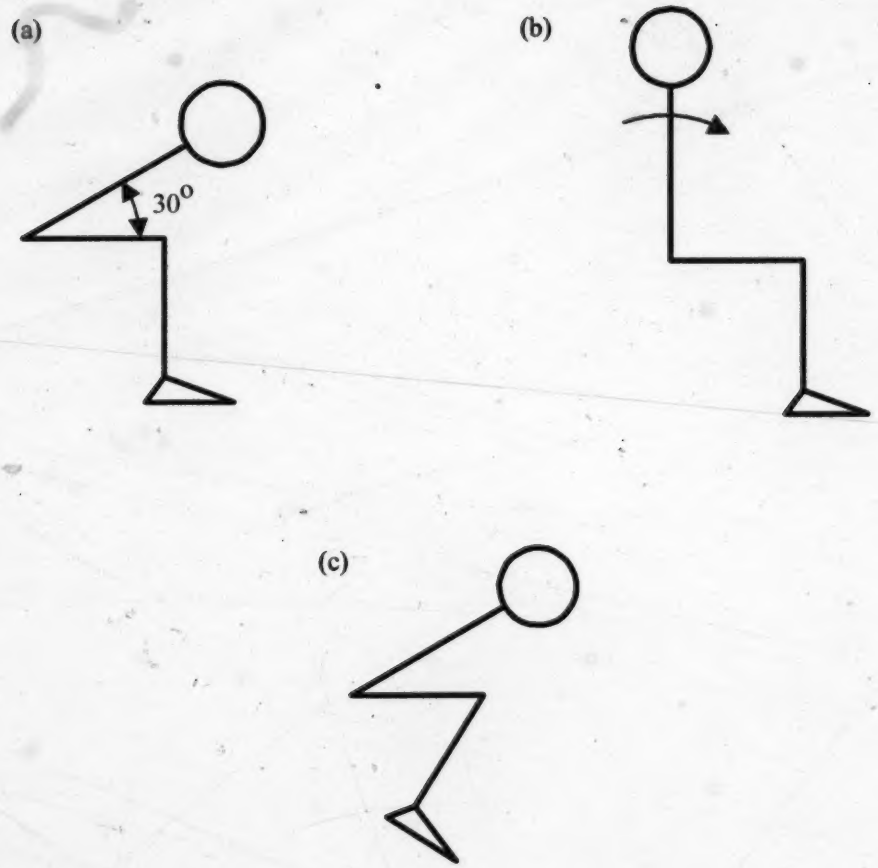

Figure 3-3: Three STS strategies analyzed in this study. (a) Feet are placed flat on ground and trunk is initially flexed forward; (b) Feet are placed flat on ground, trunk is upright, but flexing with initial angular velocity; (c) Feet are pulled back such that toe is directly below whole body center of mass.

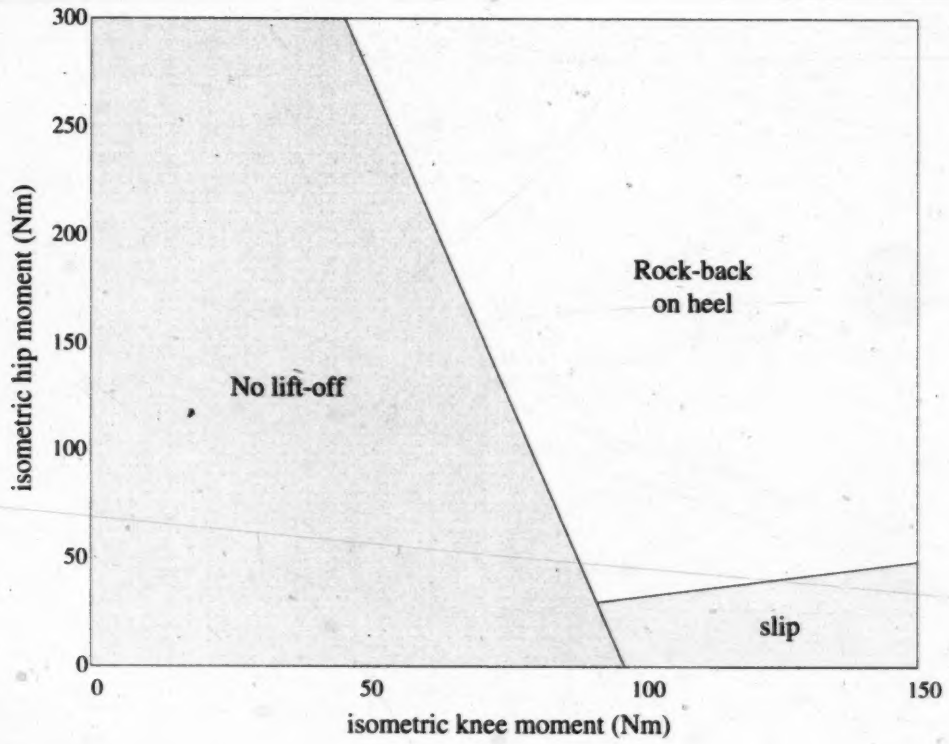

Figure 3-4: Flat foot static trials – failure regions.

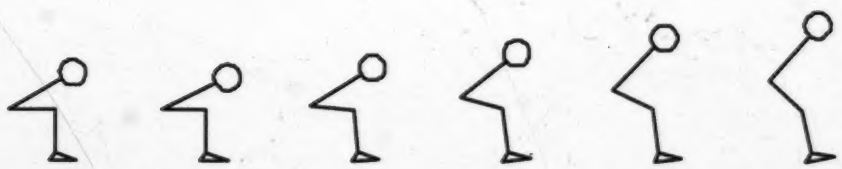

Figure 3-5: Stick figure illustration of rock-back failure. Isometric knee moment = 100 Nm, isometric hip moment = 100 Nm.

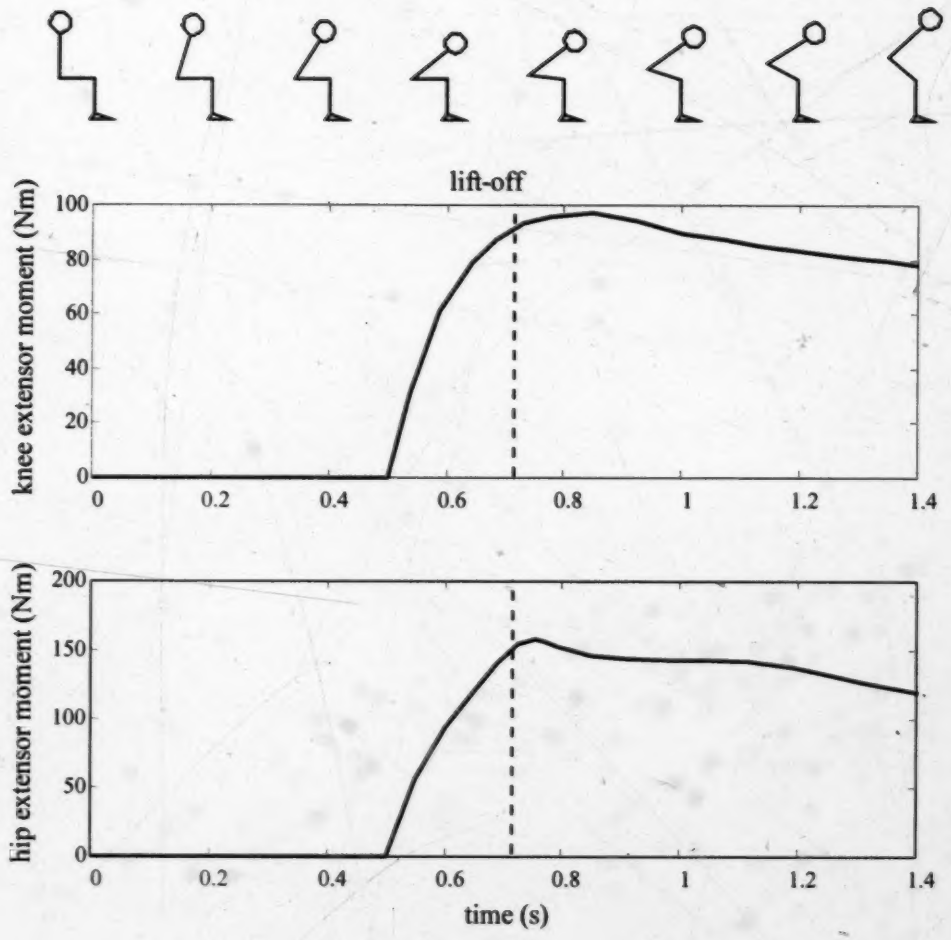

Figure 3-6: Successful STS using the flat foot dynamic strategy. Initial trunk velocity = 75 deg/s. Isometric knee moment = 100 Nm, isometric hip moment = 150 Nm. Stimulus delay = 0.5 s.

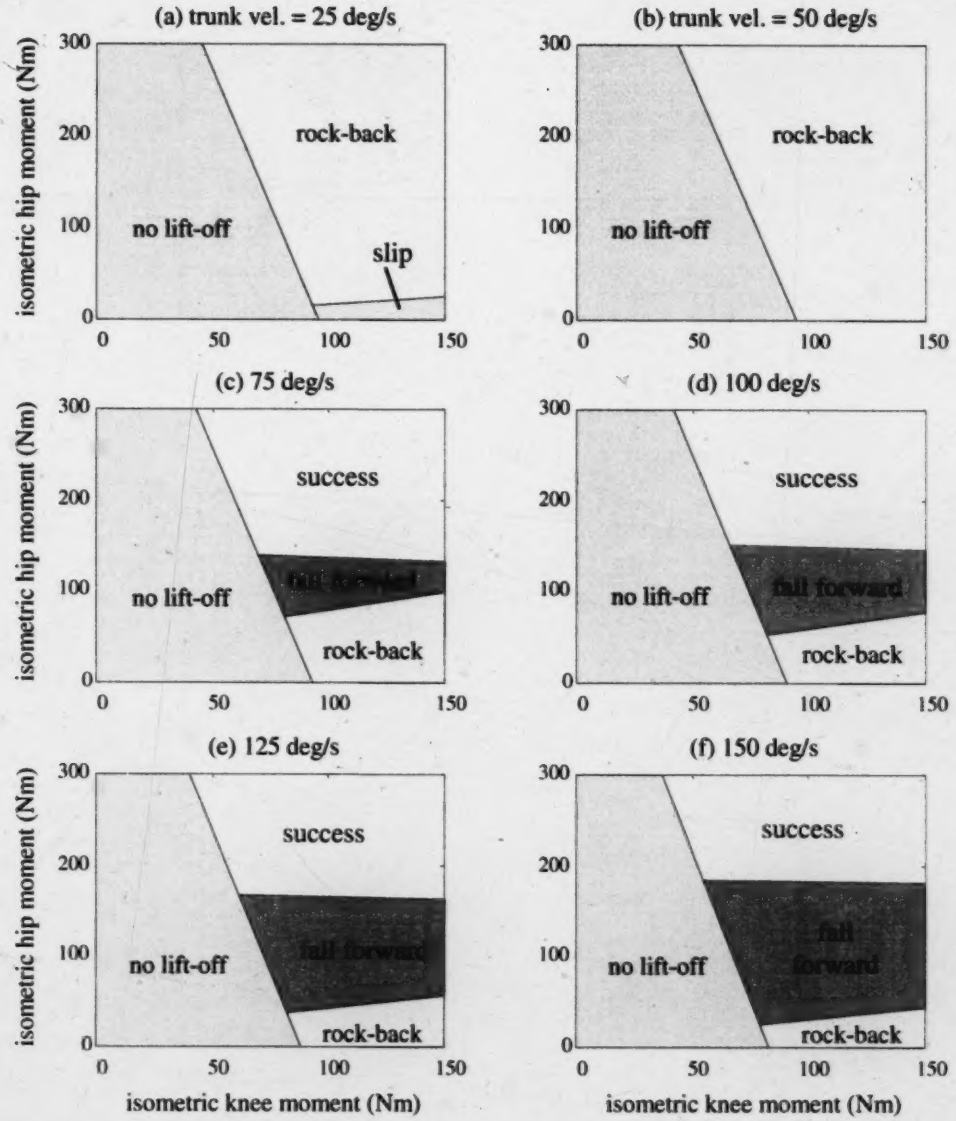

Figure 3-7: Success and failure regions for flat foot dynamic trials.

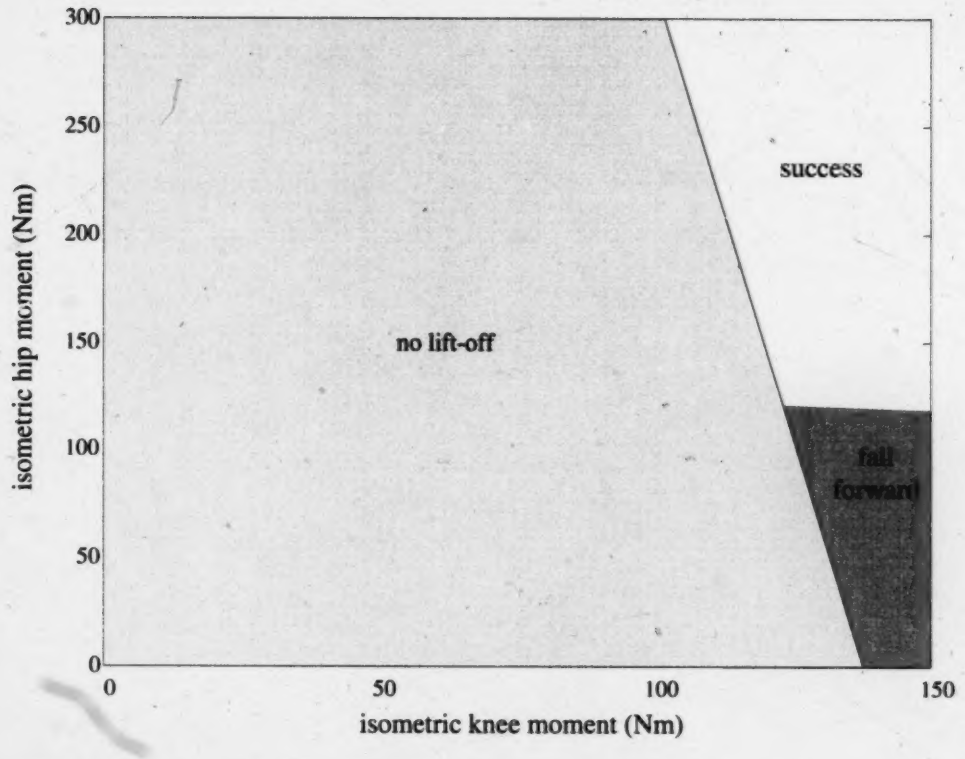

Figure 3-8: Trials starting from the Kralj position – failure and success regions.

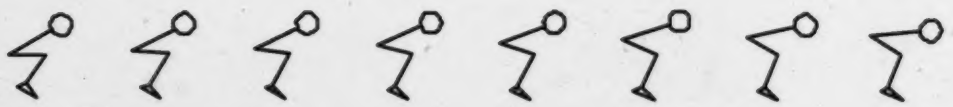

Figure 3-9: Stick figure illustration of a fall-forward failure from the Kralj position. Isometric knee moment = 130 Nm, isometric hip moment = 100 Nm.

4 Passive gait in the medially linked knee-ankle-foot orthosis

4.1 Abstract

The passive dynamics of the lower extremities can theoretically be exploited to improve paraplegic gait in the medially linked knee-ankle-foot orthosis. Swing phase of gait was modeled such that active muscle forces were zero. It was found that passive swing phase was possible for a small range of initial kinematic conditions, which must be generated during the pre-swing (double support) phase. If any initial segment angle or angular velocity is altered by more than approximately 5%, passive swing will not occur properly. The mechanical energy cost of passive swing at an optimal step length between 0.45 and 0.50m was, on average, 0.82 J/kg.m (normalized with respect to body mass and distance travelled). The average duration of optimal swing phase was 0.59 s. Stiff-legged passive swing phase was found to be slower than free-knee swing phase, however it required less mechanical energy. An ideal motor at the hip that was able to deliver 26.7 Nm of hip flexion to the swing leg on demand extended the range of allowable initial conditions at toe-off by an average of 31%. A stretched elastic cable spanning the hip and knee joints was found to have a negative effect on passive swing.

4.2 Introduction

The dimensions and inertial properties of human legs are ideally suited for walking. Evolution has engineered us to exploit pendulum dynamics, resulting in highly efficient gait. Investigators dating back to Borelli have suggested that swing phase in human walking is essentially ballistic, that is, governed by gravity and inertia. Thus, little to no muscle activity is necessary, and energy is largely conserved.

Paraplegic gait is far from efficient. Modern functional electrical stimulation (FES) approaches produce low walking speeds and demand a lot of strength and energy from users (Karcnik et al., 1996). The hip flexors and knee flexors/extensors are usually activated during swing phase, and fatigue occurs rapidly. Purely orthotic systems are also limited, and they place heavy demands on the upper body to transmit force through the paralyzed trunk to the legs.

Movements are awkward and exaggerated, and the legs tend to drag or the feet scuff the ground with almost every step. Hybrid orthoses are designed to address the problems of fatigue associated with the pure FES approach as well as the problems associated with the orthotic approach, but they are not completely successful. Fatigue is still rapid, and gait is still slow and inefficient.

When paraplegics perform reciprocal gait, they spend upwards of 90% of the cycle in the double support phase, compared to 20% in normal gait. Much time and effort is spent preparing for swing phase. At heel-strike, they typically stop, steady themselves, and then advance their crutches or walking frame before taking the next step. Thus, no kinetic energy is transferred from one swing phase to the next. This is one of the reasons why paraplegic gait is so much less efficient than normal gait. Paraplegics also tend to use very small steps when walking, less than 0.3 m (Kobetic et al., 1997) compared to 0.5 to 0.9 m for normal gait (Perry, 1992).

Can the passive dynamics inherent in human legs be harnessed during paraplegic gait? If so, how? And to what effect? In this chapter, we hypothesize that gait in the medially linked knee-ankle-foot orthosis (MLKAFO) may be improved by harnessing the passive dynamics inherent in the legs. Using mechanical theory, we will determine criteria that must be met for purely passive swing phase to occur. Then, we will estimate the energy required to meet those criteria and compare our results to the literature on normal and paraplegic gait. We will also examine both stiff-legged gait and free-knee gait. Presumably, free-knee gait will be more efficient, since that is what nature designed us for.

In addition, two new types of mechanical aid that could be added to the MLKAFO will be considered: 1) a stretched elastic element spanning the knee and hip joints, and 2) an ideal motor that applies a 'closing' torque to the medial joint. These aids may be compliant with the passive dynamics of the legs.

The stretched elastic cable is an unorthodox idea that came about through brainstorming. Here is how it is intended to work. One end of the cable attaches to a point on a waist belt coinciding with the anterior superior iliac spine (ASIS). The other end attaches to the upper portion of the AFO, anterior and inferior to

the knee. The cable is positioned lateral to the knee joint, remaining in tension all the time. The idea is that during the first part of swing phase, when the knee is slightly flexed, the cable will produce a small flexion moment at the knee, which will in turn prevent the toe from striking the ground. Gravity will extend the swing leg and cause the cable to pass in front of the knee, where it will promote extension, which is required at heel-strike. In addition, the cable produces a flexion moment on the swing hip. As part of this study, we assess the feasibility of the stretched cable.

The idea of mounting electric motors on orthoses is not new, however it has never proven to be practical. Nevertheless, rapid advancements in robotics promise that small, lightweight electric motors that are powerful enough for orthotic use will soon be available. Assuming it will eventually be possible to add such a motor to the medial joint of the MLKAFO, we analyzed its role as an aid for "passive" swing phase.

4.2.1 Theory of passive gait

Mochon and McMahon (1980) established the theory that the swing phase of human gait could be accomplished completely without muscle activity in their seminal paper on "ballistic walking". A decade later, McGeer (1990) proved it using anthropometrically scaled models that were able to walk down mild slopes without any motors or actuators. Both physical and computer-based, McGeer's models successfully demonstrated stable, repeatable ballistic gait. The modest energy losses due to joint friction and ground impact were compensated by gravity. Recently, Coleman et al. (2001) demonstrated that a simple biped machine that could not stand, could produce stable gait.

Since these landmark papers, passive gait has been the topic of many studies in a wide range of disciplines, from theoretical biology to robotics. Electromyographic analyses of normal walking support the assertion that muscle activity is minimal during swing phase (Winter, 1991). Other studies have shown that adults and children tend to walk and at "resonant" frequencies that are determined by the dynamics of their limbs (Holt and Hamill, 1995), and evidence has been found that the human nervous system utilizes passive dynamics to

control the swing leg (Eng et al., 1997). Many roboticists have built sophisticated anthropometric machines that perform passive gait (e.g. Garcia et al., 1998, Goswami et al., 1998). In addition to humans and robots, passive dynamics have been identified in the gait of horses and other quadrupeds (Witte el al., 1995, Formalsky et al., 2000). Abundant is the evidence that the most efficient control strategies exploit the passive dynamics of the swing leg as a means to conserve energy.

The present study was motivated by the lack of theory concerning the exact mechanical conditions required for passive gait. Mochon and McMahon asserted that in order for passive swing to succeed, certain conditions must be met. At toe-off, the legs must be positioned correctly, and the segments must have sufficient initial velocity. If these conditions are not met, passive dynamics will not yield a suitable swing phase – for example, the toe may strike the ground. McGeer had to give his walking machines a push by hand to initiate the first swing phase. Sometimes, the push was too strong or too weak, and the machine would stumble before entering a stable gait cycle. It has been established that toe-off conditions are the key to passive gait, but details are lacking. With this study, we aim to elucidate this matter through rigorous analysis.

Despite its efficiency, there is some energy loss during passive swing phase due to viscosity and friction of the joints. Then, a relatively large amount of energy is lost at heel-strike due to the impact on the foot, which acts as a shock absorber (Salathe et al., 1990). McGeer's machines recovered energy by descending in the gravitational field. For humans (or anthropometric robots) walking on level surfaces, the lost energy must be recovered during double support phase. This energy comes from muscles or actuators.

The MLKAFO, like many gait orthoses designed for paraplegia, includes a knee joint that can be locked in full extension. The orthosis can therefore be used for free-knee gait or stiff-legged gait, of which the latter is more common in clinical practice. Stiff-legged passive gait was the first topic of McGeer's research, and the topic of many subsequent studies in robotics. Kuo (2001) determined the preferred speed-step length relationship for stiff-legged gait using

a simple model. Reisinger and Moskovitz (1999) specifically studied stiff-legged gait, concluding that an impulsive torque at the hip during double support phase was sufficient to recover energy lost due to heel-strike. The magnitude of the required torque depended largely on the parameters of the ground impact model.

4.2.2 Hypotheses

H4. Passive swing phase is feasible and beneficial during gait in the medially linked knee-ankle-foot orthosis. Put differently, gait in the MKLAFO can be improved by harnessing the passive dynamics inherent in the legs.

H5. Passive gait in the medially linked knee-ankle-foot orthosis can be improved by a powered hip actuator or an elastic element across the knee.

The following additional hypothesis was made in this study:

1. Free-knee gait is more efficient than stiff-legged gait.

4.3 Methods

4.3.1 Models

Because it well represents the constraints of the MLKAFO, we used a 2-dimensional, 3-segment sagittal plane model of swing phase similar to the one proposed by Mochon and McMahon (1980). It is depicted in Figure 4-1. The following major alteration was made: passive elastic and damping reactions were assigned to the knee and hip joints, representing the inherent physiological reactions due to bone, ligaments, etc.. The joint reaction equations used were taken from Davy and Audu (1987).

The AFO component of the MLKAFO is designed to be rigid. It is therefore satisfactory that the model treats the swing leg shank and foot as a single segment. Our model assumes that the stance leg remains rigid throughout swing phase, due to FES of the quadriceps. It also assumes that the point of rotation between the stance leg and foot is a fixed point on the ground. The upper body mass was located entirely at the hip.

The equations of motion were carefully derived using Newton-Euler analysis. They are provided in Appendix B. The equations required 16 parameters characterizing the subject's body – for each segment: mass, length, moment of inertia, and distance to the center of mass; as well as the mass of the upper body,

plus three geometrical variables to describe the foot as a triangle. Given the segment positions and velocities at toe-off, simulations were performed using a fourth/fifth order Runge-Kutta numerical integration with variable step size, from the MATLAB software library (MATLAB, 1999).

The model was designed to simulate passive swing phase of free-knee gait with the stance leg fully extended at all times. A similar two-segment model was devised to simulate stiff-legged gait. To address hypothesis H5, the model was equipped with the following additional features: a passive elastic cable spanning the hip and knee joints, and an ideal torque generator at the hip. They are described in more detail in the corresponding sections below.

The models were initially validated by being given a wide range of initial conditions and body segment parameters and executed over a period of several seconds with all damping elements removed. Total mechanical energy was computed throughout these trials to ensure that the models were conservative.

In addition, the behavior of the basic 3-segment model was compared to normal gait. A sample of actual data recorded from normal gait was used (Vaughan et al., 1992). The body segment parameters of the actual subject and the conditions at toe-off were input to the model, and a simulation was produced. Some muscle activity was apparent during the swing phase of normal gait, hence it was not entirely passive. However, the muscle forces were weak enough to provide a basis for comparison. The trajectories of the swing leg hip and knee joints predicted by the model were compared to the actual gait data.

4.3.2 Subjects - Randomized sample of population

Normally, in theoretical modeling studies, a single "typical" individual's body parameters are used. This approach will not necessarily produce results that are applicable to other body types in the population. It cannot necessarily be assumed that all anthropometric variations will exhibit similar dynamic behavior.

In this study, a sample of individuals representing an entire population was incorporated. Each subject's total body height, H, and mass, M, were randomly determined according to probability distributions based on anthropometric data

(NASA, 1978). The following equations were used to generate the body height (in cm) and weight (in kg) of random subjects.

Male subjects:

$$H = 177 - 2.04x + 7.65y \qquad (4\text{-}1)$$

$$M = 78.5 + 8.42x + 8.93y \qquad (4\text{-}2)$$

Female subjects:

$$H = 162 - 1.02x + 7.14y \qquad (4\text{-}3)$$

$$M = 58 + 7.14x + 6.12y \qquad (4\text{-}4)$$

Where x and y are independent random variables generated from a normal probability distribution (mean = 0, standard deviation = 1). An equal number of male and female subjects were sampled.

Once subject height and mass were determined, the parameters of the individual segments were estimated according to well-established scaling methods (Dempster and Gaughran, 1967, Chandler et al., 1975). In order to ensure that not all subjects had the same proportions, segment lengths and masses were perturbed by a random factor drawn from a normal probability distribution having a mean of zero and a standard deviation of one percent.

4.3.3 Definition of "successful swing phase"

It was necessary to identify the primary objectives of swing phase such that trials could be declared successful or failed. Swing phase was considered "successful" when all three of the following conditions were met:

1. Toe clearance – the toe never came into contact with the ground. This is equivalent to saying the swing foot contacted the ground heel-first.
2. Knee extension – the knee was fully extended at the instant of heel-strike (up to 5 degrees of flexion permitted).
3. Step length consistency – the step lengths at toe-off and at heel-strike did not differ by more than 10%. Step length was defined as the horizontal distance between the toes (or the heels) when both feet are in contact with the ground.

4.3.4 Trials 1 – Initial conditions and energy cost

Figure 4-2 illustrates the input/output scheme that was used in this study. The initial conditions of the 3-segment model – that is, the angles and angular velocities at toe-off – can be described as a five-element vector, $\Phi = \{s, \phi_1, \dot{\phi}_1, \dot{\phi}_2, \dot{\phi}_3\}$, where s is initial step length (calculated at toe-off), ϕ_1 is the angle of the stance leg, and $\dot{\phi}_1, \dot{\phi}_2, \dot{\phi}_3$ are the angular velocities of the three segments.

Due to the closed geometry at toe-off (the toe must contact the ground), only two independent variables are necessary to define the initial position of the model, which is essentially a four-bar linkage. The method to determine ϕ_2, ϕ_3 based on s and ϕ_1 is described in Appendix B. The three segment angular velocities at toe-off are all independent, however they must satisfy the condition that the toe has upward velocity. This constraint is described in Appendix B as well.

A set of initial conditions was given to the model, and a simulation was performed. The result was either successful or failed, as per the definition stated in the previous section. If the trial was unsuccessful, the cause of failure was returned (i.e. toe struck ground, knee flexed at heel-strike, or step length was inconsistent).

First, we sought to determine a set of initial conditions that would result in successful swing phase. This was defined as the *passive swing locus* (PSL). It was impossible to analytically determine the PSL due to the complexity of the equations of motion, so an estimate was made by testing discrete points throughout the domain. A point was defined from actual gait data, Φ_A. The first simulation was performed at Φ_A, and the result was recorded as successful or unsuccessful. Next, a nearby point was chosen by taking a small step in one of the dimensions. This process was repeated until a reasonable estimate of the PSL was found. PSLs were estimated for 10 male and 10 female subjects (randomly generated). The estimated PSL was interpreted in terms of size, shape and how difficult it would be to yield a point within it by the end of pre-swing.

Next, *energy cost* was estimated. It was assumed that all kinetic energy would be lost in the double-support phase following successful swing phase, based on our observations of paraplegic gait. Energy cost was therefore defined as the kinetic energy at toe-off plus the drop in potential energy between toe-off and heel-strike. This is the amount of energy that must be put into the body during the following double support phase in order to achieve another successful, passive swing phase.

Energy cost was calculated for each point in the PSL for each subject. The point that produced a perfectly consistent step length and had the lowest energy cost was defined as the *optimal toe-off condition*. The *optimal energy cost* was defined as the energy cost at this point. Optimal energy costs were determined for all subjects. Karcnik et al. (1996) normalized energy cost by dividing it by the subject's body mass and the distance traveled. Thusly, we also normalized optimal energy costs. The durations of passive swing phase were computed as well.

4.3.5 Trials 2 – Free-knee gait versus stiff-legged gait

The two-segment model with the swing leg knee fixed in full extension was used to simulate stiff-legged gait. Without swing knee flexion, toe clearance is technically impossible for the 2-dimensional model. Therefore, the first criterion of successful swing phase was ignored. It was assumed that toe clearance would be accomplished via lateral tilting (see next chapter), and that that would not significantly alter the dynamics in the sagittal plane. The second criterion, regarding knee extension at heel-strike, was also unnecessary, because the model continually enforced knee extension. The step length consistency criterion was maintained.

As before, the swing toe was required to have upward velocity at toe-off. The toe and heel were allowed to dip below the ground once. Then, they were required to rise above the ground. Finally, the heel would descend back to the ground, and thus swing phase was terminated.

PSLs were generated in the same manner as the free-knee trials, however only three independent input variables were required to define a set of initial

conditions: step length, and the rotational velocities of the two segments. Energy cost was calculated for each point in the PSL, and the optimal value was determined by the method described in section 4.3.4. Optimal energy costs were compared for stiff-legged gait and free knee gait for each subject. A paired t-test was used to determine if a significant difference existed. Durations of swing phase were also compared to determine if one mode of gait was slower than the other.

4.3.6 Trials 3 – Stretched elastic cable

Two stretched elastic cables were added to the 3-segment free-knee model as illustrated in Figure 4-3. The cables were considered to be a linear springs that obey Hooke's Law. They are described by two parameters: elasticity coefficient, k, and unstretched length, l. The points of attachment were chosen to be the ASIS (on the upper body) and a point on the shank segment displaced 1/5th of the shank length below the knee and 1/10th of the shank length anterior to the knee. .

The values of k and l were first chosen arbitrarily (k = 1000 N/m, l = 0.10 m), and the volume of the PSL was estimated by the method described in section 4.3.4 above. An objective function was defined using PSL "volume," $V = f(k,l)$, the number of points found in the PSL using the fixed step sizes in each dimension. Optimal values of k and l were sought using a basic gradient (hill-climbing) algorithm. The resulting volume-maximized PSL was compared to the PSL calculated previously without the elastic cable.

Energy costs were calculated, incorporating the potential energy of the stretched spring.

4.3.7 Trials 4 – Ideal motor at hip joint

The ideal motor was conceived as an aid that would become active when needed. When the conditions at toe-off were insufficient (outside of the PSL calculated in the first part of this study), the motor would supply an extension torque to the swing leg knee and a concomitant flexion torque to the stance leg. This, we reasoned, would augment toe clearance and increase the terminal step length.

The magnitude of the motor torque was first chosen to be $T = 20$ Nm, a value typically observed during normal gait. The torque remained constant until the swing leg thigh (segment 2) passed the stance leg – in other words, when the angle of the medial joint was zero. Then, the motor deactivated and external torque instantly became zero. To find the optimal torque magnitude, the PSL volume as a function of torque magnitude was used as an objective function, $V = f(T)$. The optimal value of T, maximizing V, was sought using a basic gradient (hill-climbing) algorithm.

The mass of the motor and batteries were neglected in the model.

4.4 Results

4.4.1 Validation of the models

It was first confirmed that the basic 3-segment model was conservative. Total mechanical energy remained constant when it was executed without damping elements. The 2-segment stiff-legged version and the version with the elastic cable were also found to conserve mechanical energy.

Figure 4-4 shows the results of the basic 3-segment model compared to actual gait data. The model was given the same body segment parameters as the male able-bodied subject (height 188 cm, mass 64.9 kg), and the same initial conditions at toe-off. Although the model predicted a longer duration of swing phase (0.65 s) compared to actual data (0.54 s), the trajectories were similar. The model predicted the toe striking the ground at 0.25 s, which of course did not occur in actual gait. Discrepancies may be due to weak muscle actions, which were present throughout the actual swing phase.

4.4.2 Passive swing locus and optimal energy cost

The heights and weights of the 20 randomly generated subjects are shown in Figure 4-5. A typical simulation of the 3-segment free-knee model is illustrated in Figure 4-6. The PSL corresponding to each subject was not easy to visualize, because it exists in five dimensions. 2-dimensional "slices" were generated by fixing three of the coordinates while varying the fourth and fifth through a range. Figure 4-7 shows a typical example of these slices for one of the male subjects. The initial conditions from actual gait are indicated by a red square. The actual

subject had a height of 188 cm and a weight of 65 kg, which are very close to the subject represented in Figure 4-7. Note that the initial conditions from actual gait lie outside of the calculated PSL, and result in the toe striking the ground.

From Figure 4-7, it is clear that the toe clearance criterion dominated the lower left portion of the graphs, while the knee extension criterion dominated the upper right. The step length criterion came into play on either side of the PSL when the angular velocities of segments 1 and 2 were small or large. Small velocities indicated a terminal step length that is much shorter than the initial step length, while large velocities indicated a longer step length. All 20 subjects produced different PSLs, but the same basic shape occurred. Typically, a point could be found in the "thickest" part of the PSL that would allow a 5 to 12% change in any one of the segment velocities without departing from the PSL. The narrow extremities of the PSL were less tolerant to error.

Passive swing was possible for almost any step length up to about half of the subject's height. Optimal toe-off conditions were always found in configurations where the initial step length was extremely small. Optimal energy cost was indexed by step length and plotted in Figure 4-8. Data is shown for all 20 subjects. However, the four shortest female subjects were unable to perform passive swing phase with a step length greater than 0.75 m. A strong positive correlation between energy cost and step length is seen. The energy costs in the "thick" (tolerant) regions of the PSL were significantly higher than the optimal energy costs, usually by a factor of 1.6 to 1.9.

Normalized energy cost took on a very different shape in terms of step length. Figure 4-9 shows the same data from Figure 4-8 normalized. Minimal normalized energy costs are seen for step lengths of 0.45 and 0.50 m.

For comparison, data from two published reports on the energetics of normal and paraplegic gait are given in Table 4-1. The values reported in this table involve total energy consumption over the whole gait cycle, not just swing phase. Our calculations represent pure mechanical energy requirements.

Table 4-1; Energy cost of gait from literature

	Energy cost per step (J)	Normalized energy cost (J/kg.m)
Normal gait (Gage et al., 1995)	66.9	1.8†
Normal gait (Karcnik et al., 1996)	-	3.3
Paraplegic gait (Karcnik et al., 1996)	218.4†	14.0

† Calculated from values given; not reported directly.

The duration of successful passive swing phase ranged from 0.37 to 0.72 s over all step lengths greater than 0.30 m and all subjects. The mean duration at the optimal points was 0.59 s, and the standard deviation was 0.041 s.

4.4.3 Free-knee gait versus stiff-legged gait

Figure 4-10 illustrates a typical simulation of the two-segment, stiff-legged gait model. The PSL for stiff-legged gait had a peculiar shape. A typical example is illustrated using 2-dimensional slices in Figure 4-11. Stiff-legged PSLs had roughly the same shape for all subjects. It became smaller and more disconnected at smaller step lengths. At the "thickest" part of the PSL, changes in stance leg velocity up to approximately 10% were permitted, and swing leg velocity could generally be any value between -0.5 and 0.5 rad/s.

There was a minimum value of step length below which successful swing phase was impossible. The minimum step length varied from subject to subject, with a mean value of 0.28 m. As with free-knee gait, optimal energy cost had a positive correlation with step length. Short steps required less energy. Figure 4-12 illustrates the relationship between step length and energy cost. When energy cost was normalized, the positive correlation with step length was retained, however the curve appeared to flatten out for small step lengths. Figure 4-13 illustrates the relationship between normalized optimal energy cost and step length.

Stiff-legged gait was determined to have lower optimal energy costs than free-knee gait for all step lengths (p-value = 0.02, paired t-test). This assertion held true for normalized energy costs as well (p-value = 0.01, paired t-test).

Swing phase duration for stiff-legged gait ranged from 0.51 to 0.94 s over all step lengths greater than 0.30 m and all subjects. The mean duration at the

optimal points was 0.78 s, and the standard deviation was 0.054 s. Compared to free-knee gait, optimal stiff-legged swing phase required significantly more time to execute (p-value < 0.0001, standard z-test).

4.4.4 Stretched elastic cable

For the initial values of k = 1000 N/m and l = 0.10 m, not one point in the PSL could be found. It was assumed to not exist at that point – hence, passive swing was not possible. The value of k was adjusted to 500 N/m, and a small PSL was found. From that starting point, the gradient search algorithm was unable to find a local maximum for PSL volume. Instead, it found a trough of maximum volumes where k = 0.00 N/m and l = any value. In other words, the PSL was largest when the spring was reduced to nothing. The presence of the spring reduced the PSL in size (for some values of k and l, it could not be found). Minimum energy cost also increased when the elastic cable was present.

4.4.5 Ideal motor

The ideal motor had the effect of expanding the PSL for all subjects. In the 2-dimensional slices shown in Figure 4-14, it is clear that the motor overcame several conditions that were inadequate for passive swing phase. The ideal motor had the greatest influence when segment velocities at toe-off were low. Overall, it increased the "volume" of the PSL by an average of 31%.

The optimal motor torque varied from subject to subject. The mean optimal value was 26.7 Nm (st. dev. 6.9 Nm). For step lengths between 0.5 and 0.8 m, the energy drawn from the motor ranged from 2.8 to 9.4 J per step, with a mean value of 4.5 J.

4.5 Discussion

This computer modeling study provides a theoretical basis for MLKAFO control systems that exploit the passive dynamics of the swing leg. An in-depth examination of passive swing phase verified that it is a quick, mechanically efficient process, however very specific dynamic conditions at toe-off must be met.

4.5.1 Free-knee passive swing phase

The results of this study suggest that passive swing phase can be achieved in the MLKAFO brace with knees free or locked. However, the conditions required at toe-off are fairly strict. The passive swing locus was found to be narrow in terms of how much the segment angular velocities at toe-off could vary. It is the objective of the pre-swing phase to produce these velocities using FES activated muscles and upper body influence. If segment velocities are off by as little as 5%, passive swing phase will not occur properly. Whether or not the pre-swing phase can be controlled so precisely is a question for further study.

The energy cost of free-knee passive gait was, as expected, very small. Compared to the published values shown in Table 4-1, our simulations required much less energy. However, the comparison is only somewhat valid. Firstly, the published values involve the entire gait cycle, whereas our calculations only involved swing phase. Furthermore, we did not consider the physiological inefficiencies of muscle stimulation. For example, the stance leg, although it does no mechanical work, requires energy to remain stimulated. Our calculations simply determine the pure mechanical costs of passive gait, and serve only as a baseline.

Our analysis suggests a control strategy for FES assisted passive gait. A controller could be designed that predetermines the PSL for a specific user and uses it as a goal state. The double support phase would be assigned the task of producing toe-off conditions within the PSL. This will be done by active muscle stimulation. Ideally, the region of the PSL that yields minimal energy cost should be targeted to minimize muscle fatigue and physiological cost. A desirable feature of this control strategy is that failure can be predicted and possibly corrected before it happens. For example, if toe-off should occur when the state is outside of the PSL, the controller will be able to anticipate failure, the type of failure and take the necessary action to prevent it from happening.

It seems likely that normal gait may use a strategy similar to this. In Figure 4-7(b), the point from recorded normal gait is shown just outside the minimal energy cost region of the estimated PSL. We found that when Φ_A was

used as input to the model, the toe collided with the ground in mid-swing. The data from normal gait, however, indicated some muscle activity during swing phase. Perhaps the sophisticated biological control system sensed that conditions for passive swing were not met, and as a result, generated flexion forces at the swing leg knee and hip to compensate. The simulations of the ideal motor (see Figure 4-14(b)) did not quite correct for the point Φ_4, but when the motor torque was increased to 20 Nm, successful swing phase resulted.

The control system just described requires some very accurate sensory input to determine the dynamic conditions precisely at the instant of toe-off. Rate gyroscopes would be ideal. Segment angular velocities would be measured directly, and angles could be determined by integration. Pressure sensors mounted in the soles of the AFO, one under the toe and one under the ankle, could detect events of toe-off and heel-strike. Alternatively, or complimentarily, a system of accelerometers could be used (Williamson and Andrews, 2001).

4.5.2 Stiff-legged versus free-knee gait

Stiff-legged passive gait was possible assuming toe clearance could be achieved via lateral tipping. It was much slower than free-knee gait, but less costly in terms of energy. The latter conclusion was contrary to our third hypothesis, stated in the introduction. The reason why stiff-legged gait yielded lower energy costs than free-knee gait is because the segments of the swing leg must be moving very quickly when the knee is unlocked in order to swing through with toe clearance. The angular velocity of the swing leg in stiff-legged gait moves relatively slowly at toe-off, thus the kinetic energy is reduced. Since our calculation of energy cost relies mainly on kinetic energy at toe-off, stiff-legged gait yielded lower values. The energy cost of lateral tipping (for toe clearance) is not known.

In practice, most users prefer the stiff-legged mode, because there is no fear of buckling during stance phase and double support phase, should the quadriceps fail. The obvious drawback of stiff-legged gait is that it does not look natural, which is a serious concern for many orthotic users. Moreover, in stiff-legged mode, some force or moment is required to accelerate the trailing leg such

that passive swing can occur. The hip flexor muscles are deep and inaccessible to surface FES (Nandurkar et al., 2001). The rectus femoris, which spans the hip and knee joints, can provide some hip flexion, but probably not enough. External actuation of the medial joint during pre-swing is a possibility that needs to be practically explored.

4.5.3 Effect of elastic elements on ballistic walking

Although it was an interesting idea, the elastic cable failed to produce the desired effect. It provided no benefit to passive gait, and in fact, it made it more difficult to perform and more costly in terms of energy. Even if its use were theoretically feasible, the elastic cable would be very awkward to apply in practice. It would have to be attached to mounts that position it lateral to the leg, otherwise it would rub against the thigh. And it would have to be worn outside of the pants, which would look very unusual indeed.

4.5.4 Ideal motor at hip joint

The results for the ideal motor simulations were positive. They indicated that a small amount of torque provided to the medial joint could avert failure during swing phase if the necessary toe-off conditions were not met. The motor effectively increased the amount of error permitted during pre-swing at the cost of external electrical energy.

The proposed function of the ideal motor requires a great deal of sensory information. First, the instant of toe-off must be known. A pressure sensor mounted under the metatarsus or toe of the swing foot would be capable of detecting this event. At that instant, the three segment angles must be known as well as their angular velocities. This necessitates a sophisticated sensor array, as discussed in section 4.5.1. The motor controller would use that information to determine if the conditions were within the PSL (via look-up tables or a very quick simulation). If not, the motor would activate and provide a constant torque until the medial joint passes the neutral position. To detect that event, an additional angle sensor mounted on the joint or motor may be required, unless the existing sensors are capable of accurately determining the hip angles.

Of course, ideal motors do not exist in reality. No motor produces a perfect, steady torque independent of joint velocity, and no motor is 100% efficienct. The actual energy consumption of a motor at the medial joint will be a number of times greater than the mechanical energy provided. Even though our results indicate that, theoretically, a motor providing torque across the medial joint can greatly assist the swing phase of MLKAFO gait with very small bursts of energy, the practical issues may turn out to be insurmountable.

4.5.5 Model assumptions

It should be noted that equations 4-1 through 4-4 are based on data from a survey of American Air Force personnel and their spouses. It was the most comprehensive anthropometric data available. The paraplegic population may differ somewhat, as SCI subjects tend towards obesity and generally have disproportionately light legs due to muscle atrophy. Unfortunately, no data specific to paraplegia was available. Our sample likely included some subjects with heights and weights concurrent with the paraplegic population.

Several simplifying assumptions were made when developing the models for this study. We addressed one major limitation of the original Mochon and McMahon ballistic walking model by treating the knee not as a locking device, but instead as a free joint with intrinsic elastic and damping properties. A limitation of our model is that it treated interaction between the stance leg and ground as a frictionless pin joint. This is certainly reasonable during the first part of MLKAFO swing phase, when the stance leg rotates about the point of heel contact. However, when the stance leg becomes vertical, the foot begins to "roll" over the ground until the metatarsal joint becomes the center of rotation. Thus, in reality, the stance leg does not maintain a fixed point of rotation. Because the rolling stance foot is difficult to model, for the sake of simplicity we assumed that the point of rotation remains fixed throughout the swing phase. This is a common assumption for swing phase models.

4.5.6 Further work

As discussed above, the feasibility of using FES to produce toe-off conditions for passive swing phase needs to be analyzed. Such a system would

require sophisticated closed loop control with advanced sensory feedback. Can such a system produce the strict dynamic requirements for passive gait? Could it anticipate failure and take corrective action in time to prevent things such as toe collision during swing phase? A theory for passive MLKAFO gait was established in this study. Now, the practical issues can be explored. Also, motorization of the medial joint ought to be practically considered.

Ideally, the models should have been validated using actual MLKAFO gait data. However, such data was not available at the time of this study, so normal gait data was used. Detailed motion capture of actual paraplegic subjects walking in the MLKAFO is crucial to the continuation of this research.

The need for toe clearance placed major constraints on the PSL. There are a number of ways to augment toe clearance, including lateral tipping (see next chapter) and ankle dorsiflexion. Active control of the ankle during swing phase is commonly observed in normal gait (Winter, 1991). FES induced dorsiflexion is a fairly popular technique in paraplegic gait (eg. Kobetic et al., 1997), however the rigid AFO component of the MLKAFO prevents it. Alterations to the ankle of the MLKAFO might be considered as a means to increase toe clearance thereby relaxing the constraint that it puts on the conditions necessary at toe-off.

4.6 References

Chandler RF, Clauser CE, McConville JP, Reynolds HM, Young JW. *Investigation of inertial properties of the human body, Final report, Apr. 1, 1972 – Dec. 1974*, AMRL-TR-74-137, Aerospace Medical Research Laboratories, Wright-Patterson Air Force Base, Dayton, Ohio, 1975.

Coleman MJ, Garcia M, Mombaur K, Ruina A. Prediction of stable walking for a toy that cannot stand, *Phys Rev E*, 64:022901, 2001.

Davy DT, Audu ML. A Dynamic optimization technique for predicting muscle forces in the swing phase of gait, *Journal of Biomechanics*, 20(2):187-201, 1987.

Dempster WT, Gaughran GRL. Properties of body segments based on size and weight. *American Journal of Anatomy*, 120(1):33-54, 1967.

Eng JJ, Winter DA, Patla AE. Intralimb dynamics simplify reactive control strategies during locomotion. *Journal of Biomechanics*, 30(6):581-588, 1997.

Formalsky A, Chevallereau C, Perrin B. On ballistic walking locomotion of a quadruped, *International Journal of Robotics Research*, 19(8):743-761, 2000.

Gage JR, Deluca PA, Renshaw TS. Gait analysis: principles and applications. *Journal of Bone and Joint Surgery*, 77-A(10):1607-1623, 1995.

Garcia M, Chatterjee A, Ruina A, Coleman M. The simplest walking model: stability, complexity, and scaling. *Transactions of the ASME Journal of Biomechanical Engineering*, 120:281-288, 1998.

Goswami A, Thuilot B, Espiau B. A study of the passive gait of a compass-like biped robot: symmetry and chaos. *International Journal of Robotics Research*, 17(12):1282-1301, 1998.

Holt KG, Hamill J. Energetic cost and stability during human walking at the preferred stride frequency. *Journal of Motor Behavior*, 27(2):164-178, 1995.

Karcnik T, Kralj A, Bajd T. Crutch assisted FES gait and upright stability assessment. In: Pedotti A, Ferrarin M, Quintern J, Riener R (eds) *Neuroprosthetics: from Basic Research to Clinical Applications*, Springer-Verlag, Berlin, 1996.

Kobetic R, Triolo RJ, Marsolais EB. Muscle selection and walking performance of multichannel FES systems for ambulation in paraplegia, *IEEE Transactions on Rehabilitation Engineering*. 5(1):23-9, 1997.

Kuo AD. A simple model of bipedal walking predicts the preferred speed-step length relationship, *Trans ASME J Biomech Eng*, 123(6):264-269, 2001.

MATLAB version 5.3, The MathWorks Inc., Natick, MA, 1999.

McGeer T. Passive dynamic walking, *International Journal of Robotics Research*, 9(2):62-82, 1990.

Mochon S, McMahon TA. Ballistic walking, *Journal of Biomechanics*, 13:49-57, 1980.

Nandurkar S, Marsolais EB, Kobetic R. Percutaneous implantation of iliopsoas for functional neuromuscular stimulation, *Clin Orthop & Rel Res*, 389:210-217, 2001.

NASA. *Anthropometric Sourcebook,* NASA Reference Publication No. 1024, Houston TX, 1978.

Perry J. *Gait Analysis: Normal and Pathological Function*, Thorofare, New Jersey, Slack, 1992.

Reisinger KD, Moskowitz GD. Bipedal locomotion: stopping and the standing/balance gait, *Int J Robot Res*, 18(3):333-343, 1999.

Salathe EP Jr, Arangio GA, Salathe EP. The foot as a shock absorber. *Journal of Biomechanics*, 23(7):655-659, 1990.

Vaughan CL, Davis BL, O'Connor JC. *Dynamics of Human Gait*, 1st edition, Human Kinetics Publishers, 1992.

Williamson R, Andrews BJ. Detecting absolute human knee angle and angular velocity using accelerometers and rate gyroscopes, *Med Biol Eng Comput*, 39(3):294-302, 2001.

Winter DA. *The biomechanics and motor control of human gait*, University of Waterloo Press, Waterloo, Canada, 1991.

Witte H, Lesch C, Preuschoft H, Loitsch C. Gaits of horses: Are they ruled by oscillations? *Pferdeheilkunde*, 11(3):199, 1995.

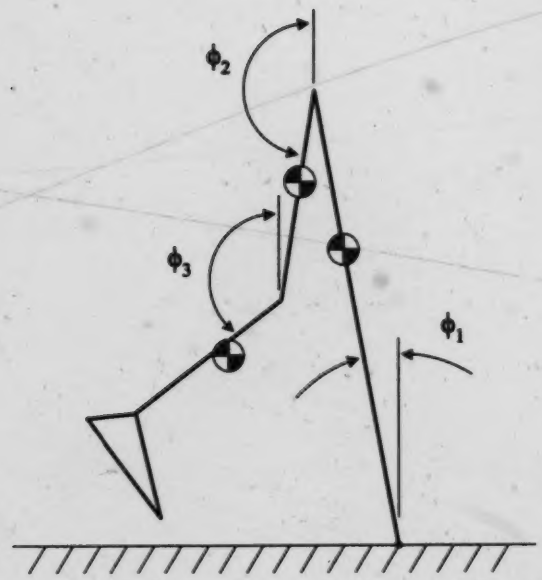

Figure 4-1: The ballistic walking model consists of three rigid bodies connected as a compound pendulum. The ankle is fused; shank & foot comprise one segment. All segment angles were measured relative to the vertical, counterclockwise (+)ve.

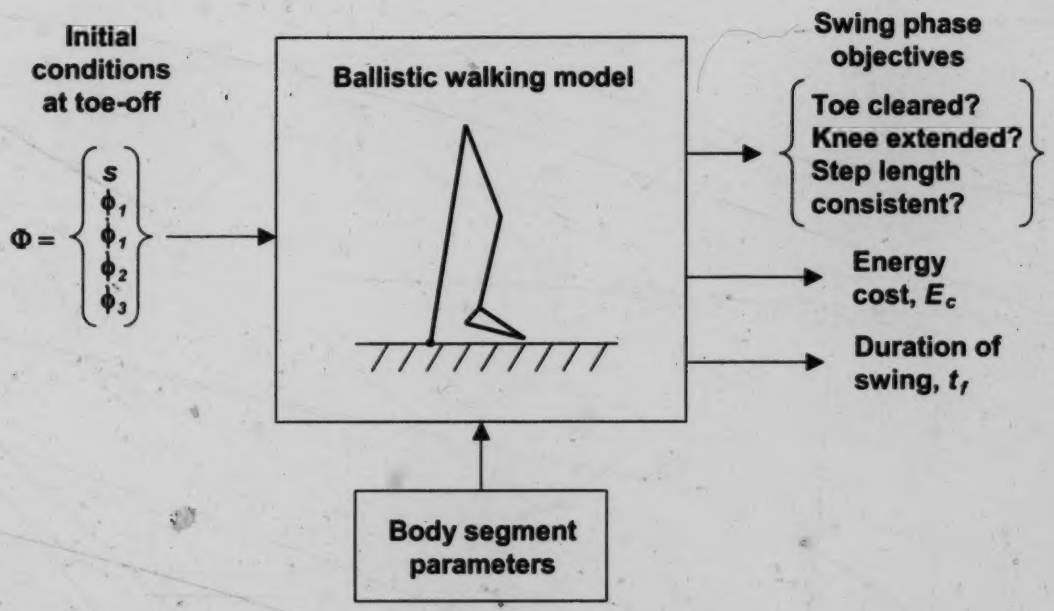

Figure 4-2: Illustration of modeling methodology. Initial conditions at toe-off (segment angles and angular velocities) are input. The success or failure of swing phase is output. The energy cost is returned in the case of successful swing phase.

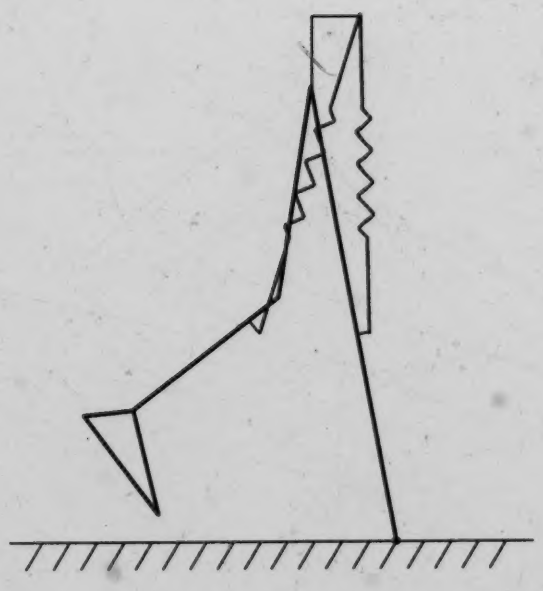

Figure 4-3: The 3-segment model equipped with stretched elastic cables spanning the hip and knee.

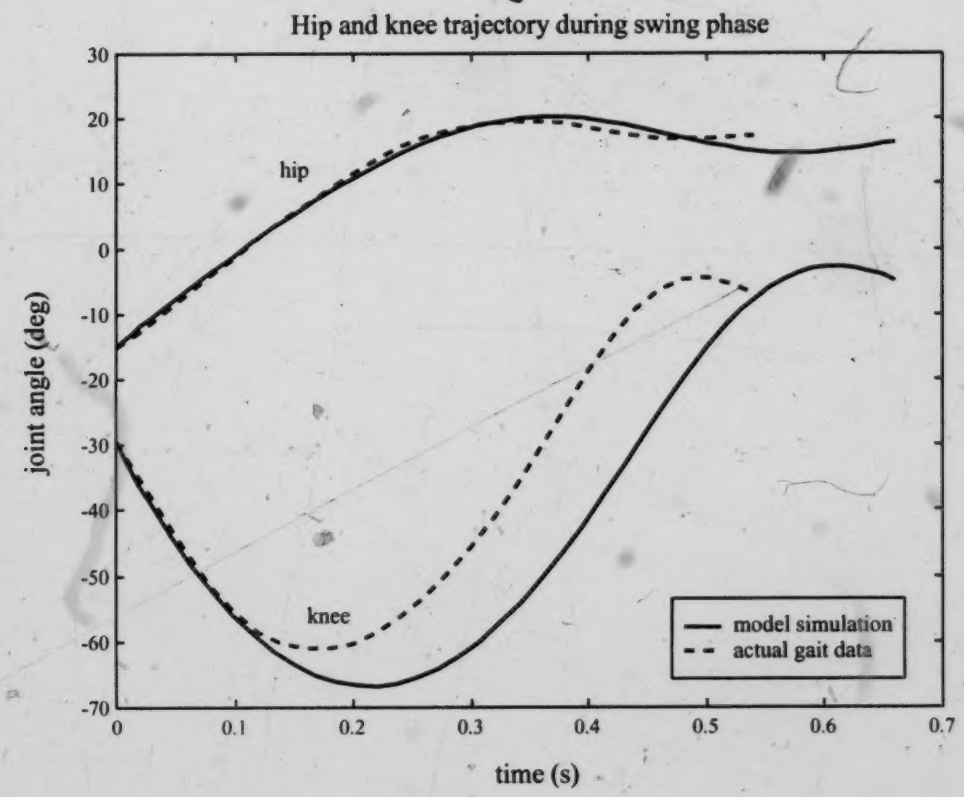

Figure 4-4: Comparison of model simulation to actual gait data. (+)ve joint angle indicates extension; (-)ve indicates flexion.

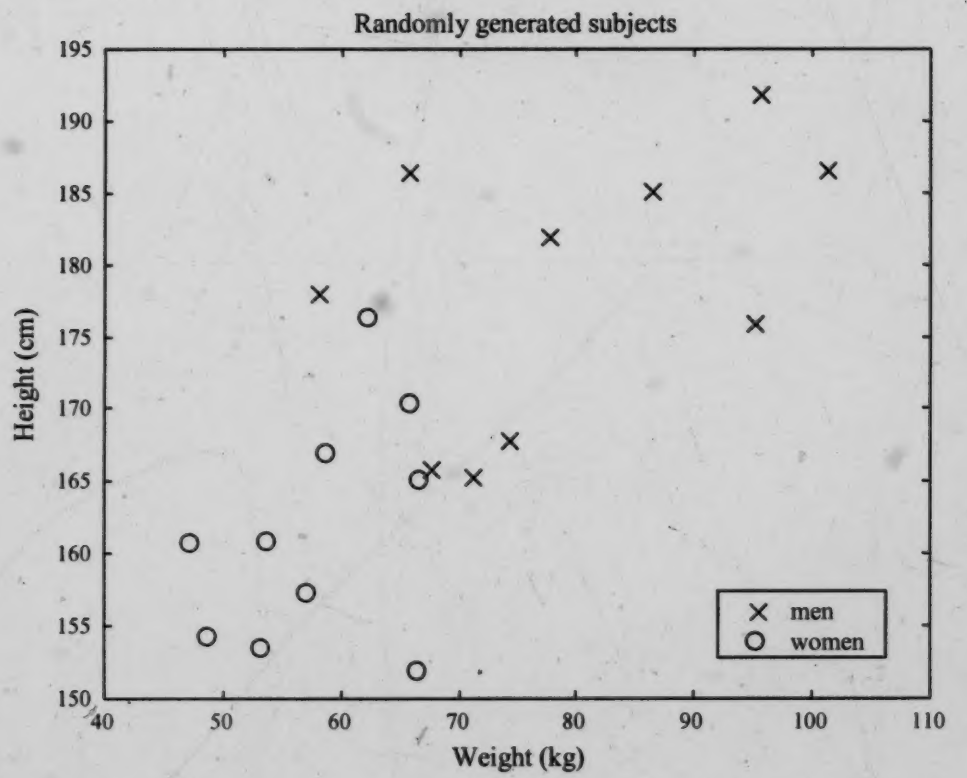

Figure 4-5: Shown here are the heights and weights of the 10 male and 10 female subjects that were randomly generated to participate in this study.

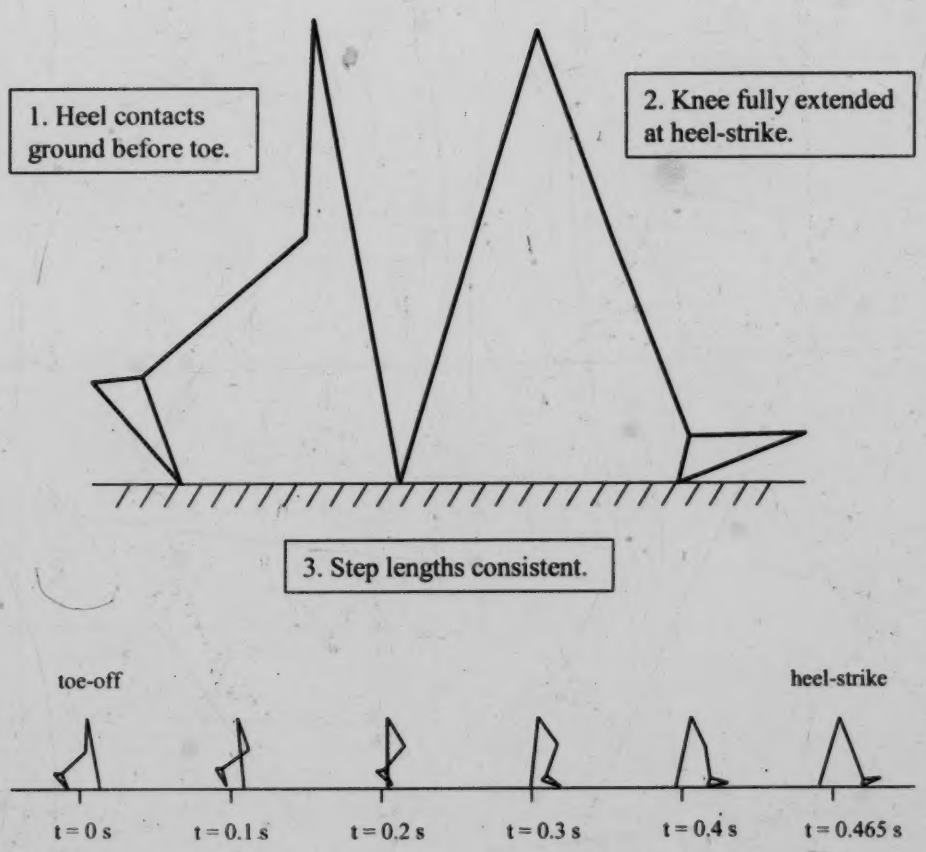

Figure 4-6: A typical successful simulation. All three swing phase criteria are satisfied.

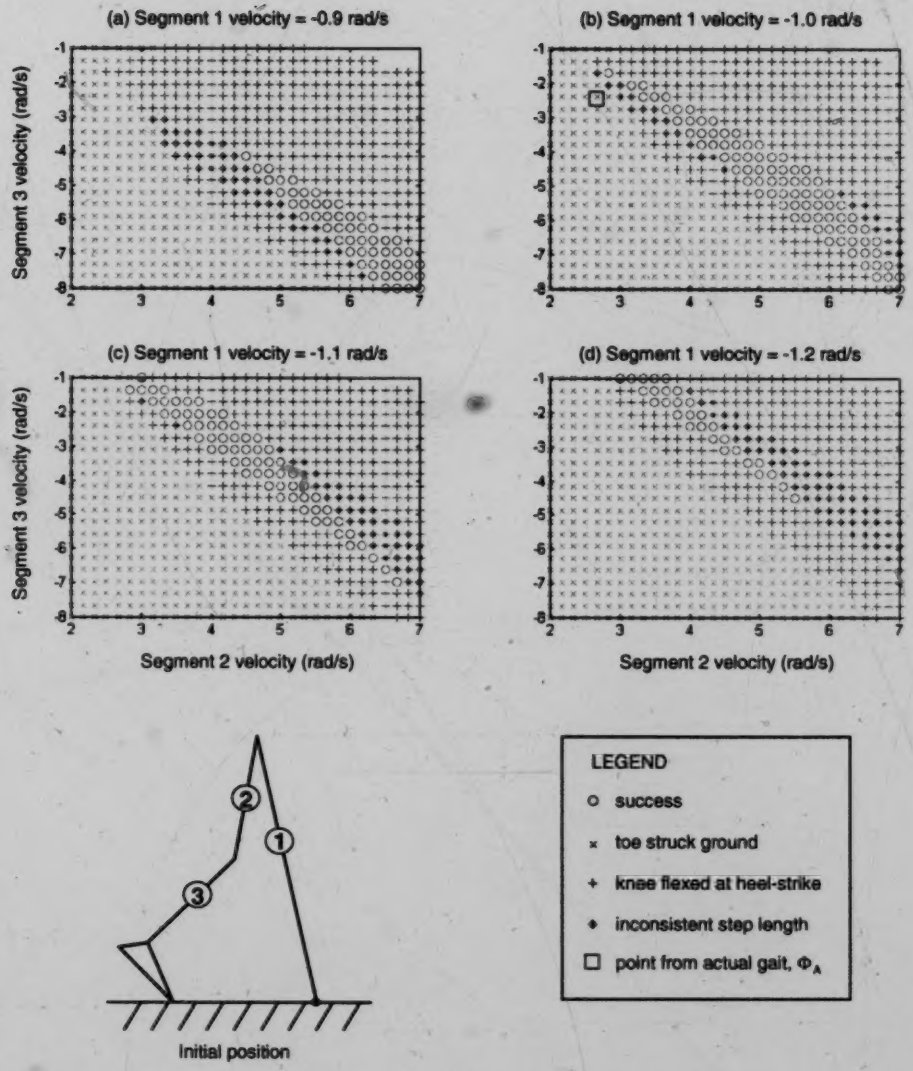
(a) Segment 1 velocity = -0.9 rad/s
(b) Segment 1 velocity = -1.0 rad/s
(c) Segment 1 velocity = -1.1 rad/s
(d) Segment 1 velocity = -1.2 rad/s
Segment 3 velocity (rad/s)
Segment 2 velocity (rad/s)
LEGEND
success
toe struck ground
knee flexed at heel-strike
inconsistent step length
point from actual gait, Φ_A
Initial position

Figure 4-7: Four 2-dimensional "slices" through the 5-dimensional input space. Points within the PSL are indicated by the symbol 'o'. All other symbols indicate the various modes of failure (see legend). Male subject, H = 186 cm, W = 65.9 kg, initial step length = 0.62 m. Velocities given are relative to the ground, counterclockwise (+)ve.

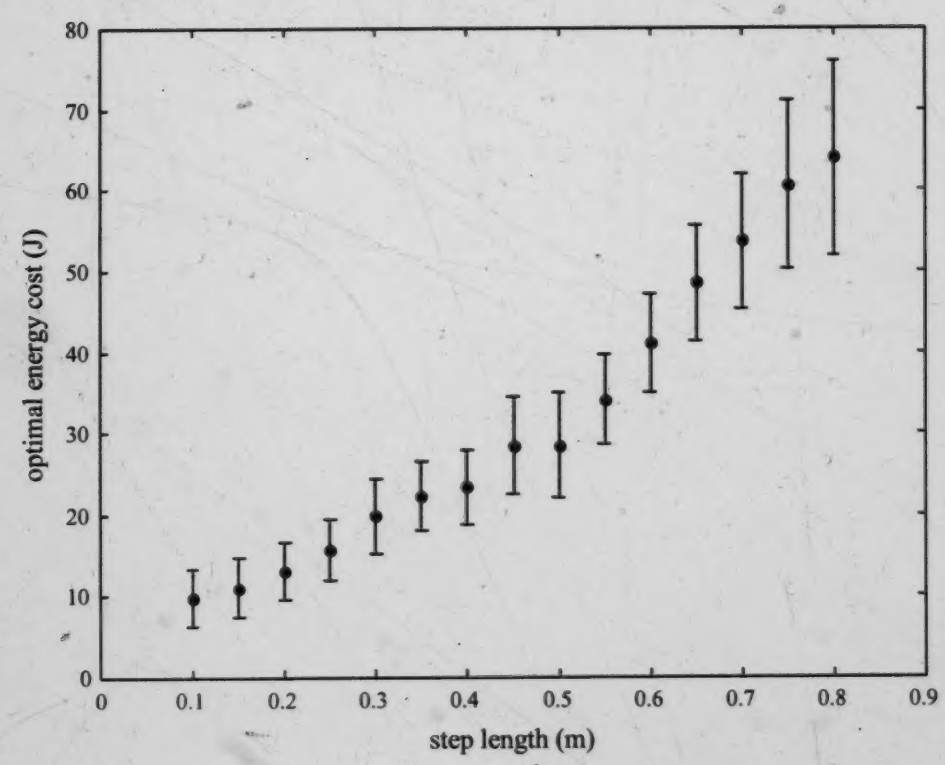

Figure 4-8: Optimal energy cost versus step length for free-knee gait. Points represent mean values; error bars indicate one standard deviation range. Data for all 20 subjects represented, however 4 female subjects were unable to produce step length > 0.75 m.

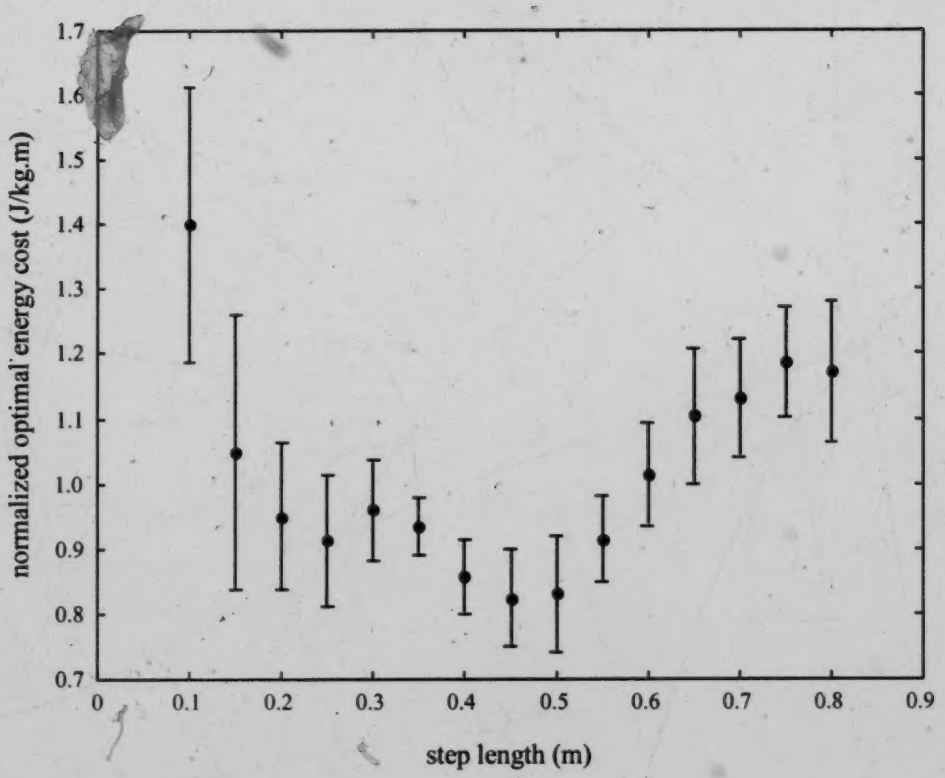

Figure 4-9: Energy cost was normalized by dividing by subject mass and step length.

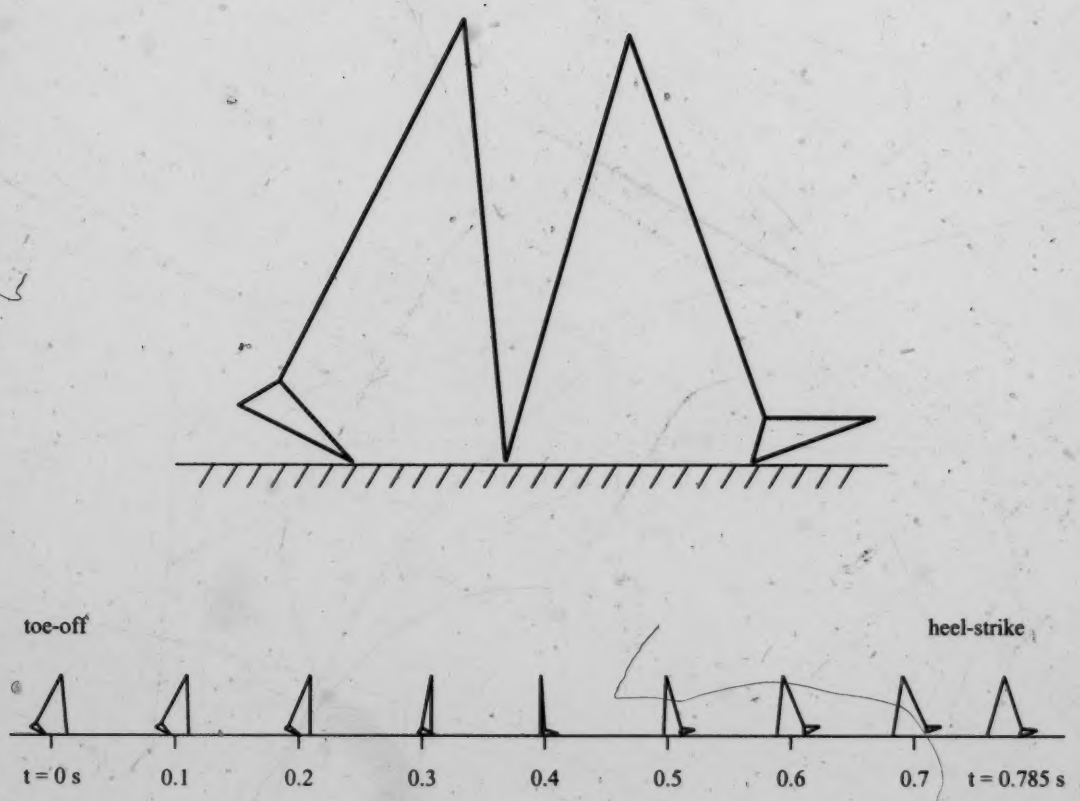

Figure 4-10: A successful simulation of stiff-legged gait. The only criterion, consistent step length, is satisfied.

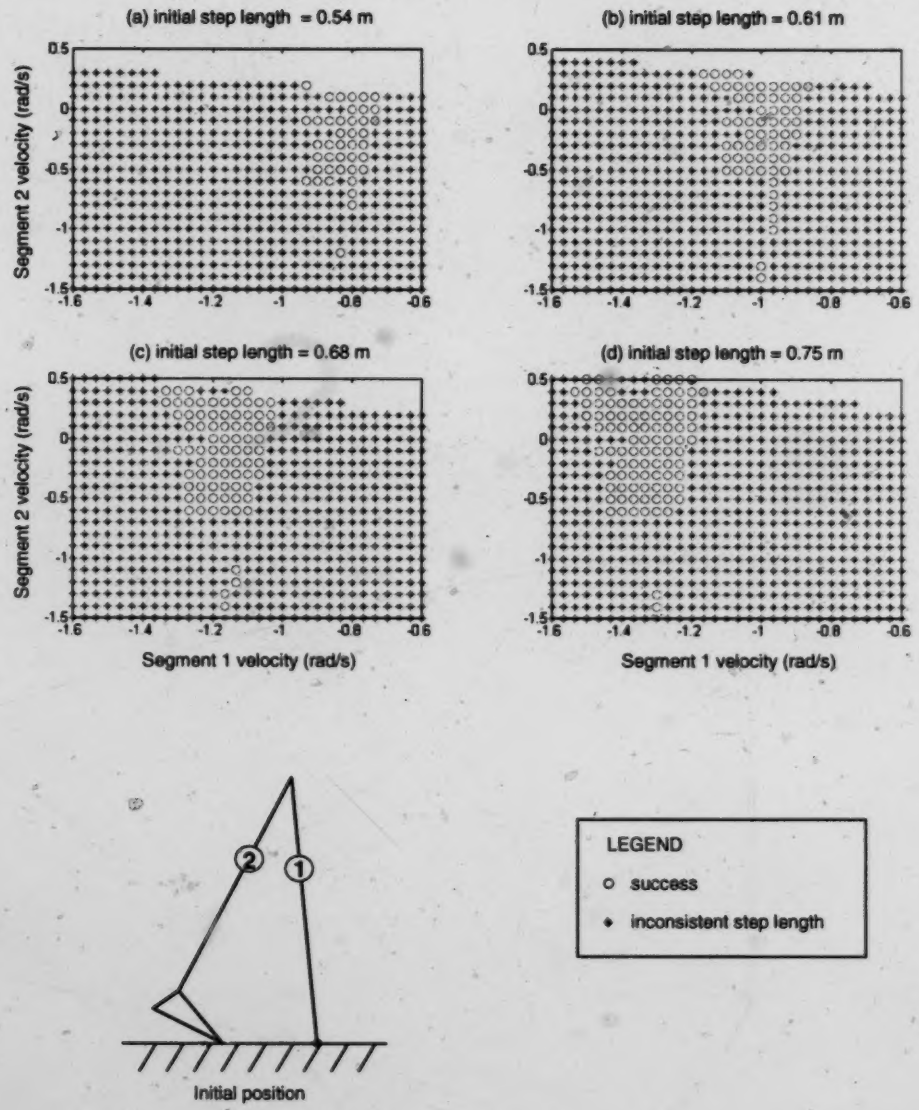

Figure 4-11: Stiff legged gait. Four 2-dimensional "slices" through the 3-dimensional input space. Points within the PSL are indicated by the symbol 'o'. All other symbols indicate failure due to inconsistent step length. Male subject, H = 186 cm, W = 65.9 kg. Velocities given are relative to the ground, counterclockwise (+)ve.

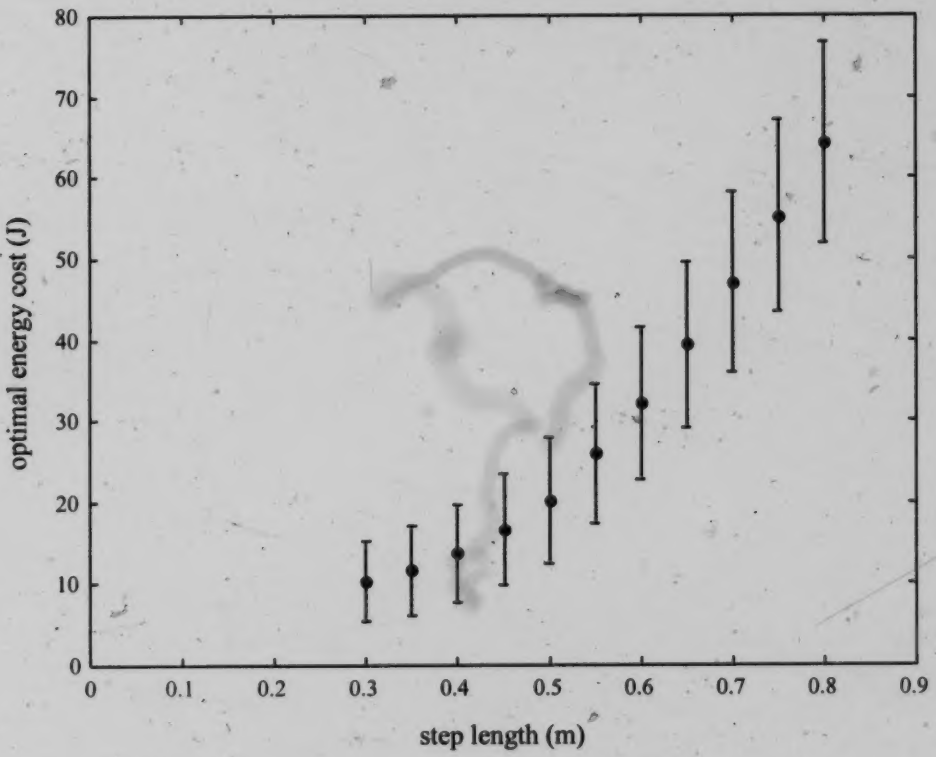

Figure 4-12: Optimal energy cost versus step length for stiff-legged gait. Points represent mean values; error bars indicate one standard deviation range. Data for all 20 subjects represented.

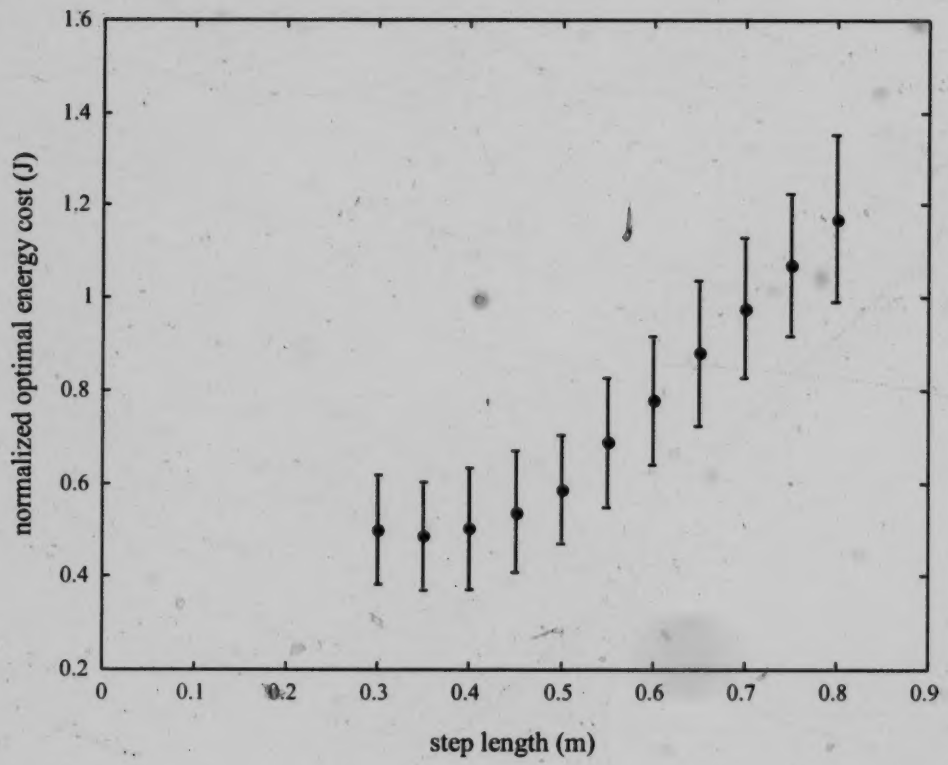

Figure 4-13: Optimal energy cost was normalized by dividing by subject mass and step length.

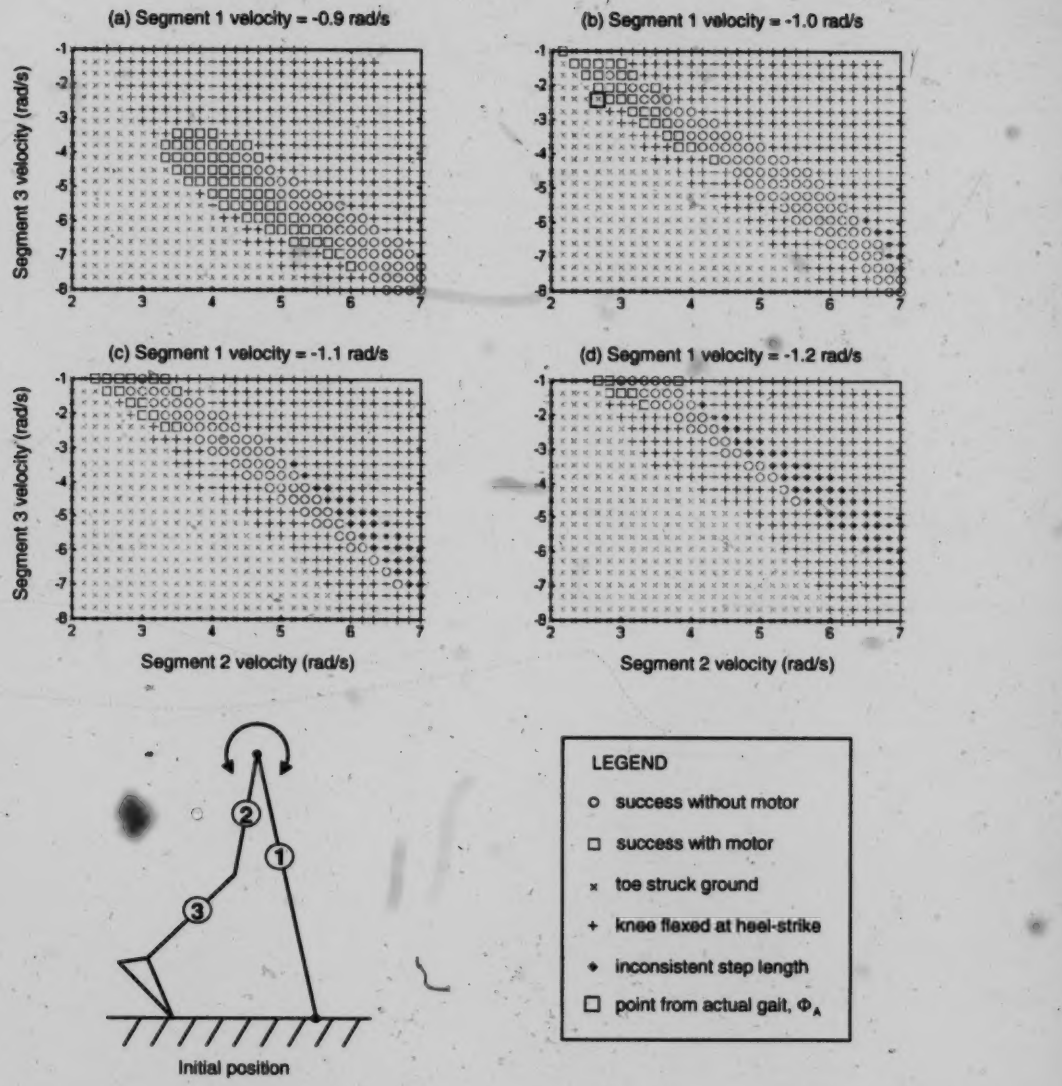
(a) Segment 1 velocity = -0.9 rad/s
(b) Segment 1 velocity = -1.0 rad/s
(c) Segment 1 velocity = -1.1 rad/s
(d) Segment 1 velocity = -1.2 rad/s
Segment 3 velocity (rad/s)
Segment 2 velocity (rad/s)
LEGEND
success without motor
success with motor
toe struck ground
knee flexed at heel-strike
inconsistent step length
point from actual gait, Φ_A
Initial position

Figure 4-14: Swing phase with ideal motor at hip joint. The motor was active outside of the PSL (indicated by the symbol 'o'). Some failure points were transformed into success points by the motor (indicated by blue squares). Male subject, H = 186 cm, W = 65.9 kg, initial step length = 0.62 m, motor torque = 14.0 N.m. Velocities given are relative to the ground, counterclockwise (+)ve.

5 Dynamic lateral articulation of the rigid trunk produces foot clearance in MLKAFO gait

5.1 Abstract

Paraplegic gait in the medially linked knee-ankle-foot orthosis is limited due to a lack of above-waist components to address paralysis of the abdomen. Proposed in this study is a method of rocking the upper body from side to side to cause the feet to lift. One paraplegic subject (T12) and two able-bodied subjects demonstrated this technique. When holding handrails, the paraplegic subject was able to raise his feet for an average duration of 0.44 s, which is not quite sufficient for gait. Some other assistance will have to be found to facilitate gait for this particular subject. The able-bodied subjects were able to walk at speeds up to 0.73 m/s using the rocking trunk strategy. Two different modes of rocking were observed – one in which the upper body rotated in the opposite direction to that of the lower body (in the frontal plane), and one where both bodies moved in the same direction. The first mode was preferred by the able-bodied subjects, while the second mode was used by the paraplegic subject when he was not holding the hand rails. When he did hold the handrails, he used the first mode.

5.2 Introduction

The medially linked knee-ankle-foot orthosis (MLKAFO) is a hybrid orthosis designed for FES assisted paraplegic gait. In normal gait, there are several mechanisms that combine to lift the swing leg foot and keep it from contacting the ground until heel-strike: knee flexion, ankle dorsiflexion, hip adduction, plantar flexion of the stance leg ankle, pelvic tilt, etc.. The MLKAFO precludes hip adduction and ankle dorsiflexion and plantar flexion. In stiff-legged mode, it also prevents knee flexion, leaving foot clearance solely up to pelvic tilt.

Current paraplegic gait systems, including orthoses and pure FES systems, require large upper limb forces to produce the pelvic tilt necessary for foot clearance. The arms must bear a large portion of the body weight (through crutches or other walking aids) and displace the upper body to one side. The shoulder girdle, however, is poorly adapted for excessive weight bearing; many paraplegics already suffer from shoulder overuse syndromes (Goldstein et al.,

1997, Sinnott et al., 2000). The motivation for the present study was to explore the possible role of the trunk as a "spinal engine" that may relieve the arms during FES gait.

The MLKAFO is superior to other linked KAFO systems in terms of rigidity in the frontal plane. The medial joint is a direct attachment between the two KAFOs, whereas hip-knee-ankle-foot orthoses, such as the Louisiana State University Reciprocating Gait Orthosis (LSU-RGO), connect the KAFOs indirectly through two hip joints and an intermediate trunk segment. The superior rigidity of the MLKAFO prevents the legs from coming into contact each other during swing phase, i.e. "scissoring." Because of its superior rigidity, the MLKAFO brace is well suited for reciprocal gait involving rotation of the lower extremities in the frontal plane, the purpose of which is to lift the swing foot from the ground.

A major drawback of the MLKAFO is that, since it has no components above the waist, the paralyzed trunk is unrestrained. Volitional upper body forces are ineffectively coupled to the pelvis due to paralysis of the abdominal musculature. In a static context, to rotate the lower body such that a foot is raised, the subject must displace his upper body far to the opposite side. Upper body forces are then translated through the flexed ligamentous spine. As illustrated in Figure 5-1(a), this method requires pronounced flexion of the spine, which poses an injury risk, especially if repeated often.

The external oblique muscles, which connect the lateral portion of the rib cage to the pelvis, can be activated through surface FES (Licht, 1967). Bilateral stimulation promotes trunk rigidity in the frontal plane. Due to their lateral points of origin and insertion, the oblique muscles can carry large moments – created by the arms – through the abdomen. This is illustrated in Figure 5-1(b). It is hypothesized that constant, open loop FES of the obliques during gait will reduce the amount of spinal flexion necessary for MLKAFO gait. It should also promote lateral stability of the trunk.

The external obliques can play a more dynamic role by creating lateral movements of the spine, oscillating the upper body from side to side. The

stimulated muscles would then oppose the momentum of the upper body, resulting in a beneficial force couple on the pelvis. In theory, this method reduces the amount of lateral spinal flexion necessary for MLKAFO gait, thus reducing injury risk. As well, it could relieve the arms.

The purpose of this study is to analyze the rocking motion described above. Experiments involving one paraplegic subject and two able-bodied subjects provided data, which served as a preliminary assessment of the feasibility of rocking gait. The dynamics were further investigated using a computer model, which was validated by the experimental data.

5.2.1 "Spinal engine"

The idea of articulating the trunk during gait to produce useful moments on the lower extremities is not a new one. Gracovetsky (1988) put forward the idea in his book, *The Spinal Engine*. He proposed that the spine and paraspinal muscles are major players in all forms of vertebrate locomotion. In humans, the spinal engine is the means by which the spine and paraspinal muscles commute momentum and forces between the upper and lower body. Trunk momentum, he argues, is subtle, but instrumental in normal gait.

Gracovetsky's theory has been independently supported (perhaps unwittingly) by researchers such as Callaghan et al. (1999), who measured lateral flexion moments through the lumbosacral cross section during normal gait. Maximum moments occurred at toe-off, and minimum moments occurred at heel-strike. This is what we would expect given that the purpose of the lateral trunk moment is to create foot clearance. At faster walking speeds, moments increased.

Perhaps the most dramatic example of the spinal engine in action is the biped robot developed by Li et al. (1993). The robot consisted of a heavy inverted pendulum atop a pair of anthropometrically scaled legs. Driven by an electric motor, the pendulum would rock left and right, like a metronome, producing moments that were transmitted to the lower extremities. This produced the foot clearance necessary for swing phase. The robot could walk, but it would topple over unless an operator guided it by hand.

Bauby and Kuo (2000) concluded that passive stiff-legged gait is possible, however active control is required to stabilize the lateral motion of the lower body. Earlier, Kuo (1999) suggested five methods of stabilizing the lower body of a stiff-legged walking robot. One of these methods was rocking torso motion, which Kuo did not pursue. He preferred a method of modulating step width through hip adduction.

There are no reports of paraplegic gait systems that prescribe lateral motion of the trunk to produce foot clearance. The flaccidity of the paralyzed trunk likely makes it impossible to harness trunk movements.

5.2.2 Hypotheses

H6. Stiff-legged gait in the medially linked knee-ankle-foot orthosis can be improved by FES of the trunk.

The following additional hypotheses were made in this study:

1. A subject with a low thoracic injury can use external forces on his arms to produce moments that cause pelvic tilt, lifting a foot.
2. When there are no external forces on the arms, one can oscillate one's trunk causing the feet to lift alternately at frequencies compatible with passive gait.
3. Stiff-legged gait is possible in the MLKAFO without the use of arms if a strategy of rocking the trunk side to side is used to produce foot clearance.

5.3 Methods

This study can be divided into three parts: Paraplegic experiments, able-bodied experiments, and computer modeling. In each part, lateral rocking of the trunk was performed (or simulated) in order to lift the feet alternately.

5.3.1 Subjects

Three human subjects were recruited. Subject A was a paraplegic male – age 67, height 168 cm, mass 86 kg, with a complete spinal cord injury at T12. Subject A suffered from hip contractures, which made him unstable in the sagittal plane when standing. For three months prior to the test, he performed exercises to reduce the contractures. During these exercises, he was put into MLKAFO braces, lifted to a standing posture and held in place for up to 30 minutes. He was also

asked to lie supine at home for at least one hour a day. By the end of the three months, the contractures were reduced, but still apparent.

The other participants were two able-bodied males: Subject B – age 23, height 168 cm, mass 62 kg; Subject C – age 28, height 182 cm, mass 80 kg.

5.3.2 Apparatus – MLKAFO and safety frame

The MLKAFO braces used in this study were fitted and constructed by a licensed orthotist at the Glenrose Rehabilitation Hospital, Department of Prosthetics and Orthotics. One is shown in Figure 5-2. The braces consisted of a pair of knee-ankle-foot orthoses with uniaxial knee joints that could be firmly locked in full extension by a sliding metal clamp. The KAFOs were connected via a uniaxial joint, which was located in the subject's sub-peritoneal region (crotch).

To prevent falls for paralyzed subject A, a large support frame equipped with a safety harness was used. The harness was attached to an overhead bar by a slackened rope, which applied no external force to the subject during trials. A fabric strap attached to the frame was slung horizontally behind the subject a few inches below waist level. When the subject leaned against it, the strap would provide a horizontal force on his buttocks. The strap was necessary when the subject stood without holding the handrails.

5.3.3 Instrumentation

Motion during the human trials was recorded using a four-camera Vicon 140 motion analysis system (Vicon, 1995). Thirteen reflective markers were attached to the brace and anatomical landmarks on the subject's back indicating the orientation of the key body segments. A micro switch was attached to the sole of each shoe. When pressed, the switch triggered a light emitting diode (LED) mounted on the heel of the shoe. The LED was visible both to the operators and the motion analysis cameras. Each LED, when lit, would indicate that the foot was in contact with the ground. The 3-dimensional coordinates of all markers and active LEDs were recorded at 60 Hz. The data was low-pass filtered (second-order Butterworth filter) at a cutoff frequency of 5 Hz. Residual analysis showed that the movements were slow, smooth and contained virtually no signal above 5 Hz. A sample is shown in Figure 5-4.

From the marker and LED data, the lateral trunk flexion angle was calculated. The lateral displacement of the upper body was also computed. It was defined as the horizontal displacement of the marker located at T1. By averaging peak-to-peak values and dividing by two, mean amplitudes of trunk flexion and translation were computed. The frequency of rocking was calculated by simply dividing number of cycles by time.

The duration of each foot lift was determined directly from the LED data. For each foot, a mean duration of foot lift was calculated by averaging the duration of all the lifts in a trial. If the foot failed to lift at all during a given cycle, its duration was treated as zero, and it was included in the calculation of the mean duration.

5.3.4 Trials 1 – Paraplegic subject

Subject A donned the braces and harness, and stood holding on to the handrails. The knee joints of the brace were locked in full extension. He was asked to raise his feet one at a time by rocking laterally. A large floor mirror was provided so that the subject could see his feet during the trials. His movements were recorded. Next, subject A was asked to let go of the handrails. While holding his arms to his chest, he was again asked to lift his feet alternately by rocking side to side. Several trials were recorded with and without the use of the handrails. Attempts were made to walk passively in the MLKAFO as well.

5.3.5 Trials 2 – Able-bodied subjects

As with the paraplegic subject, after donning the MLKAFO brace and locking the knees, the able-bodied subjects were asked to lift their feet alternately by rocking in place. While doing so, they were instructed to hold their arms to their chest. Several trials were recorded. After the rocking trials, subjects B and C were asked to walk. Again, arms were held to the chest. Several trials were recorded at various walking speeds.

5.3.6 Models

Rocking in the frontal plane was simulated using two simple two-segment, two degree-of-freedom rigid body models. They both consisted of an upper body segment, representing the head, arms and trunk, connected to a lower body

segment, representing the pelvis and legs, via the lumbosacral joint, which was treated as a simple pin joint. The first model, illustrated in Figure 5-3(a), was a simple inverted pendulum with a linear, torsional spring at the lumbosacral joint. The equations of motion were derived using Netwon-Euler analysis, which is detailed in Appendix C.

The model was linearized by assuming small angles ($\sin\phi \cong \phi$, $\cos\phi \cong 1$) and small angular velocities ($\dot{\phi}^2 \cong 0$). Written in matrix form, the linearized equations of motion are

$$\underbrace{\begin{bmatrix} I_1 + m_1 l_1^2 + m_2 L_1^2 & m_2 L_1 l_2 \\ m_2 L_1 l_2 & I_2 + m_2 l_2^2 \end{bmatrix}}_{J} \begin{Bmatrix} \ddot{\phi}_1 \\ \ddot{\phi}_2 \end{Bmatrix} = \underbrace{\begin{bmatrix} (m_1 l_1 + m_2 L_1) g - k & k \\ k & m_2 l_2 g - k \end{bmatrix}}_{K} \begin{Bmatrix} \phi_1 \\ \phi_2 \end{Bmatrix}$$

Assume that harmonic solutions exist that can be written in the form

$$\begin{Bmatrix} \phi_1 \\ \phi_2 \end{Bmatrix} = \begin{Bmatrix} A_1 \\ A_2 \end{Bmatrix} e^{i\omega t}$$

Where A_1 and A_2 represent harmonic amplitudes of the segments. Values for resonant frequency, ω, are found by solving the equation:

$$\det(J\omega^2 + K) = 0$$

Anthropometric data from the human subjects were used. Segment lengths, masses, locations of centers of mass, and moments of inertia were estimated using well-established scaling methods (Dempster and Gaughran, 1967, Chandler et al., 1975).

The second model, illustrated in 5-3(b), was a non-linear representation of frontal plane rocking that included the abdominal oblique muscles and a foot-ground interaction model.

On either side of the lumbosacral joint were external oblique muscles originating from the most inferior ribs and inserting at the iliac crests. The common Hill-type muscle model described in section 1.6.6 was used to simulate FES of the knee extensors. Force-length and force-velocity properties of the contractile element were derived using anatomical values gathered from radiographic measurements of the lumbar musculature of healthy men (Stokes and

Gardner-Morse, 1999). Isometric forces were scaled down by a factor of 0.5 to simulate the reduction of strength associated with FES.

Collisions between the feet and ground were handled by treating the sole of the shoe as a coupled spring and dashpot, i.e. deformable. This approach has been shown to produce more accurate results than traditional coefficient of restitution methods (Kaplan and Heegaard, 2000).

The non-linear model was validated by confirming that total mechanical energy was conserved (ground collisions were removed for this). The model was also given experimental data from the hands-free trials of subject A, and virtually no moment was required at the foot-ground contact point to replicate the motion.

5.3.7 Trials 3 – non-linear model simulations

The rocking motion was simulated using the non-linear model in order to determine feasible rocking frequencies and to observe corresponding flexion angles. Initial conditions (segment angles and angular velocities) were taken from arbitrary instants from the successful hands-free rocking trials of subjects A, B and C. Simulations were executed from these starting points.

Periodic activation signals were applied to the muscles. The signals were square waves that were full on for half of the stimulation period and completely off for the other half. The left signal was out of phase with the right signal – that is, while one was on, the other was off. The frequency of the stimulation signals was varied until the model produced a full cycle in which each foot lifted once and the final kinematic conditions were within 10% of the initial conditions.

5.4 Results

5.4.1 Paraplegic subject

Subject A required assistance from operators to perform sit-to-stand in the brace. Due to his hip contractures, he could not stand freely. He easily performed the rocking motion while holding on to the handrails. He would laterally flex his trunk in the direction of the foot he wanted to lift, and displace his upper body in the opposite direction by pulling with his arms. For example, to raise his left foot, he would pull his upper body to the right, and flex his trunk to the left. This is clearly illustrated in Figure 5-5, which shows the lateral trunk flexion and lateral

displacement of the upper body, as well as the lifting of the feet. This method of raising a foot by flexing the trunk toward it was dubbed *mode I*.

Only when leaning against the horizontal strap attached to the frame could subject A stand without holding on to the handrails. For short periods of time (15-45s), he was able to fold his arms across his chest and rock side to side, lifting his feet alternately. He performed the rocking motion in a different manner than when he used the handrails. In the no-hands trials, he flexed his trunk in the direction opposite of the foot that he wanted to raise. His upper body displaced in that direction as well. This was dubbed *mode II*. The feet tended to rise only when the trunk was largely flexed and displaced. Data from a typical no-hands trial are shown in Figure 5-6.

The trial summary shown in Figure 5-7 suggested a negative correlation between the rocking frequency and the amount of trunk flexion. The method of least squares was used to determine a "best fit" line, also shown in the Figure, with a slope of –11.9 Hz/deg. However, the t-statistic was insufficient to assert that amplitude of trunk flexion was dependent upon rocking frequency (p-value = 0.08).

There were, however, significant differences between the handrail trials and the no hands trials, in terms of frequency, mean trunk flexion, lateral translation and duration of foot lift. A summary is given in Table 5-1. Values listed in parentheses are standard deviations.

Table 5-1: Summary of rocking trials for paraplegic subject A

Type of trials	Mode	Frequency (Hz)	Trunk flexion (deg)	Lateral translation (mm)	Duration of foot lift (s)
handrails	I	0.59 (0.057)	6.4 (0.87)	126 (12)	0.44 (0.050)
no hands	II	0.46 (0.072)	8.9 (1.67)	178 (16)	0.18 (0.103)

Subject A rocked at significantly higher frequencies using the handrails than when not (p-value = 0.009, standard t-test). He also flexed his trunk less (p-value = 0.022) and there was less translation of the T1 marker (p-value = 0.0007). The duration of foot lift was significantly less for the no hands trials (p-value = 0.008).

All attempts by subject A to walk in the MLKAFO failed. He was unable to advance his feet.

5.4.2 Able-bodied subjects

Subjects B and C were both able to perform the rocking motion with ease, and both were able to walk without using their arms. Walking did require some effort. One or two early trials were aborted when the subjects lost balance and had to unfold and "windmill" their arms. There were no actual falls.

While just rocking, both subjects always used mode I. That is, the trunk flexed laterally towards the side of the raised foot, and the T1 marker did not travel very far laterally. When initiating the periodic cycle, there was often a large amount of flexion in the direction opposite to the foot that rose first. Then, a steady mode I cycle was established and maintained. Rocking frequencies varied from 0.42 to 0.88 Hz. Mean trunk flexion angles varied from 5.5 to 19 degrees. Duration of foot lift varied from 0.35 to 0.95 s

Subjects B and C each performed eight walking trials. Subject B used rocking mode I in six of his trials; subject C used rocking mode I in seven of his trials. In the other three trials, mode II was observed. In subject B's last walking trial, he made a very irregular transition from mode II to mode I over several steps. This is shown in Figure 5-8.

During the walking trials, step frequencies between 0.43 and 0.89 Hz were observed. Walking speeds ranged from 0.187 to 0.730 m/s. Figure 5-9 shows the frequency and amplitudes of the various trials of subject B and C. For the rocking trials only, a significant negative correlation between rocking frequency and trunk flexion angle was observed in the able-bodied rocking trials, based on a least squares linear model (p-value < 0.0001). No similar correlation could be inferred from the walking trials (p-value $= 0.23$).

5.4.3 Computer models

The linear model revealed a hyperbolic relationship between resonant frequency squared and lumbosacral stiffness. For the body parameters of Subject A, this relationship is described by the following equation.

$$k = \frac{528\omega^4 + 16740\omega^2 + 97200}{103.6\omega^2 + 841}$$

where ω is in units of Hz and k in units of Nm/rad.

The relationship is illustrated in Figure 5-10(a). The upper half of the hyperbola corresponds to mode I rocking, and the lower half to mode II. Real values for resonant frequency could only be found for mode I. As shown in Figure 5-10(b), lumbosacral stiffness of at least 116 Nm/rad was required for rocking to occur. This is essentially a stability criterion. Any resonant frequency can be obtained by increasing lumbosacral stiffness.

The non-linear model was able to produce successful rocking cycles (one foot lifted, then the other, returning to a point within 10% of the initial conditions). It did so using both rocking modes. 36 simulation trials were performed in all, 12 for each subject. 31 of the trials were successful; five failed. All successful trials exhibited rocking mode I. Frequencies were observed from 0.32 to 1.01 Hz. Mode I frequencies tended to be higher (mean 0.67 Hz) than Mode II (mean 0.51 Hz). No statistical analysis was performed because the results were influenced by our choice of initial conditions, which was not randomized. Foot lift duration ranged from 0.33 to 0.98 s. The amplitude of trunk flexion ranged from 4.7 to 20.3 deg.

When executed for longer than one cycle, the non-linear model typically became unstable, rocking out of control or failing to lift the feet alternately, after two to five cycles.

5.5 Discussion

This study serves as a basis for stiff-legged MLKAFO gait involving dynamic lateral trunk articulation, or rocking. To date, no hybrid systems use dynamic rocking to lift the feet, but the results of this study suggest that it might be useful. We demonstrated that a rocking strategy is capable of producing lower body movements that alternately lift the feet, however some additional assistance is required for paraplegic gait.

5.5.1 Major findings

The paraplegic subject (T12) could produce foot clearance only when holding the handrails, and even then, not consistently. Our first hypothesis was therefore not verified. The subject's feet would lift from the ground for an average of 0.44 s. We know from the previous chapter that passive stiff-legged swing phase is theoretically possible, but it requires approximately 0.5 to 0.9 s to execute. While the rocking trunk could create useful movement of the lower extremities in the frontal plane, it was not quite sufficient to facilitate passive gait.

Without the use of his arms, the paraplegic subject could not cause his feet to lift reliably enough for passive swing phase. This might have been due to the weakness of his partially paralyzed trunk muscles. However, since he was capable of lifting the feet while holding the handrails, we deduced that the abdominal muscles were capable of transmitting the necessary moments through the trunk. While not using the handrails, it probably became an issue of stability – rocking vigorously presented a risk of falling. The subject would rock more briskly when he saw that his feet were not lifting, but there was a limit to how hard he would go.

The able bodied subjects and the computer simulations demonstrated durations of foot lift up to almost a full second. Thus, it is possible to rock hands-free and raise the feet for sufficient periods of time for passive swing, when the lateral trunk flexors are properly stimulated. Our second hypothesis holds for the able-bodied subjects, but not the paraplegic subject. In the model, the external oblique muscles were controlled by an open loop scheme. It was therefore not surprising that long cycles could not be maintained. Closed loop control of stimulation may be able to stabilize the cycle over longer terms. Also, voluntary action of the arms may contribute to stability.

The able-bodied subjects both used the rocking trunk strategy to perform gait in the MLKAFO. Therefore, our third hypothesis is true, at least for these subjects. They were observed to use both rocking modes while walking.

5.5.2 Mode I vs. mode II

Two different modes of rocking were observed in this study. In mode I, the lower segment rotated one way in the frontal plane, while the upper segment rotated in the opposite direction. As a result, the body's center of mass did not move laterally as much as it did in mode II, where both segments rotated in the same direction. Hence, mode I involved less translation of the upper body center of mass.

The two modes observed suggest a system similar to a double mass-spring. Indeed, our linear model was an analog of that – an inverted double pendulum. Our model showed that mode I rocking was possible at any frequency, so long at the lumbosacral stiffness was sufficiently high (always greater than 116 Nm/rad). Mode II oscillations were not theoretically possible due to the absence of moment reactions between the feet and ground. The non-linear model involved such moment reactions due to the separation of the feet, however it too was unable to produce mode II rocking.

The able-bodied subjects used rocking mode I in all of the rocking trials and in the majority of the walking trials. Why they preferred this mode to the other is not entirely clear. Mode I appeared more comfortable for the subjects, probably because it did not make them feel off balance. The paraplegic subject used mode I exclusively when he was holding on to the handrails, and mode II for all of his hands-free trials. It is not clear why he preferred mode II. Slightly greater flexion of the trunk was measured when the paraplegic subject used mode II. Perhaps with weakened abdominal obliques, mode II is more effective.

5.5.3 Frequency vs. amplitude

The negative correlation between frequency and amplitude of trunk flexion in the able-bodied trials was not particularly surprising. In a simple mass-spring system, increasing the spring stiffness attains higher frequencies. If peak force is held constant, the amplitude will have an inverse squared relationship with frequency. If the muscles are thought of as variable-stiffness springs (Bergmark, 1989), it can be hypothesized that the able-bodied subjects achieved higher frequencies by increasing the activation of the abdominal obliques thereby

increasing the stiffness of the trunk. This was confirmed by the results of our linear model. However, no frequency-amplitude correlation was observed during the walking trials.

In the non-linear model, amplitude varied little. This might be expected since the initial conditions were preselected. Furthermore, peak muscle stimulation was not varied, hence the effective stiffness of the trunk was not varied (although it may have been somewhat affected by the first-order delay of muscle forces).

5.5.4 Further work

A follow-up study is necessary to determine if subjects with completely paralyzed abdominal muscles can lift the feet by rocking with FES applied to the obliques. Constant and cyclical open loop stimulation should be testing, and failing that, closed loop techniques should be examined. Modeling should be extended into three dimensions to explore the full kinetic and geometric issues of rocking and walking. An EMG study of able-bodied subjects walking in the MLKAFO could reveal much more about the behavior of the trunk muscles during rocking and walking. Additional insight into the natural control strategy could be gained if gait were perturbed by unexpected obstacles, (for example in the manner of Eng et al., 1997). Methods should be considered that address hip contractures, such as standing exercises and perhaps FES of the gluteal muscles.

5.6 Bibliography

Andrews BJ, Baxendale RH, Katakis J, Cliquet A, Paul JP, Freeman PA. Restoration of locomotion in spinal cord injured subjects using surface FES, In: *Functional Electrical Stimulation*, pp. 1-8, IEEE publications (PG S9), London, UK, 1986.

Andrews BJ, Cliquet A, Olin M, Burnham R, Thrasher TA. Paraplegic locomotion: a linked knee-ankle-foot hybrid FES system, *Proc. IFESS'97*, pp. 165-167, Simon Fraser University, Burnaby, Canada, August 1997.

Bauby CE, Kuo AD. Active control of lateral balance in human walking, *Journal of Biomechanics*, 33(11):1433-1440, 2000.

Bergmark A. Stability of the lumbar spine: a study in mechanical engineering, *Acta Orthop Scand*, supplement 230, vol. 60, 1989.

Callaghan JP, Patla AE, McGill SM. Low back three-dimensional joint forces, kinematics, and kinetics during walking, *Clinical Biomechanics*, 14(3):203-216, 1999.

Chandler RF, Clauser CE, McConville JP, Reynolds HM, Young JW. *Investigation of inertial properties of the human body, Final report, Apr. 1, 1972 – Dec. 1974*, AMRL-TR-74-137, Aerospace Medical Research Laboratories, Wright-Patterson Air Force Base, Dayton, Ohio, 1975.

Cliquet A, Nene AV, Barnett R, Andrews BJ. FNS augmentation of reciprocating HKAFO and KAFO braces, *Proceedings 2nd Vienna International Workshop on FES*, Austria, pp. 83-87, 1986.

Cliquet A. Paraplegic Locomotion with Neuromuscular Electrostimulation System. Dissertation, University of Strathclyde, 1988.

Cliquet A., Baxendale R.H., Andrews B.J. Paraplegic locomotion and its metabolic energy expenditure, In: *Comprehensive Neurologic Rehabilitation*, vol. 3, Ed Rose, Jones & Vrbova, pp. 139-146, Demos, USA, 1989.

Davoodi R., Andrews B. J. Modeling and control of FES standing in paraplegia: possibility of unassisted standing-up, *Proceedings IFESS'97*, pp. 93-94, Simon Fraser University, Burnaby, Canada, August 1997.

Dempster WT, Gaughran GRL. Properties of body segments based on size and weight. *American Journal of Anatomy*, 120(1):33-54, 1967.

Eng JJ, Winter DA, Patla AE. Intralimb dynamics simplify reactive control strategies during locomotion. *Journal of Biomechanics*, 30(6):581-588, 1997.

Gracovetsky S. *The Spinal Engine*, Springer-Verlag, Wein-New York, 1988.

Goldstein B, Young J, Escobedo EM. Rotator cuff repairs in individuals with paraplegia, *American Journal of Physical Medicine & Rehabilitation*, 76:316-322, 1997.

Kaplan ML, Heegaard JH. Energy-conserving impact algorithm for the heel-strike phase of gait, *Journal of Biomechanics*, 33(6):771-775, 2000.

Kralj A, Bajd T. *Functional electrical stimulation: standing and walking after spinal cord injury*. 1st edition CRC Press, pp. 97-102, 1989.

Kuo AD. Stabilization of lateral motion in passive dynamic walking, *International Journal of Robotics Research*, 18(9):917-930, 1999.

Li Q, Takanishi A, Kato I. Learning control for a biped walking robot with a trunk, In: *Proc '93 International Conference on Intelligent Robots and Systems*, Yokohama, Japan, pp. 1771-1777, July 1993.

Licht S. *Therapeutic Electricity and Ultraviolet Radiation*. Waverly Press, Baltimore, 1967.

McGeer T. Passive dynamic walking, *International Journal of Robotics Research*, 9(2):62-82, 1990.

Sinnott KA, Milburn P, McNaughton H. Factors associated with thoracic spinal cord injury, lesion level and rotator cuff disorders, *Spinal Cord*, 38(12):748-753, 2000.

Stokes IAF, Gardner-Morse M. Quantitative anatomy of the lumbar musculature, *Journal of Biomechanics*, 32(3):311-316, 1999.

Vicon 140 version 1.0, Movement analysis hardware & software, Oxford Metrics Ltd, Oxford, 1996.

Watanabe T, Futami R, Hoshimiya N, Handa Y. An approach to a muscle model with a stimulus frequency-force relationship for FES relationships. *IEEE Transactions on Rehabilitation Engineering*, 7(1):12-18, 1999.

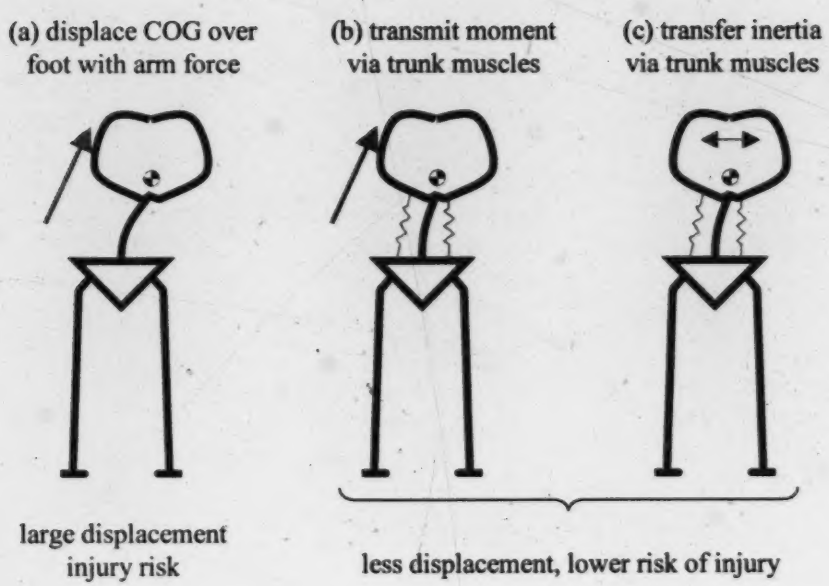
(a) displace COG over foot with arm force
(b) transmit moment via trunk muscles
(c) transfer inertia via trunk muscles
large displacement injury risk
less displacement, lower risk of injury

Figure 5-1: Three methods of generating foot clearance in MLKAFO.

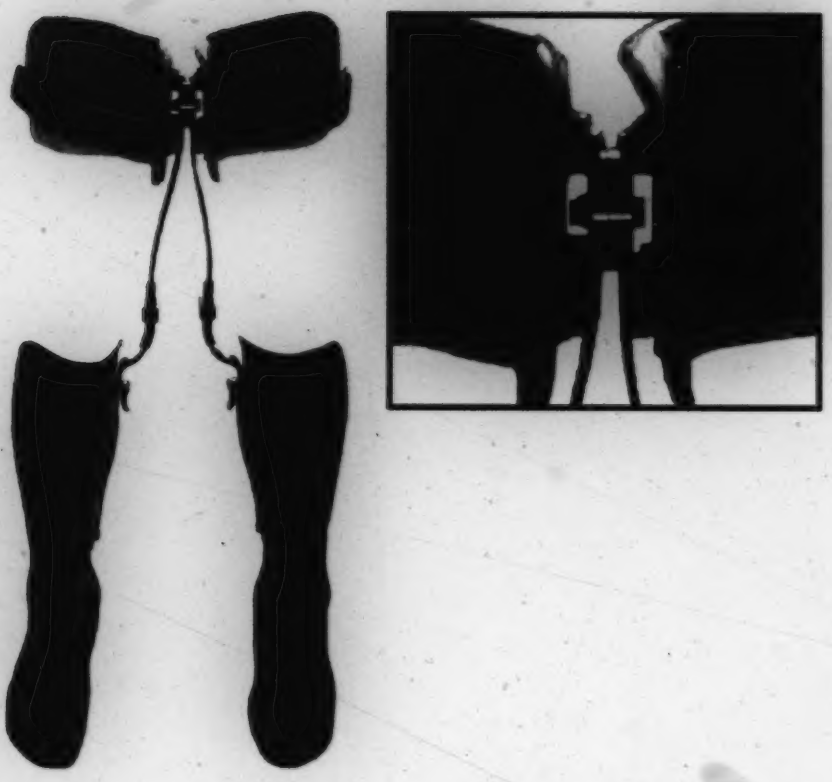

Figure 5-2: The medially linked knee-ankle-foot orthosis designed for FES-assisted paraplegic gait. (Inset) Close-up view of uniaxial medial joint.

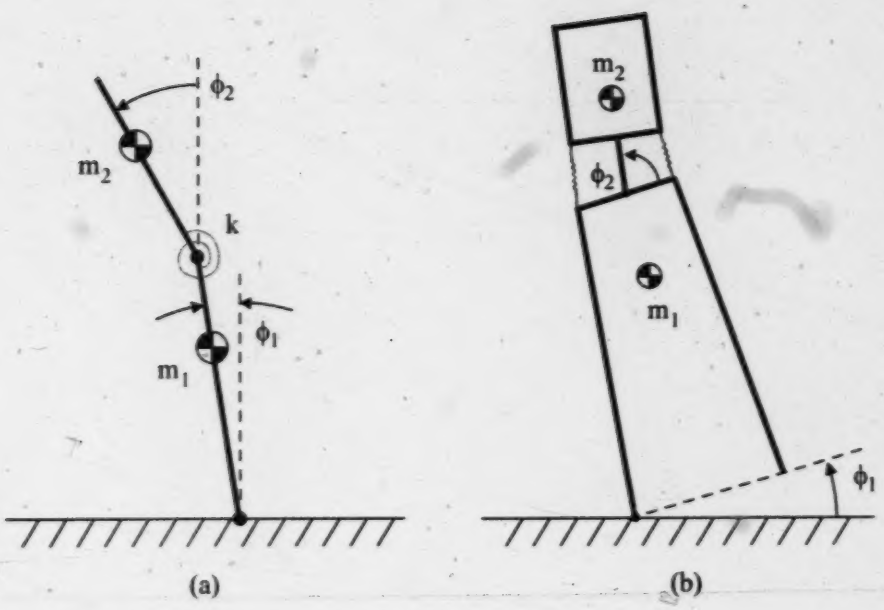

Figure 5-3: Two-segment, two degree-of-freedom frontal plane models of a person rocking laterally in the MLKAFO brace. (a) "Linear" inverted pendulum model, (b) non-linear model with foot-ground interaction.

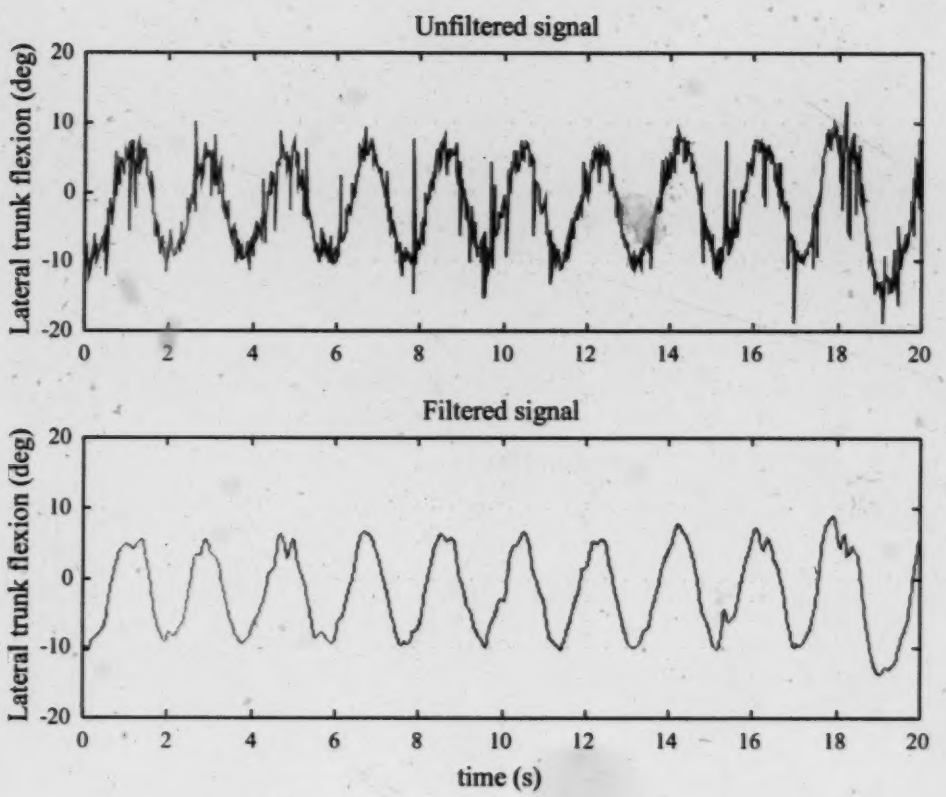

Figure 5-4: Experimental data (subject A, trial 2) smoothed by a low-pass, second order Butterworth filter with a cut-off frequency of 5 Hz.

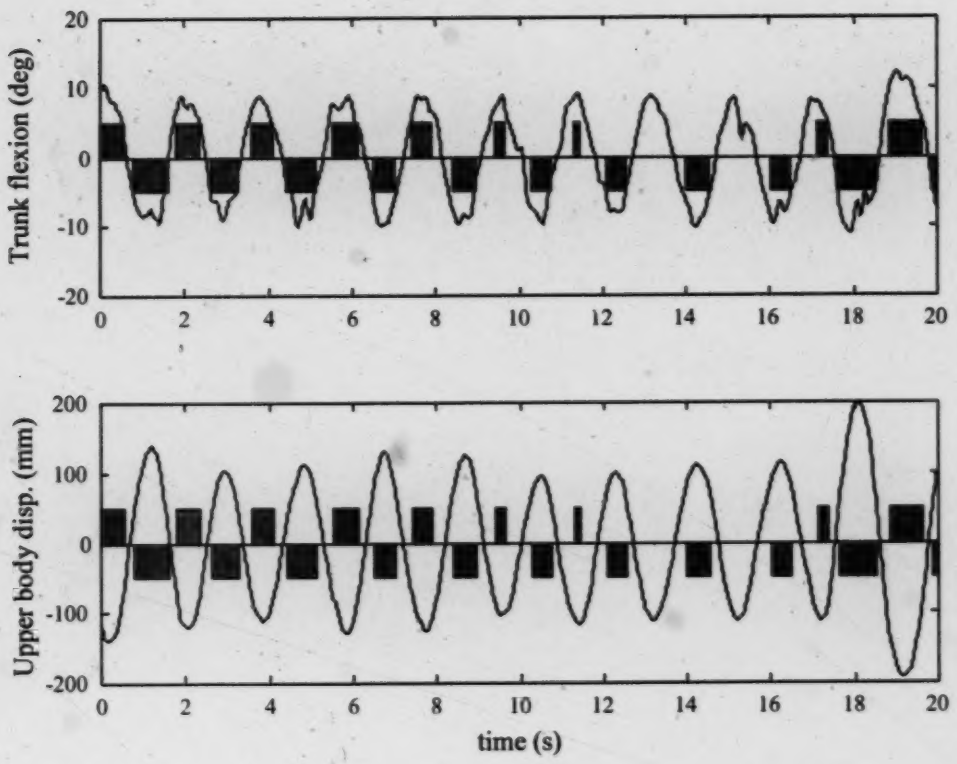

Figure 5-5: Subject A rocking in MLKAFO while holding handrails (mode I). By convention, (+)ve trunk flexion is to the left. Shaded rectangles indicate periods when a foot is raised: above zero indicates that the left foot is off the ground, below zero indicates the right foot. Horizontal displacement of the T1 marker shown in bottom graph.

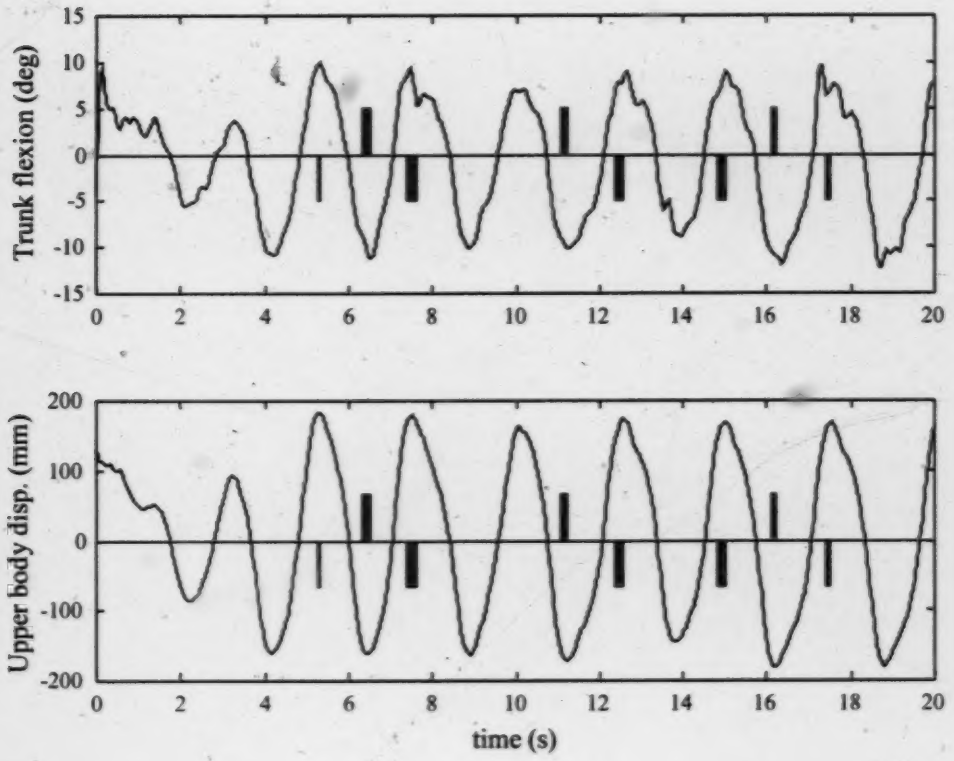

Figure 5-6: Subject A rocking in MLKAFO without hands (mode 2). By convention, (+)ve trunk flexion is to the left. Shaded rectangles indicate periods when a foot is raised: above zero indicates that the left foot is off the ground, below zero indicates the right foot. Horizontal displacement of the T1 marker shown in bottom graph.

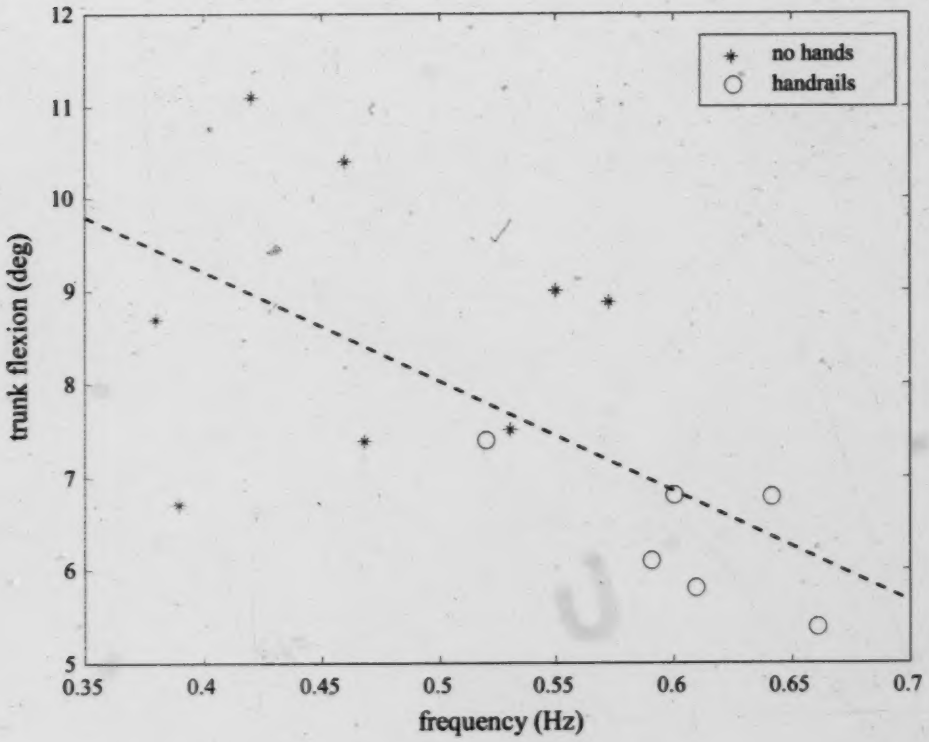

Figure 5-7: Mean trunk flexion angle versus rocking frequency from subject A trials. 'o' indicate handrail trials; '*' for no hands trials. Dashed line is the best fit through least squares regression.

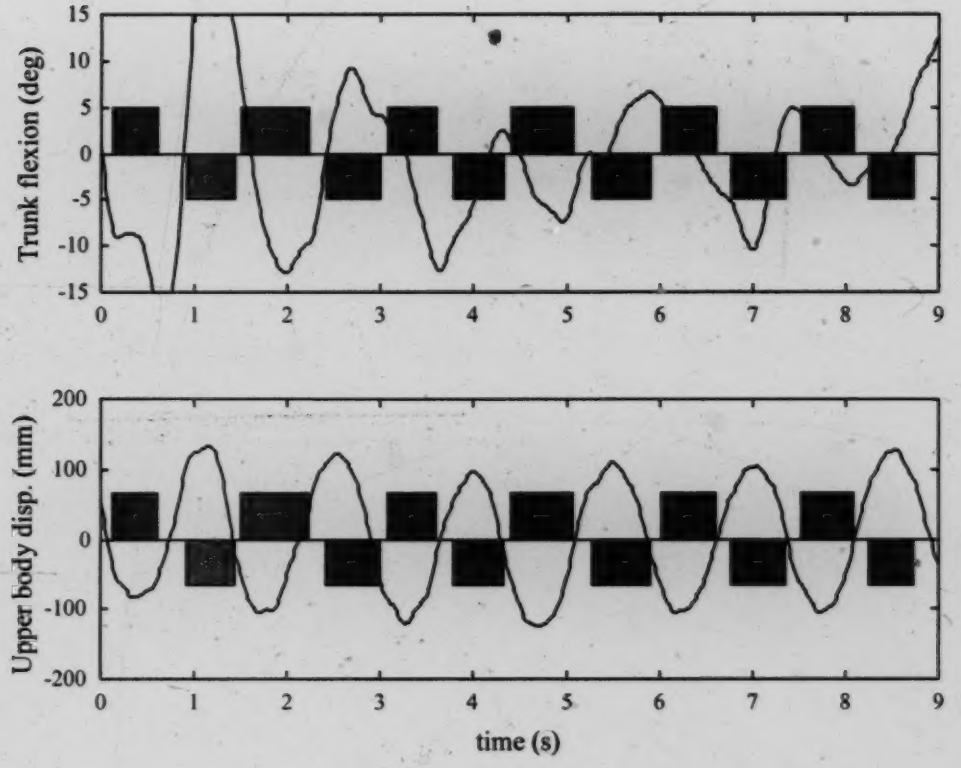

Figure 5-8: Subject B walking in MLKAFO, changing from mode II to mode I. (+)ve trunk flexion is to the left. Shaded rectangles indicate periods when a foot is raised: above zero indicates that the left foot is off the ground, below zero indicates the right foot. Horizontal displacement of the T1 marker shown in bottom graph.

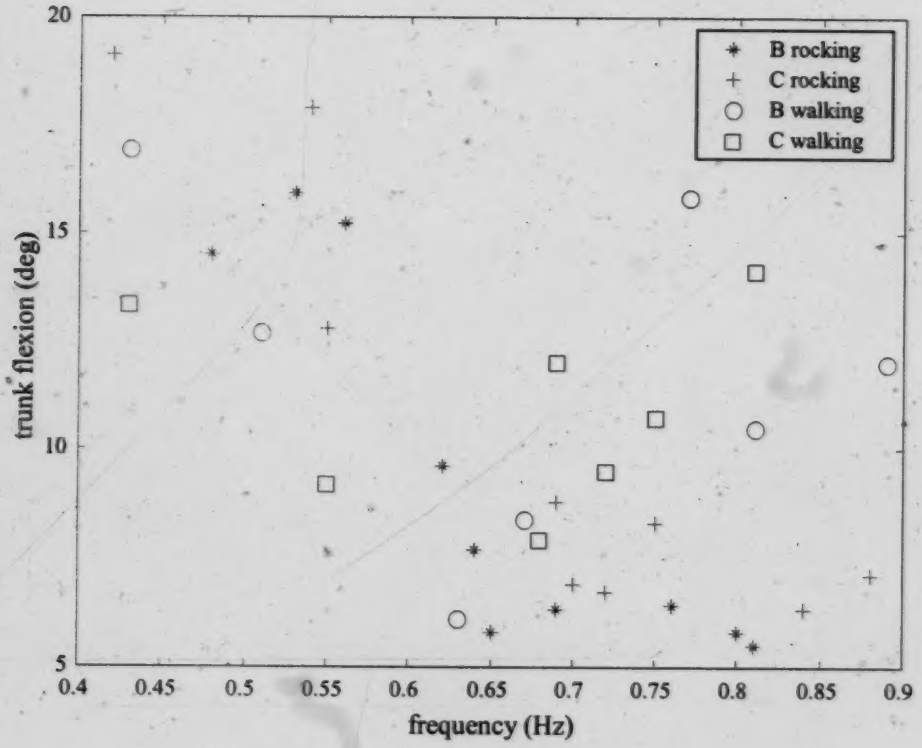

Figure 5-9: Mean trunk flexion angle versus rocking frequency from able bodied trials.

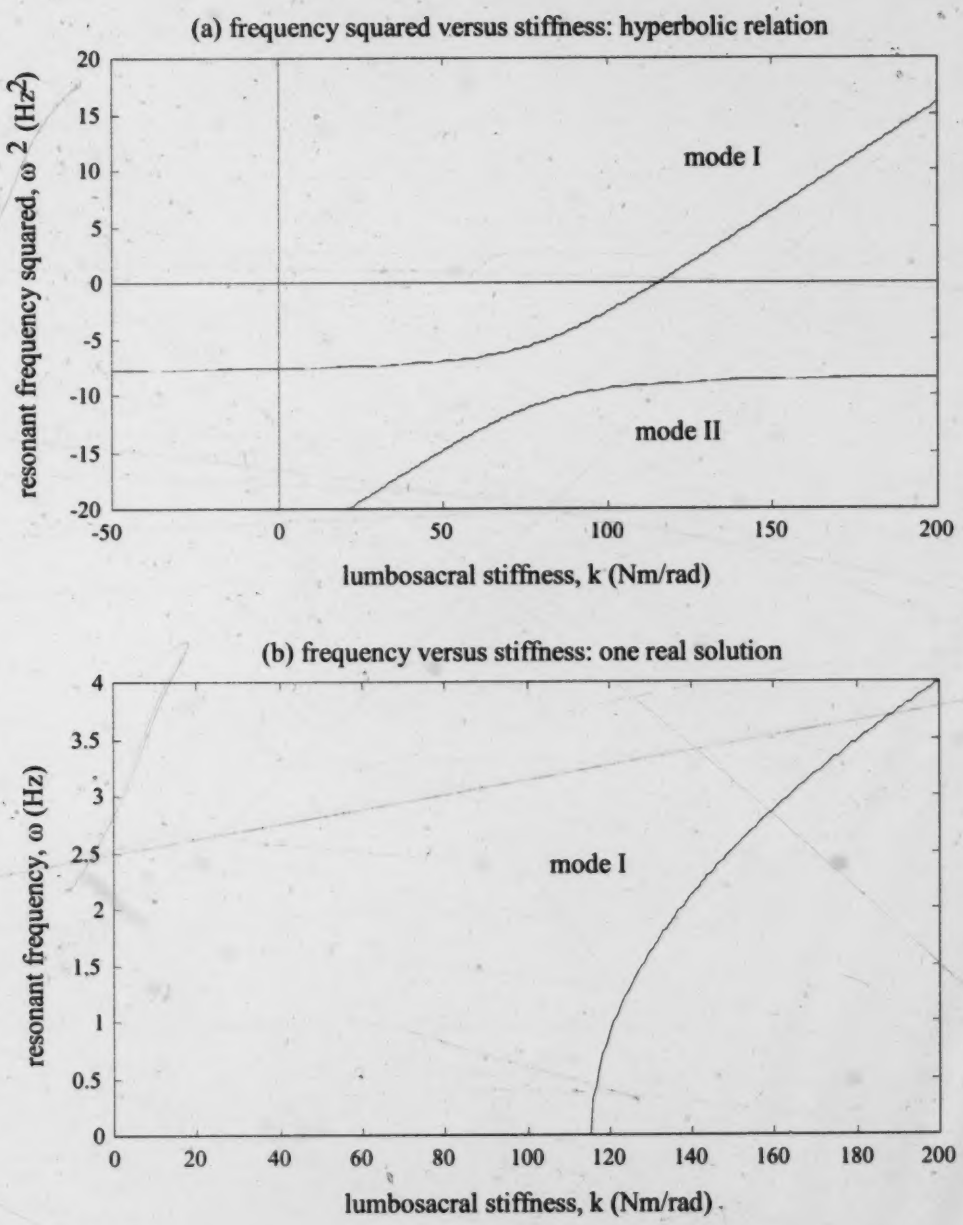
(a) frequency squared versus stiffness: hyperbolic relation
resonant frequency squared, ω 2 (Hz2)
mode I
mode II
lumbosacral stiffness, k (Nm/rad)
(b) frequency versus stiffness: one real solution
resonant frequency, ω (Hz)
mode I
lumbosacral stiffness, k (Nm/rad)

Figure 5-10: Frequency vs. stiffness relationship according to linear model (specfic to body parameters of Subject A).

6 Adaptive neuro-fuzzy control of paraplegic gait: reinforcement learning versus supervised learning

6.1 Abstract

An adaptive fuzzy network was designed to control paraplegic gait using a hybrid orthosis. The network adapted its own rule base using two distinct methodologies of machine learning: supervised learning and reinforcement learning. A biomechanical model of the swing leg in a powered hybrid orthosis was the subject of the controller. The swing leg included an electric motor at the hip and a Hill-type muscle model of the knee extensors. An optimized open loop controller developed in a previous study was used to train the supervised learning controller. The supervised learning controller was able to converge to a control strategy similar to that of the optimized open loop controller in approximately 10 trials. It outperformed the open loop controller by being able to cope with small perturbations in the system parameters. The penalty-based reinforcement learning controller, using simple binary feedback signals representing the objectives of swing phase, was able to find to a successful control strategy in usually about 150 trials. Once trained, it produced trajectories similar to the optimized open loop controller, even though it was given no information. The reinforcement learning controller had the added ability to continually readapt to large changes in the system parameters, which caused the other controllers to fail. When fatigue of the knee extensors was simulated, the reinforcement learning controller learned to compensate by increasing hip flexion moment. When initialized with a rule base from the supervised learning controller, the reinforcement learning controller was able to converge to a successful strategy in typically less than 30 trials.

6.2 Introduction

This study was motivated by the need to automate the design of controllers for paraplegic gait in the medially linked knee-ankle foot orthosis (MLKAFO). The MLKAFO is a hybrid orthosis. It consists of a mechanical brace to constrain some of the joints of the lower extremities, and FES of the knee extensors to actuate the legs. The dynamics of gait and neuromuscular stimulation are highly non-linear, thus robust non-linear controllers are required.

Over the decades, there have been many approaches to FES control. Traditional open loop systems are limited in that they do not adapt to the user – the user must adapt to them – nor can they adapt to a changing environment. Most open loop controllers only function well when all conditions are near perfect, which is rarely the case in paraplegic gait.

Today, the trend is towards closed loop controllers. Closed loop FES controllers are necessarily more complex than their open loop cousins. They require sensors, which are proving to be successful (Williamson and Andrews, 2001), and high performance electronics to rapidly process feedback signals. They also require advanced algorithms that are able to handle the highly non-linear system.

At the heart of every closed loop controller is a rule base that defines its behavior. Developing a complex rule base manually is a painstaking process with many pitfalls. Fuzzy logic is a closed loop control scheme that greatly simplifies the rule base design process, because it uses semantic variables. Fuzzy rules can be expressed as logical if-then statements such as, "if knee angle is LARGE, then quadriceps stimulation is SMALL." Fuzzy rule bases are extremely well suited for human interpretation. Fuzzy logic FES controllers using hand-crafted rule bases have been successful (Ng and Chizeck, 1993).

Control schemes based on neural networks allow for machine learning techniques that enable the controller to create its own rule base. Neuro-fuzzy controllers are those that place a fuzzy rule base into neural network architecture such that they may incorporate machine learning. These systems are considered to have the best of both worlds.

Supervised learning (SL) describes a class of machine learning controllers that learn from expert knowledge. Through back-propagation, these controllers learn to mimic the behavior of the expert.

Reinforcement learning (RL) is a special class of machine learning methods that learn through interacting with the environment and receiving reinforcements (rewards and penalties). These methods require no prior knowledge about the plant. They also have the advantage of being able to

continually update their rule base, and adapt to changes in the system. Neuro-fuzzy controllers that use RL have the advantage of being able to use prior expert knowledge, coded as fuzzy rules, which effectively "jump start" the learning process (Berenji, 1993, Davoodi and Andrews, 1998).

In this study, we theoretically analyze an adaptive neuro-fuzzy controller for the swing phase of MLKAFO gait. SL is compared to RL in terms of how quickly they converge on a rule base that works, and also in terms of how well they deal with perturbations to the system. As a basis for comparison for both learning methods, an optimized open loop controller from a previous study was used (Bielen, 1993). Finally, we test the idea of jump starting the RL controller with previously acquired knowledge to accelerate the learning rate.

6.2.1 Hypotheses

H7. A particular closed loop electrical stimulator for paraplegic gait can be improved with reinforcement learning.

The following additional hypotheses were made:

1. A SL closed loop AFN controller that uses an optimized open loop control scheme as training data will adapt and outperform the optimized open loop controller.
2. A RL based closed loop AFN controller that uses no prior data will find a unique control scheme that outperforms the open loop and SL controllers.
3. The SL controller will converge faster than the RL controller.
4. The RL controller can be initialized with the rule base developed by the SL controller, and it will continuously adapt to new environment parameters.

6.3 Methods

6.3.1 Model of the swing leg

A very simple 2-segment model of the human swing leg was used. It is illustrated in Figure 6-1. Essentially, it is a compound pendulum consisting of a thigh segment and a shank & foot segment. The hip joint was assumed to be attached to an inertial frame of reference. The equations of motion were derived using Newton-Euler analysis and are provided in Appendix D.

Passive elastic and damping reactions were assigned to the knee and hip joints, representing the inherent physiological reactions due to bone, ligaments, et cetera. The joint reaction equations used were taken from Davy and Audu (1987). The common Hill-type muscle model described in section 1.6.6 was used to simulate FES of the knee extensors (vasti). The hip extension moment was applied by a motor with a first-order response.

Body segment parameters were calculated for a typical male of 75 kg mass and 1.80 m height according to the scaling methods of Dempster (1955). The maximum isometric moment of the knee extensors was initially set to 50 Nm.

The model was implemented using MATLAB software on a Sun workstation. The differential equations were solved using a numerical integration method (4/5-order Runge-Kutta with adaptive step size). The initial conditions of the dynamic system were taken from actual gait data of a normal male (Vaughan, 1992). As we saw in chapter 4, these conditions were insufficient to produce passive swing phase – therefore, some active control is required.

In this swing leg model, there are two control signals (hip torque and quadriceps stimulation), and two state feedback signals (hip and knee angle).

6.3.2 Adaptive Fuzzy Network

An Adaptive Fuzzy Network (AFN) with particular network structure and algorithms suitable for reinforcement learning was developed. The AFN was a trainable, universal, nonlinear function approximator with adjustable parameters. As illustrated in Figure 6-2, it consists of four neural network layers:

1. The input fuzzification layer uses Gaussian membership functions to determine the "fitness" of each input variable to each rule. Each membership function was defined by three variables corresponding to center, width and kurtosis. These generalized Gaussian membership functions are differentiable and therefore adjustable by gradient based learning algorithms.
2. The rule evaluation layer uses the fuzzy logic AND (product) operation to combine all inputs to each rule at the active level.
3. The composition layer uses "sum-normalization" to combine weighted fuzzy singleton into a real-valued output signal. The normalization procedure

enhances highly applicable rules and prevents the learning from slowing down when all rules' active levels are low.

4. The squash layer normalizes the real-valued output signal to a value in the interval [0 1] using the following sigmoid

$$z = 1/(1+e^{\frac{s}{s0}})$$

where *s0* determines the sigmoid shape. z was then scaled to the actual output range using a linear transformation.

6.3.2.1 Supervised Learning controller

Two independent SL AFN controllers were developed, one for hip torque control, and another for quadriceps stimulation control. Both used two inputs, the hip and knee joint angles, and provided two outputs, hip torque and quadriceps stimulation pulse width. Each of these AFN controllers used five Gaussian membership functions for each input and defined 25 fuzzy rules using the Sugeno-style inference method with fuzzy singletons (Sugeno, 1985, Wang and Andrews, 1994). Both of these were trained using a basic gradient following back propagation algorithm. An energy-optimized open loop control scheme was used as the training data for the SL controller (Bielen, 1993).

6.3.2.2 Reinforcement Learning controller

Two separate RL controllers were also developed, one for hip torque control, and the other for quadriceps stimulation. The RL controllers were each built around two AFNs. Like the SL controllers, the RL controllers used hip and knee angles for input.

Reinforcement feedback was provided at the end of the trials in the form of three binary variables. The variables were equal to 1 or 0 indicating whether a criteria of swing phase was met or not met, respectively. The three criteria for successful swing phase were defined: (1) foot clearance greater than zero at all times during the swing phase, (2) hip angle never greater than 0.7 radians, and (3) knee extension (between -0.1 and 0.1 radians) at heel-strike. The RL controller acted only on negative reinforcement signals (zeros), i.e. it penalized and did not reward.

The RL controller learned using Williams' REINFORCE algorithm (Williams 1992). Figure 6-3 illustrates the operational scheme of one RL controller. An Action Net (AN) acts as an adaptive closed-loop controller whose performance is evaluated by an Evaluation Net (EN). Both AN and EN use an AFN as a trainable component. The AN has a Stochastic Search Unit (SSU) inserted before the output squash layer. The SSU is a stochastic search engine that introduces controllable noise into the output. The noise is a normally distributed random variable with mean determined by the AFNa and variance controlled by the evaluation signal, v. The SSU scatter range decreases as control performance improves, becoming zero when an optimal solution is found.

The AFN inside the EN used nine Gaussian membership functions for each input, as opposed to five in the AFN within the AN. The resulting rule base consisted of 81 rules. The larger rule base was to ensure that there was accurate reinforcement predication. The learning rules for EN parameters used Sutton's Temporal Differences algorithm (Sutton, 1988). The *TD Error*, $\hat{r}$, is a secondary reinforcement that indicates the variation between two sequential states. It is computed from external reinforcement r and predicted reinforcement v from the AFN.

6.3.3 Trials

First, the supervised learning controller was trained using the optimized open loop controller as training data. The number of trials – that is, the number of swing phase cycles that need to be performed – was noted as a measure of the rate of convergence. Then, the isometric knee extensor moment was multiplied by a factor between 0.5 and 2.0 to simulate fatigue and potentiation. The behavior of the trained SL controller was noted.

The RL controller was initialized with arbitrary rules and executed repeatedly until a solution was found that routinely achieved the objectives of swing phase. The convergence rate and resulting control scheme was observed.

Finally, the RL controller was initialized with the rule base from the SL controller. Then the gains on the hip motor and the isometric knee extensor

muscle moment were varied between 0.5 and 1.7, and thus its ability to adapt to new conditions was evaluated.

Even though the rule base from the trained SL controller provided prior knowledge only for the Action Net, but none for the Evaluation Net, the RL controller could still get a jump start. The reasons are as follows. The learning of the Action Net is a RL task in that the desired signal is not provided. On the other hand, the learning of the Evaluation Net is basically a SL task where the desired signal is provided by the environment in the form of penalty or reward. The difference between EN learning and the common SL is that these desired signals (reinforcements) are delayed binary signals.

6.4 Results

6.4.1 SL controller

The SL controller was able to converge to a successful control strategy in 12 trials. From there, it produced results very similar to the optimized open loop controller. Figure 6-4 compares the SL controller signal to the optimized open loop controller signal.

The SL controller was able to produce successful swing phase when the isometric knee extensor moment was reduced to 0.86 of its original value, thus simulating muscle fatigue. The SL controller successfully compensated by increasing the stimulus. The open loop controller failed under these conditions. Below a factor of 0.86, the SL controller could not create sufficient knee moments due to saturation of the muscle recruitment curve.

Simulating muscle potentiation, the isometric knee extensor moment could be increased by a factor up to 1.7 of its original value. The controller compensated by simply reducing the pulse width output. The open loop controller could not respond at all to potentiation, and produced hyperextension at the knees.

6.4.2 RL controller

The RL controller converged on a unique control strategy after about 150 trials. As shown in Figure 6-6, it provided hip torque at the initial swing phase to flex the leg and clear the ground, then provided quadriceps stimulation at the terminal swing phase to extend the knee and prepare for stance. Figure 6-5 shows

the three-dimensional control surfaces produced by the RL controller. This new control scheme is completely unlike the optimized open loop controller and its student, the SL controller. However, it works.

Figure 6-7 shows the two-dimensional phase plane of the swing leg trajectory. Starting from the initial position, the controller should control the leg trajectory to avoid foot collision (FC <0 zone) and extreme hip flexion (HA > 0.7 zone), then reach the successful end position (knee extension, -0.1 < KA < 0.1).

6.4.3 Jump-starting the RL controller with prior knowledge

When the rule base from the trained SL controller was imported to the AN of the RL controller, and the system parameters were changed, the RL controller could converge to a new solution in typically 20-30 trials. Figure 6-5 shows the control signals from the jump-started RL controller after the isometric knee extensor moment was multiplied by 0.40 (simulating severe fatigue). Convergence to this scheme took 29 trials.

When given significant variations in body mass and geometric parameters, the RL controllers converged to new solutions in usually less than 30 trials.

6.5 Discussion

The advantage of SL is that it can rapidly clone knowledge from supervisors. However, it requires knowledgeable supervisors. RL is a relatively new machine learning methodology, which has the advantage of self-learning without supervisors. It tends to learn slowly due to a lack of informative teaching signals. By combining SL and RL, controllers are possible that rapidly learn a successful control strategy using SL based on one particular model. Then, without further supervision, it can readapt to changes in the plant using RL.

Neural networks can modify the internal network parameters during learning, but the internal parameters are hard to comprehend for a human. Fuzzy logic systems are better suited for incorporating human knowledge in expressive fuzzy rule format with noise and fault tolerance, but the rules are not necessarily easy to obtain. By combining fuzzy logic with a neural network, as in the AFN, we can incorporate prior human knowledge and previous learning experiences in

the fuzzy rule base and use neural network learning algorithms to adjust rules by learning from example, or by trial and error.

6.5.1 Major findings

The results clearly indicate that SL is capable of finding a solution faster than RL (in the order of 10-20 times faster). This is because the SL controller has the benefit of expert information, which guides it towards a known solution. The RL controller must wander without a map, so to speak, to find its solution. We found it very interesting that the solution found by the RL controller was completely different than the solution learned by the SL controller. Yet, it produced desired results. RL may be very useful in finding unique solutions to other difficult, non-linear control problems concerning hybrid orthoses.

The SL controller outperformed its open loop teacher due to the fact that it utilizes state feedback. This was seen when fatigue was simulated. Open loop control is limited to very narrow ranges of operation, whereas closed loop control can respond to some perturbations and irregularities in function.

The feasibility of RL with an AFN was demonstrated. Although a specific biomechanical model was used representing a specific implementation of a hybrid FES orthosis, the control method is general purpose. The method requires no knowledge of the neuromuscular plant and can automatically adapt to differences between patients and time varying changes such as muscle fatigue. The RL controllers' use of partial training to re-adapt to new patients is practical for clinical application. In contrast to non-adaptive fuzzy logic networks, the teaching does not require a human expert to handcraft the fuzzy rules.

The RL controller succeeded where the SL and open loop controllers failed. This was because the RL controller is constantly updating its rule base. When a drastic change in system parameters occurs, the RL controller will seek a new solution, and often find it in 2-3 dozen trials.

This study also serves as an example of how multiple learning techniques can be combined to produce a highly effective controller. First, an open loop controller was designed and optimized in terms of energy minimization. The optimized open loop scheme served as training data for the closed loop supervised

learning controller, which adapted its fuzzy rule base accordingly. Once the fuzzy rule base had been defined, reinforcement learning could take over, enabling the system to react to changes in the musculoskeletal system due to fatigue, et cetera.

6.5.2 Future work

The next logical step in this line of research is to build a closed loop stimulator based on the algorithms discussed, and test it on actual human subjects. This study establishes the theory, but the model used was very simplistic and possibly too abstract to accurately represent the neuromuscular system. Closed loop control systems for FES gait have enjoyed a great deal of success on paper, but few have been successfully implemented in practice.

The AFN can be further improved by incorporating network structure optimization and scale-up capability via such techniques as genetic algorithms, ID3 type inductive machine learning or space clustering. Chiang et al. (1997) combined genetic algorithms with RL to train a fuzzy logic controller. The genetic algorithm was used to adjust fuzzy output consequence labels. R. Davoodi et al. (1998) used genetic algorithms to adjust the membership function parameters of fuzzy logic controller for neuroprosthetic control. However, it was found that genetic algorithms required a large number of trials to converge. RL was more efficient.

6.6 References

Andrews, B.J. Hybrid FES orthosis for paraplegic locomotion, *Studies in Health Technology and Informatics*, IOS Press, 5:50-56, 1992.

Bielen J. The feasibility of a powered brace for paraplegic gait: preliminary results of computer simulation study. Technical report, Department of Applied Sciences in Medicine, University of Alberta, Edmonton, Canada, April 1993.

Berenji HR. Adaptive fuzzy control with reinforcement learning. In: *Proceedings of American Control Conference*, pp. 1840-1844, San Francisco, CA, 1993.

Chiang CK, Chung HY, Lin JJ. A self-learning fuzzy logic controller using genetic algorithms with reinforcements, *IEEE Transactions on Fuzzy Systems*, 5(3), 1997.

Davoodi R, Andrews BJ. Modeling and control of FES standing in paraplegia: Unassisted standing up, *Proceedings of IFESS 97*, Burnaby, Canada, 1997.

Davoodi R, Andrews BJ. Computer simulation of FES standing up in paraplegia: a self-adaptive fuzzy controller with reinforcement learning, *IEEE Transactions on Rehabilitation Engineering*, 6(2):151-161, 1998.

Davy DT, Audu ML. A Dynamic optimization technique for predicting muscle forces in the swing phase of gait, *Journal of Biomechanics*, 20(2):187-201, 1987.

Ng SK, Chizeck HJ. A fuzzy logic gait event detector for FES using Firmware Transitional Logic, *Proc IEEE (EMBS) 10th Ann Internat Conf*, 1562-1563, 1993.

Sugeno, M. *Industrial applications of fuzzy control*. Elsevier Science Pub. Co., 1985.

Sutton, R.S. Learning to predict by methods of temporal differences, *Machine Learning*, 3:9-44, 1988.

Veltink, P.H., Chizeck, H.J., Crago, P.E., and el Bialy, A. Nonlinear joint angle control for artificially stimulated muscle, *IEEE Transactions on Biomedical Engineering*, 39(4):368-380, 1992.

Wang, F. And Andrews, B.J. Adaptive fuzzy logic controller for FES- computer simulation study, *Proc. of Ann. Int. Conf. Of IEEE/EMBS*, 16:406-407, 1994.

Williams, R.J. Simple statistical gradient-following algorithms for connectionist reinforcement learning, *Machine Learning*, 8:229-256, 1992.

Williamson R, Andrews BJ. Detecting absolute human knee angle and angular velocity using accelerometers and rate gyroscopes, *Med Biol Eng Comput*, 39(3):294-302, 2001.

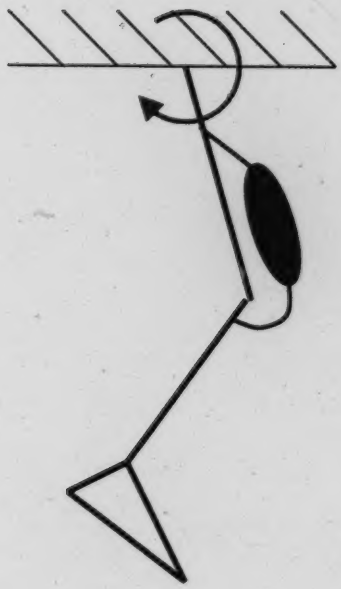

Figure 6-1: 2-segment sagittal plane model of swing leg. This is the same model as used in Bielen, 1993.

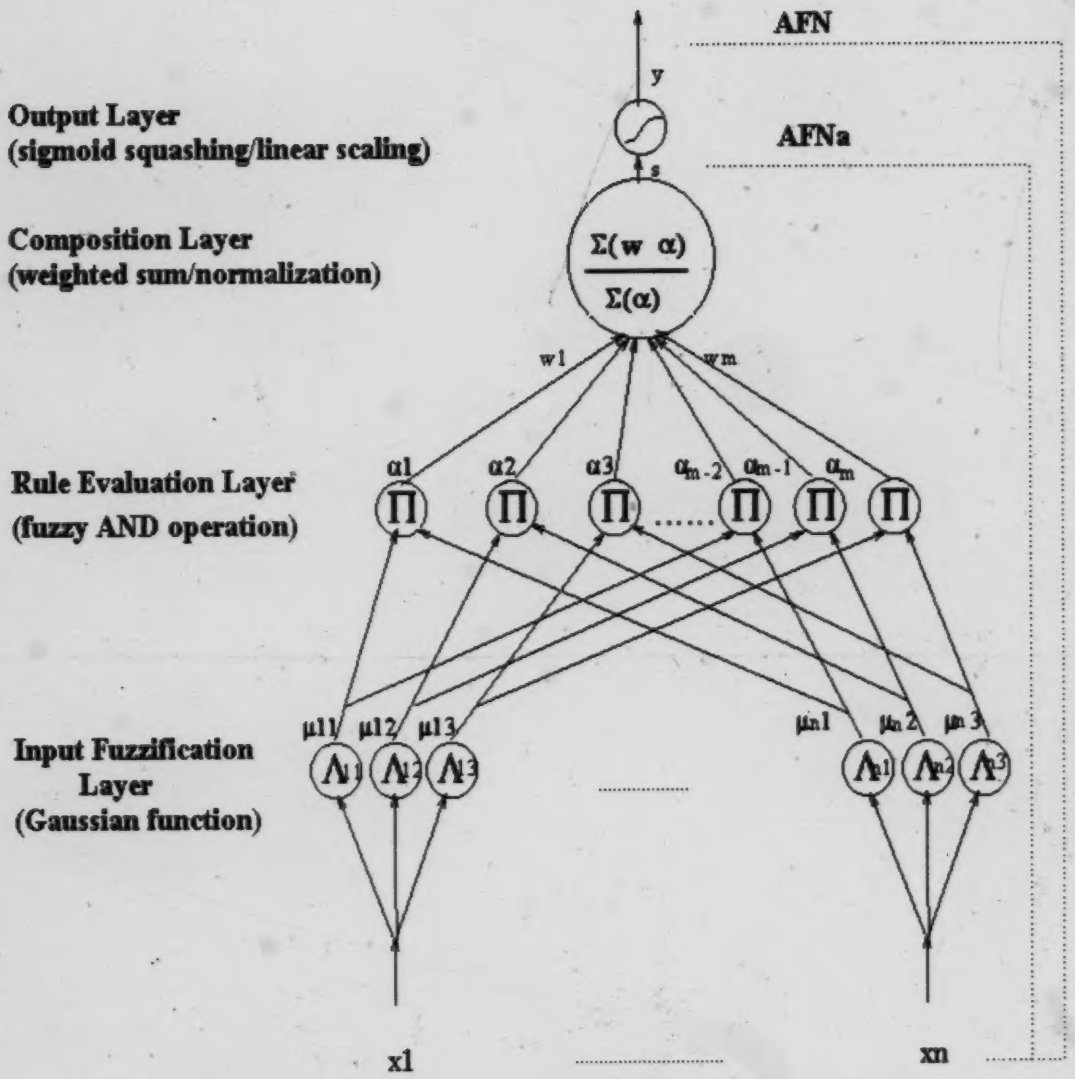

Figure 6-2: Schematic diagram of the Adaptive Fuzzy Network, which processes n input variables according to m fuzzy rules, and produces a single variable output. AFNa refers to the AFN that omits the final squashing function.

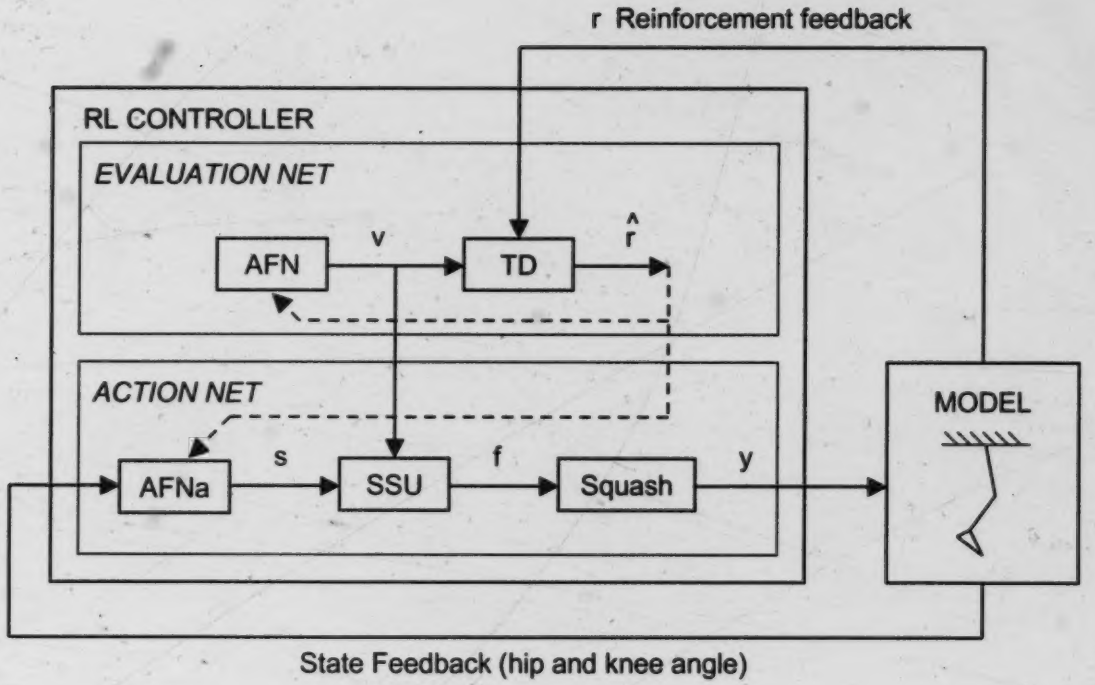

Figure 6-3: Reinforcement learning control scheme. The Action Net performs as an adaptive closed loop controller. It consists of an AFN, a Stochastic Search Unit (SSU), and a Squash layer. The Evaluation Net evaluates the performance of the Action Net based on reinforcement feedback via a Temporal Difference (TD) unit and an AFN separate from the action net.

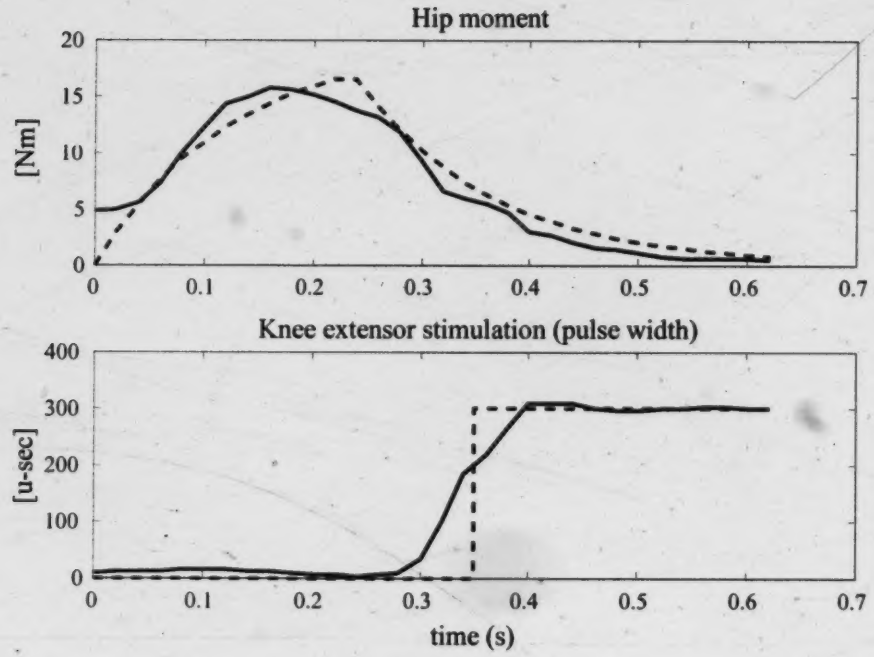

Figure 6-4: The SL controller learned to mimic the open loop controller (dotted lines) after only 10 trials.

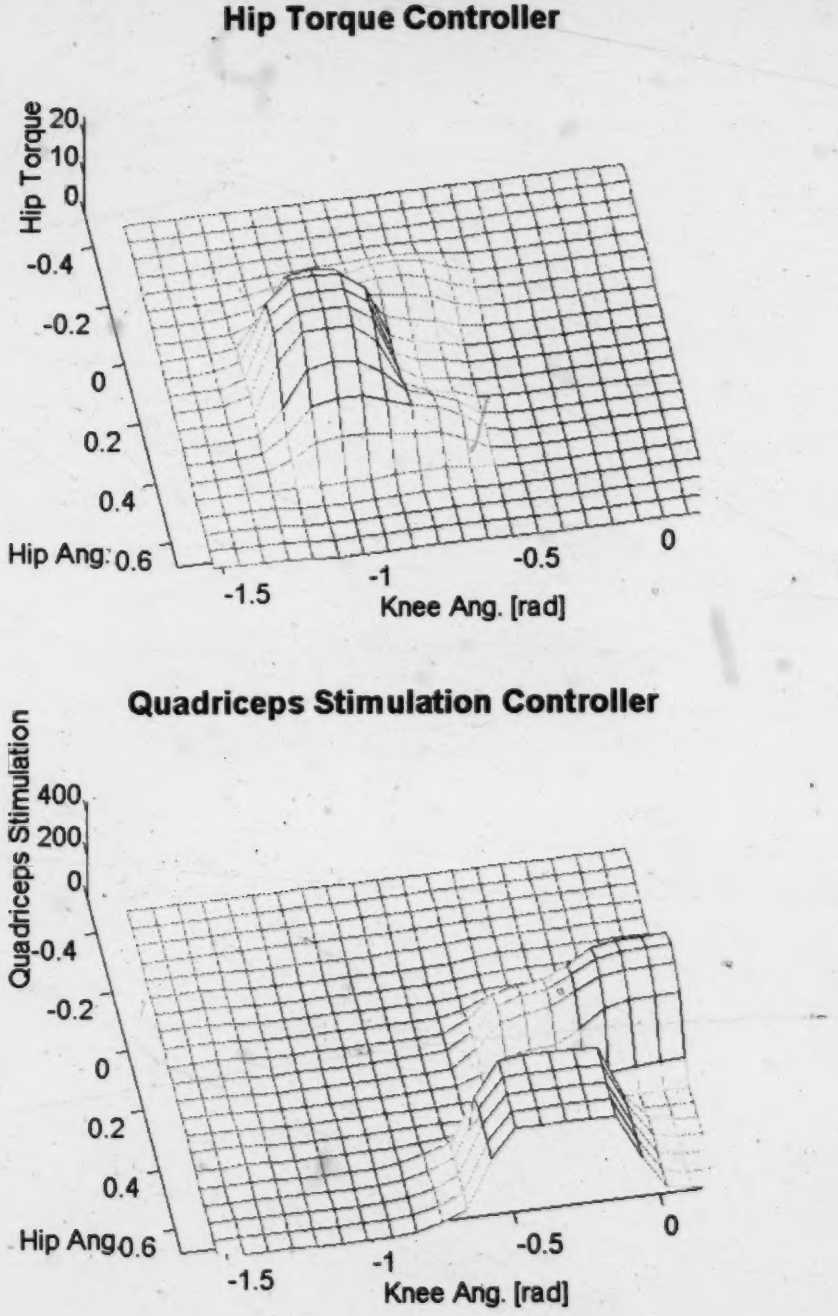

Figure 6-5: Control surfaces for the adapted RL controller. Hip torque given in units of Nm; Quadriceps stimulation given in units of μs (pulse width).

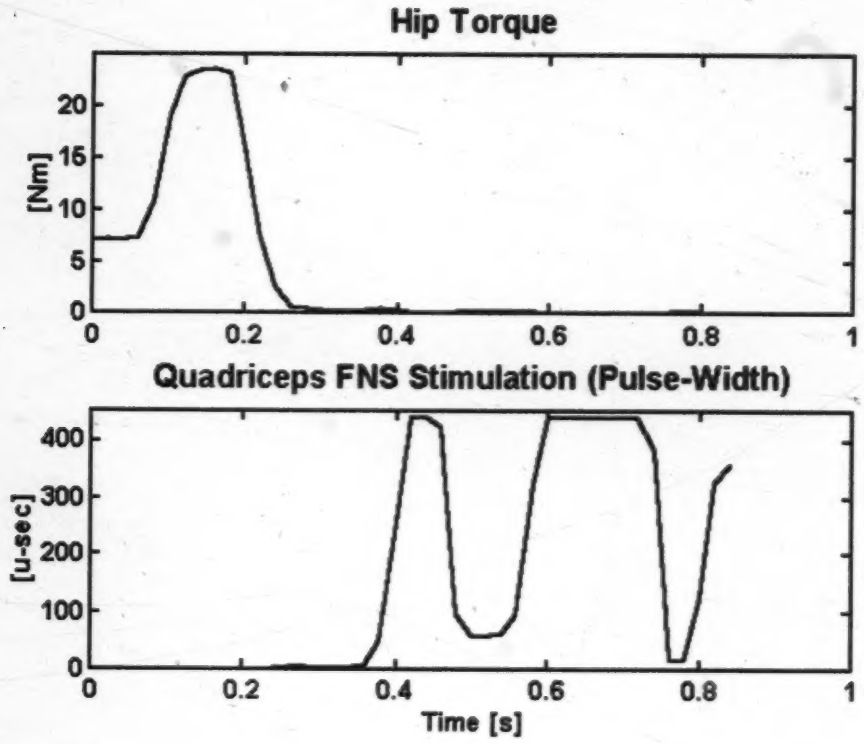

Figure 6-6: The RL controller converged to this unique scheme after 150 trials. No prior knowledge of the plant was used.

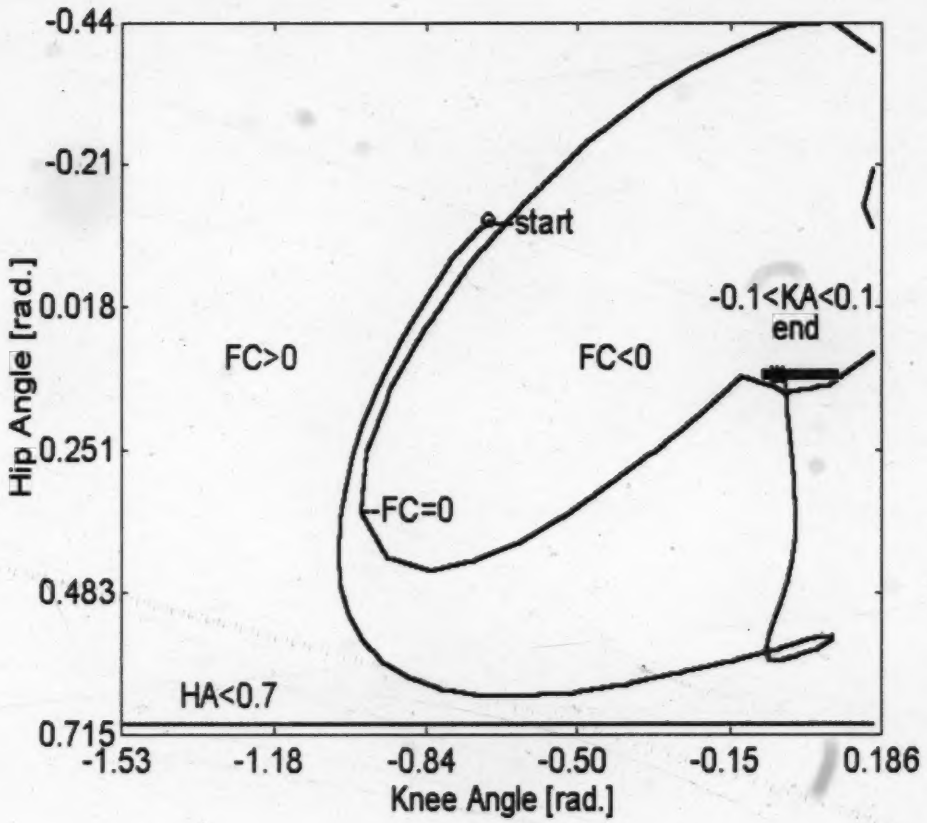

Figure 6-7: Phase plane of swing phase trajectory of RL controller. Regions indicated for foot clearance (FC), knee angle (KA), hip angle (HA).

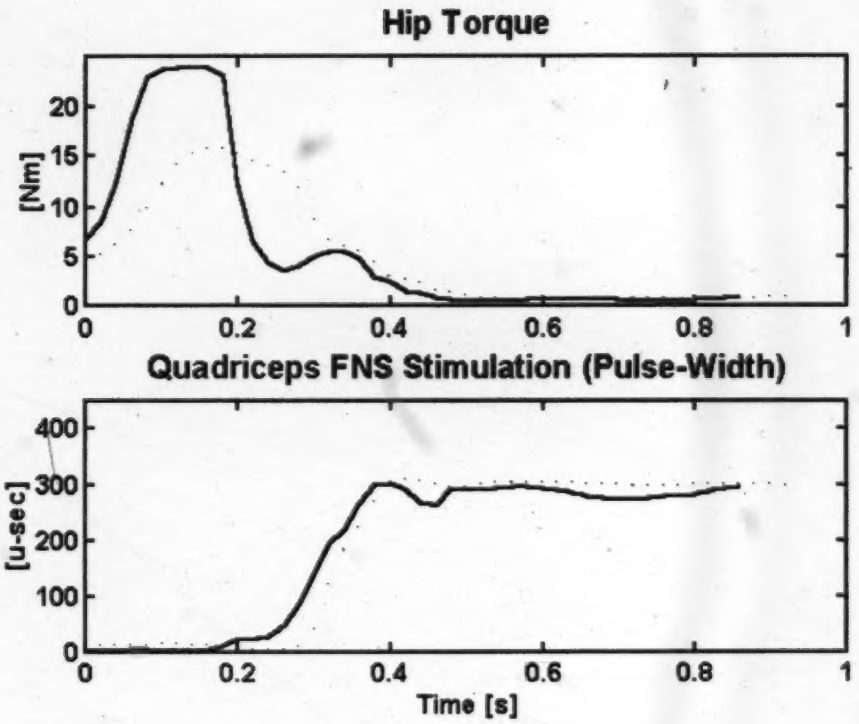

Figure 6-8: The RL controller re-adapted after isometric muscle force was cut in half (in 29 trials). Dotted lines indicate the expert knowledge provided by the trained SL controller.

7 General discussion and conclusions

7.1 Discussion

In essence, this thesis is a proposal for a new generation of hybrid orthoses that utilize novel biomechanical theories and advanced control concepts. It is a collection of ideas, each focusing on a particular shortcoming of current hybrid FES systems. These ideas share a common goal, which is to bring about new devices that will enable paraplegics to stand and walk more effectively than before. Such devices would vastly improve one's independence and quality of life after spinal cord injury.

Current hybrid orthoses are limited in several ways. Those with mechanical components above the waist are bulky and difficult to don and doff, while those without leave the paralyzed trunk unrestrained and potentially unstable. Subjects normally deal with trunk instability using their arms. Standing and walking require huge loads on the arms, which is problematic because many paraplegics already suffer from shoulder overuse syndromes. Proposed in Chapters 2, 3 and 5 are techniques aimed at relieving the arms. Another major limitation of current hybrid orthoses is the rapid rate at which electrically stimulated muscles fatigue. This problem can be addressed by simply reducing the mechanical energy requirements of those muscles, which is largely the approach taken in Chapters 3 through 6. There is a trend in hybrid orthoses today towards closed loop control. Advances in sensor and microprocessor technology are making possible sophisticated closed loop controllers, however the design of such controllers is still an extremely difficult task due to the complexity of FES-assisted gait. Proposed in Chapter 6 is a method of automating this design process. Many of the techniques analyzed in this thesis showed promise and ought to be developed further to bring about the new generation of hybrid orthoses.

The MLKAFO was chosen as the central focus of this thesis. It is a mechanical brace that is considered superior to other braces in its class due to its rigidity in the frontal plane and its lack of above-waist components. Each chapter in this thesis presents the analysis of a specific idea (or group of similar ideas). The first idea proposed was to overcome the lack of stability of the paralyzed

trunk by electrically stimulating the paraspinal muscles. The second idea was a new sit-to-stand strategy for paraplegics involving trunk momentum. Thirdly, an improvement to the efficiency and control of paraplegic gait was proposed that harnessed the passive dynamics of the legs. Fourth, a strategy of rocking the trunk from side to side was advocated for MLKAFO gait. Lastly, an advanced machine learning method for closed loop FES control of gait was considered. Altogether, these ideas form a basis for a new generation of hybrid orthoses.

Following is a summary of how my results reflect upon the original hypotheses (first stated in section 1.1):

H1. *Higher levels of spinal cord injury result in lower trunk stability.*
Inconclusive. An insufficient number of SCI subjects were recruited to address this hypothesis. In order to provide sufficient data, at least a dozen subjects should be recruited, representing a broad range of injury levels. In pursuing this hypothesis, however, a novel measurement protocol was designed for objectively assessing trunk stability in the context of spinal cord injury. Such a methodology has never been presented before, and the one developed here could have important clinical application. For example, the measurement could be used as part of SCI classification – an indication in severity of trunk dysfunction. Furthermore, this objective trunk stability measurement would be well suited to assess the efficacy of treatment methods, including the pioneering cellular treatments aimed at spinal cord regeneration.

H2. *Open loop functional electrical stimulation of the erector spinae muscles will improve trunk stability after SCI.*
Inconclusive. Open loop stimulation of the lumbar erector spinae significantly improved stability measurements for one subject (see Table 2-5), but failed to have any affect on the other (Table 2-6). The FES method investigated was very simplistic, involving open loop control and only two channels of stimulation. In future attempts, more trunk muscles should be targeted, such as the external obliques for resistance to lateral

perturbations and/or a greater portion of the erector spinae (more electrodes).

H3. *Thrusting the rigid trunk forward before lift-off during sit-to-stand in conjunction with hip extension moment will reduce required knee moment.*
Rejected. It was found that trunk momentum did not significantly reduce the requirements of the knee extensors. However, when starting from a position with the feet flat on the ground, initial trunk momentum was required to prevent rock-back failures (Figure 3-7). This is the first time such a conclusion has been reached. A standard three-segment model of STS was used to investigate this hypothesis.

H4. *Passive swing phase is feasible and beneficial during gait in the medially linked knee-ankle-foot orthosis.*
Accepted. Passive swing phase was successfully simulated using a sagittal plane model of gait. However, it was only possible given a very small range of kinematic conditions at toe-off (Figure 4-7). This suggests an entirely new control scheme that activates muscles during the double support phase with the goal of producing these precise conditions. The study designed to investigate this hypothesis employed a novel method of generating body parameters for a random sample of subjects. This technique could be used in any biomechanical modeling studies that aim to make conclusions across a broad population.

H5. *Passive gait in the medially linked knee-ankle-foot orthosis can be improved by a powered hip actuator or an elastic element across the knee.*
The first part of this hypothesis was accepted, and the second part rejected. An ideal motor supplying a moment to the medial link was able to prevent failures during swing phase when the toe-off conditions were slightly off (Figure 4-14). Such a motor, if practically installed over the medial joint on the brace, could respond to an 'error prediction' signal generated by the forward dynamics model given the conditions at toe-off. The elastic element, on the other hand, proved to have no beneficial effect.

H6. *Stiff-legged gait in the medially linked knee-ankle-foot orthosis can be improved by functional electric stimulation of the trunk.*

This hypothesis was not really verified, but the results were somewhat supportive. The able-bodied subjects were able to perform stiff-legged gait in the MLKAFO by oscillating their trunks laterally to produce foot clearance (Figure 5-9). The SCI subject, however, could not lift the feet reliably enough for steady gait (e.g. Figure 5-6). Also, the SCI subject tended to use a different rocking than the able-bodied subjects. A computer model indicated that a certain level of trunk stiffness is required to produce harmonic oscillations in a rocking mode where the trunk rotates in the opposite direction to the lower extremities (Figure 5-10). This method of articulating the trunk to produce foot clearance – the spinal engine – is not new, but this pilot study presents the first investigation of how it might be used in paraplegic gait.

H7. *A particular closed loop electrical stimulator for paraplegic gait can be improved with reinforcement learning.*

Supported. Reinforcement learning improved the swing phase controller by enabling it to develop unique control strategies without supervision (Figure 6-6). Although it was slow to converge – 150 trials – it was able to cope with ongoing changes to the system, whereas the open loop and supervised learning controllers failed. Furthermore, the reinforcement learning controller could be initialized with an expert rule base instead of starting from scratch. This technique suggests an entirely new generation of intelligent controllers for paraplegic gait that adapt to specific control tasks without human supervision.

7.2 Conclusions

From the results of the studies, the following conclusions were made:

1. Trunk instability is a serious problem for persons with SCI. Many cannot sit unassisted and resist small perturbations without using their arms. Trunk instability is likely the main reason why excessive arm loads are necessary during paraplegic STS and gait.

2. Unassisted STS is theoretically possible for isometric knee moments as low as 50-70 Nm, if (1) the subject sits with feet flat on the ground and knees flexed at right angles, (2) the hip extensors are stimulated with isometric moments of up to 200 Nm, and (3) the trunk is flexed at a rate of at least 75 deg/s, which is very rapid.
3. Trunk momentum prior to lift-off in STS does not significantly reduce the required hip and knee moments. The purpose of the trunk momentum is to carry the body's center of mass to a position above the feet.
4. Passive swing phase during MLKAFO gait is theoretically possible if certain precise kinematic conditions are met at toe-off. It is therefore the duty of the pre-swing phase to produce the necessary joint angles and velocities.
5. Passive gait is more energy efficient when the knees are locked than when the knees are free during swing phase. The drawback is that stiff-legged gait is slower, more awkward looking, and ground clearance is more difficult to achieve. On the other hand, there is no risk of knee buckling during stiff-legged gait.
6. Oscillating the upper body laterally can produce ground clearance for stiff-legged gait. Only able-bodied subjects were able to successfully produce this movement. Computer models showed that a certain amount of lumbosacral stiffness or active control of the lateral trunk flexors is required.
7. Neuro-fuzzy reinforcement learning control is feasible for a basic swing phase controller

7.3 Future work

Now that some groundwork has been laid regarding improvements to the MLKAFO hybrid orthosis, the new techniques should be developed. Following is a list of the main follow-up studies that need to be done:

1. More data is required to address hypotheses H1 and H2. More SCI subjects with thoracic injuries should be recruited, and their trunk

stability measured on the apparatus. FES trunk stimulation should be expanded to include more of trunk muscles, particularly the abdominal obliques, and more levels of the erector spinae. If possible, the apparatus should be equipped to produce more controlled perturbations, perhaps by electric motor or hydraulic piston.

2. The sit-to-stand strategy that was theorized in Chapter 3 should be tested on human subjects. SCI subjects should be recruited, and experiments should be devised to measure the effect of the trunk momentum during STS. Also, the strength of electrically stimulated hip extensors needs to be measured. Able-bodied subjects should also be recruited for EMG experiments, measuring the specific trunk muscle activity during STS.
3. The feasibility of a passive gait controller needs to be analyzed. A computer model of pre-swing phase may give insight into the control issues concerning the production of the toe-off conditions necessary for passive swing phase. Once an effective control scheme is found, an FES controller should be built and tried out on SCI subjects.
4. Subjects with mid-thoracic injuries should attempt the oscillating trunk strategy for stiff-legged gait. Open loop FES should be applied to their abdominal oblique muscles to see if stiffening the trunk improves their gait and/or reduces their shoulder loads. Closed loop FES should be attempted as well to better regulate the trunk movement.
5. The adaptive neuro-fuzzy controller should be built and tried out on human subjects. The controller worked beautifully on our computer model, but how will it behave on living subjects?

Appendix A – equations of motion for sagittal plane sit-to-stand model

Three-segment inverted pendulum model of sit-to-stand

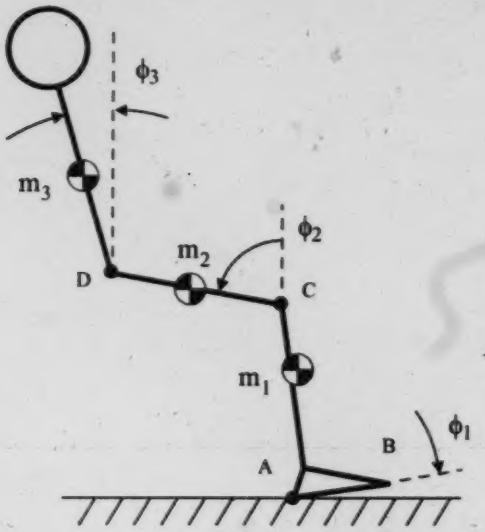

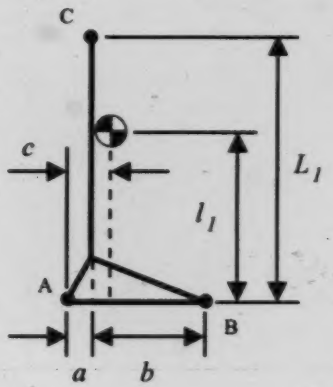

Define:

$\vec{r}$ is a position vector from the point of ground contact to segment 1 COM.

$\vec{R}$ is a position vector from the point of ground contact to the knee joint (point C).

CASE 1: Segment 1 rotates about the heel ($\phi_1 > 0$)

$$\vec{r} = \begin{bmatrix} \cos\phi_1 & -\sin\phi_1 \\ \sin\phi_1 & \cos\phi_1 \end{bmatrix} \begin{Bmatrix} c \\ l_1 \end{Bmatrix} \tag{A-1}$$

$$\vec{R} = \begin{bmatrix} \cos\phi_1 & -\sin\phi_1 \\ \sin\phi_1 & \cos\phi_1 \end{bmatrix} \begin{Bmatrix} a \\ L_1 \end{Bmatrix} \tag{A-2}$$

CASE 2: Segment 1 rotates about the toe ($\phi_1 < 0$)

$$\vec{r} = \begin{bmatrix} \cos\phi_1 & -\sin\phi_1 \\ \sin\phi_1 & \cos\phi_1 \end{bmatrix} \begin{Bmatrix} c-a-b \\ l_1 \end{Bmatrix} \tag{A-3}$$

$$\vec{R} = \begin{bmatrix} \cos\phi_1 & -\sin\phi_1 \\ \sin\phi_1 & \cos\phi_1 \end{bmatrix} \begin{Bmatrix} -b \\ L_1 \end{Bmatrix} \tag{A-4}$$

Derivation:

segment 1

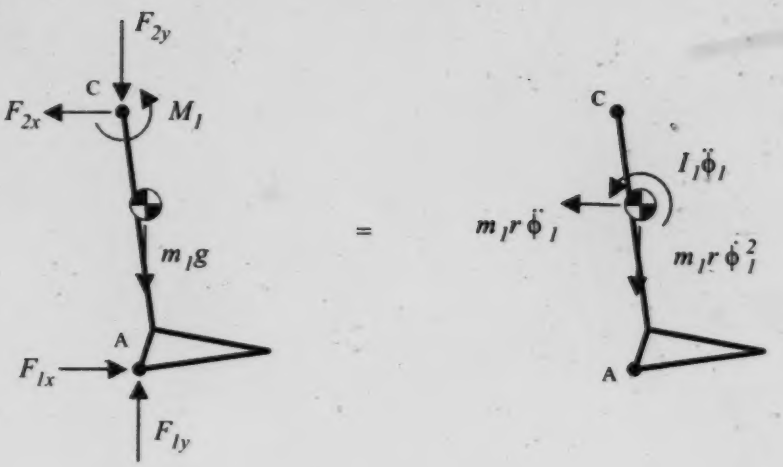

$$\sum F_x = F_{1x} - F_{2x} = -m_1 r_y \ddot{\phi}_1 - m_1 r_x \dot{\phi}_1^2 \qquad \text{(A-5)}$$

$$\sum F_y = F_{1y} - F_{2y} - m_1 g = m_1 r_x \ddot{\phi}_1 - m_1 r_y \dot{\phi}_1^2 \qquad \text{(A-6)}$$

$$\sum M_A = M_1 - m_1 g r_x - F_{2y} R_x + F_{2x} R_y = (I_1 + m_1 r^2)\ddot{\phi}_1 \qquad \text{(A-7)}$$

segment 2

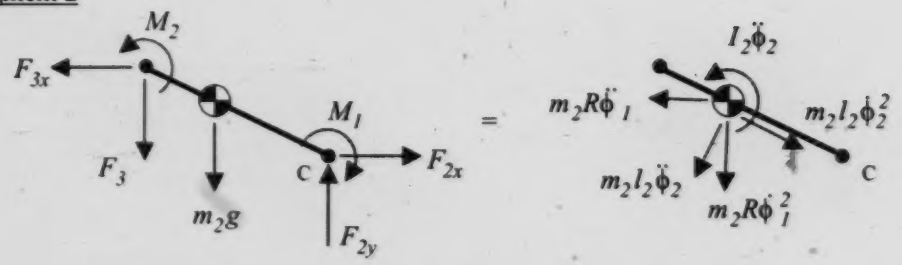

$$\sum F_x = F_{2x} - F_{3x} = -m_2 R_y \ddot{\phi}_1 - m_2 R_x \dot{\phi}_1^2 - m_2 l_2 \ddot{\phi}_2 \cos\phi_2 + m_2 l_2 \dot{\phi}_2^2 \sin\phi_2 \qquad \text{(A-8)}$$

$$\sum F_y = F_{2y} - F_{3y} - m_2 g = m_2 R_x \ddot{\phi}_1 - m_2 R_y \dot{\phi}_1^2 - m_2 l_2 \ddot{\phi}_2 \sin\phi_2 - m_2 l_2 \dot{\phi}_2^2 \cos\phi_2 \qquad \text{(A-9)}$$

$$\sum M_C = M_2 - M_1 + m_2 g l_2 \sin\phi_2 + F_{3x} L_2 \cos\phi_2 + F_{3y} L_2 \sin\phi_2 =$$
$$(I_2 + m_2 l_2^2)\ddot{\phi}_2 + m_2 l_2 (R_y \cos\phi_2 - R_x \sin\phi_2)\ddot{\phi}_1 + m_2 l_2 (R_y \sin\phi_2 + R_x \cos\phi_2)\dot{\phi}_1^2 \qquad \text{(A-10)}$$

segment 3

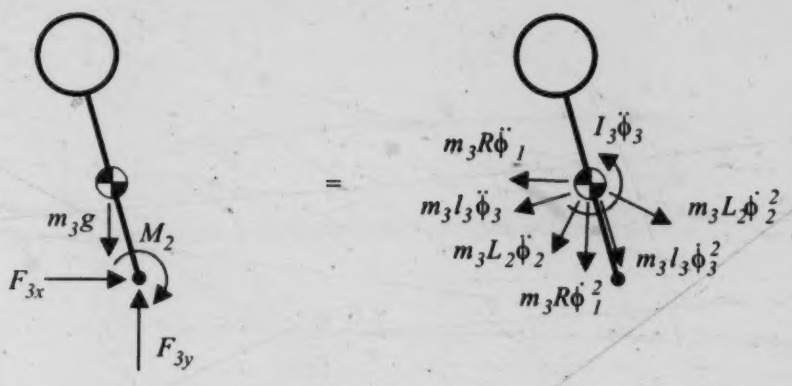

$$\sum F_x = F_{3x} = -m_3R_y\ddot{\phi}_1 - m_3R_x\dot{\phi}_1^2 - m_3L_2\ddot{\phi}_2\cos\phi_2 + m_3L_2\dot{\phi}_2^2\sin\phi_2 - m_3l_3\ddot{\phi}_3\cos\phi_3 + m_3l_3\dot{\phi}_3^2\sin\phi_3 \quad \text{(A-11)}$$

$$\sum F_y = F_{3y} - m_3g = m_3R_x\ddot{\phi}_1 - m_3R_y\dot{\phi}_1^2 - m_3L_2\ddot{\phi}_2\sin\phi_2 - m_3L_2\dot{\phi}_2^2\cos\phi_2 - m_3l_3\ddot{\phi}_3\sin\phi_3 - m_3l_3\dot{\phi}_3^2\cos\phi_3 \quad \text{(A-12)}$$

$$\sum M_D = -M_2 + m_3gl_3\sin\phi_3 = (I_3 + m_3l_3^2)\ddot{\phi}_3 + m_3l_3(R_y\cos\phi_3 - R_x\sin\phi_3)\ddot{\phi}_1 + m_3l_3(R_y\sin\phi_3 + R_x\cos\phi_3)\dot{\phi}_1^2 + m_3L_2l_3\ddot{\phi}_2\cos(\phi_3 - \phi_2) + m_3L_2l_3\dot{\phi}_2^2\sin(\phi_3 - \phi_2) \quad \text{(A-13)}$$

Combining equations A-10, A-11 and A-12 yields

$$(m_2l_2 + m_3L_2)(R_y\cos\phi_2 - R_x\sin\phi_2)\ddot{\phi}_1 + (I_2 + m_2l_2^2 + m_3L_2^2)\ddot{\phi}_2 + m_3L_2l_3\ddot{\phi}_3\cos(\phi_3 - \phi_2) = M_2 - M_1 + (m_2l_2 + m_3L_2)g\sin\phi_2 + (m_2l_2 - m_3L_2)(R_y\sin\phi_2 + R_x\cos\phi_2)\dot{\phi}_1^2 + m_3L_2l_3\dot{\phi}_3^2\sin(\phi_3 - \phi_2) \quad \text{(A-14)}$$

Combining equations A-5 through A-9, A-11 and A-12 yields

$$(I_1 + m_1r^2 + (m_2 + m_3)R^2)\ddot{\phi}_1 + (m_2l_2 + m_3L_2)(R_y\cos\phi_2 - R_x\sin\phi_2)\ddot{\phi}_2 + m_3l_3(R_y\cos\phi_3 - R_x\sin\phi_3)\ddot{\phi}_3 = M_1 - (m_1r_x + (m_2 + m_3)R_x)g + (m_2l_2 + m_3L_2)(R_y\sin\phi_2 + R_x\cos\phi_2)\dot{\phi}_2^2 + m_3l_3(R_y\sin\phi_3 + R_x\cos\phi_3)\dot{\phi}_3^2 \quad \text{(A-15)}$$

Equations A-13, A-14 and A-15 can be written in matrix form as follows

$$[I]\{\ddot{\phi}\} = [G]\{\dot{\phi}^2\} + \{g\} + \{M\} \qquad \text{(A-16)}$$

where ...

$$\{\ddot{\phi}\} = \begin{Bmatrix} \ddot{\phi}_1 \\ \ddot{\phi}_2 \\ \ddot{\phi}_3 \end{Bmatrix} \quad \text{and} \quad \{\dot{\phi}^2\} = \begin{Bmatrix} \dot{\phi}_1^2 \\ \dot{\phi}_2^2 \\ \dot{\phi}_3^2 \end{Bmatrix}$$

(I inertia matrix)

$$I_{11} = I_1 + m_1 r^2 + (m_2 + m_3)R^2$$
$$I_{12} = I_{21} = (m_2 l_2 + m_3 L_2)(R_y \cos\phi_2 - R_x \sin\phi_2)$$
$$I_{13} = I_{31} = m_3 l_3 (R_y \cos\phi_3 - R_x \sin\phi_3)$$
$$I_{22} = I_2 + m_2 l_2^2 + m_3 L_2^2$$
$$I_{23} = I_{32} = m_3 L_2 l_3 \cos(\phi_3 - \phi_2)$$
$$I_{33} = I_3 + m_3 l_3^2$$

(G gyroscopic matrix)

$$G_{11} = G_{22} = G_{33} = 0$$
$$G_{12} = -G_{12} = (m_2 l_2 + m_3 L_2)(R_y \sin\phi_2 + R_x \cos\phi_2)$$
$$G_{13} = -G_{13} = m_3 l_3 (R_y \sin\phi_3 + R_x \cos\phi_3)$$
$$G_{23} = -G_{23} = m_3 L_2 l_3 \sin(\phi_3 - \phi_2)$$

(gravitational vector)

$$g = \begin{Bmatrix} (m_1 r_x + (m_2 + m_3)R_x)g \\ (m_2 l_2 + m_3 L_2)g \sin\phi_2 \\ m_3 l_3 g \sin\phi_3 \end{Bmatrix}$$

(internal moment vector)

$$M = \begin{bmatrix} 1 & 0 \\ -1 & 1 \\ 0 & -1 \end{bmatrix} \begin{Bmatrix} M_1 \\ M_2 \end{Bmatrix}$$

This is a system of second-order ordinary differential equations for which no analytical solution is known.

CASE 3: Foot is flat on the ground ($\phi_1 = 0$) and segment 1 is stationary.

Define x as the distance from the heel to the center of pressure (COP).

segment 1

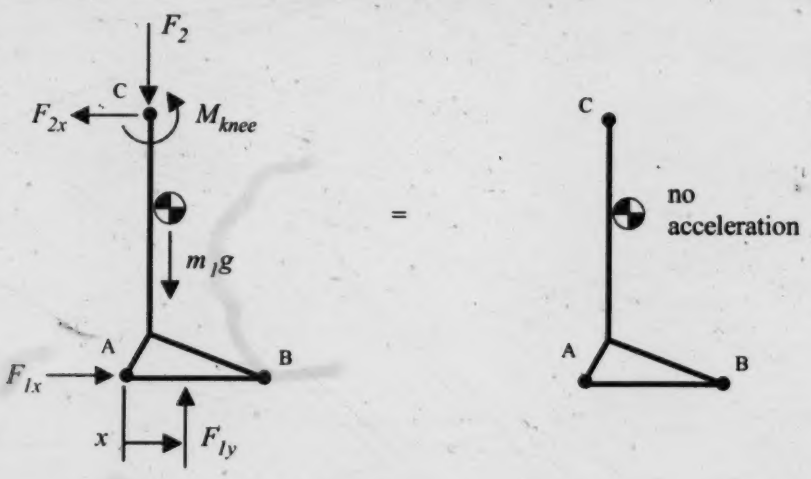

$$\sum M_A = M_{knee} + F_{1y}x - m_1 gc + F_{2x}L_1 - F_{2y}a = 0 \qquad \text{(A-17)}$$

Let $\dot{\phi}_1 = 0$ and $\ddot{\phi}_1 = 0$, then solve for $\ddot{\phi}_2$ and $\ddot{\phi}_3$ using equations A-13 and A-14. Confirm that the COP is underneath the foot, i.e. $0 < x < a + b$.

$$x = \frac{aF_{2y} - L_1 F_{2x} + cm_1 g - M_{knee}}{F_{2y} + m_1 g} \qquad \text{(A-18)}$$

where (equations A-8 and A-11)

$$F_{2x} = (m_3 L_2 + m_2 l_2)(\dot{\phi}_2^2 \sin\phi_2 - \ddot{\phi}_2 \cos\phi_2) + m_3 l_3 (\dot{\phi}_3^2 \sin\phi_3 - \ddot{\phi}_3 \cos\phi_3) \qquad \text{(A-19)}$$

and (equations A-9 and A-12)

$$F_{2y} = (m_2 + m_3)g - (m_2 l_2 + m_3 L_2)(\dot{\phi}_2^2 \cos\phi_2 + \ddot{\phi}_2 \sin\phi_2) - m_3 l_3 (\dot{\phi}_3^2 \cos\phi_3 + \ddot{\phi}_3 \sin\phi_3) \qquad \text{(A-20)}$$

If $x < 0$, then segment 1 begins rotating about the heel (go to CASE 1). If $x > a + b$, then segment 1 begins rotating about the toe (go to CASE 2). Otherwise, segment 1 remains stationary and CASE 3 is valid.

Appendix B – equations of motion for sagittal plane ballistic walking model

Three-segment inverted pendulum model of passive swing phase

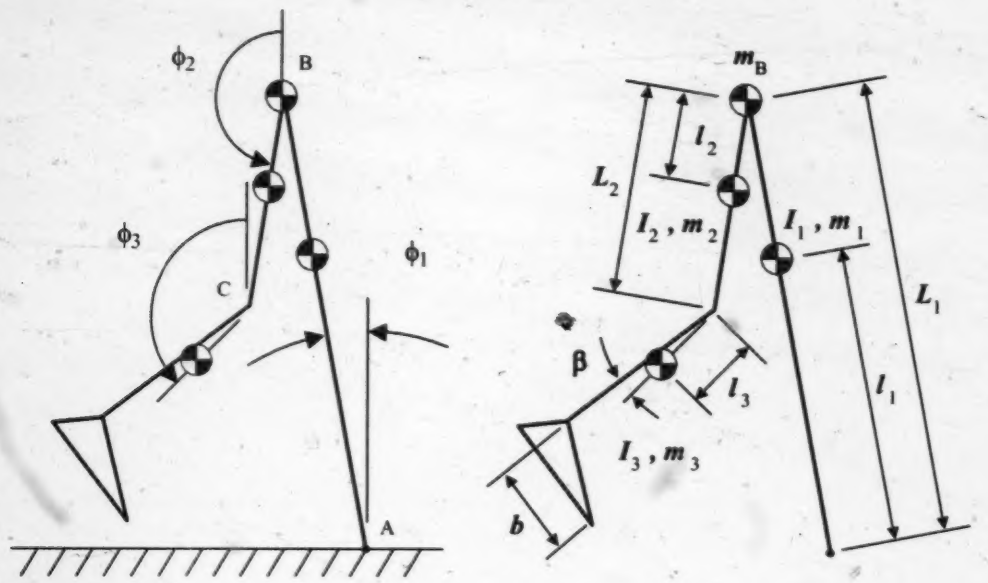

Derivation:

segment 1

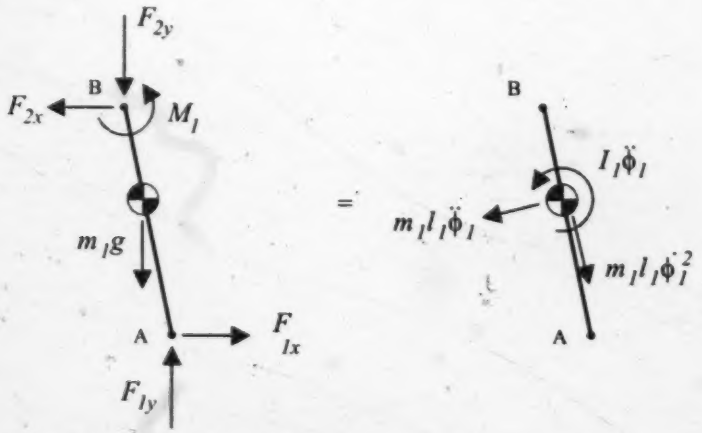

$$\sum F_x = F_{1x} - F_{2x} = -m_1 l_1 \ddot{\phi}_1 \cos\phi_1 + m_1 l_1 \dot{\phi}_1^2 \sin\phi_1 \qquad \text{(B-1)}$$

$$\sum F_y = F_{1y} - F_{2y} - m_1 g = -m_1 l_1 \ddot{\phi}_1 \sin\phi_1 - m_1 l_1 \dot{\phi}_1^2 \cos\phi_1 \qquad \text{(B-2)}$$

$$\sum M_A = M_1 + m_1 g l_1 \sin\phi_1 + F_{2y} L_1 \sin\phi_1 + F_{2x} L_1 \cos\phi_1 = (I_1 + m_1 l_1^2)\ddot{\phi}_1 \qquad \text{(B-3)}$$

point mass B (upper body)

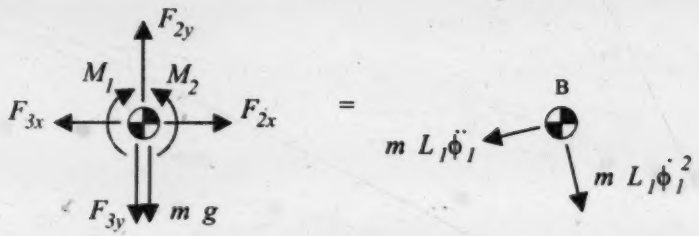

$$\sum F_x = F_{2x} - F_{3x} = -m_B L_1 \ddot{\phi}_1 \cos\phi_1 + m_B L_1 \dot{\phi}_1^2 \sin\phi_1 \tag{B-4}$$

$$\sum F_y = F_{2y} - F_{3y} - m_2 g = -m_B L_1 \ddot{\phi}_1 \sin\phi_1 - m_B L_1 \dot{\phi}_1^2 \cos\phi_1 \tag{B-5}$$

$$\sum M_B = M_2 - M_1 = 0 \tag{B-6}$$

segment 2

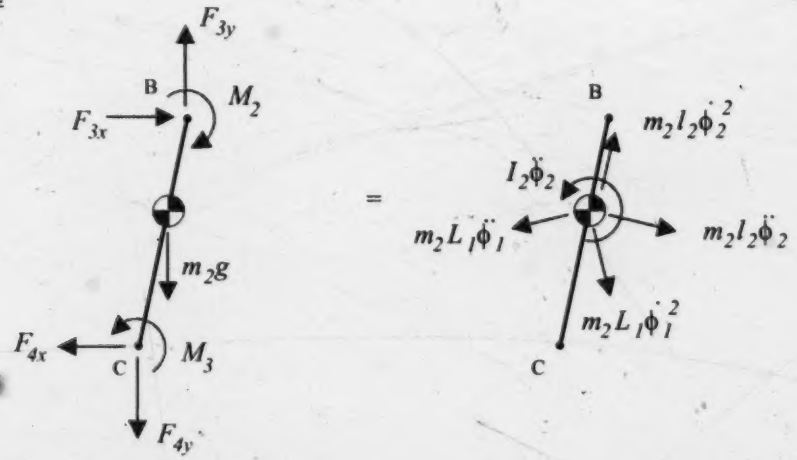

$$\sum F_x = F_{3x} - F_{4x} = -m_2 L_1 \ddot{\phi}_1 \cos\phi_1 + m_2 L_1 \dot{\phi}_1^2 \sin\phi_1 - m_2 l_2 \ddot{\phi}_2 \cos\phi_2 + m_2 l_2 \dot{\phi}_2^2 \sin\phi_2 \tag{B-7}$$

$$\sum F_y = F_{3y} - F_{4y} - m_2 g = -m_2 L_1 \ddot{\phi}_1 \sin\phi_1 - m_2 L_1 \dot{\phi}_1^2 \cos\phi_1 - m_2 l_2 \ddot{\phi}_2 \sin\phi_2 - m_2 l_2 \dot{\phi}_2^2 \cos\phi_2 \tag{B-8}$$

$$\sum M_B = M_3 - M_2 + m_2 g l_2 \sin\phi_2 + F_{4y} L_2 \sin\phi_2 + F_{4x} L_2 \cos\phi_2 = m_2 L_1 l_2 \dot{\phi}_1^2 \sin(\phi_2 - \phi_1) + m_2 L_1 l_2 \ddot{\phi}_1 \cos(\phi_2 - \phi_1) + (I_2 + m_2 l_2^2)\ddot{\phi}_2 \tag{B-9}$$

segment 3

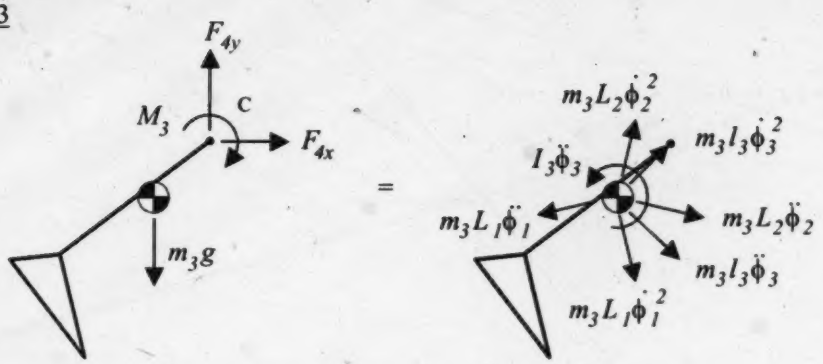

$$\sum F_x = F_{4x} = -m_3 L_1 \ddot{\phi}_1 \cos\phi_1 + m_3 L_1 \dot{\phi}_1^2 \sin\phi_1 - m_2 L_2 \ddot{\phi}_2 \cos\phi_2 + m_2 L_2 \dot{\phi}_2^2 \sin\phi_2 - m_3 l_3 \ddot{\phi}_3 \cos\phi_3 + m_3 l_3 \dot{\phi}_3^2 \sin\phi_3 \quad \text{(B-10)}$$

$$\sum F_y = F_{4y} - m_3 g = -m_3 L_1 \ddot{\phi}_1 \sin\phi_1 - m_3 L_1 \dot{\phi}_1^2 \cos\phi_1 - m_3 L_2 \ddot{\phi}_2 \sin\phi_2 - m_3 L_2 \dot{\phi}_2^2 \cos\phi_2 - m_3 l_3 \ddot{\phi}_3 \sin\phi_3 - m_3 l_3 \dot{\phi}_3^2 \cos\phi_3 \quad \text{(B-11)}$$

$$\sum M_B = -M_3 + m_3 g l_3 \sin\phi_3 = m_3 L_1 l_3 \dot{\phi}_1^2 \sin(\phi_3 - \phi_1) + m_3 L_1 l_3 \ddot{\phi}_1 \cos(\phi_3 - \phi_1) + m_3 L_2 l_3 \dot{\phi}_2^2 \sin(\phi_3 - \phi_2) + m_3 L_2 l_3 \ddot{\phi}_2 \cos(\phi_3 - \phi_2) + (I_3 + m_3 l_3^2) \ddot{\phi}_3 \quad \text{(B-12)}$$

Combining equations B-9, B-10 and B-11 yields

$$(m_2 l_2 + m_3 L_2) L_1 \ddot{\phi}_1 \cos(\phi_2 - \phi_1) + (I_2 + m_2 l_2^2 + m_3 L_2^2) \ddot{\phi}_2 + m_3 L_2 l_3 \ddot{\phi}_3 \cos(\phi_3 - \phi_2) = M_3 - M_2 + (m_2 l_2 + m_3 L_2) g \sin\phi_2 - (m_2 l_2 + m_3 L_2) L_1 \dot{\phi}_1^2 \sin(\phi_2 - \phi_1) + m_3 L_2 l_3 \dot{\phi}_3^2 \sin(\phi_3 - \phi_2) \quad \text{(B-13)}$$

Combining equations B-3 through B-8, B-10 and B-11 yields

$$(I_1 + m_1 l_1^2 + (m_B + m_2 + m_3) L_1^2) \ddot{\phi}_1 + (m_2 l_2 + m_3 L_2) L_1 \ddot{\phi}_2 \cos(\phi_2 - \phi_1) + m_3 L_1 l_3 \ddot{\phi}_3 \cos(\phi_3 - \phi_1) = M_2 + (m_1 l_1 + (m_B + m_2 + m_3) L_1) g \sin\phi_1 + (m_2 l_2 + m_3 L_2) L_1 \dot{\phi}_2^2 \sin(\phi_2 - \phi_1) + m_3 L_1 l_3 \dot{\phi}_3^2 \sin(\phi_3 - \phi_1) \quad \text{(B-14)}$$

Equations B-12, B-13 and B-14 can be written in matrix form as follows

$$[I]\{\ddot{\phi}\} = [G]\{\dot{\phi}^2\} + \{g\} + \{M\} \qquad \text{(B-15)}$$

where

$$\{\ddot{\phi}\} = \begin{Bmatrix} \ddot{\phi}_1 \\ \ddot{\phi}_2 \\ \ddot{\phi}_3 \end{Bmatrix} \quad \text{and} \quad \{\dot{\phi}^2\} = \begin{Bmatrix} \dot{\phi}_1^2 \\ \dot{\phi}_2^2 \\ \dot{\phi}_3^2 \end{Bmatrix}$$

(inertia matrix)

$$I = \begin{bmatrix} (I_1 + m_1 l_1^2 + (m_B + m_2 + m_3)L_1^2) & (m_2 l_2 + m_3 L_2)L_1 \cos(\phi_2 - \phi_1) & m_3 L_1 l_3 \cos(\phi_3 - \phi_1) \\ (m_2 l_2 + m_3 L_2)L_1 \cos(\phi_2 - \phi_1) & (I_2 + m_2 l_2^2 + m_3 L_2^2) & m_3 L_2 l_3 \cos(\phi_3 - \phi_2) \\ m_3 L_1 l_3 \cos(\phi_3 - \phi_1) & m_3 L_2 l_3 \cos(\phi_3 - \phi_2) & (I_3 + m_3 l_3^2) \end{bmatrix}$$

(gyroscopic matrix)

$$G = \begin{bmatrix} 0 & (m_2 l_2 + m_3 L_2)L_1 \sin(\phi_2 - \phi_1) & m_3 L_1 l_3 \sin(\phi_3 - \phi_1) \\ -(m_2 l_2 + m_3 L_2)L_1 \sin(\phi_2 - \phi_1) & 0 & m_3 L_2 l_3 \sin(\phi_3 - \phi_2) \\ -m_3 L_1 l_3 \sin(\phi_3 - \phi_1) & -m_3 L_2 l_3 \sin(\phi_3 - \phi_2) & 0 \end{bmatrix}$$

(gravitational vector) (internal moment vector)

$$g = \begin{Bmatrix} (m_1 l_1 + (m_B + m_2 + m_3)L_1)g \sin\phi_1 \\ (m_2 l_2 + m_3 L_2)g \sin\phi_2 \\ m_3 l_3 g \sin\phi_3 \end{Bmatrix} \qquad M = \begin{bmatrix} 1 & 0 \\ -1 & 1 \\ 0 & -1 \end{bmatrix} \begin{Bmatrix} M_2 \\ M_3 \end{Bmatrix}$$

This is a system of second-order ordinary differential equations for which no analytical solution is known.

The initial angles ϕ_2 and ϕ_3 can be determined given step length, s, and ϕ_1 as follows.

First define

$$\alpha = \pi - \arctan\left(\frac{s - b - L_1 \sin\phi_1}{L_1 \cos\phi_3}\right) \tag{B-16}$$

then

$$\phi_2 = \alpha + \arccos\left(\frac{L_2^2 - b^2 - L_3^2 + (s - b - L_1 \sin\phi_1)^2 + (L_1 \cos\phi_1)^2}{2dL_2}\right) \tag{B-17}$$

$$\phi_3 = \alpha - \arccos\frac{b^2 + L_3^2 - L_2^2 + (s - b - L_1 \sin\phi_1)^2 + (L_1 \cos\phi_1)^2}{2d\sqrt{b^2 + L_3^2}} - \arctan\frac{b}{L_3} + \beta \tag{B-18}$$

The following inequality must be satisfied in order for the toe to be initially moving upwards.

$$L_1\dot{\phi}_1 \sin\phi_1 + L_2\dot{\phi}_2 \sin\phi_2 + L_3\dot{\phi}_3 \sin(\phi_3 - \beta) + b\dot{\phi}_3 \cos(\phi_3 - \beta) < 0 \tag{B-19}$$

Inclusion of elastic cables spanning hip and knee.

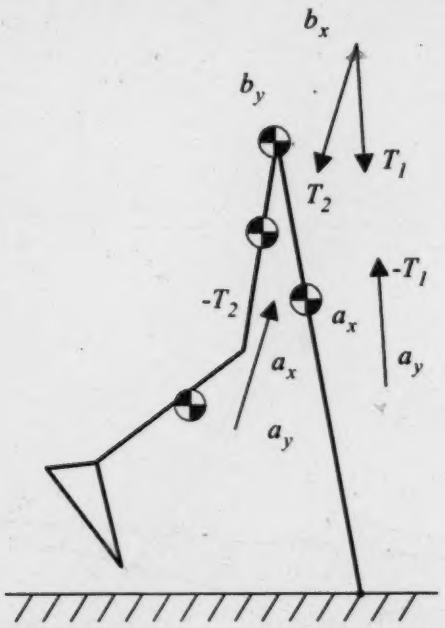

Define

$$\vec{r}_1 = \begin{bmatrix} \cos\phi_1 & -\sin\phi_1 \\ \sin\phi_1 & \cos\phi_1 \end{bmatrix} \begin{Bmatrix} a_x \\ L_1 - L_2 - a_y \end{Bmatrix} \quad \text{(B-20)}$$

$$\vec{r}_2 = L_1 \begin{Bmatrix} -\sin\phi_1 \\ \cos\phi_1 \end{Bmatrix} + \begin{Bmatrix} b_x \\ b_y \end{Bmatrix} \quad \text{(B-21)}$$

$$\vec{r}_3 = L_1 \begin{Bmatrix} -\sin\phi_1 \\ \cos\phi_1 \end{Bmatrix} + L_2 \begin{Bmatrix} -\sin\phi_2 \\ \cos\phi_2 \end{Bmatrix} + \begin{bmatrix} \cos\phi_3 & -\sin\phi_3 \\ \sin\phi_3 & \cos\phi_3 \end{bmatrix} \begin{Bmatrix} a_x \\ a_y \end{Bmatrix} \quad \text{(B-22)}$$

Cable tension determined by Hooke's Law:

$$\vec{T}_1 = k\left(1 - \frac{l}{\|\vec{r}_1 - \vec{r}_2\|}\right)(\vec{r}_1 - \vec{r}_2) \quad \text{(B-23)}$$

$$\vec{T}_2 = k\left(1 - \frac{l}{\|\vec{r}_3 - \vec{r}_2\|}\right)(\vec{r}_3 - \vec{r}_2) \quad \text{(B-24)}$$

Equation B-15 remains the same except for the addition of the cable terms:

$$[I]\{\ddot{\phi}\} = [G]\{\dot{\phi}^2\} + \{g\} + \{M\} + \{T\} \quad \text{(B-25)}$$

where

$$T = \begin{bmatrix} -r_{1x}T_{1y} + r_{1y}T_{1x} + b_x(T_{1y} + T_{2y}) - b_y(T_{1x} + T_{2x}) \\ T_{2x}L_2\cos\phi_2 + T_{2y}L_2\sin\phi_2 \\ (a_xT_{2y} - a_yT_{2x})\cos\phi_3 - (a_xT_{2x} - a_yT_{2y})\sin\phi_3 \end{bmatrix}$$

Appendix C – equations of motion for frontal plane rocking models

Model 1: two-segment inverted pendulum model of frontal plane rocking.

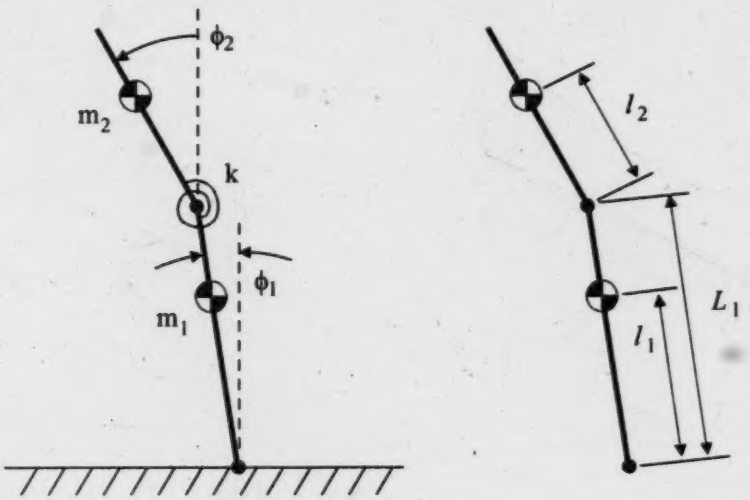

Derivation:

segment 1

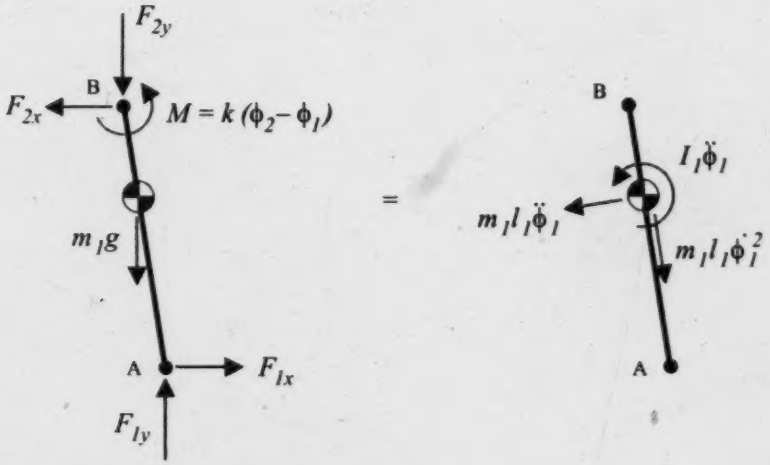

$$\sum F_x = F_{1x} - F_{2x} = -m_1 l_1 \ddot{\phi}_1 \cos\phi_1 + m_1 l_1 \dot{\phi}_1^2 \sin\phi_1 \qquad \text{(C-1)}$$

$$\sum F_y = F_{1y} - F_{2y} - m_1 g = -m_1 l_1 \ddot{\phi}_1 \sin\phi_1 - m_1 l_1 \dot{\phi}_1^2 \cos\phi_1 \qquad \text{(C-2)}$$

$$\sum M_A = k(\phi_2 - \phi_1) + m_1 g l_1 \sin\phi_1 + F_{2y} L_1 \sin\phi_1 + F_{2x} L_1 \cos\phi_1 = (I_1 + m_1 l_1^2)\ddot{\phi}_1 \qquad \text{(C-3)}$$

segment 2

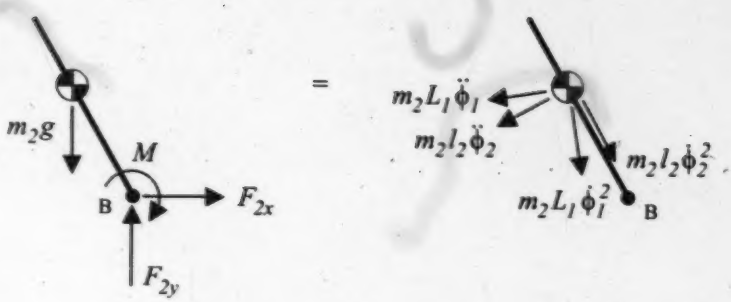

$$\sum F_x = F_{2x} = -m_2L_1\ddot{\phi}_1\cos\phi_1 - m_2l_2\ddot{\phi}_2\cos\phi_2 + m_2L_1\dot{\phi}_1^2\sin\phi_1 + m_2l_2\dot{\phi}_2^2\sin\phi_2 \quad \text{(C-4)}$$

$$\sum F_y = F_{2y} - m_2g = -m_2L_1\ddot{\phi}_1\sin\phi_1 - m_2l_2\ddot{\phi}_2\sin\phi_2 - m_2L_1\dot{\phi}_1^2\cos\phi_1 - m_2l_2\dot{\phi}_2^2\cos\phi_2 \quad \text{(C-5)}$$

$$\sum M_B = -k(\phi_2 - \phi_1) + m_2gl_2\sin\phi_2 = (I_2 + m_2l_2^2)\ddot{\phi}_2 + m_2L_1l_2\ddot{\phi}_1\cos(\phi_2 - \phi_1) + m_2L_1l_2\dot{\phi}_1^2\sin(\phi_2 - \phi_1) \quad \text{(C-6)}$$

Reaction forces are eliminated by substitution. Combining equations C-3, C-4 and C-5 yields:

$$-k\phi_1 + k\phi_2 + m_1gl_1\sin\phi_1 + m_2gL_1\sin\phi_1 = (I_1 + m_1l_1^2 + m_2L_1^2)\ddot{\phi}_1 + m_2l_2L_1\ddot{\phi}_2\cos(\phi_2 - \phi_1) - m_2l_2L_1\dot{\phi}_2^2\sin(\phi_2 - \phi_1) \quad \text{(C-7)}$$

Model 2: two-segment model of frontal plane rocking with variable foot contact.

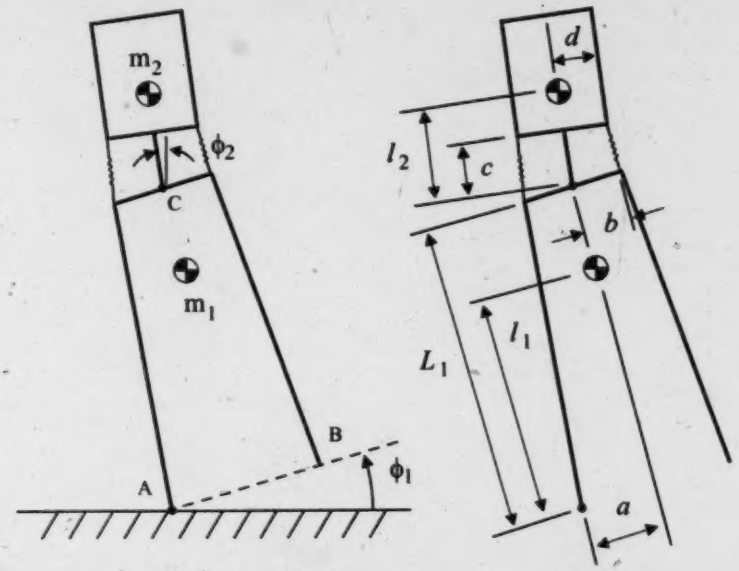

Let $\vec{r}$ be a position vector from the point of ground contact to segment 1 COM, and $\vec{R}$ be a position vector from the point of ground contact to the lumbosacral joint (point C).

segment 1

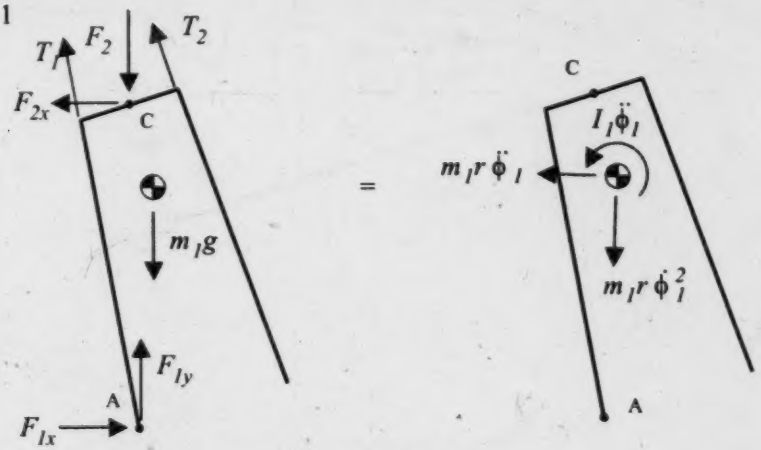

$$\sum F_x = F_{1x} - F_{2x} + T_{1x} + T_{2x} = -m_1 r_y \ddot{\phi}_1 - m_1 r_x \dot{\phi}_1^2 \qquad \text{(C-8)}$$

$$\sum F_y = F_{1y} - F_{2y} - m_1 g + T_{1y} + T_{2y} = m_1 r_x \ddot{\phi}_1 - m_1 r_y \dot{\phi}_1^2 \qquad \text{(C-9)}$$

$$\sum M_A = b(T_{1x} - T_{2x})\sin(\phi_2 - \phi_1) - b(T_{1y} - T_{2y})\cos(\phi_2 - \phi_1) - \\ - m_1 g r_x - F_{2y} R_x + F_{2x} R_y = (I_1 + m_1 r^2)\ddot{\phi}_1 \qquad \text{(C-10)}$$

segment 2

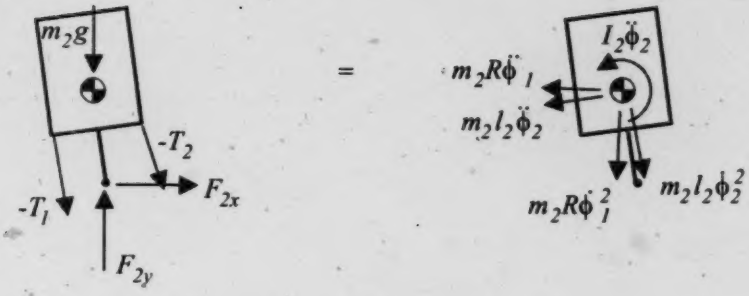

$$\sum F_x = F_{2x} - T_{1x} - T_{2x} = -m_2R_y\ddot{\phi}_1 - m_2R_x\dot{\phi}_1^2 - m_2l_2\ddot{\phi}_2\cos\phi_2 + m_2l_2\dot{\phi}_2^2\sin\phi_2 \quad \text{(C-11)}$$

$$\sum F_y = F_{2y} - m_2g - T_{1y} - T_{2y} = m_2R_x\ddot{\phi}_1 - m_2R_y\dot{\phi}_1^2 - m_2l_2\ddot{\phi}_2\sin\phi_2 - m_2l_2\dot{\phi}_2^2\cos\phi_2 \quad \text{(C-12)}$$

$$\begin{aligned}\sum M_C = {} & m_2gl_2\sin\phi_2 + (c(T_{1y}+T_{2y}) - d(T_{1x}-T_{2x}))\sin(\phi_2-\phi_1) + \\ & (c(T_{1x}+T_{2x}) + d(T_{1y}-T_{2y}))\cos(\phi_2-\phi_1) - F_{3x}L_2\cos\phi_2 + F_{3y}L_2\sin\phi_2 = \\ & (I_2 + m_2l_2^2)\ddot{\phi}_2 + m_2l_2(R_y\cos\phi_2 - R_x\sin\phi_2)\ddot{\phi}_1 + m_2l_2(R_y\sin\phi_2 + R_x\cos\phi_2)\dot{\phi}_1^2\end{aligned} \quad \text{(C-13)}$$

Combining equations C-14, C-15 and C-16 yields

$$\begin{aligned}& (I_1 + m_1r^2 + m_2R^2)\ddot{\phi}_1 + m_2l_2(R_y\cos\phi_2 - R_x\sin\phi_2 +)\ddot{\phi}_2 = \\ & b(T_{1x}-T_{2x})\sin(\phi_2-\phi_1) - b(T_{1y}-T_{2y})\cos(\phi_2-\phi_1) + (T_{1x}+T_{2x})R_y - \\ & (T_{1y}+T_{2y})R_x - (m_1r_x + m_2R_x)g + m_2l_2(R_y sim\phi_2 + R_x\cos\phi_2)\dot{\phi}_2^2\end{aligned} \quad \text{(C-14)}$$

Muscle force vectors $\bar{T}_1$ and $\bar{T}_2$ are determined by the muscle model based on the corresponding muscle length vectors and rates of change below.

$$\bar{L}_1 = \begin{bmatrix}\cos(\phi_2-\phi_1) & -\sin(\phi_2-\phi_1)\\ \sin(\phi_2-\phi_1) & \cos(\phi_2-\phi_1)\end{bmatrix}\begin{Bmatrix}-d\\ c\end{Bmatrix} + \begin{Bmatrix}b\\ 0\end{Bmatrix} \quad \text{(C-15)}$$

$$\frac{d}{dt}\bar{L}_1 = (\dot{\phi}_2 - \dot{\phi}_1)\begin{bmatrix}-\sin(\phi_2-\phi_1) & -\cos(\phi_2-\phi_1)\\ \cos(\phi_2-\phi_1) & -\sin(\phi_2-\phi_1)\end{bmatrix}\begin{Bmatrix}-d\\ c\end{Bmatrix} + \begin{Bmatrix}b\\ 0\end{Bmatrix} \quad \text{(C-16)}$$

$$\bar{L}_2 = \begin{bmatrix}\cos(\phi_2-\phi_1) & -\sin(\phi_2-\phi_1)\\ \sin(\phi_2-\phi_1) & \cos(\phi_2-\phi_1)\end{bmatrix}\begin{Bmatrix}d\\ c\end{Bmatrix} - \begin{Bmatrix}b\\ 0\end{Bmatrix} \quad \text{(C-17)}$$

$$\frac{d}{dt}\bar{L}_2 = (\dot{\phi}_2 - \dot{\phi}_1)\begin{bmatrix}-\sin(\phi_2-\phi_1) & -\cos(\phi_2-\phi_1)\\ \cos(\phi_2-\phi_1) & -\sin(\phi_2-\phi_1)\end{bmatrix}\begin{Bmatrix}d\\ c\end{Bmatrix} - \begin{Bmatrix}b\\ 0\end{Bmatrix} \quad \text{(C-18)}$$

Appendix D – equations of motion for sagittal plane swing phase model

Two-segment compound pendulum model of swing phase

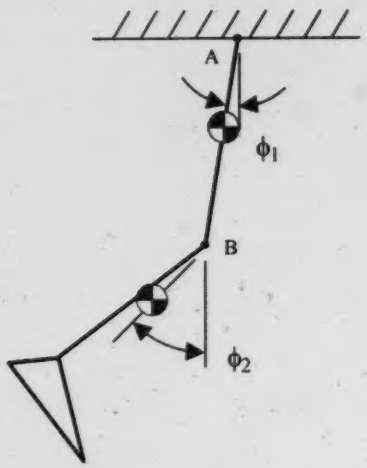

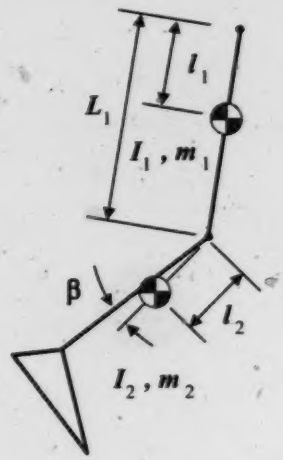

Derivation:

<u>segment 1</u>

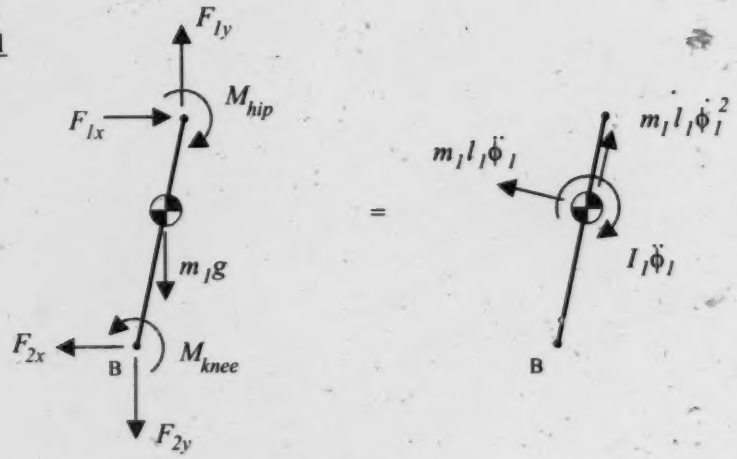

$$\sum F_x = F_{1x} - F_{2x} = -m_1 l_1 \ddot{\phi}_1 \cos\phi_1 + m_1 l_1 \dot{\phi}_1^2 \sin\phi_1 \qquad \text{(D-1)}$$

$$\sum F_y = F_{1y} - F_{2y} - m_1 g = m_1 l_1 \ddot{\phi}_1 \sin\phi_1 + m_1 l_1 \dot{\phi}_1^2 \cos\phi_1 \qquad \text{(D-2)}$$

$$\sum M_A = M_{hip} - M_{knee} - m_1 g l_1 \sin\phi_1 - F_{2y} L_1 \sin\phi_1 + F_{2x} L_1 \cos\phi_1 = (I_1 + m_1 l_1^2)\ddot{\phi}_1 \qquad \text{(D-3)}$$

segment 2

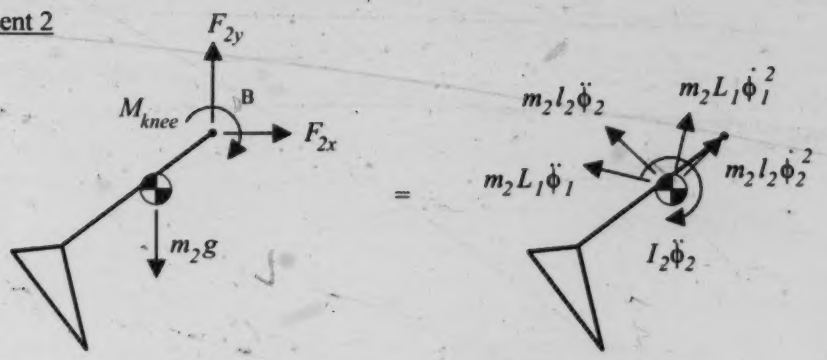

$$\sum F_x = F_{2x} = -m_2 L_1 \ddot{\phi}_1 \cos\phi_1 + m_2 L_1 \dot{\phi}_1^2 \sin\phi_1 - m_2 l_2 \ddot{\phi}_2 \cos\phi_2 + m_2 l_2 \dot{\phi}_2^2 \sin\phi_2 \quad \text{(D-4)}$$

$$\sum F_y = F_{2y} - m_2 g = m_2 L_1 \ddot{\phi}_1 \sin\phi_1 + m_2 L_1 \dot{\phi}_1^2 \cos\phi_1 + m_2 l_2 \ddot{\phi}_2 \sin\phi_2 + m_2 l_2 \dot{\phi}_2^2 \cos\phi_2 \quad \text{(D-5)}$$

$$\sum M_B = M_{knee} - m_2 g l_2 \sin\phi_2 = m_2 L_1 l_2 \dot{\phi}_1^2 \sin(\phi_2 - \phi_1) + m_2 L_1 l_2 \ddot{\phi}_1 \cos(\phi_2 - \phi_1) + (I_2 + m_2 l_2^2)\ddot{\phi}_2 \quad \text{(D-6)}$$

Combining equations D-3, D-4 and D-5 yields

$$(I_1 + m_1 l_1^2 + m_2 L_1^2)\ddot{\phi}_1 + m_2 L_1 l_2 \ddot{\phi}_2 \cos(\phi_2 - \phi_1) = M_{hip} - M_{knee} - (m_2 l_2 + m_3 L_2) g \sin\phi_2 + m_2 L_1 l_2 \dot{\phi}_2^2 \sin(\phi_2 - \phi_1) \quad \text{(D-7)}$$